# Friend or Foe? Unraveling the Effects of UV-A1 on Plant Growth and Photosynthesis

Xuguang Sun

**Propositions**

1. Studying how plants respond to UV-A in a vertical farm unravels its role in nature.
   (this thesis)

2. Supplemental UV-A radiation for commercial plant cultivation is a waste of money and energy.
   (this thesis)

3. Journal selection for a scientific paper mirrors picking stocks based on their potential for returns.

4. Obsession with science steals life away.

5. Fitness of entire nations is more important than winning Olympic medals.

6. The coverage of surveillance cameras in the public spaces ensures the safety of citizens.

Propositions belonging to the thesis, entitled
Friend or Foe? Unraveling the Effects of UV-A1 on Plant Growth and Photosynthesis

Xuguang Sun
Wageningen, 26 November 2024

# Friend or Foe?

# Unraveling the Effects of UV-A1 on Plant Growth and Photosynthesis

Xuguang Sun

**Thesis committee**

**Promotor**
Prof. Dr Leo F.M. Marcelis
Professor of Horticulture and Product Physiology
Wageningen University & Research

**Copromotors**
Dr Elias Kaiser
Assistant professor, Horticulture and Product Physiology
Wageningen University & Research
Associate professor, Institute of Agriculture and Life Sciences
Seoul National University, South Korea

Prof. Dr Tao Li
Institute of Environment and Sustainable Development in Agriculture
Chinese Academy of Agricultural Sciences, Beijing, China

**Other members**
Prof. Dr Paul Struik, Wageningen University & Research
Prof. Dr David Kramer, Michigan State University, USA
Prof. Dr Susanne Neugart, Georg-August-Universität, Göttingen, Germany
Dr Titta Kotilainen, Natural Resources Institute Finland, Helsinki, Finland

This research was conducted under the auspices of the C.T. de Wit Graduate School for Production Ecology and Resource Conservation (PE&RC)

# Friend or Foe?

# Unraveling the Effects of UV-A1 on Plant Growth and Photosynthesis

Xuguang Sun

**Thesis**

submitted in fulfilment of the requirements for the degree of doctor
at Wageningen University
by the authority of the Rector Magnificus,
Prof. Dr C. Kroeze,
in the presence of the
Thesis Committee appointed by the Academic Board
to be defended in public
on Tuesday 26 November 2024
at 1:00 p.m. in the Omnia Auditorium

Xuguang Sun
Friend or Foe?
Unraveling the Effects of UV-A1 on Plant Growth and Photosynthesis
185 Pages

PhD thesis, Wageningen University, Wageningen, the Netherlands (2024)
With references, with summary in English.

ISBN 978-94-6510-248-1
DOI https://doi.org/10.18174/673044

# Contents

# CHAPTER 1

## General introduction

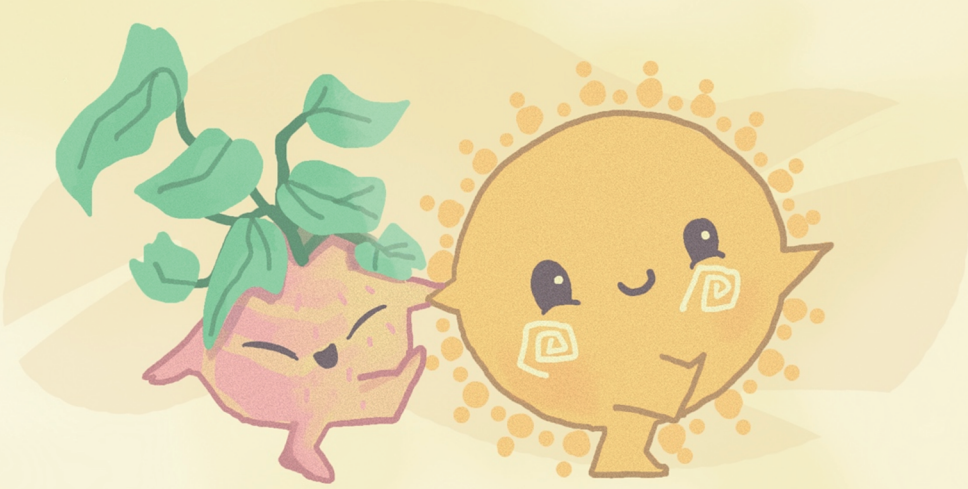

Xuguang Sun

Chapter 1

# UV-A radiation and its redefinition: from sunlight to LEDs

Ultraviolet radiation (UV; 100–400 nm) is an important part of solar radiation, which consists of UV-A (315–400 nm), UV-B (280–315 nm) and UV-C (100-280 nm). Only UV-B and UV-A can reach the biosphere, while UV-C is filtered out by ozone (Björn, 2015). Although UV radiation is often considered as deleterious, recent studies show that UV-A and UV-B can positively regulate performance and postharvest behavior of fruit, vegetable and ornamental crops when applied properly (Neugart & Schreiner, 2018). UV-B signaling and its effects on major physiological processes in plants, as well as its prospective horticultural applications, have been well explored (Wargent et al., 2009, 2015; Wargent & Jordan, 2013). Compared to UV-B, knowledge gaps exist in our current understanding of plant processes in response to UV-A (Verdaguer et al., 2017), even though in nature, UV-A accounts for ~95% of all solar UV radiation (Kerr & Fioletov, 2008). Besides, crops in greenhouses are exposed to varying levels of UV radiation depending on covering materials (Li et al., 2015; Timmermans et al., 2020). Moreover, the use of UV-A in vertical farms is less common compared to other parts of the spectrum like blue, red and far-red light.

Recently, it has been proposed to divide UV-A into two regions based on the photoreceptors involved in UV responses of the plants (Fig. 1), long-wavelength UV-A (defined as 350–400 nm, UV-A1) shares phototropins and cryptochromes with blue light (400–500 nm), whereas short-wavelength UV-A (315–350 nm; UV-A2) is perceived by UV Resistance Locus 8 (UVR8) (Christie, 2007; Rai et al., 2021). However, there is no conclusive evidence to show that UV-A has its own photoreceptor. Further, plant responses to UV-A, as mediated by these photoreceptors, have so far been poorly investigated. Thus, the function of UV-A in affecting plant growth and physiology is still unclear. Recently, novel LED technology with peak wavelength in the UV-A1 waveband provide the opportunity to manipulate UV-A1 radiation in photobiology studies. However, the energy conversion efficacy of UV-A2 LEDs is lower than 5% and their application in large-scale experiments continues to be expensive.

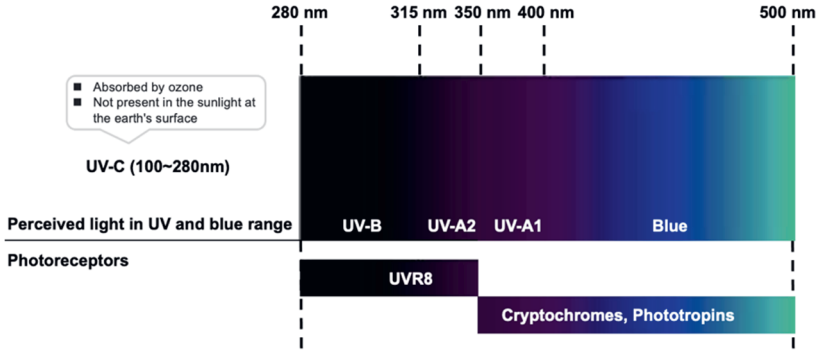


**Figure 1.** Photoreceptor-mediated light perception of higher plants in UV and blue light. Modified from Heijde & Ulm (2012).



# Plants in response to UV-A radiation is still ambiguous

## Current limitations of UV-A research

The effects of UV-A on plant growth and physiology have not been systematically investigated and there has been little agreement, mainly due to varying experimental approaches often without clear descriptions of the applied spectrum and intensity. Three types of experimental approaches have mainly been used to study plant responses to UV-A (Verdaguer et al., 2017): i) plants growing in climate rooms, using supplemental UV-A lamps; ii) plants growing in the field with cut-off filters for reducing natural UV-A exposure; iii) plants growing in the field with the supplemental UV lamps. However, each of these approaches has significant shortcomings in terms of elucidating the effects of UV-A (these are elaborated on below), and consequently these approaches limited fundamental research on how UV-A affects plants. Furthermore, UV-A may affect plants across different temporal scales, influencing processes on the short term (seconds -hours) such as photosynthesis and photoinhibition, as well as on the long term (days-weeks) like plant growth, photosynthetic acclimation, and photoprotective responses, which remain unclear and require further investigation.

## Plant growth under UV-A

Conflicting results exist on the effects of UV-A on plant growth, even for the same species. For instance, UV-A reduced stem length and leaf area in *Cucumis sativus* and *Lactuca sativa* (Krizek et al., 1997, 1998), and biomass in *Gossypium hirsutum*, *Triticum aestivum*, *Amaranthus tricolor* and *Sorghum bicolor* (Kataria et al., 2013; Qian et al., 2020). On the other hand, UV-A increased leaf area in *Arabidopsis thaliana*, *Solanum lycopersicum* and *L. sativa*, as well as total biomass in *Laurus nobilis* (Bernal et al., 2015; Biswas & Jansen, 2012; Chen et al., 2019; Kang et al., 2018). Partially, these conflicting findings may be explained by the response to a specific dose of UV-A. Indeed, we do not know much about the dose-response relationship of plants to UV-A, and how this relationship might differ across species. Several studies suggest that the intensity of photosynthetically active radiation (PAR) may affect plant responses to UV-A. For example, specific ratios of intensity of PAR: UV-B: UV-A affected flavonoid concentrations in leaves (Neugart et al., 2019). Besides, UV-A ameliorated the damage induced by UV-B at lower (600 μmol $m^{-2}$ $s^{-1}$) but not at higher PAR (1500 μmol $m^{-2}$ $s^{-1}$; Caldwell et al., 1994). Although these studies have shown the responses of plants to specific ratios of intensity of UV-A: UV-B: PAR, little has been known on the potential interactions between UV-A and PAR.

## Photosynthetic acclimation under UV-A

Photosynthetic acclimation is well-known as a process by which plants adjust the composition and function of their photosynthetic apparatus in response to environmental changes, occurring over a timeline that ranges from seconds to months (Walters, 2005). This process enables plants to optimize plant growth and carbon fixation while mitigating stress-induced damage. When leaves are grown under monochromatic red light, they develop a collection of symptoms of photosynthetic malfunctioning in plants (e.g. low $CO_2$ assimilation rate and photosynthetic capacity, low maximum quantum yield of photosystem II, low chlorophyll content, and unresponsive stomata) (Matsuda et al., 2004; Trouwborst et al., 2016). UV-A has a similar function as blue light in alleviating the “red light syndrome” (Zhang et al., 2020), via alleviating the curling downwards of leaves and maintaining leaf photosynthetic functioning. However, effects of blue light are not equivalent to those of UV-

A1 radiation, and UV-A1 showed weaker and later transcriptome-wide responses (Zhang et al., 2023). Moreover, an increase in net leaf photosynthetic rate upon blue light exposure (25–60%) was associated with increases in stomatal, chloroplast and mesophyll cell numbers, as well as chlorophyll contents (Hogewoning et al., 2010; Liu et al., 2018). These studies indicated that blue light is essential for normal photosynthetic functioning. Compared to blue light, it is likely that UV-A causes photo-oxidative stress, due to its high energy content per photon. Therefore, UV-A exposure may induce the up-regulation of photoprotective capacity to alleviate the damaging effects of abiotic stresses through several plant processes such as accumulation of biochemical compounds (i.e. UV-screening compounds) and non-photochemical quenching (Barnes et al., 2015; Murchie & Ruban, 2020; Tokutsu et al., 2021). I hypothesize that acclimation to UV-A can result in tolerance against abiotic stress such as high light and fluctuating light intensity. So far, it is still unclear how photoprotection may be induced by pre-exposure to UV-A and through which pathways this may occur.

Considering that UV-A1 may share photoreceptors with blue light, and studies on effects of UV-A1 on leaf photosynthetic acclimation have so far received limited attention, it is worthwhile to explore the similarities and differences between UV-A1 and blue light effects on leaf photosynthetic acclimation, including its wavelength dependency. Besides, background illumination is likely to alter any response mediated by photoreceptors. To my knowledge, only few studies have been conducted on leaf photosynthetic acclimation to UV-A. Sea buckthorn (*Hippophae rhamnoides*) that was exposed to solar UV-A for 90 days showed reduced water and chlorophyll b contents, coupled with an increase in carotenoid concentrations, which might be a pre-acclimation strategy to help plants retain their photochemical capacity and photosynthesis rate under UV-A (Yang & Yao, 2008). There are conflicting results on photochemical efficiency (fraction of light energy converted into chemical energy during photosynthesis) acclimated to UV-A (Pessarakli, 2005): long-term exposure to solar (and therefore dynamically changing) UV-A did not affect photochemical efficiency in *Eucalyptus nitens* seedlings (Close et al., 2007). Thus, the effects of UV-A on photosynthetic acclimation are still rather inconclusive, as these may depend on intensity and spectrum, among other factors. Further studies of UV-A effects on photosynthetic acclimation, using clearly defined and highly controlled UV-A and PAR doses, are therefore warranted.

Chapter 1

## Does UV-A power leaf photosynthesis?

The standard definition of PAR, the range from 400 to 700 nm, is largely agreed upon, as in this waveband, leaves utilize light energy to power photosynthesis (McCree, 1971). However, wavelengths <400 nm can still be photosynthetically active. Early studies showed that UV in the 300-350 nm range can stimulate leaf photosynthesis (Halldal, 1964; Leod & Kanwisher, 1962). Also, chlorophyll b has minor absorption peaks at 334 and 357 nm, and carotenoids have minor absorption peaks at 300 nm (Kusuma et al., 2020; Lichtenthaler, 1987). To date, to the best of our knowledge, only four studies (mentioned below) regarding leaf photosynthesis in response to UV-A have been conducted, and they arrive at conflicting conclusions: when solar PAR (~500 μmol $m^{-2}$ $s^{-1}$) was supplemented with UV-A at a peak wavelength of 340 nm during photosynthesis measurement, photosynthesis was increased by 8–10% in several species, compared to photosynthesis with the 400 nm supplement (Mantha et al., 2001). In another study, photosynthesis in *Sorghum bicolor* was increased by 1.2% when illumination from a xenon-arc lamp (cut-off below 311 nm) that emitted UV radiation was added to PAR (250 μmol $m^{-2}$ $s^{-1}$; Johnson & Day, 2002). In the above two studies, UV-A1 light intensity was provided based on the specific PAR of outdoor sunlight under the tree canopy; however, the exact values were not specified. Turnbull et al. (2013) reported that UV-A in sunlight (midday UV-A intensity of up to 160 μmol $m^{-2}$ $s^{-1}$) increased photosynthesis by 12% in *Pimelea ligustrina* at a PAR intensity of up to 1995 μmol $m^{-2}$ $s^{-1}$, compared to the transmission of PAR alone. However, another study in *Geranium antrorsum* under natural sunlight coupled with UV screening films showed that UV-A exposure (midday UV-A intensity of up to 50 μmol $m^{-2}$ $s^{-1}$) reduced photosynthesis, when measured at background PAR intensities of up to 1700 μmol $m^{-2}$ $s^{-1}$ (Salter et al., 2018). Among these four studies, three did not clarify which exact spectrum was used. Also, sunlight was used in all studies, thus light intensity may not have been constant, which may affect the conclusions drawn from these results. Besides, it remains unclear to what extent the effects of UV-A on photosynthesis may vary among different species. Further investigation is needed to assess how different growth environments modulate the effects of UV-A on photosynthesis. Such investigation should use a well-controlled and clearly described plant growth and measurement setup.

A new definition of PAR, namely ePAR (400-750 nm), was recently proposed by Zhen et al. (2021), based on far-red radiation together with shorter-wavelength red light it has been demonstrated to enhance photosynthesis (Emerson et al., 1957; Zhen et al., 2019; Zhen & Bugbee, 2020; Zhen & van Iersel, 2017). Despite several studies showing that wavelengths <400 nm can be photosynthetically active, the definition of ePAR has so far not been modified. A possible reason could be that UV-A provides only ca. 7% of all radiation in the 400-700 nm waveband (ASTM, 2013). It is unclear how strongly photosynthesis may increase with increases of intensity of specific parts of the UV-A waveband. I hypothesize that the quantum yield of photosynthesis decreases, the further the peak wavelength of UV-A is away from the visible range. This reduction may be caused by pigment excitation transfer from e.g. flavonoids to chlorophylls becoming less efficient the further the UV-A wavelength is away from PAR. Besides, compared to the quantum yield under PAR, the UV screening compounds in the epidermis likely serve as the main reason for the reduced quantum yield under UV-A by preventing further UV radiation from reaching the chloroplasts (Caldwell et al., 1983). Additionally, given that UV-A has high energy per photon, it may not only drive photosynthesis but also induce photodamage. Prolonged exposure to UV-A raises the question whether photosynthesis declines and how plants activate photoprotection mechanisms in response to longer-term UV-A exposure.



# About the thesis

In this thesis, I aim to identify and quantify how UV-A1 affects plant growth, leaf photosynthesis and photosynthetic acclimation.

The following hypotheses were investigated in detail:

- Plant responses to UV-A1 radiation are genotype and background irradiance dependent (**Chapter 2**).
- UV-A1 radiation and blue light trigger photosynthetic and photoprotective acclimation following a shallow gradient pattern, which becomes stronger the longer the peak wavelength is (**Chapter 3**).
- UV-A1 powers photosynthesis and causes photoinhibition in a wavelength-dependent manner (**Chapter 4**).

- Longer-term UV-A1 exposure (24-72 h) stresses plants, but plants can successfully acclimate by adjusting their photosynthetic apparatus (**Chapter 5**).

This thesis consists of six chapters: a general introduction (**Chapter 1**, this chapter), four research chapters (**Chapters 2-5**) and a general discussion (**Chapter 6**). The outline of **Chapters 2-5** is displayed in Figure 2.

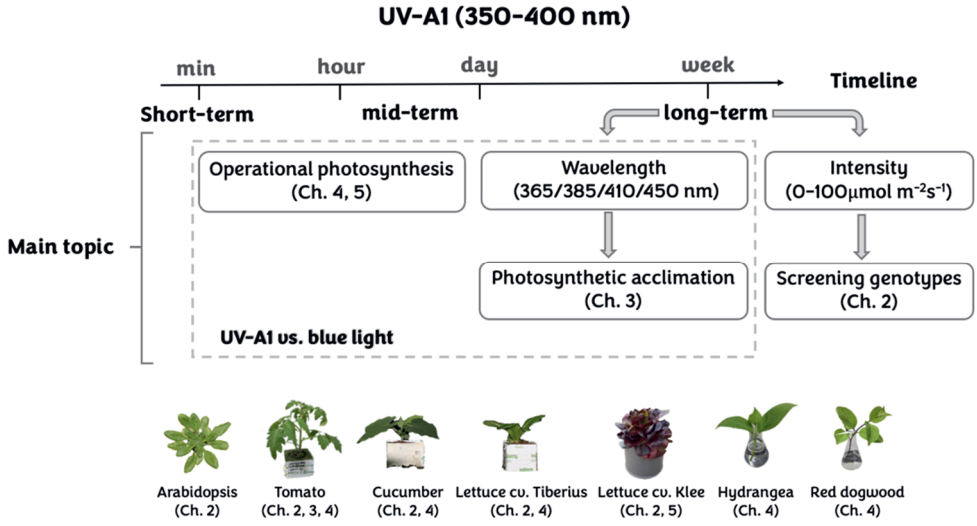


**Figure 2.** Structure of thesis. Effects of UV-A1 radiation on leaf and plant level. Plant growth, photosynthesis, photosynthetic acclimation, photoinhibition and photoprotection are the main focus of investigating how plants respond to UV-A1.

**Chapter 2** investigates the extent to which plant genotypes differ in their response to UV-A1, and how their responses to UV-A1 depend on the photosynthetic photon flux density (PPFD). To elucidate this, several horticultural (tomato, cucumber, and two lettuce cultivars) and a model species (*Arabidopsis thaliana*) were grown under low and high PPFD, each of which is paired with three UV-A1 intensities.

**Chapter 3** aims to compare how acclimation to several wavelengths in the UV-A1 and blue light range affects leaf photosynthetic and photoprotective performance in tomato, and consequently how such acclimation prepares plants for subsequent exposure to fluctuating and high light intensities. Tomato plants were initially grown under hybrid red and blue light,

and another four treatments are supplemented with the same light intensity at several peak wavelengths under UV-A1 and blue light.

**Chapter 4** aims to quantify the photosynthetic quantum yield of UV-A1. Measurements of photosynthesis were conducted in leaves of six genotypes (from different growth conditions) at four spectra and a range of intensities.



**Chapter 5** focuses on whether photoinhibition caused by UV-A1 would suppress photosynthesis continuously, if applied for 24-72 h, and how this may interact with red/blue light effects. Lettuce seedlings were exposed to three independent experiments varying in light intensity and duration: photosynthesis under light treatments and standard spectrum, chlorophyll fluorescence, plant growth and leaf pigmentation were monitored.

In **Chapter 6**, I discuss the findings of this thesis. A comprehensive overview of UV-A1 effects on plant growth, leaf photosynthesis and photosynthetic acclimation is presented, by relating the findings of this thesis to the existing literature, as well as a comparison of the similarities and differences between UV-A1 and blue light. I also provides insights on the role of UV-A1 on plants in nature and perspectives for future research on this topic.

# References

ASTM. (2013). Standard Tables for Reference Solar Spectral Irradiances : Direct Normal and Hemispherical on 37° Tilted Surface. *ASTM*. https://doi.org/10.1520/G0173-03R12.2

Barnes, P. W., Flint, S. D., Ryel, R. J., Tobler, M. A., Barkley, A. E., & Wargent, J. J. (2015). Rediscovering leaf optical properties: New insights into plant acclimation to solar UV radiation. *Plant Physiology and Biochemistry*, *93*, 94–100. https://doi.org/10.1016/j.plaphy.2014.11.015

Bernal, M., Verdaguer, D., Badosa, J., Abadía, A., Llusià, J., Peñuelas, J., Núñez-Olivera, E., & Llorens, L. (2015). Effects of enhanced UV radiation and water availability on performance, biomass production and photoprotective mechanisms of Laurus nobilis seedlings. *Environmental and Experimental Botany*. https://doi.org/10.1016/j.envexpbot.2014.06.016

Biswas, D. K., & Jansen, M. A. K. (2012). Natural variation in UV-B protection amongst arabidopsis thaliana accessions. *Emirates Journal of Food and Agriculture*. https://doi.org/10.9755/ejfa.v24i6.14681

Björn, L. O. (2015). History Ultraviolet-A, B, and C. *UV4Plants Bulletin*. https://doi.org/10.19232/uv4pb.2015.1.12

Caldwell, M. M., Flint, S. D., & Searles, P. S. (1994). Spectral balance and UV-B sensitivity of soybean: a field experiment. *Plant, Cell & Environment*, *17*(3), 267–276. https://doi.org/10.1111/j.1365-3040.1994.tb00292.x

Caldwell, M. M., Robberecht, R., & Flint, S. D. (1983). Internal filters: Prospects for UV-acclimation in higher plants. *Physiologia Plantarum*, *58*(3), 445–450. https://doi.org/10.1111/j.1399-3054.1983.tb04206.x

Chen, Y., Li, T., Yang, Q., Zhang, Y., Zou, J., Bian, Z., & Wen, X. (2019). UVA radiation is beneficial for yield and quality of indoor cultivated lettuce. *Frontiers in Plant Science*, *10*. https://doi.org/10.3389/fpls.2019.01563

Christie, J. M. (2007). Phototropin blue-light receptors. *Annu Rev Plant Biol*, *58*, 21–45. https://doi.org/10.1146/annurev.arplant.58.032806.103951

Close, D. C., McArthur, C., Hagerman, A. E., Davies, N. W., & Beadle, C. L. (2007). Phenolic acclimation to ultraviolet-A irradiation in *Eucalyptus nitens* seedlings raised across a nutrient environment gradient. *Photosynthetica*. https://doi.org/10.1007/s11099-007-0006-4

Emerson, R., Chalmers, R., & Cederstrand, C. (1957). Some Factors Influencing the Long-Wave Limit of Photosynthesis. *Proceedings of the National Academy of Sciences*, *43*(1), 133–143. https://doi.org/10.1073/pnas.43.1.133

Halldal, P. (1964). Ultraviolet action spectra of photosynthesis and photosynthetic inhibition in a green and a red alga. *Physiologia Plantarum*, *17*(2), 414–421. https://doi.org/10.1111/j.1399-3054.1964.tb08174.x

Heijde, M., & Ulm, R. (2012). UV-B photoreceptor-mediated signalling in plants. *Trends in Plant Science,*, *17*(4), 230–237. https://doi.org/10.1016/j.tplants.2012.01.007

Hogewoning, S. W., Trouwborst, G., Maljaars, H., Poorter, H., van Ieperen, W., & Harbinson, J. (2010). Blue light dose-responses of leaf photosynthesis, morphology, and chemical composition of *Cucumis sativus* grown under different combinations of red and blue light. *Journal of Experimental Botany*. https://doi.org/10.1093/jxb/erq132

Johnson, G. A., & Day, T. A. (2002). Enhancement of photosynthesis in Sorghum bicolor by ultraviolet radiation. *Physiologia Plantarum*. https://doi.org/10.1034/j.1399-3054.2002.1160415.x

Kang, S., Zhang, Y., Zhang, Y., Zou, J., Yang, Q., & Li, T. (2018). Ultraviolet-a radiation stimulates growth of indoor cultivated tomato (Solanum lycopersicum) seedlings. *HortScience*. https://doi.org/10.21273/HORTSCI13347-18

Kataria, S., Guruprasad, K. N., Ahuja, S., & Singh, B. (2013). Enhancement of growth, photosynthetic performance and yield by exclusion of ambient UV components in C3 and C4 plants. *Journal of Photochemistry and*

*Photobiology B: Biology*. https://doi.org/10.1016/j.jphotobiol.2013.08.013

Kerr, J. B., & Fioletov, V. E. (2008). Surface ultraviolet radiation. *Atmosphere-Ocean*. *46*(1), 159–184. https://doi.org/10.3137/ao.460108

Krizek, D. T., Britz, S. J., & Mirecki, R. M. (1998). Inhibitory effects of ambient levels of solar UV-A and UV-B radiation on growth of cv. New Red Fire lettuce. *Physiologia Plantarum, 103*(1), 1–7. https://doi.org/10.1034/j.1399-3054.1998.1030101.x

Krizek, D. T., Mirecki, R. M., & Britz, S. J. (1997). Inhibitory effects of ambient levels of solar UV-A and UV-B radiation on growth of cucumber. *Physiologia Plantarum*, *100*(4), 886–893. https://doi.org/10.1111/j.1399-3054.1997.tb00014.x

Kusuma, P., Pattison, P. M., & Bugbee, B. (2020). From physics to fixtures to food: current and potential LED efficacy. *Horticulture Research*. https://doi.org/10.1038/s41438-020-0283-7

Li, D., Li, Z., Zheng, Y., Liu, C., & Lu, L. (2015). Optical performance of single and double glazing units in the wavelength 337-900nm. *Solar Energy*, *122*, 1091–1099. https://doi.org/10.1016/j.solener.2015.10.028

Lichtenthaler, H. K. (1987). Chlorophylls and Carotenoids: Pigments of Photosynthetic Biomembranes. *Methods in Enzymology*. https://doi.org/10.1016/0076-6879(87)48036-1

Liu, X. Y., Jiao, X. L., Chang, T. T., Guo, S. R., & Xu, Z. G. (2018). Photosynthesis and leaf development of cherry tomato seedlings under different LED-based blue and red photon flux ratios. *Photosynthetica*. https://doi.org/10.1007/s11099-018-0814-8

Mantha, S. V., Johnson, G. A., & Day, T. A. (2001). Evidence from action and fluorescence spectra that UV-Induced violet-blue-green fluorescence enhances leaf photosynthesis¶. *Photochemistry and Photobiology*. https://doi.org/10.1562/0031-8655(2001)0730249efaafs2.0.co2

Matsuda, R., Ohashi-Kaneko, K., Fujiwara, K., Goto, E., & Kurata, K. (2004). Photosynthetic characteristics of rice leaves grown under red light with or without supplemental blue light. *Plant and Cell Physiology*, *45*(12), 1870–1874. https://doi.org/10.1093/pcp/pch203

Leod, G. C. M., & Kanwisher, J. (1962). The quantum efficiency of photosynthesis in ultraviolet light. Physiologia Plantarum, 15(3), 581–586. https://doi.org/10.1111/j.1399-3054.1962.tb08061.x

McCree, K. J. (1971). The action spectrum, absorptance and quantum yield of photosynthesis in crop plants. *Agricultural Meteorology*. https://doi.org/10.1016/0002-1571(71)90022-7

Murchie, E. H., & Ruban, A. V. (2020). Dynamic non-photochemical quenching in plants: from molecular mechanism to productivity. *Plant Journal*, *101*(4), 885–896. https://doi.org/10.1111/tpj.14601

Neugart, S., & Schreiner, M. (2018). UVB and UVA as eustressors in horticultural and agricultural crops. *Scientia Horticulturae, 234,* 370–381.. https://doi.org/10.1016/j.scienta.2018.02.021

Neugart, S., Tobler, M. A., & Barnes, P. W. (2019). Different irradiances of UV and PAR in the same ratios alter the flavonoid profiles of: Arabidopsis thaliana wild types and UV-signalling pathway mutants. *Photochemical and Photobiological Sciences*. https://doi.org/10.1039/c8pp00496j

Pessarakli, M. (2005). Handbook of photosynthesis. In *Handbook of Photosynthesis, Second Edition*. https://doi.org/10.1201/9781420027877

Qian, M., Rosenqvist, E., Flygare, A. M., Kalbina, I., Teng, Y., Jansen, M. A. K., & Strid, Å. (2020). UV-A light induces a robust and dwarfed phenotype in cucumber plants (*Cucumis sativus* L.) without affecting fruit yield. *Scientia Horticulturae, 263, 109110.* https://doi.org/10.1016/j.scienta.2019.109110

Rai, N., Morales, L. O., & Aphalo, P. J. (2021). Perception of solar UV radiation by plants: photoreceptors and mechanisms. *Plant Physiology*, *186*(3), 1382–1396. https://doi.org/10.1093/PLPHYS/KIAB162

Salter, W. T., Turnbull, T. L., Rennenberg, H., & Adams, M. A. (2018). Solar UV upregulates photoprotection but slows photosynthesis in subalpine Australian Plants. *Arctic, Antarctic, and Alpine Research*, *49*(4), 673–685. https://doi.org/10.1657/aaar0017-024

Timmermans, G. H., Hemming, S., Baeza, E., van Thoor, E. A. J., Schenning, A. P. H. J., & Debije, M. G. (2020).

Advanced optical materials for sunlight control in greenhouses. *Advanced Optical Materials*, *8*(18). https://doi.org/10.1002/adom.202000738

Tokutsu, R., Fujimura-Kamada, K., Yamasaki, T., Okajima, K., & Minagawa, J. (2021). UV-A/B radiation rapidly activates photoprotective mechanisms in Chlamydomonas reinhardtii. *Plant Physiology*, *185*(4), 1894–1902. https://doi.org/10.1093/plphys/kiab004

Trouwborst, G., Hogewoning, S. W., van Kooten, O., Harbinson, J., & van Ieperen, W. (2016). Plasticity of photosynthesis after the 'red light syndrome' in cucumber. *Environmental and Experimental Botany*, *121*, 75–82. https://doi.org/10.1016/j.envexpbot.2015.05.002

Turnbull, T. L., Barlow, A. M., & Adams, M. A. (2013). Photosynthetic benefits of ultraviolet-A to Pimelea ligustrina, a woody shrub of sub-alpine Australia. *Oecologia*. https://doi.org/10.1007/s00442-013-2640-9

Verdaguer, D., Jansen, M. A. K., Llorens, L., Morales, L. O., & Neugart, S. (2017). UV-A radiation effects on higher plants: Exploring the known unknown. In *Plant Science*. https://doi.org/10.1016/j.plantsci.2016.11.014

Walters, R. G. (2005). Towards an understanding of photosynthetic acclimation. *Journal of Experimental Botany*. https://doi.org/10.1093/jxb/eri060

Wargent, J. J., Gegas, V. C., Jenkins, G. I., Doonan, J. H., & Paul, N. D. (2009). UVR8 in Arabidopsis thaliana regulates multiple aspects of cellular differentiation during leaf development in response to ultraviolet B radiation. *New Phytologist*. https://doi.org/10.1111/j.1469-8137.2009.02855.x

Wargent, J. J., & Jordan, B. R. (2013). From ozone depletion to agriculture: Understanding the role of UV radiation in sustainable crop production. In *New Phytologist*. https://doi.org/10.1111/nph.12132

Wargent, J. J., Nelson, B. C. W., Mcghie, T. K., & Barnes, P. W. (2015). Acclimation to UV-B radiation and visible light in *Lactuca sativa* involves up-regulation of photosynthetic performance and orchestration of metabolome-wide responses. *Plant Cell and Environment*, *38*(5), 929–940. https://doi.org/10.1111/pce.12392

Yang, Y. Q., & Yao, Y. (2008). Photosynthetic responses to solar UV-A and UV-B radiation in low-and high-altitude populations of Hippophae rhamnoides. *Photosynthetica*, *46*(2). https://doi.org/10.1007/s11099-008-0056-2

Zhang, Y., Kaiser, E., Zhang, Y., Zou, J., Bian, Z., Yang, Q., & Li, T. (2020). UVA radiation promotes tomato growth through morphological adaptation leading to increased light interception. *Environmental and Experimental Botany*. https://doi.org/10.1016/j.envexpbot.2020.104073

Zhang, Y., Sun, X., Aphalo, P. J., Zhang, Y., Cheng, R., & Li, T. (2023). Ultraviolet-A1 radiation induced a more favorable light-intercepting leaf-area display than blue light and promoted plant growth. *Plant Cell and Environment*, *46*(10), 1–16. https://doi.org/10.1111/pce.14727

Zhen, S., & Bugbee, B. (2020). Far-red photons have equivalent efficiency to traditional photosynthetic photons: Implications for redefining photosynthetically active radiation. *Plant Cell and Environment*, *43*(5), 1259–1272. https://doi.org/10.1111/pce.13730

Zhen, S., Haidekker, M., & van Iersel, M. W. (2019). Far-red light enhances photochemical efficiency in a wavelength-dependent manner. *Physiologia Plantarum*, *167*(1), 21–33. https://doi.org/10.1111/ppl.12834

Zhen, S., van Iersel, M., & Bugbee, B. (2021). Why far-Red photons should be included in the definition of photosynthetic photons and the measurement of horticultural fixture efficacy. *Frontiers in Plant Science*, *12*(June), 10–13. https://doi.org/10.3389/fpls.2021.693445

Zhen, S., & van Iersel, M. W. (2017). Far-red light is needed for efficient photochemistry and photosynthesis. *Journal of Plant Physiology*, *209*, 115–122. https://doi.org/10.1016/j.jplph.2016.12.004

# CHAPTER 2

## Plant responses to UV-A1 radiation are genotype and background irradiance dependent

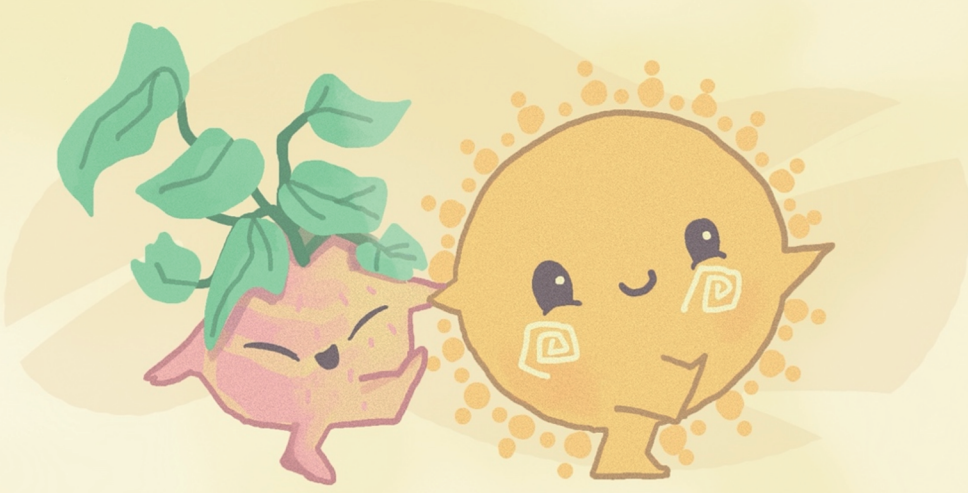

Xuguang Sun, Elias Kaiser, Pedro J. Aphalo, Leo F. M. Marcelis, Tao Li

*Published in Environmental and Experimental Botany (2024)*
*https://doi.org/10.1016/j.envexpbot.2023.105621*

# Abstract

A large fraction of solar UV radiation that reaches the Earth's surface is in the UV-A1 waveband (350-400 nm). Despite its prevalence, it is unknown how strongly plant genotypes differ in their response to UV-A1, and how their responses to UV-A1 depend on the photosynthetic photon flux density (PPFD). We grew several horticultural (tomato, cucumber, and two lettuce cultivars) and a model species (*Arabidopsis thaliana*) under low (LL; 150 µmol $m^{-2}$ $s^{-1}$) and high PPFD (HL; 550 µmol $m^{-2}$ $s^{-1}$), each of which was paired with UV-A1 (peaking at 365 nm) at irradiances of 0, 20, and 100 µmol $m^{-2}$ $s^{-1}$. Arabidopsis was the most strongly affected, as under LL, addition of UV-A1 resulted in early flowering, changes in leaf shape, and strong decreases in shoot dry weight (~40%). In all species, UV-A1 exposure induced photoinhibition (low $F_v/F_m$) only under LL, but not under HL. Under HL, exposure to UV-A1 also induced strong decreases in the concentrations of UV-absorbing compounds and anthocyanins in arabidopsis (Columbia-0) and lettuce cv. Klee, but not in other genotypes. Altogether, we found that UV-A1 had only mild effects on the morphology of horticultural species (e.g. petiole angle, leaf shape and curvature), did not significantly alter biomass or leaf biochemical compound concentrations, and these effects were almost entirely unaffected by background PPFD. In contrast, these traits were strongly affected by UV-A1 in arabidopsis, highlighting the importance of not relying solely on model species when exploring environmental effects on plants. We conclude that plant responses to UV-A1 radiation depend on genotype and background irradiance.

**Keywords**:

UV-A1, plant growth, leaf biochemical compounds, photoinhibition

# 1. Introduction

Ultraviolet radiation (UV; 100–400 nm) is a substantial component of solar radiation, and is typically classified as UV-A (315–400 nm), UV-B (280–315 nm) and UV-C (100-280 nm) (Verdaguer et al., 2017). Only UV-B and UV-A reach the Earth's biosphere, while UV-C is filtered out by ozone and oxygen (Reed, 2010). The mechanisms of UV-B signaling in key physiological processes of plants, including potential applications of UV-B in horticulture, are relatively well studied (Jenkins, 2014; Wargent et al., 2015; Wargent & Jordan, 2013). Unlike UV-B, UV-A does not seem to have its own photoreceptor, but likely long-wavelength UV-A (defined as 350-400 nm, UV-A1) shares phototropins and cryptochromes with blue light (400-500 nm), while short-wavelength UV-A (315-350 nm; UV-A2) is sensed mainly by UVR8 (Christie, 2007; Rai et al., 2021). Knowledge of UV-A effects on plant responses is rather limited (Verdaguer et al., 2017), even though in nature, UV-A accounts for ~95% of all solar UV radiation (Kerr & Fioletov, 2008). UV-A photon irradiance is equivalent to ~5-12% of photosynthetically active radiation (PAR; 400-700 nm), while >80% of all UV-A photons are in the UV-A1 region. So far, the few studies that exist on the topic have presented conflicting results: while several studies reported that UV-A reduced stem length and leaf area in cucumber (*Cucumis sativus*) and lettuce (*Lactuca sativa*) (Krizek et al., 1997, 1998; Qian et al., 2021), as well as biomass in cotton (*Gossypium hirsutum*), wheat (*Triticum aestivum*), amaranth (*Amaranthus tricolor)* and sorghum (*Sorghum bicolor*) (Kataria et al., 2013), others have reported that UV-A increased leaf area in *Arabidopsis thaliana*, tomato (*Solanum lycopersicum*) and both leaf area and biomass in lettuce (Bernal et al., 2015; Biswas & Jansen, 2012; Chen et al., 2019; Hooks et al., 2021; Ng, 2019; Zhang et al., 2020).

Possible explanations for these conflicting results are listed below. First, exposure to UV-A1 could result in very different photomorphogenesis and growth compared to UV-A2 due to its dependence on a different photoreceptor. However, this needs to be explored experimentally, as studies comparing the effects of UV-A1 and UV-A2 have so far been very few, and have been limited to gene expression and transcriptome-wide responses (Rai et al., 2019, 2021). Second, effects of UV-A on plant growth are expected to be dose-dependent, which reflects the

diversity and plasticity of plants for long-term acclimation (Aphalo & Sadras, 2021); also, this dependence could be species-specific, leading to variations in their perception and response to UV-A. Third, UV-A can drive photosynthesis (McCree, 1971; Verdaguer et al., 2017), but its contribution (relative to that of PAR) towards carbon gain by the plant remains unclear. Last, interactions between UV and photosynthetic photon flux density (PPFD) affect plant growth (Caldwell et al., 1994; Neugart et al., 2019), but the effects of UV-A alone (i.e., without UV-B) still require elucidation.

Studies of plant UV photobiology are often limited by light source availability. UV-B and UV-A, including black light blue fluorescent tubes and UV-absorbing filters have been used to manipulate UV radiation in previous studies (e.g., Albert & Mcleod, 2012; Morales et al., 2010; Rai et al., 2019; Siipola et al., 2015; White & Jahnke, 2002). Recently, LEDs with emission peaks in the UV-A1 waveband have become available at low cost, thereby substantially increasing the opportunities for manipulating UV-A1 radiation in photobiology studies (Chen et al., 2019; He et al., 2021; Kelly & Runkle, 2023; Lee et al., 2019; Zhang et al., 2020). Although LEDs emitting at wavelengths <365 nm (340 nm and 325 nm) are also available, their energy conversion efficacy is lower (i.e. < 5% below 350 nm vs. > 50% above 365 nm) and their use in large-scale experiments remains very expensive (Rai et al., 2021). Further, in some studies that used UV-A fluorescent tubes (Biswas & Jansen, 2012), no data of the spectrum was provided. However, fluorescent tubes tend to have a broader spectrum than LEDs, so any effects of UV-A in these studies will likely not have been due to UV-A1 alone. Finally, in several experiments conducted outdoors, filters were used to remove UV-A and UV-B from sunlight simultaneously, or UV-B only (Kataria et al., 2013; Rai et al., 2021), making it difficult to quantify UV-A1 effects separately, especially under the highly variable conditions that are typically encountered in nature (Kaiser et al., 2018).

Due to its short wavelength and correspondingly high energy content per photon as well as relative abundance in sunlight, UV-A can cause photoinhibition (Hakala-Yatkin et al., 2010; Kataria et al., 2013; Krizek et al., 1998). Using chlorophyll *a* fluorescence (CF), the effects of photoinhibition on leaf photochemistry can be assessed by measuring the maximum quantum efficiency of photosystem II photochemistry ($F_v/F_m$), which is related to the number of closed

photosystem II reaction centers in dark-adapted leaves. Acclimation to solar UV radiation likely increases leaf photoprotective capacity (Aphalo & Sadras, 2021; Bruce et al., 2007): specifically, UV-absorbing compounds in the epidermis (flavonoids and related phenylpropanoid derivatives) act as sunscreen pigments to prevent UV from reaching the mesophyll. Furthermore, flavonoids in the mesophyll have antioxidant properties, contributing to protection from photooxidative stress (Agati & Tattini, 2010; Barnes et al., 2016). Besides, anthocyanin located in the mesophyll engages in free-radical scavenging, protecting chloroplasts from photoinhibition and photooxidative stress (Agati & Tattini, 2010). Apart from its putative effects on photoinhibition, UV-A, similarly to other abiotic stresses, may lead to faster flowering in annuals (Xu et al., 2014).



This study aims to explore how UV-A1 affects plant growth and its underlying traits across four plant species, and how their responses to UV-A1 depend on PPFD. We hypothesized that: i) UV-A1 radiation has genotype-specific effects on plant growth, morphology and leaf biochemical compounds; ii) UV-A1 radiation is an environmental stressor which reduces biomass and induces photoinhibition, depending on irradiance. We used UV-A1 LEDs (peaking at 365 nm) in a controlled environment to systematically investigate the effects of UV-A1 on plant growth and several leaf physiological traits in horticultural (tomato, cucumber, and two lettuce cultivars) as well as a model species (*Arabidopsis thaliana*). These horticultural species were selected, as they are typical leafy greens and vegetable seedlings that are often cultivated in controlled environments, and developing a proper light recipe is thus essential for their cultivation.

# 2. Materials and methods

## 2.1 Plant material and growth conditions

Seeds of tomato cv. Moneymaker, cucumber cv. Xiamei No.2, romaine lettuce cv. Tiberius and butterhead lettuce cv. Klee were sown in rockwool plugs (Grodan, Roermond, the Netherlands) with one seed per plug, and germinated in a growth room at a PPFD of 150 μmol $m^{-2}$ $s^{-1}$, using white dimmable LED lamps (PanAmGreenlight, Jinhua, China; for spectra see Fig. S1B and

Table S1). The photoperiod was 16 h, day/night temperatures were 22/20 °C, relative humidity was 65-70%, and $CO_2$ partial pressure was ~410 μmol $mol^{-1}$. Air temperature was regularly and diligently monitored by the experimenter with a climate sensor (TR-76Ui-S, T&D Co. Ltd., Nagano, Tokyo, Japan), and was very close to the setpoint. Arabidopsis (accession Columbia-0) was germinated under identical conditions as the other species, except for a lower PPFD (100 μmol $m^{-2}$ $s^{-1}$) with a shorter photoperiod (10 h).

Cucumber and tomato seedlings were transferred to rockwool cubes (10 cm × 10 cm × 7 cm; Grodan) upon unfolding of the first and second true leaf, respectively. Seedlings of lettuce and arabidopsis were transferred to smaller rockwool cubes (7.5 cm × 7.5 cm × 5 cm; Grodan) upon unfolding of the second and tenth true leaf, respectively. Plants were then distributed over six growth units with dimensions of 115 cm × 70 cm × 115 cm each (length × width × height), which were located in one growth room. Opaque black-white plastic films were wrapped around each unit, which harbored one treatment, with the white side facing the plants, to avoid light contamination between units. Two ventilation fans (12 V, 0.90 A, 0.5 $m^3$ $min^{-1}$) were installed on both sides of each unit to ensure air circulation; the installation height was close to the LED lamps, in order to get rid of the heat emitted by the lamps. A UV-A dimmable LED lamp (ZWS01D-LED120-180, PanAnGreenlight, Jinhua, China; for spectra see Fig. 1) with peak wavelength at 365 nm and half-wave width between 358 and 383 nm was installed in between two white dimmable LED lamps (the same brand as the UV-A lamp) at the top of each growth unit. A cooling system, including central air conditioning and ventilation fans, was used to provide uniform air in the growth chamber.

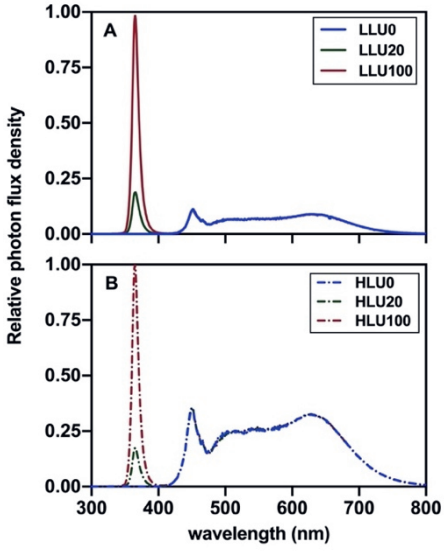


**Figure 1.** Normalized spectral photon irradiance corresponding to the three UV-A1 treatments at two background irradiances. A low (panel A: LL; 150 µmol $m^{-2}$ $s^{-1}$) and a high PPFD (panel B: HL; 550 µmol $m^{-2}$ $s^{-1}$) were used, each of which was paired with three UV-A1 irradiances of 0, 20, and 100 µmol $m^{-2}$ $s^{-1}$, which are referred as LLU0, LLU20, LLU100, HLU0, HLU20, and HLU100, respectively.

## 2.2 Experimental setup

### *Genotype screening experiment*

This experiment was set up to investigate whether plant responses to UV-A1 are genotype-specific, and to what extent UV-A1 and PPFD affect plant growth interactively. A low (LL; 150 µmol $m^{-2}$ $s^{-1}$) and a high PPFD (HL; 550 µmol $m^{-2}$ $s^{-1}$) were used, each of which was paired with three UV-A1 irradiances of 0, 20, and 100 µmol $m^{-2}$ $s^{-1}$, resulting in six treatments. The daily UV-A1 dose was calculated by using a spectral weighing function according to Flint and Caldwell (2003). These treatments are hereafter referred to as LLU0, LLU20, LLU100, HLU0, HLU20, and HLU100, respectively. Information on irradiance and spectra of each treatment are shown in Table 1 and Fig.1, respectively. Light treatments were randomly distributed between the six growth units. The position of the light treatments in the growth room was randomly switched whenever a new round of cultivation was started. Every other day, plants inside each treatment were rotated and relocated relative to each other, to avoid position effects on plant growth. Irradiance was regularly adjusted by altering the height of the platform to

maintain the same irradiance at the top of the plants during plant growth, and was measured using a spectroradiometer (Avaspec-2048CL, Avantes, Apeldoorn, the Netherlands). At any time, two plant species were grown per unit, with 6-10 plants per species. Per unit, two lifting platforms (i.e. one per species) were installed, to repeatedly adjust the distance (50 cm) between the top of the canopy and the LEDs, thereby ensuring identical PPFD and UV-A1 irradiance during plant growth.

**Table 1.** Experimental lighting setup.

| Treatment | PPFD ($\mu mol \cdot m^{-2} \cdot s^{-1}$) | FR ($\mu mol \cdot m^{-2} \cdot s^{-1}$) | UV-A1 ($\mu mol \cdot m^{-2} \cdot s^{-1}$) | Daily UV-A1 dose ($KJ \cdot m^{-2} \cdot s^{-1}$) | Total PFD ($\mu mol \cdot m^{-2} \cdot s^{-1}$) | Radiation energy ($W \cdot m^{-2}$) |
|---|---|---|---|---|---|---|
| LLU0 | 150 | 8 | 0 | 0 | 158 | 0.31 |
| LLU20 | 150 | 8 | 20 | 7 | 178 | 0.38 |
| LLU100 | 150 | 8 | 100 | 35 | 258 | 0.64 |
| HLU0 | 550 | 30 | 0 | 0 | 580 | 1.16 |
| HLU20 | 550 | 30 | 20 | 7 | 600 | 1.22 |
| HLU100 | 550 | 30 | 100 | 35 | 680 | 1.48 |

**Note:** PPFD, photosynthetic photon flux density (400-700 nm); FR, far-red radiation (700-800 nm); UV-A1, long-wavelength UV-A radiation (350-400 nm); daily UV-A1 dose was weighed by using a biologic spectral weighing function according to Flint and Caldwell (2003); total PFD, total photon flux density.

Plants were treated for 13 days, at a photoperiod was 16 h, day/night temperatures were ~22/22±2 °C in the low PPFD growth units, ~25± 2/22±1 °C in the high PPFD growth units, relative humidity was 65-70%, $CO_2$ partial pressure was ~410 μmol $mol^{-1}$. Air temperatures in all experimental units were regularly and diligently checked by the experimenter; no difference in environmental conditions among UV-A1 treatments under the same PPFD was observed. Plants were regularly watered by hand with a modified Hoagland nutrient solution (tomato and cucumber: pH = 5.8, EC = 1.8 dS $m^{-1}$; lettuce and arabidopsis: pH = 5.8, EC = 1.6 dS $m^{-1}$). Per genotype and light treatment, plants were grown for three rounds, which were considered to be three replicates.

### *UV-A1 dose response experiment*

This experiment was used to fine-map responses to a larger number of UV-A1 doses within the 0-100 µmol $m^{-2}$ $s^{-1}$ range, in a selected genotype. Lettuce cv. Tiberius was used in this experiment, as in the *genotype screening experiment* it was the most sensitive genotype among the horticultural species (i.e., excluding arabidopsis). Plants were grown under six UV-A1 irradiances, i.e. 0, 10, 30, 50, 70 and 100 µmol $m^{-2}$ $s^{-1}$. PPFD was maintained at 150 µmol $m^{-2}$ $s^{-1}$. Ten plants were grown per treatment, and this was repeated in three separate rounds. All other conditions were identical to those of the *genotype screening experiment* at low PPFD.

## 2.3 Measurements



Measurements were conducted on five plants per round of cultivation. In lettuce and arabidopsis, five plants were randomly selected from ten plants to conduct all destructive measurements, while another five plants were used for all other measurements; in tomato and cucumber, five plants were randomly selected from six plants, and all measurements were performed on these five plants.

#### *2.3.1 Plant growth and morphological traits*

Analysis of plant growth and morphological traits was carried out 13 days after the start of treatments. Fresh and dry weights of leaves, petioles and stems were destructively determined. Plant organs were dried for 48 h at 80 °C in a ventilated oven (DHG-9070A, Shanghai Jinghong, Shanghai, China). Stem length was measured using a ruler, and was defined as the distance from the intersection of the shoot and root to the shoot apical meristem. Inflorescence length in arabidopsis was defined as the distance from the intersection of shoot and root to the tip of the inflorescence. Leaf area was measured using a leaf area meter (LI-3100C, Li-Cor Biosciences, Lincoln, Nebraska, USA). Specific leaf area (SLA; $cm^2$ $g^{-1}$) was calculated by dividing leaf area by leaf dry weight. Dry mass partitioning to each organ was calculated by dividing dry weight of each organ to total shoot dry weight. Dry mass content was calculated by dividing shoot dry weight by shoot fresh weight.

### *2.3.2 Leaf optical properties*

Light reflectance (Rf) and transmittance (Tr) of the adaxial side of the leaf in the PAR range (400-700 nm) were measured on the uppermost fully expanded leaves with a spectrometer (Ocean optics USB2000+, Dunedin, USA), in combination with two integrating spheres (FOIS-1, ISP-REF, Ocean Optics). Leaf light absorptance (Ab) was calculated as Ab=1−(Rf+Tr).

### *2.3.3. Maximum quantum yield of photosystem II ($F_v/F_m$)*

To assess maximum quantum yield of photosystem II ($F_v/F_m$), maximum ($F_m$) and minimum ($F_o$) chlorophyll *a* fluorescence of uppermost fully expanded leaves of dark-adapted plants ($\geqslant$ 20 min of dark adaptation) were measured, using a chlorophyll *a* fluorescence imager (IMAG-MAXI; Heinz Walz, Effeltrich, Germany). The measuring beam irradiance was 1 μmol $m^{-2}$ $s^{-1}$, and maximum flash irradiance was 8,000 μmol $m^{-2}$ $s^{-1}$. $F_v/F_m$ was calculated as $(F_m-F_o)/ F_m$ (Baker, 2008).

### *2.3.4. Leaf biochemical compounds*

In lettuce and cucumber, samples were taken from the youngest fully expanded leaves, in tomato they were taken from the third and fourth leaf counting from the top, and in arabidopsis they were taken from all expanded leaves. All samples were collected on the 13$^{th}$ day of treatment during the sixth hour of the photoperiod. Whole leaves were immersed in liquid nitrogen and then stored at -80 °C until further analysis.

### *Chlorophylls and carotenoids*

Fresh samples (0.1 g) were ground in liquid nitrogen, using a high-throughput tissue grinder (SCIENTZ-48, Xinzhi, Ningbo, China), and then incubated in 10 mL 95% ethanol in the dark at 4 °C, for 24h. After centrifugation for 5 min at 4 °C, the absorbance of the extract was measured at 470, 649, 664 and 750 nm, using a spectrophotometer (UV-1800, Shimadzu, Japan). The concentrations of chlorophyll *a*, chlorophyll *b*, their sum and ratio (on a mass basis),

as well as total carotenoid contents, were calculated using the equations derived by Lichtenthaler & Buschmann (2001).

***Anthocyanin***

Fresh samples (0.1 g) were ground as described above, incubated with 600 µL of extraction buffer (99% methanol and 1% HCl), and vortexed. The extracts were placed in an ultrasonic bath with ice water for 10 minutes and then incubated overnight at 4 °C in the dark. After extraction, 400 µL of water and 400 µL of chloroform were added. Absorbance (A) of extracts was measured at 530 and 657 nm, using a microplate reader (Infinite 200 PRO, TECAN, Switzerland), and anthocyanin content was expressed as: Anthocyanin = ($A_{530}$-0.33*$A_{657}$) / fresh weight (Liu et al., 2018a), where $A_{530}$ and $A_{657}$ are absorbance at 530 and 657 nm, respectively.



***UV-absorbing compounds***

Fresh samples (0.1 g) were ground as described above, and incubated with 5 mL of acidified methanol solution (70% methanol, 29% $H_2O$ and 1% HCl) at -20°C, for 48 h. Absorbance of extracts was scanned in the 240−400 nm range, with 2 nm resolution, using a microplate reader (Infinite 200 PRO), and the concentration of UV-absorbing compounds was expressed as absorbance (A) $cm^{-2}$. For estimation of extracted UV-absorbing compounds, mostly phenolic metabolites, absorbance at 365 nm was used (Barnes et al., 2016).

## 2.4 Statistics

Statistical analyses were performed in R (version 4.1.3., R Core Development Team, 2022). The Q-Q plot was used to test the distribution of data graphically, and the *bartlett.test* was used to test the homogeneity of variance of residuals. Linear mixed effects models were fitted using the *lme* function in the *nlme* package and with cultivation round as a block, from the comparison of fits that allow the error variance to depend on UV-A1. This was followed with a factorial analysis of variance (ANOVA) to assess the effects of the factors, i.e. UV-A1 irradiance, PPFD,

and their interaction. When the ANOVA indicated an interaction ($p < 0.05$), the response to UV-A1 was assessed within each PPFD. When the effect of UV-A1 irradiance was significant ($p < 0.05$), a post-hoc test was used to assess the significance of differences between pairs of UV-A1 treatments under each PPFD; this was done using the function *glht* in the *multcomp* package, using *Tukey* as the linear hypothesis. Tukey's HSD (honestly significant difference) was used to fit pairwise contrasts ($p$-values were adjusted for multiple comparisons) to assess the effect of UV-A1 treatments under each PPFD on the parameters. Additionally, within the UV-A1 dose response experiment, to estimate the linear relationship of UV-A1 irradiance and measured parameters, simple linear regressions were tested using the function *lm*. Each repetition was considered as a block. Data are presented as mean ± standard error (SE) of three blocks (n=3).

# 3. Results

## 3.1 Plant growth and morphological traits

Background irradiance (i.e., 150 vs. 550 μmol $m^{-2}$ $s^{-1}$ of white light) had strong effects on almost all growth traits in all species (Figs. 2, 3), except for total leaf area in tomato (Fig. 3F). In contrast, UV-A1 barely affected plant appearance (Fig. 2) or growth (Fig. 3) at either PPFD, except for some responses in arabidopsis and both lettuce cultivars. Arabidopsis and lettuce showed several responses: Leaf area of lettuce cv. Klee was increased by 11% at LLU20, compared to LLU0 (Fig. 3I). Leaf area and shoot dry weight of arabidopsis in LLU20 were decreased by 7% and 13%, respectively, compared to LLU0 (Fig. 3E, J). Effects of PPFD and UV-A1 irradiance did mostly not interact, except for leaf area in lettuce cv. Klee ($P_{UxI}$= 0.01; Fig. 3I), which was increased by UV-A1 (highest value at 20 μmol $m^{-2}$ $s^{-1}$ UV-A1) under LL, while under HL there was no detectable UV-A1 effect. In addition, UV-A1 remarkably reduced shoot dry weight and leaf area near-linearly in lettuce cv. Tiberius, which was grown under a larger number of intermediate UV-A1 irradiance at LL (red symbols in Fig. 3C, H). Cucumber showed the least sensitive response to UV-A1 (Fig. 3B).

Both UV-A1 and PPFD strongly affected inflorescence formation in arabidopsis, based on visual observation: under LLU0, closed flower buds were observed at the final harvest, and inflorescence tended to increase in length with higher UV-A1 under LL (Fig. 2C). Under HL, arabidopsis formed inflorescences even when no UV-A1 was applied, but inflorescence formation was hastened by UV-A1 (Fig. 2B). UV-A1 also affected leaf shape in arabidopsis, and leaf angle in tomato and lettuce cv. Tiberius: when arabidopsis was grown under LLU100, the leaf edges were more visibly rounded and leaves were much flatter, compared with LLU0. This phenomenon was not observed under HL, as the edges of leaf blades were strongly curved downwards in all cases (Figs. 2; S2). Further, petioles of tomato and lettuce cv. Tiberius tended to be more upright upon increases of UV-A1 irradiance under LL (Fig. S2). These UV-A1 effects were not observed under HL (Fig. S2).

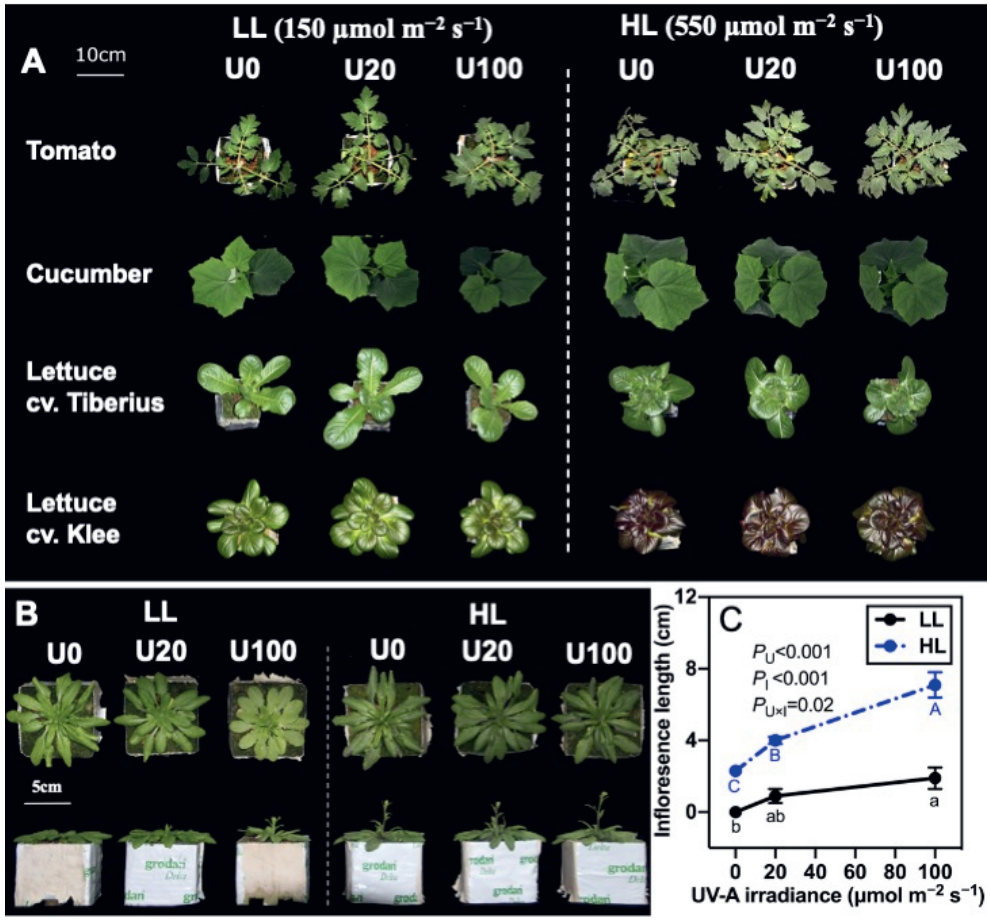


**Figure 2.** Plant morphology responses to UV-A1 radiation. Three UV-A1 irradiances were applied, i.e. 0, 20 and 100 µmol $m^{-2}$ $s^{-1}$ at low (LL; 150 µmol $m^{-2}$ $s^{-1}$) and high (HL; 550 µmol $m^{-2}$ $s^{-1}$) PPFD for 13 days. A and B show plant morphology of horticultural species and arabidopsis, respectively, under the various treatments; C: inflorescence length of arabidopsis. Different capital and lowercase letters (in C) indicate statistically significant differences among UV-A1 treatments under HL and LL, respectively ($p < 0.05$). The numbers (in C) provide *p*-values for the main effects of UV-A1 ($P_U$) and PPFD ($P_I$), and the interaction between them ($P_{U×I}$). Error bars show ± SE (n = 3, where each replicate represents the mean of five biological replicates).

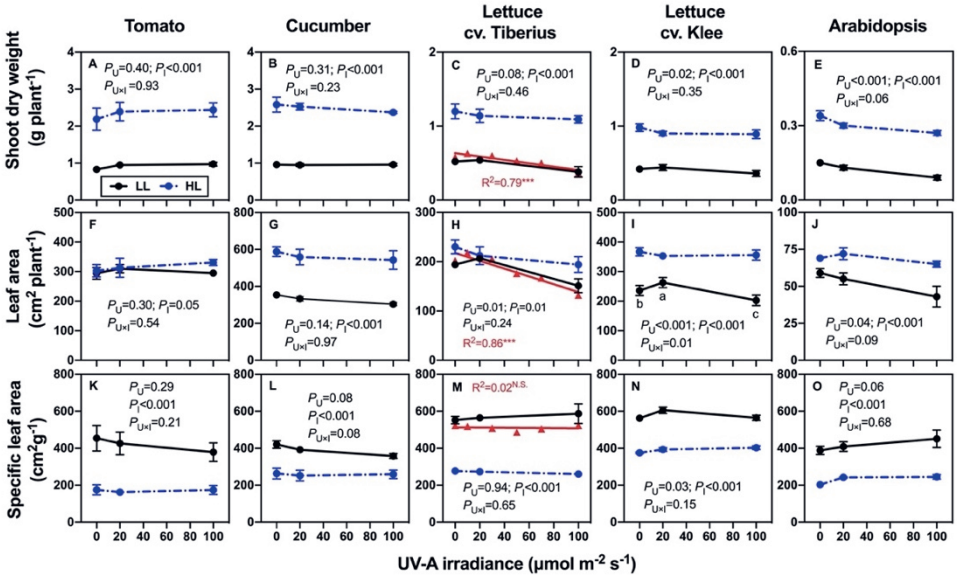


**Figure 3.** Effects of UV-A1 radiation on growth of tomato, cucumber, lettuce (cvs. Tiberius and Klee) and arabidopsis. Plants were grown under three UV-A1 irradiances (i.e. 0, 20 and 100 µmol $m^{-2}$ $s^{-1}$) paired with low (LL, 150 µmol $m^{-2}$ $s^{-1}$; black solid line) and high (HL, 550 µmol $m^{-2}$ $s^{-1}$; blue dotted line) PPFD for 13 days. Additionally, lettuce cv. Tiberius (C, H, M) was grown under six UV-A1 irradiances (i.e. 0, 10, 30, 50, 70 and 100 µmol $m^{-2}$ $s^{-1}$) at LL (red solid line). A-E: shoot dry weight; F-J: leaf area; K-O: specific leaf area. The numbers in each panel provide *p*-values for the main effects of UV-A1 ($P_U$) and PPFD ($P_I$), and the interaction between them ($P_{U\times I}$). The red line and numbers in panels C, H, and M represent the best-fit model as determined by simple linear regression and asterisks indicate the significance of the linear relationship (∗*P*<0.05, ∗∗*P*<0.01, ∗∗∗*P*<0.001). Different lowercase letters (in I) indicate statistically significant differences among UV-A1 treatments under LL ($p < 0.05$). Error bars show ± SE (n = 3, where each replicate represents the mean of five biological replicates).

## 3.2 Leaf biochemical compounds

In all species, HL promoted the accumulation of almost all leaf metabolites per unit leaf area (Fig. 4). UV-A1 had comparably smaller effects on chlorophyll and carotenoid concentrations, except for a strong increase under LLU20 and a strong decrease under LLU100 in arabidopsis, with visible differences in leaf greenness (Figs. 3A; 4E, J). Concentrations of anthocyanin and UV-absorbing compounds dropped with UV-A1 at HL in most species, and did so especially strongly in arabidopsis and lettuce cv. Klee (Fig. 4P-T). However, at LL, concentrations of anthocyanin and UV-absorbing compounds hardly responded to UV-A1 in tomato, cucumber and lettuce cv. Tiberius (Fig. 4U-Y).

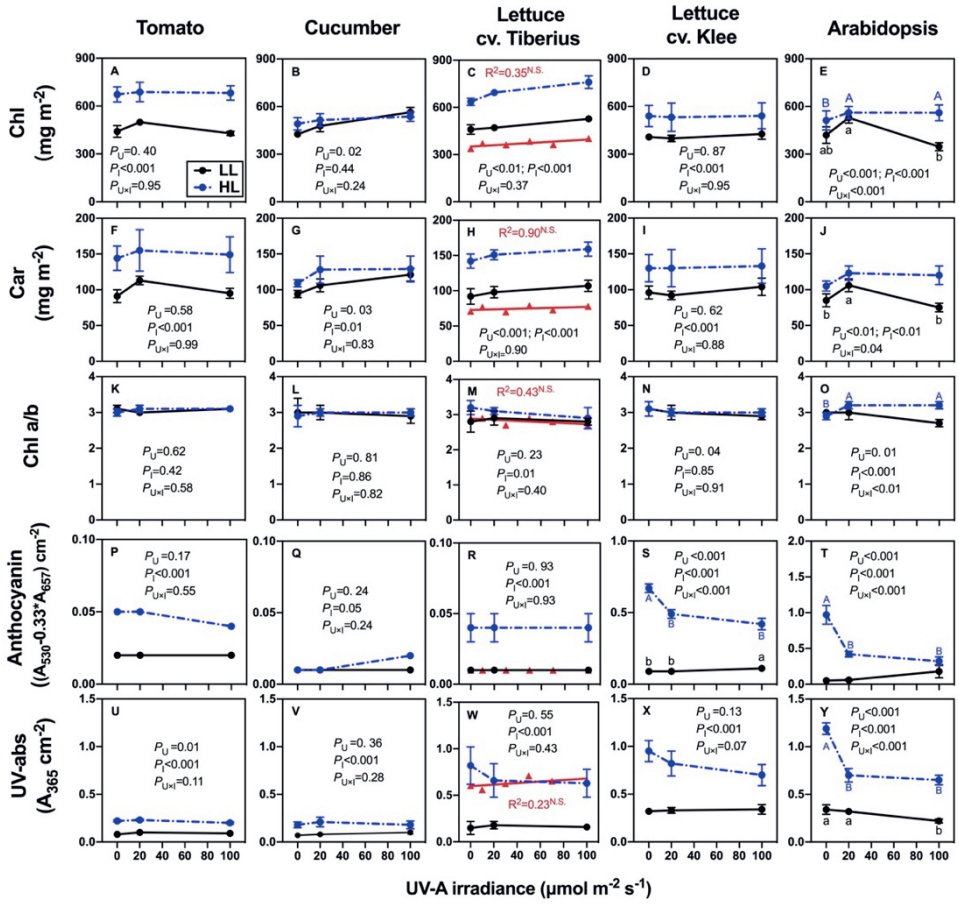


**Figure 4.** Effects of UV-A1 radiation on leaf biochemical compounds of tomato, cucumber, lettuce (cvs. Tiberius and Klee) and arabidopsis. Three UV-A1 irradiances were applied, i.e, 0, 20 and 100 µmol $m^{-2}$ $s^{-1}$ at low (LL; 150 µmol $m^{-2}$ $s^{-1}$; black solid line) and high (HL; 550 µmol $m^{-2}$ $s^{-1}$; blue dotted line) PPFD for 13 days. Additionally, lettuce cv. Tiberius (C, H, M, R, W) was grown under six UV-A1 irradiances, i.e. 0, 10, 30, 50, 70 and 100 µmol $m^{-2}$ $s^{-1}$ (red solid line) at LL. A-E: chlorophyll concentration, F-J: carotenoids, K-O: Chla/b, P-T: anthocyanin, U-Y: UV-absorbing compounds. Different capital (in E, S, T and Y) and lowercase letters (in E and S) indicate statistically significant differences among UV-A1 treatments under HL and LL, respectively ($p < 0.05$). The numbers in each panel provide *p*-values for the main effects of UV-A1 ($P_U$) and PPFD ($P_I$), and the interaction between them ($P_{U\times I}$). The red line and numbers in the panels C, H, M, R and W represent the best-fit model as determined by simple linear regression and asterisks indicate the significance of the linear relationship (∗$P$<0.05, ∗∗$P$<0.01, ∗∗∗$P$<0.001). Error bars show mean ± SE (n = 3, where each replicate represents the mean of five biological replicates).

### 3.3 $F_v/F_m$ and leaf light absorptance

UV-A1 reduced $F_v/F_m$ near-linearly under LL, but in most cases there was no reduction under HL (Figs. 5A-E). In cucumber, UV-A1 had a similar, but small, reducing effect on $F_v/F_m$ at both PPFD, while an interaction between PPFD and UVA-1 was observed in lettuce cv. Klee and arabidopsis. Unlike $F_v/F_m$, leaf light absorption by leaves was weakly affected by UV-A1, but a high PPFD tended to increase absorptance, albeit with genotype-specific effects: Leaves of lettuce cv. Klee were colored purple when grown under HL (Fig. 2A), resulting in high overall leaf light absorptance (Fig. 5I), which was especially increased in the green and red range of the visible spectrum (Fig. S3D). In arabidopsis, leaf light absorptance increased under HL (Fig. 5J).



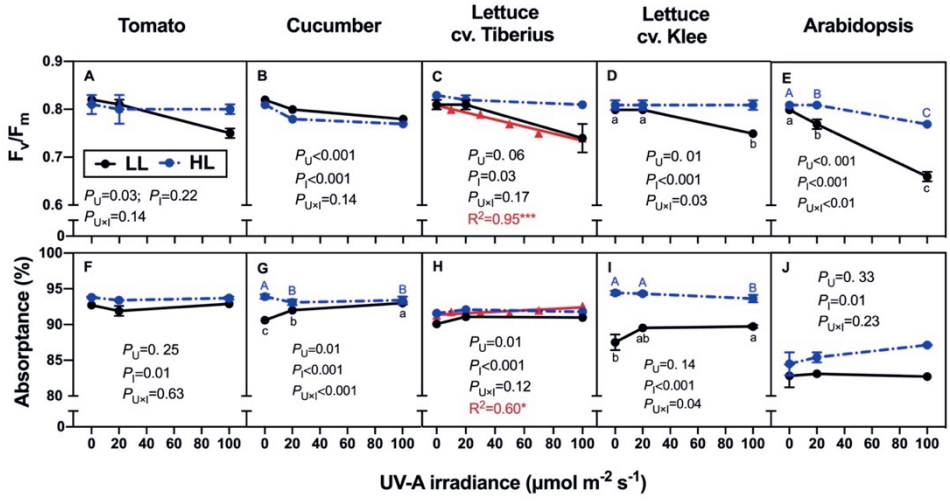


**Figure 5.** Effects of UV-A1 radiation on maximum quantum yield of photosystem II ($F_v/F_m$) and leaf light absorptance in the PAR range (400-700 nm) of tomato, cucumber, lettuce (cvs. Tiberius and Klee) and arabidopsis. Three UV-A1 irradiances were applied, i.e, 0, 20 and 100 µmol $m^{-2}$ $s^{-1}$ at low (LL; 150 µmol $m^{-2}$ $s^{-1}$; black solid line) and high (HL; 550 µmol $m^{-2}$ $s^{-1}$; blue dotted line) PPFD for 13 days. Additionally, lettuce cv. Tiberius (C, H) was grown under six UV-A1 irradiances, i.e. 0, 10, 30, 50, 70 and 100 µmol $m^{-2}$ $s^{-1}$ (red solid line) at LL. A-E: $F_v/F_m$, F-G: leaf light absorptance. Different capital (in E, G and I) and lowercase letters (in D, E, G and I) indicate statistically significant differences among UV-A1 treatments under HL and LL, respectively ($p < 0.05$). The numbers in each panel provide *p*-values for the main effects of UV-A1 ($P_U$) and PPFD ($P_I$), and the interaction between them ($P_{U×I}$). The red line and numbers in the panels C and H represent the best-fit model as determined by simple linear regression and asterisks indicate the significance of the linear relationship (∗$P$<0.05, ∗∗$P$<0.01, ∗∗∗$P$<0.001). Error bars show ± SE (n = 2, which each replicate represents the mean of five biological replicates).

# 4. Discussion

Several horticultural and a model species (*Arabidopsis thaliana*) were grown under a range of UV-A1 irradiances, at two background PPFD, and their growth and leaf physiological traits were explored. To our knowledge, this is the first controlled-environment study of its kind: thanks to recent advances in LED technology, we were able to use narrowband UV-A1 LEDs peaking at 365 nm at irradiances up to 100 µmol $m^{-2}$ $s^{-1}$, which could not be realized previously. We found that plant growth and leaf biochemical compound concentrations in response to UV-A1 radiation are genotype-specific, and UV-A1 radiation-induced leaf photoinhibition depends on the background irradiance. When designing this experiment, we chose to add UV-A1 radiation to two background PPFD, resulting in different total PFD among the treatments (Table 1). Although this approach is not perfect, the alternative – namely keeping PFD identical between treatments by lowering PPFD with increments in UV-A1 radiation – seemed like an even worse alternative, as this would have resulted in strongly different rates of photosynthesis among treatments. Nevertheless, possible unintended consequences of our experimental design include increased plant temperature as indicated by the higher radiation energy under high PFD condition, and potentially slightly higher photosynthesis rates under increased UV-A1 radiation which drives photosynthesis to some extent (McCree, 1971; Turnbull et al., 2013).

## 4.1 UV-A1 radiation: stimulus or stressor?

Whether UV-A1 radiation functions as stimulus or stressor for plant growth and development has been the subject of ongoing debate (Rai et al., 2021; Verdaguer et al., 2017). UV-A1 is considered to be a regulator, as it shares photoreceptors with blue light, i.e. phototropins and cryptochromes, which determine many aspects of plant processes (Lin, 2000; Takahashi & Murata, 2008). UV-A1 can also be considered a stressor, owing to its short wavelength and thus high energy per photon, which can effectively induce photoinhibition or even photodamage to photosystem II (Takahashi et al., 2010).

As a stimulus for plant growth and development, UV-A1 radiation functions similarly to blue light in eliminating the so-called "red light syndrome": when plants are grown under monochromatic red light, they form an abnormal plant morphology as well as photosynthetic machinery, and the addition of small quantities of either blue or UV-A1 radiation can revert this syndrome (Zhang et al., 2020). Earlier studies reported that under indoor cultivation, adding ~20 μmol $m^{-2}$ $s^{-1}$ UV-A1 radiation stimulated biomass accumulation by ~20% both in tomato and lettuce (Chen et al., 2019; Zhang et al., 2020). Similar findings were also reported by others in tomato, lettuce and kale (He et al., 2021; Kang et al., 2018; Lee et al., 2019). Our recent study again illustrated that UV-A1 treated plants had a greater leaf area than blue light, thereby promoting plant growth (Zhang et al., 2023). Such a strong positive regulation of plant growth was not observed in this study (Fig. 2), which is logical given that the white background light contained ample amounts of blue light (20%; Table S1).



The role of UV-A1 as a stressor that exerts oxidative pressure (Neugart & Schreiner, 2018) was obvious in our data, given the photoinhibition (i.e. decreased $F_v/F_m$, Fig. 5) that occurred when UV-A1 was paired with LL. Chen at al. (2019) reported similar findings, where exposure to 30 μmol $m^{-2}$ $s^{-1}$ UV-A1 radiation induced photoinhibition in lettuce. However, the photoinhibition that occurred in most genotypes did not seem to have strong effects on growth (Fig. 2). Interestingly, our data further suggest that UV-A1-induced photoinhibition was counteracted under HL in all genotypes, except in cucumber (Fig. 5A-E). This may be attributed to the high light build-up of increased photosynthetic and photoprotective capacity (Hoffmann et al., 2015; Kang et al., 2021). Furthermore, the higher concentration of UV-absorbing compounds under HL may have prevented some of the UV-A1 penetrating to the mesophyll, avoiding further damage (Fig. 4U-Y; Bidel et al., 2007; Caldwell et al., 1983); and higher concentrations of carotenoids under HL may have also contributed to mitigating photoinhibition through non-photochemical quenching (Horton et al., 1996; Shih et al., 2000).

In arabidopsis, the appearance of an inflorescence under LL and the longer inflorescence length under HL when paired with UV-A1 could also be considered as an indicator of plant stress (Figs. 2C, 5E). Early flowering in arabidopsis can maintain high fitness under UV-A1 radiation, by shifting much of the carbon fixation towards the inflorescence (Gnan et al., 2017; Fig. 2C).

Also, a possible higher plant temperature under UV-A1 may have promoted developmental rates and rate of flowering in arabidopsis (Fig. 2C; Kazan & Lyons, 2016). The reduction in growth observed in arabidopsis (Fig. 2) is likely attributed to UV-A1 promoting flowering development, which in turn constrains plant growth, rather than a direct consequence of UV-A1 exposure (Blümel et al., 2015; Koelewijn, 2004). On the other hand, previous studies have reported that cryptochrome 2 absorbs UV-A1 radiation and participates in regulating the flowering-time gene CONSTANS, thereby accelerating flowering (Guo et al., 1998; Suárez-López et al., 2001). In this context, it is difficult to conclude whether UV-A1 directly stimulated flowering via cryptochrome 2, or whether the stress as well as possible higher plant temperature exerted by UV-A1 indirectly led to early flowering.

Based on our observations of plant morphology and growth (Figs. 2, 3), tomato, cucumber and lettuce cv. Klee could be considered as UV-A1 tolerant plants, whereas arabidopsis and lettuce cv. Tiberius are UV-A1 sensitive plants as they clearly showed reductions in growth due to UV-A1 exposure. Plants possess several mechanisms to protect themselves from UV-induced damage, including hairs and waxes on the leaf surface (Holmes & Keiller, 2002), photoprotective pigments, non-photosynthetic quenching (Bassi and Dall'Osto, 2021), chloroplast movement (Haupt & Scheuerlein, 1990), et al. In this context, UV sensitivity is likely affected by a range of underlying traits, and our data do not allow to conclude a clear answer as to which traits separate sensitive from tolerant genotypes.

## 4.2 Does UV-A1 radiation up or down-regulate UV-screening compound accumulation?

Effects of UV-A radiation on the buildup of leaf secondary metabolites are inconclusive and controversial (Verdaguer et al., 2017). Flavonoids, a major group of secondary metabolites, are considered to be UV-screening compounds. In our study, UV-A1 radiation hardly affected the accumulation of UV-screening compounds under LL, except for lettuce cv. Klee and arabidopsis, which showed only slight increments at UV-A1 irradiance of 100 µmol $m^{-2}$ $s^{-1}$ (Fig. 4P-Y). Our recent study reported that UV-A1 radiation caused weaker increases in transcript abundance of genes in the flavonoid biosynthetic pathway than blue light (Zhang et al., 2023).

In this context, the substantial fraction of blue light in the background spectra (20%) was probably sufficient to fully excite the pathway of cryptochrome-mediated UV-screening compound biosynthesis (Fig. 4P-Y; Table S1; Brelsford et al. 2019). Consequently, UV-A1 radiation did not have any effects on the accumulation of UV-screening compounds. Under HL, interestingly, UV-A1 radiation significantly reduced the concentrations of anthocyanin and UV-absorbing compounds in lettuce cv. Klee and arabidopsis, but not in other genotypes (Fig. 4P-T), which means the accumulation of UV-screening compounds under UV-A1 radiation depends on both plant genotype and background irradiance. The production of anthocyanin is regulated by light and corresponding photoreceptors (Liu et al., 2018b). Moreover, the chemical structure of the pigments can also be altered by high light or UV radiation, thus leading to pigment degradation (Woodward et al., 2009). Our results challenge the view that UV radiation can promote the accumulation of secondary metabolites (Lee et al., 2014; Neugart & Schreiner, 2018; Verdaguer et al., 2017). Altogether, the mechanisms underlying the interactive effects between UV-A1 and growth irradiance on the concentration of UV-screening compounds seem rather complex, and further exploration using photoreceptor mutants as well as pigment chemical structure analysis might be needed.



## 4.3 Responses of arabidopsis to the environment are not necessarily representative of other species

As a model species, arabidopsis has been used widely to explore physiological and developmental processes in plants, including photoreceptor functions (Inoue et al., 2008; Jenkins, 2014; Takemiya et al., 2005). In this study, surprisingly, UV-A1 radiation had relatively minor effects on growth in most horticultural species, but strongly reduced biomass by up to ~40% in arabidopsis (Fig. 3E). Also, UV-A1 had much stronger effects on photoinhibition (reduced $F_v/F_m$) in arabidopsis than in the other tested species, and induced or accelerated floral initiation in both low and high PPFD (Figs. 2C, 5E). Additionally, arabidopsis showed notable changes in leaf shape when grown under UV-A1 radiation (Fig. 2B). Hence, many responses in arabidopsis to UV-A1 deviated from those found in the other species. Similarly, in other studies the rate and degree of chloroplast movement were much stronger in arabidopsis compared to those of many other species (Königer & Bollinger, 2012), as was the

extent of blue light-induced stomatal opening (Vialet-Chabrand et al., 2021). Curiously, these examples all seem to show a larger sensitivity in arabidopsis to photoreceptor-mediated processes that respond to either blue light or UV-A1. In this context, extrapolation of research results from arabidopsis to horticultural species should be treated with caution.

# 5. Conclusions

Our study describes how strongly plant species differ in their response to UV-A1 radiation, and how their responses to UV-A1 radiation depend on background irradiance. We show that i) the addition of UV-A1 radiation to white light reduces growth in *Arabidopsis*, but barely affects growth in three horticultural species, ii) the addition of UV-A1 radiation to white light induced photoinhibition under low light but not under high light in all tested species, and iii) UV-A1 radiation and background irradiance interactively affects UV-screening compound concentrations in *Arabidopsis* and lettuce cv. Klee, but not in the other genotypes. We conclude that plant responses to UV-A1 radiation are genotype and background irradiance-dependent under indoor cultivation with full spectrum white light. This study highlights the importance of interactive effects of other light spectra on UV-A1 radiation-mediated plant processes, which is highly relevant when designing UV-A plant photobiology studies, as the spectrum of background light plays an important role.

# References


Agati, G., & Tattini, M. (2010). Multiple functional roles of flavonoids in photoprotection. *New Phytologist*, *186*(4), 786–793. https://doi.org/10.1111/j.1469-8137.2010.03269.x

Albert, A., & Mcleod, A. R. (2012). Beyond the Visible : A handbook of best practice in plant UV photobiology. In *Beyond the Visible : A handbook of best practice in plant UV photobiology* (Issue January). https://doi.org/10.31885/9789521083631

Aphalo, P. J., & Sadras, V. O. (2021). Explaining pre-emptive acclimation by linking information to plant phenotype. *Journal of Experimental Botany*. https://doi.org/10.1093/jxb/erab537

Baker, N. R. (2008). Chlorophyll fluorescence: A probe of photosynthesis in vivo. *Annual Review of Plant Biology*, *59*, 89–113. https://doi.org/10.1146/annurev.arplant.59.032607.092759

Barnes, P. W., Tobler, M. A., Keefover-Ring, K., Flint, S. D., Barkley, A. E., Ryel, R. J., & Lindroth, R. L. (2016). Rapid modulation of ultraviolet shielding in plants is influenced by solar ultraviolet radiation and linked to alterations in flavonoids. *Plant Cell Environ*, *39*(1), 222–230. https://doi.org/10.1111/pce.12609

Bassi, R., & Dall'Osto, L. (2021). Dissipation of Light Energy Absorbed in Excess: The Molecular Mechanisms. *Annual Review of Plant Biology, 72*, 47–76. https://doi.org/10.1146/annurev-arplant-071720-015522

Bernal, M., Verdaguer, D., Badosa, J., Abadía, A., Llusià, J., Peñuelas, J., Núñez-Olivera, E., & Llorens, L. (2015). Effects of enhanced UV radiation and water availability on performance, biomass production and photoprotective mechanisms of Laurus nobilis seedlings. *Environmental and Experimental Botany*. https://doi.org/10.1016/j.envexpbot.2014.06.016

Bidel, L. P. R., Meyer, S., Goulas, Y., Cadot, Y., & Cerovic, Z. G. (2007). Responses of epidermal phenolic compounds to light acclimation: In vivo qualitative and quantitative assessment using chlorophyll fluorescence excitation spectra in leaves of three woody species. *Journal of Photochemistry and Photobiology B: Biology*, *88*(2–3), 163–179. https://doi.org/10.1016/j.jphotobiol.2007.06.002

Biswas, D. K., & Jansen, M. A. K. (2012). Natural variation in UV-B protection amongst arabidopsis thaliana accessions. *Emirates Journal of Food and Agriculture*. https://doi.org/10.9755/ejfa.v24i6.14681

Blümel, M., Dally, N., & Jung, C. (2015). Flowering time regulation in crops-what did we learn from Arabidopsis? *Current Opinion in Biotechnology*, *32*, 121–129. https://doi.org/10.1016/j.copbio.2014.11.023

Bruce, T. J. A., Matthes, M. C., Napier, J. A., & Pickett, J. A. (2007). Stressful "memories" of plants: Evidence and possible mechanisms. *Plant Science*, *173*(6), 603–608. https://doi.org/10.1016/j.plantsci.2007.09.002

Caldwell, M. M., Flint, S. D., & Searles, P. S. (1994). Spectral balance and UV-B sensitivity of soybean: a field experiment. *Plant, Cell & Environment*. https://doi.org/10.1111/j.1365-3040.1994.tb00292.x

Caldwell, M. M., Robberecht, R., & Flint, S. D. (1983). Internal filters: Prospects for UV-acclimation in higher plants. *Physiologia Plantarum*, *58*(3), 445–450. https://doi.org/10.1111/j.1399-3054.1983.tb04206.x

Chen, Y., Li, T., Yang, Q., Zhang, Y., Zou, J., Bian, Z., & Wen, X. (2019). UVA Radiation Is Beneficial for Yield and Quality of Indoor Cultivated Lettuce. *Frontiers in Plant Science*, *10*. https://doi.org/10.3389/fpls.2019.01563

Christie, J. M. (2007). Phototropin blue-light receptors. *Annu Rev Plant Biol*, *58*, 21–45. https://doi.org/10.1146/annurev.arplant.58.032806.103951

Flint, S. D., & Caldwell, M. M. (2003). Field testing of UV biological spectral weighting functions for higher plants. *Physiologia Plantarum, 117(1)*, 145–153. https://doi.org/10.1034/j.1399-3054.2003.1170118.x

Gnan, S., Marsh, T., & Kover, P. X. (2017). Inflorescence photosynthetic contribution to fitness releases Arabidopsis thaliana plants from trade-off constraints on early flowering. *PloS ONE*, *12*(10), 1–13. https://doi.org/10.1371/journal.pone.0185835

Guo, H., Yang, H., Mockler, T. C., & Lin, C. (1998). Regulation of flowering time by Arabidopsis photoreceptors. *Science*, *279*(5355), 1360–1363. https://doi.org/10.1126/science.279.5355.1360

Hakala-Yatkin, M., Mantysaari, M., Mattila, H., & Tyystjarvi, E. (2010). Contributions of visible and ultraviolet parts of sunlight to photoinhibition. *Plant Cell Physiol*, *51*(10), 1745–1753. https://doi.org/10.1093/pcp/pcq133

Haupt, W., & Scheuerlein, R. (1990). Chloroplast movement. *Plant, Cell & Environment, 13*(7), 595–614. https://doi.org/10.1111/j.1365-3040.1990.tb01078.x

He, R., Zhang, Y., Song, S., Su, W., Hao, Y., & Liu, H. (2021). UV-A and FR irradiation improves growth and nutritional properties of lettuce grown in an artificial light plant factory. *Food Chemistry*, 345, 128727. https://doi.org/10.1016/j.foodchem.2020.128727

Hoffmann, A. M., Noga, G., & Hunsche, M. (2015). High blue light improves acclimation and photosynthetic recovery of pepper plants exposed to UV stress. *Environmental and Experimental Botany*, *109*, 254–263. https://doi.org/10.1016/j.envexpbot.2014.06.017

Holmes, M. G., & Keiller, D. R. (2002). Effects of pubescence and waxes on the reflectance of leaves in the ultraviolet and photosynthetic wavebands: A comparison of a range of species. *Plant, Cell and Environment, 25*(1), 85–93. https://doi.org/10.1046/j.1365-3040.2002.00779.x

Hooks, T., Masabni, J., Sun, L., & Niu, G. (2021). Effect of pre-harvest supplemental uv-a/blue and red/blue led lighting on lettuce growth and nutritional quality. *Horticulturae*, *7*(4), 1–14. https://doi.org/10.3390/horticulturae7040080

Horton, P., Ruban, A. V., & Walters, R. G. (1996). Regulation of light harvesting in green plants. *Annual Review of Plant Physiology and Plant Molecular Biology*, *47*(1), 655–684. https://doi.org/10.1146/annurev.arplant.47.1.655

Inoue, S. I., Kinoshita, T., Takemiya, A., Doi, M., & Shimazaki, K. I. (2008). Leaf positioning of Arabidopsis in response to blue light. *Molecular Plant*, *1*(1), 15–26. https://doi.org/10.1093/mp/ssm001

Jenkins, G. I. (2014). The UV-B photoreceptor UVR8: from structure to physiology. *Plant Cell*, *26*(1), 21–37. https://doi.org/10.1105/tpc.113.119446

Kaiser, E., Morales, A., & Harbinson, J. (2018). Fluctuating light takes crop photosynthesis on a rollercoaster ride. *Plant Physiology, 176(2)*, 977–989. https://doi.org/10.1104/pp.17.01250

Kang, C., Zhang, Y., Cheng, R., Kaiser, E., Yang, Q., & Li, T. (2021). Acclimating Cucumber Plants to Blue Supplemental Light Promotes Growth in Full Sunlight. *Frontiers in Plant Science*, *12*(November), 1–14. https://doi.org/10.3389/fpls.2021.782465

Kang, S., Zhang, Y., Zhang, Y., Zou, J., Yang, Q., & Li, T. (2018). Ultraviolet-a radiation stimulates growth of indoor cultivated tomato (Solanum lycopersicum) seedlings. *HortScience*. https://doi.org/10.21273/HORTSCI13347-18

Kataria, S., Guruprasad, K. N., Ahuja, S., & Singh, B. (2013). Enhancement of growth, photosynthetic performance and yield by exclusion of ambient UV components in $C_3$ and $C_4$ plants. *Journal of Photochemistry and Photobiology B: Biology*. https://doi.org/10.1016/j.jphotobiol.2013.08.013

Kazan, K., & Lyons, R. (2016). The link between flowering time and stress tolerance. *Journal of Experimental Botany, 67(1)*, 47–60. https://doi.org/10.1093/jxb/erv441

Kelly, N., & Runkle, E. S. (2023). End-of-production Ultraviolet A and Blue Light Similarly Increase Lettuce Coloration and Phytochemical Concentrations. *HortScience*, *58*(5), 525–531. https://doi.org/10.21273/HORTSCI17108-23

Kerr, J. B., & Fioletov, V. E. (2008). Surface ultraviolet radiation. In *Atmosphere - Ocean*. https://doi.org/10.3137/ao.460108

Koelewijn, H. P. (2004). Rapid change in relative growth rate between the vegetative and reproductive stage of the life cycle in Plantago coronopus. *New Phytologist*, *163*(1), 67–76. https://doi.org/10.1111/j.1469-

8137.2004.01078.x

Königer, M., & Bollinger, N. (2012). Chloroplast movement behavior varies widely among species and does not correlate with high light stress tolerance. *Planta*, *236*(2), 411–426. https://doi.org/10.1007/s00425-012-1619-9

Krizek, D. T., Britz, S. J., & Mirecki, R. M. (1998). Inhibitory effects of ambient levels of solar UV-A and UV-B radiation on growth of cv. New Red Fire lettuce. *Physiologia Plantarum*, *103*(1), 1–7. https://doi.org/10.1034/j.1399-3054.1998.1030101.x

Krizek, D. T., Mirecki, R. M., & Britz, S. J. (1997). Inhibitory effects of ambient levels of solar UV-A and UV-B radiation on growth of cucumber. *Physiologia Plantarum*, *100*(4), 886–893. https://doi.org/10.1034/j.1399-3054.1997.1000414.x

Lee, J. H., Oh, M. M., & Son, K. H. (2019). Short-Term Ultraviolet (UV)-A Light-Emitting Diode (LED) Radiation Improves Biomass and Bioactive Compounds of Kale. *Frontiers in Plant Science*. https://doi.org/10.3389/fpls.2019.01042

Lee, M. J., Son, J. E., & Oh, M. M. (2014). Growth and phenolic compounds of Lactuca sativa L. grown in a closed-type plant production system with UV-A, -B, or -C lamp. *J Sci Food Agric, 94*(2), 197–204. https://doi.org/10.1002/jsfa.6227

Lichtenthaler, H. K., & Buschmann, C. (2001). Chlorophylls and Carotenoids: Measurement and Characterization by UV-VIS Spectroscopy. *Current Protocols in Food Analytical Chemistry*, *1*(1), F4.3.1-F4.3.8. https://doi.org/10.1002/0471142913.faf0403s01

Lin, C. (2000). Plant blue-light receptors. In *Trends in Plant Science*. https://doi.org/10.1016/S1360-1385(00)01687-3

Liu, C. C., Chi, C., Jin, L. J., Zhu, J., Yu, J. Q., & Zhou, Y. H. (2018a). The bZip transcription factor HY5 mediates CRY1a-induced anthocyanin biosynthesis in tomato. *Plant Cell and Environment*, *41*(8), 1762–1775. https://doi.org/10.1111/pce.13171

Liu, Y., Tikunov, Y., Schouten, R. E., Marcelis, L. F. M., Visser, R. G. F., & Bovy, A. (2018b). Anthocyanin biosynthesis and degradation mechanisms in Solanaceous vegetables: A review. *Frontiers in Chemistry*, *6*(MAR). https://doi.org/10.3389/fchem.2018.00052

McCree, K. J. (1971). The action spectrum, absorptance and quantum yield of photosynthesis in crop plants. *Agricultural Meteorology*. https://doi.org/10.1016/0002-1571(71)90022-7

Morales, L. O., Tegelberg, R., Brosche, M., Keinanen, M., Lindfors, A., & Aphalo, P. J. (2010). Effects of solar UV-A and UV-B radiation on gene expression and phenolic accumulation in Betula pendula leaves. *Tree Physiol*, *30*(7), 923–934. https://doi.org/10.1093/treephys/tpq051

Neugart, S., & Schreiner, M. (2018). UVB and UVA as eustressors in horticultural and agricultural crops. *Scientia Horticulturae*. https://doi.org/10.1016/j.scienta.2018.02.021

Neugart, S., Tobler, M. A., & Barnes, P. W. (2019). Different irradiances of UV and PAR in the same ratios alter the flavonoid profiles of: Arabidopsis thaliana wild types and UV-signalling pathway mutants. *Photochemical and Photobiological Sciences*. https://doi.org/10.1039/c8pp00496j

Ng, C. K. Y. (2019). Plant Cell Biology: UVA on Guard. *Current Biology*, *29*(15), R740–R742. https://doi.org/10.1016/j.cub.2019.06.036

Qian, M., Rosenqvist, E., Flygare, A. M., Kalbina, I., Teng, Y., Jansen, M. A. K., & Strid, Å. (2020). UV-A light induces a robust and dwarfed phenotype in cucumber plants (Cucumis sativus L.) without affecting fruit yield. *Scientia Horticulturae*. https://doi.org/10.1016/j.scienta.2019.109110

Qian, M., Rosenqvist, E., Prinsen, E., Pescheck, F., Flygare, A. M., Kalbina, I., Jansen, M. A. K., & Strid, A. (2021). Downsizing in plants—UV light induces pronounced morphological changes in the absence of stress. *Plant Physiology*, *187*(1), 378–395. https://doi.org/10.1093/plphys/kiab262

Rai, N., Morales, L. O., & Aphalo, P. J. (2021). Perception of solar UV radiation by plants: photoreceptors and

mechanisms. *Plant Physiology*, *186*(3), 1382–1396. https://doi.org/10.1093/PLPHYS/KIAB162

Rai, N., Neugart, S., Yan, Y., Wang, F., Siipola, S. M., Lindfors, A. V., Winkler, J. B., Albert, A., Brosché, M., Lehto, T., Morales, L. O., & Aphalo, P. J. (2019). How do cryptochromes and UVR8 interact in natural and simulated sunlight? *Journal of Experimental Botany*, *70*(18), 4975–4990. https://doi.org/10.1093/jxb/erz236

Reed, N. G. (2010). The history of ultraviolet germicidal irradiation for air disinfection. *Public Health Reports*, *125*(1), 15–27. https://doi.org/10.1177/003335491012500105

Robson, T. M., Aphalo, P. J., Banaś, A. K., Barnes, P. W., Brelsford, C. C., Jenkins, G. I., Kotilainen, T. K., Łabuz, J., Martínez-Abaigar, J., Morales, L. O., Neugart, S., Pieristè, M., Rai, N., Vandenbussche, F., & Jansen, M. A. K. (2019). A perspective on ecologically relevant plant-UV research and its practical application. *Photochemical and Photobiological Sciences*, *18*(5), 970–988. https://doi.org/10.1039/c8pp00526e

Shih, C., Grossman, A. R., Rosenquist, M., Jansson, S., Niyogi, K. K., Li, X., & Bjo, O. (2000). A pigment-binding protein essential for regulation of photosynthetic light harvesting. *Nature*, *403*(January), 391–395.

Siipola, S. M, Kotilainen, T., Sipari, N., Morales, L. O., Lindfors, A. V, Robson, T. M., & Aphalo, P. J. (2015). Epidermal UV-A absorbance and whole-leaf flavonoid composition in pea respond more to solar blue light than to solar UV radiation. *Plant Cell Environ*, *38*(5), 941–952. https://doi.org/10.1111/pce.12403

Suárez-López, P., K. Wheatley, F. Robson, H. Onouchi, F. Valverde, & G. Coupland. (2001). CONSTANS mediates between the circadian clock and the control of flowering in Arabidopsis. *Nature*, *410*(April), 1116–1120.

Takahashi, S, & Murata, N. (2008). How do environmental stresses accelerate photoinhibition? *Trends Plant Sci*, *13*(4), 178–182. https://doi.org/10.1016/j.tplants.2008.01.005

Takahashi, S, Milward, S. E., Yamori, W., Evans, J. R., Hillier, W., & Badger, M. R. (2010). The solar action spectrum of photosystem II damage. *Plant Physiology*, *153*(3), 988–993. https://doi.org/10.1104/pp.110.155747

Takemiya, A., Inoue, S., Doi, M., Kinoshita, T., & Shimazaki, K. (2005). Phototropins promote plant growth in response to blue light in low light environments. *Plant Cell*, *17*(4), 1120–1127. https://doi.org/10.1105/tpc.104.030049

Turnbull, T. L., Barlow, A. M., & Adams, M. A. (2013). Photosynthetic benefits of ultraviolet-A to Pimelea ligustrina, a woody shrub of sub-alpine Australia. *Oecologia, 173*(2), 375–385. https://doi.org/10.1007/s00442-013-2640-9

Verdaguer, D., Jansen, M. A. K., Llorens, L., Morales, L. O., & Neugart, S. (2017). UV-A radiation effects on higher plants: Exploring the known unknown. In *Plant Science*. https://doi.org/10.1016/j.plantsci.2016.11.014

Vialet-Chabrand, S., Matthews, J. S. A., & Lawson, T. (2021). Light, power, action! Interaction of respiratory energy- and blue light-induced stomatal movements. *New Phytologist*, *231*(6), 2231–2246. https://doi.org/10.1111/nph.17538

Wargent, J. J., Nelson, B. C. W., Mcghie, T. K., & Barnes, P. W. (2015). Acclimation to UV-B radiation and visible light in Lactuca sativa involves up-regulation of photosynthetic performance and orchestration of metabolome-wide responses. *Plant, Cell and Environment*. https://doi.org/10.1111/pce.12392

Wargent, J. J., Gegas, V. C., Jenkins, G. I., Doonan, J. H., & Paul, N. D. (2009). UVR8 in Arabidopsis thaliana regulates multiple aspects of cellular differentiation during leaf development in response to ultraviolet B radiation. *New Phytologist*. https://doi.org/10.1111/j.1469-8137.2009.02855.x

Wargent, J. J., & Jordan, B. R. (2013). From ozone depletion to agriculture: Understanding the role of UV radiation in sustainable crop production. In *New Phytologist*. https://doi.org/10.1111/nph.12132

White, A. L., & Jahnke, L. S. (2002). Contrasting effects of UV-A and UV-B on photosynthesis and photoprotection of β-carotene in two Dunaliella spp. *Plant and Cell Physiology*. https://doi.org/10.1093/pcp/pcf105

Woodward, G., Kroon, P., Cassidy, A., & Kay, C. (2009). Anthocyanin stability and recovery: Implications for the analysis of clinical and experimental samples. *Journal of Agricultural and Food Chemistry*, *57*(12), 5271–5278. https://doi.org/10.1021/jf900602b

Xu, M. Y., Zhang, L., Li, W. W., Hu, X. L., Wang, M. B., Fan, Y. L., Zhang, C. Y., & Wang, L. (2014). Stress-induced early flowering is mediated by miR169 in Arabidopsis thaliana. *Journal of Experimental Botany*, *65*(1), 89–101. https://doi.org/10.1093/jxb/ert353

Zhang, Y., Kaiser, E., Zhang, Y., Zou, J., Bian, Z., Yang, Q., & Li, T. (2020). UVA radiation promotes tomato growth through morphological adaptation leading to increased light interception. *Environmental and Experimental Botany*. https://doi.org/10.1016/j.envexpbot.2020.104073

Zhang, Y., Sun, X., Aphalo, P. J., Zhang, Y., Cheng, R., & Li, T. (2023). Ultraviolet-A1 radiation induced a more favorable light-intercepting leaf-area display than blue light and promoted plant growth. *Plant, Cell & Environment*, *46*(10), 1–16. https://doi.org/10.1111/pce.14727

# Supplementary material:

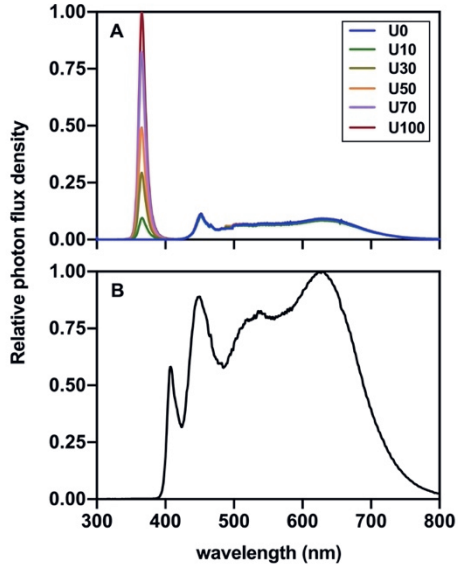


**Figure S1.** Spectral photon irradiance normalized to its maximum in each panel, in light treatments used for screening genotypes: UV-A1 dose response curve experiment (A); for germination in growth room (B).

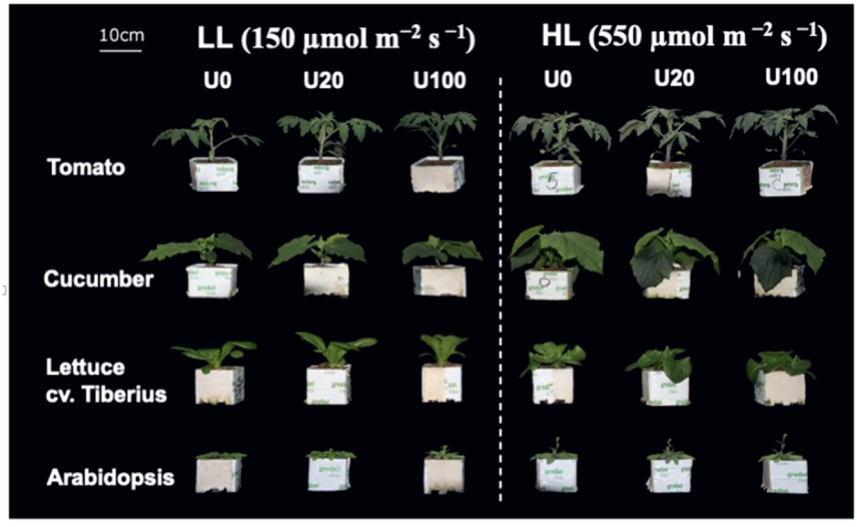


**Figure S2.** Plant morphology responses to UV-A1 radiation. Three UV-A1 irradiances were applied, i.e. 0, 20 and 100 µmol $m^{-2}$ $s^{-1}$ at low (LL; 150 µmol $m^{-2}$ $s^{-1}$) and high (HL; 550 µmol $m^{-2}$ $s^{-1}$) PPFD for 13 days.

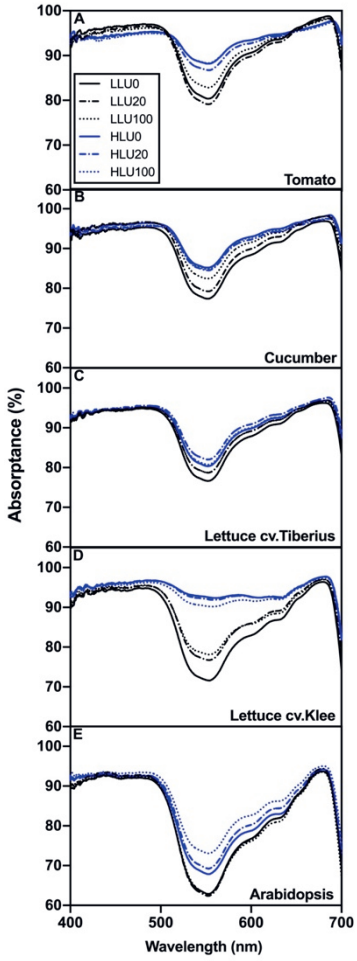


**Figure S3.** Effects of UV-A1 on leaf light absorptance in the PAR range (400-700 nm) of tomato, cucumber, lettuce cvs. Tiberius and Klee and arabidopsis. Three UV-A1 irradiances were applied, i.e. 0, 20 and 100 µmol $m^{-2}$ $s^{-1}$ at low (LL; 150 µmol $m^{-2}$ $s^{-1}$) and high (HL; 550 µmol $m^{-2}$ $s^{-1}$) PPFD for 13 days. A-E: Absorptance (%). Error bars show ± SE (n = 2, where each replicate represents the mean of five biological replicates).

**Table S1.** Spectrum distribution of white light in screening genotypes cultivation and UV-A1 dose response curve experiment.

| LEDs | Blue | Green | Red | Far Red |
|---|---|---|---|---|
| Percentage(%) | 20 | 35 | 38 | 7 |

# CHAPTER 3

## Leaf photosynthetic and photoprotective acclimation in the ultraviolet-A1 and blue light regions follow a continuous, shallow gradient

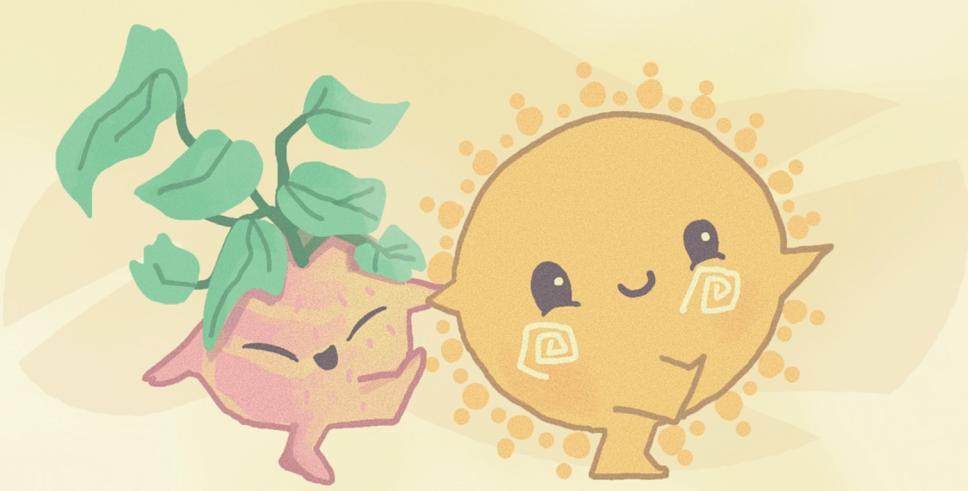

Xuguang Sun, Elias Kaiser, Leo F. M. Marcelis, Tao Li

*Published in Plant, Cell & Environment (2024)*
*https://doi.org/10.1111/pce.15256*

# Abstract

Although blue light is known to produce leaves with high photosynthetic capacity, the role of the blue-adjacent UV-A1 (350-400 nm) in driving leaf photosynthetic acclimation is less studied. Tomato plants were grown under hybrid red and blue (RB; 95/5 μmol $m^{-2}$ $s^{-1}$), as well as four treatments in which RB was supplemented with 50 μmol $m^{-2}$ $s^{-1}$ peaking at 365, 385, 410, and 450 nm, respectively. Acclimation to 365-450 nm led to a shallow gradient increase in trait values (i.e. photosynthetic capacity, pigmentation and dry mass content) as the peak wavelength increased. Furthermore, both UV-A1 and blue light grown leaves showed efficient photoprotection under high light intensity. When treated plants were transferred to fluctuating light for five days, leaves from all treatments showed increases in photosynthetic capacity, which were strongest in RB, followed by additional UV-A1 treatments; RB grown leaves showed reductions in maximum quantum yield of photosystem II, while UV-A1 grown leaves showed increases. We conclude that both UV-A1 and blue light effectively trigger photosynthetic and photoprotective acclimation, the extent of acclimation becoming stronger the longer the peak wavelength is. Acclimatory responses to UV-A1 and blue light are thus not distinct from one another, but follow a continuous gradient.

**Keywords:**

UV-A1, acclimation, steady-state photosynthesis, dynamic photosynthesis, photoprotection, tomato

# 1. Introduction

Light is the source of energy for photosynthesis, but also functions as a crucial signal for plant development and environmental acclimation (Poorter et al., 2019). Apart from light intensity, dosage, direction, and timing (e.g. Kaiser et al., 2024; van Delden et al., 2021), the spectral composition of light is crucial in plant development and growth. Among the different wavebands in the solar spectrum, blue light (400-500 nm) has long been recognized for its role in plant development (Fankhauser & Chory, 1997; Jiang et al., 2023; Lin, 2000), including photosynthetic acclimation (Hogewoning et al., 2010). The waveband directly adjacent to blue light, UV-A radiation (315-400 nm), is a primary component of solar UV radiation, and its role in shaping plant development is relatively less well studied than that of blue light. However, the investigation of its effects on plants has recently been boosted by new LED technology (Chen et al., 2019; Kelly & Runkle, 2023; Verdaguer et al., 2017; Zhang et al., 2023). Due to their narrow bandwidth, LED lamps provide the opportunity to investigate plant acclimation to various compositions of light qualities and intensities. Depending on photoreceptor involvement, the UV-A waveband can be divided into a range termed UV-A1 (350-400 nm), which is sensed by phototropins and cryptochromes, and UV-A2 (315-350 nm) which is primarily detected by UVR8 (Rai et al., 2019, 2021). While earlier studies primarily focused on the instantaneous response of photosynthesis to UV-A radiation (Johnson & Day, 2002; Mantha et al., 2001; Sun et al., 2024; Turnbull et al., 2013), the effects of photosynthetic acclimation under UV-A1, as well as its wavelength dependence, are largely unknown (Rai et al., 2021). Given that UV-A1 acts on the same photoreceptors as blue light, similarities in photosynthetic acclimation between the two wavebands can be expected. However, because UV-A1 is less strongly absorbed by chloroplasts than blue light, it is reasonable to assume that photosynthetic acclimation to UV-A1 is weaker than acclimation to blue light.

Plants acclimate to their environment through adjustments in photosynthetic biochemistry and plant morphology, to maximize their fitness under the given circumstances (Morales & Kaiser, 2020; Walters, 2005). Blue light is an important signal for the development of a normal photosynthetic apparatus (Wennicke & Schmid, 1987). Leaves grown under a mixture of red

and blue light show higher chlorophyll a/b ratios, biomass, photosynthetic capacity and photosynthetic electron transport than leaves grown under monochromatic red light (Hogewoning et al., 2010; Liang et al., 2021; Matsuda et al., 2004). The latter exhibit a phenomenon known as the "red light syndrome" (Trouwborst et al., 2016), which is characterized by a dysfunctional leaf photosynthetic apparatus: low net photosynthesis rate ($A$) and photosynthetic capacity, low maximum quantum yield of photosystem II, low chlorophyll content, and unresponsive stomata. The red light syndrome can be alleviated by adding a small amount of either UV-A1 or blue light (Franklin, 2008; Hogewoning et al., 2010; Zhang et al., 2020). However, the fact that UV-A1 radiation triggered weaker and later gene expression than blue light (Zhang et al., 2023) suggests that its effects are not equivalent to those of blue light (Zhang et al., 2020).

Both light intensity and spectrum are dynamic in nature (Durand & Robson, 2023), causing photosynthesis and photoprotection to respond dynamically. How quickly photosynthesis responds to changes in light intensity is often probed through measurements of photosynthetic induction, which describes the progressive transition of $A$ from a dark- or low light-adapted to a high light intensity (Kaiser et al., 2017a). This progress is determined by both biochemical (regeneration of ribulose 1,5-bisphosphate and the activation of Ribulose 1,5-bisphosphate carboxylase) and diffusional factors (opening of stomata; (Acevedo-Siaca et al., 2020; Kaiser et al., 2016), and its rapidity is modulated by several environmental factors (Kaiser et al., 2015, 2017a). Given that acclimation to several red/blue light ratios (including monochromatic red light) barely affected the rate of photosynthetic induction and other dynamic photosynthesis traits under fluctuating light (Zhang et al., 2019), it can be hypothesized that acclimation to UV-A1 radiation will not affect the rate of photosynthetic induction, either.

Leaves often absorb more light than they can utilize for photosynthesis, potentially leading to oxidative damage of their photosynthetic tissues (Murchie & Niyogi, 2011). To mitigate this, plants use several photoprotective mechanisms, including non-photochemical quenching (NPQ; Bassi & Dall'Osto, 2021). Based on its kinetics, NPQ can be divided into its components energy-dependent quenching ($qE$), zeaxanthin-dependent quenching ($qZ$), state transition-dependent quenching ($qT$) and photoinhibition ($qI$; Long et al., 2022). Compared to red-light

grown leaves, red/blue light-grown leaves showed a faster NPQ formation and higher steady-state NPQ (Kang et al., 2021; Zhang et al., 2019), potentially alleviating photoinhibition and maintaining photosynthesis under periods of high or strongly fluctuating light intensity. While cryptochromes are involved in ameliorating high light stress (Brelsford et al., 2019; Hoffmann et al., 2015), it is currently unclear whether acclimation to UV-A1 is similarly effective as acclimation to blue light in the build-up of photoprotective capacity. The extent of photoinhibition is partially driven by the energy per photon (Takahashi et al., 2010), suggesting that UV-A1 exposure is likely more photoinhibitive than blue light exposure. Indeed, plants grown under higher UV-A1 intensity showed stronger symptoms of photoinhibition than plants under a white background light only (Sun et al., 2024). Repairing UV-A1-induced photoinhibition requires energy (Miyata et al., 2012), which could otherwise be used for growth. It could thus be hypothesized that UV-A1 grown leaves show larger photoprotective capacity and less biomass accumulation than blue light grown leaves.



We aimed to compare how acclimation to several wavelengths in the UV-A1 and blue light range (365-450 nm) affects photosynthetic and photoprotective performance in tomato, and how such acclimation prepares plants for subsequent exposure to fluctuating and high light intensities. We hypothesized that: 1) UV-A1 is less effective than blue light in promoting photosynthetic acclimation and biomass accumulation, 2) acclimation to neither wavelength affects the rate of photosynthetic induction; 3) leaves grown under UV-A1 radiation have higher photoprotective capacity compared to those grown under blue light, and 4) photoinhibition caused by UV-A1 exposure is reversed when plants are transferred to fluctuating light intensity.

# 2. Materials and methods

## 2.1 Plant material and growth conditions

Seeds of tomato (*Solanum lycopersicum* cv. 'Moneymaker') were sown in rockwool plugs (Grodan, Roermond, the Netherlands) with one seed per plug, and germinated in a growth room at a photosynthetic photon flux density (PPFD) of 100 μmol $m^{-2}$ $s^{-1}$ white light (WL; ZWS01D-

LED120-180, PanAnGreenlight, Jinhua, China; for spectra see Fig. S1), a photoperiod of 16 h, day/night temperature of 23.4 ± 0.7 / 22.4 ± 0.5, relative humidity of 70 ± 5%, and $CO_2$ partial pressure of ~450 μmol $mol^{-1}$. Air temperature and relative humidity were monitored by a climate sensor (TR-76Ui-S; T&D, Nagano, Tokyo, Japan), $CO_2$ partial pressure was regularly and diligently monitored by the experimenter. Tomato seedlings were transferred to rockwool cubes (7.5 cm × 7.5 cm × 5 cm; Grodan) upon unfolding of the second true leaf, and distributed over five growth units (115 cm L × 70 cm W × 115 cm H), which were all set up in the same growth room. Opaque black-white plastic films were wrapped around each unit, which harbored one treatment, with the white side facing the plants, to avoid light contamination between units. Two ventilation fans (12 V, 0.90 A, 0.5 $m^3$ $min^{-1}$) were installed per unit to ensure uniform air circulation. Light was provided by a mixture of dimmable LED lamps (ZWS01D-LED120-180, PanAnGreenlight; see Fig. 1A for spectra).

### *Light spectrum treatments*

A background light intensity of 100 μmol $m^{-2}$ $s^{-1}$ was provided by a mixture of red (R; 95 μmol $m^{-2}$ $s^{-1}$, peaking at 656 nm) and blue LEDs (B; 5 μmol $m^{-2}$ $s^{-1}$, peaking at 450 nm) per treatment (Table 1). In four out of five treatments, an additional 50 μmol $m^{-2}$ $s^{-1}$ light intensity was added, using light peaking at 365, 385, 410 and 450 nm, respectively (the latter was the same LED type as that used to provide blue in the background light). These treatments are referred to as RB+365, RB+385, RB+410, RB+450, respectively, while the treatment only containing background light is referred to as RB (Table 1). Plants were treated for 10-14 days, at a photoperiod of 16 h; all other environmental factors were the same as during germination. Plants were regularly watered by hand with a modified Hoagland nutrient solution (pH: 5.8, EC: 1.8 dS $m^{-1}$). Every other day, plants inside each treatment were rotated and relocated relative to each other, to avoid position effects on plant growth. The initial distance between the top of the plants and the light panel was 60 cm. As plants grew upward, lamp output was regularly adjusted to maintain the same intensity at the top of the plants, which was measured regularly using a spectroradiometer (Avaspec-2048CL, Avantes, Apeldoorn, the Netherlands).

**Table 1.** Overview of light treatments in the experimental setup.

| Treatment | R ($\mu mol\ m^{-2}\ s^{-1}$) | B ($\mu mol\ m^{-2}\ s^{-1}$) | UV-A1 ($\mu mol\ m^{-2}\ s^{-1}$) | Total PFD ($\mu mol\ m^{-2}\ s^{-1}$) | DLI ($mol\ m^{-2}\ d^{-1}$) |
|---|---|---|---|---|---|
| RB | 95 | 5 | 0 | 100 | 5.76 |
| RB+365 | 95 | 5 | 50 | 150 | 8.64 |
| RB+386 | 95 | 5 | 50 | 150 | 8.64 |
| RB+410 | 95 | 55 | 0 | 150 | 8.64 |
| RB+450 | 95 | 55 | 0 | 150 | 8.64 |

**Note:** R, red light peaking at 656 nm; B, blue light (as background light peaking at 450 nm; as treatment light peaking at 410 and 450 nm, respectively); UV-A1, long-wavelength UV-A radiation (350-400 nm); PPFD, photosynthetic photon flux density (400-700 nm); total PFD, total photon flux density; DLI, daily light integral.

### *High light (HL) exposure*

To evaluate leaf photoprotective capacity after acclimation under light spectrum treatments for 13 days, plants were exposed to a high light intensity (1500 $\mu mol\ m^{-2}\ s^{-1}$; HL) for 30 min (spectrum in Fig. S1B).

### *Fluctuating light (FL) exposure*

To follow changes in photosynthetic capacity due to light mimicking natural sunlight, plants that had been growing under the light spectrum treatments for 10 days were exposed to FL for 5 days. For this, plants were transferred to growth units (140 cm L × 75 cm W × 115 cm H) with white LEDs (spectrum in Fig. S1B) and a programmable controller. A FL that followed a diurnal pattern and changed every 5 minutes in the range of 0-1000 $\mu mol\ m^{-2}\ s^{-1}$ was repeated daily (Fig. 1B), with an average PPFD of 406.8 $\mu mol\ m^{-2}\ s^{-1}$, and DLI of 20.6 $mol\ m^{-2}\ d^{-1}$. The photoperiod was 14 h. The position of plants relative to each other was changed daily. The distance between the top of the canopy and the LEDs was 40 cm. Other environmental conditions were identical to those described above.

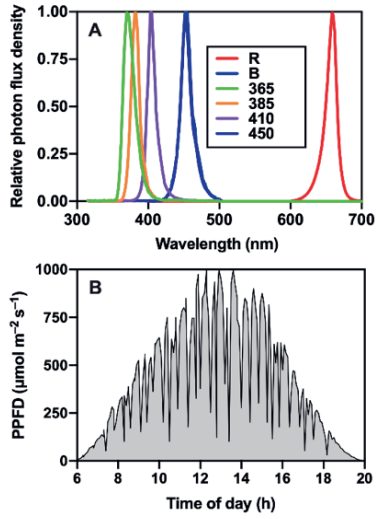


**Figure 1.** Relative photon flux density of the light spectra used for light spectrum treatments (A) and diurnal photosynthetic photon flux density (PPFD) patterns used for fluctuating light exposure (B).

## 2.2 Measurements

### *2.2.1 Destructive measurements*

Destructive measurements were conducted after 14 days of light spectrum treatments, as well as before and after 5 days of FL exposure. Fresh and dry weights of leaves, petioles and stems were determined. Plant organs were dried for 48 h at 80 °C in a ventilated oven (DHG-9070A, Shanghai Jinghong, Shanghai, China). Stem length was measured using a ruler, and was defined as the distance from the intersection between shoot and root to the shoot apex. Leaf area was measured using a leaf area meter (LI-3100C, Li-Cor Biosciences, Lincoln, NE, USA). Specific leaf area (SLA; $cm^2\ g^{-1}$) was calculated as leaf area divided by leaf dry weight. Dry mass partitioning to each organ was calculated by dividing dry weight of each organ by total shoot dry weight. Dry mass content was calculated as the ratio of shoot dry to fresh weight. The changes in shoot dry weight and leaf area before and after FL exposure were calculated as (after FL – before FL) / before FL.

### *2.2.2 Leaf light absorptance*

Light reflectance and transmittance in the 400-700 nm range of the adaxial side of the leaf were measured with a spectrometer (Ocean optics USB2000+, Dunedin, USA), in combination with two integrating spheres (FOIS-1, ISP-REF, Ocean Optics). Leaf light absorptance was calculated as 1 – reflectance – transmittance. The fully expanded third or fourth true leaves, counting from the top, were used for measurements.

### *2.2.3 Leaf biochemical components*

After 13 days of light spectrum treatments, at the sixth hour of the photoperiod, the fully expanded third or fourth true leaves, counting from the top, were collected for measurements. Whole leaves were immersed in liquid nitrogen and then stored at – 80 °C until further analysis.



#### *Chlorophyll*

Fresh samples (0.1 g) were ground in liquid nitrogen, using a high-throughput tissue grinder (SCIENTZ-48, Xinzhi, Ningbo, China), and then incubated in 10 mL 95% ethanol in the dark at 4 °C, for 24h. The absorbance of the extract was measured at 470, 649, 664 and 750 nm, using a spectrophotometer (UV-1800, Shimadzu, Japan). The concentrations of chlorophyll *a*, chlorophyll *b*, their sum and ratio (on a mass basis), as well as total carotenoid contents, were calculated using the equations derived by Lichtenthaler & Buschmann (2001).

#### *Anthocyanin*

Fresh samples (0.1 g) were ground as described above, incubated with 600 µL of extraction buffer (99% methanol and 1% HCl), and vortexed. The extracts were placed in an ultrasonic bath for 10 minutes and then dark incubated overnight at 4 °C. After extraction, 400 µL of water and 400 µL of chloroform were added. Absorbance (A) of extracts was measured at 530 and 657 nm, using a microplate reader (Infinite 200 PRO, TECAN, Switzerland), and anthocyanin content was expressed as: Anthocyanin = ($A_{530}$-0.33*$A_{657}$) / leaf area (Liu et al., 2018), where

$A_{530}$ and $A_{657}$ are absorbance at 530 and 657 nm, respectively.

***Phenolics and flavonoids***

Samples (0.1 g) were extracted with 1 mL of 80% aqueous methanol in an ultrasonic bath (10 min), and were then centrifuged (15000 × g for 10 min). Total phenolic and flavonoid concentrations were determined using the Folin Ciocalteu and the aluminum chloride colorimetric assays, respectively (Khanam et al., 2012). The absorbance was determined using a microplate reader (Infinite 200 PRO, TECAN, Switzerland). For total phenolics content, gallic acid was used as the standard reference and gallic acid equivalent (GAE) was expressed as mg per g fresh mass. For total flavonoid content, rutin was used as the standard reference and rutin equivalent (RUE) was expressed as mg per g fresh mass (Yang et al., 2021).

### *2.2.4 Photosynthesis*

Photosynthetic gas exchange and chlorophyll fluorescence measurements were performed using the LI-6800 photosynthesis system (Li-Cor Biosciences) equipped with the leaf chamber fluorometer (Li-Cor Part No.6800–01A, enclosed leaf area: 2 $cm^2$). During measurements, $CO_2$ partial pressure was 400 μbar, leaf temperature was ~25 °C, leaf-to-air vapor pressure deficit was 0.7–1.0 kPa, and air flow rate through the system was 500 μmol $s^{-1}$. Light intensity was provided by a mixture of red (90%) and blue (10%) LEDs in the fluorometer. Peak intensities of red and blue LEDs were at wavelengths of 635 and 465 nm, respectively. After 10–13 days of light spectrum treatments, photosynthesis measurements were taken on the same leaves as those used for leaf biochemical measurements. Per treatment, five biological replicates randomly selected from two batches were used for measurements.

***Steady-state photosynthesis***

To assess the responses of leaf photosynthetic gas exchange and chlorophyll fluorescence to a range of light intensities, leaves were adapted to 500 μmol $m^{-2}$ $s^{-1}$ PPFD, until photosynthesis rate ($A$) and stomatal conductance ($g_s$) were stable. Leaves were then exposed to 2000, 1500,

1000, 800, 600, 400, 200, 150, 100, 50, and 0 µmol $m^{-2}$ $s^{-1}$ PPFD. When *A* reached steady-state at each PPFD (~2 min, except for the highest light intensity, where this took 5-10 min), *A*, $g_s$, and leaf internal $CO_2$ partial pressure ($C_i$) were logged every 5 s for 0.5 min, and averaged values were used. Fluorescence yield under actinic light ($F_s$) and maximal fluorescence yield of a light-adapted leaf ($F_m$') were logged at the same time, using a rectangular saturating flash of 16000 µmol $m^{-2}$ $s^{-1}$ intensity that was applied for 500 ms, and at a data acquisition rate of 100 Hz. Photosystem II operating efficiency ($\Phi_{PSII}$) was calculated as $\Phi_{PSII} = (F_m' - F_s)/F_m'$ (Baker, 2008).

To assess the $CO_2$ response of *A*, leaves were adapted to 1000 µmol $m^{-2}$ $s^{-1}$ PPFD and 400 µbar $CO_2$, until *A* and $g_s$ were stable. Thereafter, leaves were exposed to a range of $CO_2$ partial pressures: 400, 300, 200, 100, 50, 400, 600, 800, 1000, 1200, 1500 and 2000 µbar. At each $CO_2$ partial pressure, measurements were taken when *A* had reached a steady state (3–5 min). Infra-red gas analyzers were matched at every $CO_2$ step.

To follow changes in leaf photosynthesis and respiration in plants under FL exposure, the youngest fully expanded leaf was used for measurements. Every day, leaves were exposed to 1000, 150 and 0 µmol $m^{-2}$ $s^{-1}$ PPFD respectively, using the fluorometer cuvette of the LI-6800. When *A* was stable (~3 min per step), gas exchange was logged every 5 s for 1 min, and averages of 12 values were used.

***Dynamic photosynthesis***

To evaluate gas exchange and chlorophyll fluorescence responses to step changes in PPFD, plants were adapted in a dark room for ~30 min. After that, selected leaflets were placed in the LI-6800 cuvette, and minimal ($F_0$) and maximal ($F_m$) chlorophyll fluorescence were recorded to determine the maximum quantum yield of photosystem II ($F_v/F_m$). $F_v/F_m$ was calculated as $(F_m-F_o)/ F_m$ (Baker, 2008). PPFD was then increased to 50 µmol $m^{-2}$ $s^{-1}$, and leaves were adapted at this PPFD until *A* and $g_s$ were at a steady state (approx. 20 min). Then, gas exchange was logged for 10 min at low light intensity (LL; 50 µmol $m^{-2}$ $s^{-1}$), followed by 40 min of high light intensity (HL; 1,000 µmol $m^{-2}$ $s^{-1}$), followed by another 20 min of LL. Gas exchange was

logged once every 2 s. Chlorophyll fluorescence was measured once per minute, as described above.

***Chlorophyll fluorescence imaging***

Chlorophyll fluorescence imaging were taken on both HL and FL exposed plants. $F_v/F_m$ was measured using the Imaging-PAM Chlorophyll Fluorescence System (MAXI-PAM, Heinz Walz GmbH, Effeltrich, Germany). $F_m$ and $F_o$ of dark-adapted plants (≥ 20 min of dark adaptation) were measured on the youngest fully developed leaves. Measuring beam intensity was 1 µmol $m^{-2}$ $s^{-1}$, maximum flash intensity was 8,000 µmol $m^{-2}$ $s^{-1}$. Measurements were conducted on six plants per batch after 13 days of acclimation to light spectrum treatments and on three plants per batch in the case of FL exposure. During FL exposure, measurements were conducted on days 1, 3 and 5, respectively. The percentage reduction between $F_v/F_m$ before and after HL exposure was calculated as: Reduction (%) = ($F_v/F_{m\_before\ HL}$ - $F_v/F_{m\_after\ HL}$) *100/ $F_v/F_{m\_before\ HL}$.

***Calculations***

*Analysis of steady-state leaf photosynthesis.* A non-rectangular hyperbolic function (Cannell and Thornley, 1998) was fitted to the light response curve, and the parameters light-saturated net photosynthesis rate ($A_{sat}$, µmol $m^{-2}$ $s^{-1}$), maximum apparent quantum yield (α, µmol $CO_2$ $µmol^{-1}$ photons) and mitochondrial respiration ($R_d$, µmol $m^{-2}$ $s^{-1}$) were derived. Parameters including maximum carboxylation rate ($V_{cmax}$), rate of photosynthetic electron transport ($J$) and triose phosphate use (TPU) were derived according to Sharkey (2016). For the purpose of $A/C_i$ curve fitting, the mitochondrial respiration rate ($R_d$) was estimated to be 50% of dark respiration rate ($R_{dark}$; Busch et al., 2024), and mesophyll conductance ($g_m$) at 400 µbar $CO_2$ and 1000 µmol $m^{-2}$ $s^{-1}$ was calculated using the variable $J$ method (Harley et al., 1992) using light response curve data. To obtain $g_m$, $R_d$ was assumed to be 50% of dark respiration rate, $J$ was obtained by multiplying $\Phi_{PSII}$ with incident light intensity and a scaling factor, $s$ (0.4525), and the $CO_2$ compensation point in the absence of $R_d$, Γ*, was assumed to be 57.07 µbar. Values for $s$ and Γ* were taken from Kaiser et al. (2017a), and were initially derived on tomato leaves using the

methodology by Yin et al. (2009).

*Photosynthetic induction.* Transient responses of $A$, $g_s$, and $C_i$ to a step increase in light intensity were averaged over five data points to reduce measurement noise, using a moving average filter. Photosynthetic induction state was calculated after Zipperlen & Press (1997):

$$\text{photosynthetic induction} = \frac{A - A_i}{A_f - A_i} * 100 \qquad \text{(Eq. 1)}$$

Where $A_f$ is steady-state $A$ at 1500 µmol $m^{-2}$ $s^{-1}$ PPFD (mean value over 120 s), corrected for initial $A$ at 50 µmol $m^{-2}$ $s^{-1}$ ($A_i$, mean value over 120 s before the increase in PPFD). Photosynthetic induction state 60 s after the light intensity increase, $IS_{60}$, as well as the times required to reach 50% and 90% of full photosynthetic induction, $t_{50}$-$A$ and $t_{90}$-$A$, were calculated.

*Modelling dynamic $g_s$ responses to PPFD.* An empirical model was used to quantify the speed of stomatal responses to light intensity changes (Vialet-Chabrand et al., 2017):

$$g_s = (g_{sf} - g_{si}) e^{-e^{-(\frac{\lambda - t}{k_i} + 1)}} + g_{si} \qquad \text{(Eq. 2)}$$

where $g_{si}$ and $g_{sf}$ represent steady-state $g_s$ under LL and HL respectively, t represents time, λ represents the initial time lag (time after the increase in light intensity during which no change in $g_s$ is observed), and $k_i$ represents the time constant for an increase of $g_s$. $k_i$ does not directly represent a time to reach a percentage of $g_s$, as this also depends on λ. Therefore $\tau_i$, representing the time to reach 63% of the total $g_s$ increase including λ, can be calculated as:

$$\tau_i = \lambda - k_i * [\ln(-\ln(1 - e^{-1})) - 1] \qquad \text{(Eq. 3)}$$

Where λ represents the initial time lag (time after the increase in light intensity during which no change in $g_s$ is observed), and $k_i$ represents the time constant for an increase of $g_s$. $k_i$ does not directly represent a time to reach a percentage of $g_s$, as this also depends on λ. Therefore, the time constant $\tau_i$ represents the time to reach 63% of the total $g_s$ increase. After a step decrease in light intensity, an exponential model (Vialet-Chabrand et al., 2017) was determined to be the best fit for stomatal closure in tomato leaves that had been grown under

similar conditions (Zhang et al., 2022):

$$g_s = g_{si} + (g_{sf} - g_{si}) e^{-\frac{t}{\tau_d}} \quad \text{(Eq. 4)}$$

Where the time constant $\tau_d$ represents the time to reach 63% of the total decrease in $g_s$.

*NPQ kinetics.* Separate models were fit to the induction (Equation 5) and low light relaxation (Equation 5) of NPQ to obtain their respective rate constants (*b*; Ferguson et al., 2023):

$$\text{NPQ} = a * (1 - e^{(-b*t)}) \quad \text{(Eq. 5)}$$

$$\text{NPQ} = a * (e^{(-b*t)}) + c \quad \text{(Eq. 6)}$$

Where in both equations, a represents the amplitude of the response, c is an offset to account for a non-zero intercept, and t is time. Different NPQ components were further quantified by fitting a double exponential function to NPQ relaxation (Long et al., 2022):

$$NPQ = Aq1^{(-\frac{t}{\tau q1})} + Aq2^{(-\frac{t}{\tau q2})} + Aq3 \quad \text{(Eq. 7)}$$

where *Aq1* corresponds to *qE*, *Aq2* corresponds to *qZ* and *qT*, *Aq3* corresponds to *qI*, τq1 and τq2 represent the half-lives of relation of *Aq1* and *Aq2* respectively. Curve-fitting was done using the 'solver' function in Microsoft excel. It should be noted that fitting of the entire Eqn. 7 to the NPQ relaxation data yielded unrealistically low values for *Aq3* (and correspondingly larger values for *Aq1* and *Aq2*), since during the relatively short NPQ relaxation time (20 min), NPQ did not reach a steady state – this is a prerequisite for realistic estimation of *Aq3* and thus *qI*. To solve this issue, we assigned the last recorded NPQ datapoint during NPQ relaxation as the value of *Aq3*, and fitted the rest of Eqn. 7 to the data. Since this procedure inevitably results in an overestimation of *qI* (due to steady-state NPQ having not yet been reached), we report the values here as apparent *qI*.

## 2.3 Experimental design and statistics

The experiment was designed as a completely randomized block design (Table S1). The experiment ('Light spectrum treatments') was conducted three times in a row (resulting in three blocks), with six plants per treatment and block (total: 18 plants per treatment). In each block, the position of the light treatments in the growth room was changed randomly. Additional batches of plants were treated with light spectra and subsequently exposed to HL or FL, each of which were conducted on two separate batches of plants, with six plants per treatment and batch under HL exposure (total: 12 plants) and three plants per treatment and batch under FL exposure (total: 6 plants). Except for gas exchange measurements, all measurements were conducted on all experimental plants. Gas exchange measurements were conducted on five replicate plants per treatment in two batches (three plants measured in batch 1, two plants in batch 2).



Treatment batches were treated as blocks, except for photosynthesis data, where each individual plant was treated as a replicate plant. One-way ANOVA was performed using polynomial contrasts to examine linear and quadratic trends across light spectra treatments (similar to Kaiser et al., 2019), with peak wavelength as quantitative factor. In this analysis, the quadratic component takes precedence over the linear component, i.e. if the quadratic component has a statistically significant effect ($P<0.05$), the linear component is irrelevant. In this analysis, the RB treatment was excluded, as it was applied at a lower light intensity than the other treatments. Custom contrast coefficients were applied to compare effects of the RB treatment with the average value of all RB+ treatments. Photosynthesis traits recorded during FL exposure were analyzed by a two-way ANOVA with light spectrum treatment and time of treatment as factors. Data were first tested for normality (Shapiro–Wilk test) and homogeneity of variances (Fligner–Killeen test) at $P=0.05$. When data did not fulfil the assumptions for an ANOVA, they were log-transformed, after which data fulfilled these prerequisites in all cases. For improved clarity, only $P<0.1$ are shown in figures, and $P<0.05$ are shown in bold. All analyses were performed using SPSS 24 (SPSS Inc., Chicago, IL).

# 3. Results

## 3.1 Plant morphology, growth and pigmentation

Plants grown with additional UV-A1 or blue light were visibly shorter and more compact (Fig. 2A) than the control (RB); these are typical characteristics of high light intensity treated plants. RB treated plants were significantly longer, had larger SLA as well as lower dry mass content and leaf light absorptance, than RB+ treated plants ($P_{RB} < 0.001$ in all cases; Fig. 2D-G). Dry mass partitioning within the shoot was also different in RB treated plants: partitioning to leaves was reduced whereas partitioning to petioles was increased, compared to RB+ plants (Table S2). Among the RB+ treatments, we observed significant linear response gradients with peak wavelength for shoot dry weight ($P_{lin} = 0.01$), specific leaf area (SLA) ($P_{lin} < 0.001$), dry mass content ($P_{lin} < 0.001$) and leaf light absorptance ($P_{lin} = 0.003$; Fig. 2B, D, F, G). Unlike the other traits, leaf area was unaffected by any of the treatments (Fig. 2C). The various components of shoot dry weight, i.e. leaf, stem, and petiole dry weight, also showed significant linear responses with peak wavelength, as well as a linear increase in biomass partitioning to petioles (Table S2).

RB treated plants showed reduced pigmentation than RB+ treated plants: concentrations of chlorophylls, carotenoids, anthocyanins and phenolics were all significantly reduced, whereas flavonoid concentrations were unchanged (Fig. 3). Among the RB+ treated plants, significant linear increases with peak wavelength could be observed for chlorophyll and carotenoid concentrations (Fig. 3A, C), but not for the other pigments. The chlorophyll *a*/*b* ratio was unaffected by treatments (Fig. 3B).

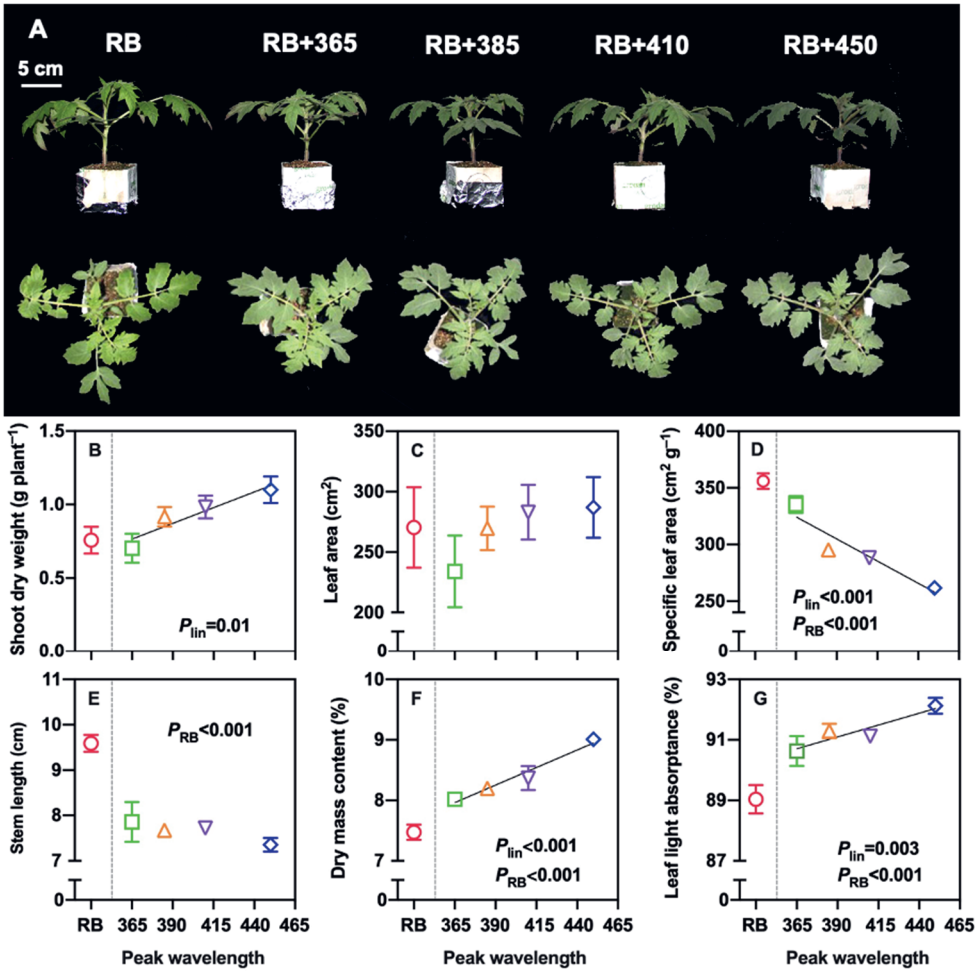


**Figure 2.** Plant morphology, growth and leaf light absorption of tomato plants acclimated to a mixture of red (R; 95 µmol $m^{-2}$ $s^{-1}$) and blue (B; 5 µmol $m^{-2}$ $s^{-1}$) light (RB), as well as additional spectra in the UV-A1 and blue region with an intensity of 50 µmol $m^{-2}$ $s^{-1}$ peaking at 365, 385, 410 and 450 nm (RB+). A: representative images of plant morphology from the side and top view; B: shoot dry weight, C: leaf area, D: specific leaf area, E: stem length, F: shoot dry mass content, G: leaf light absorptance in the 400–700 nm range. Error bars show ± standard error of means (SEM; n = 3, each replicate represents the mean of six replicate plants). SEM is visible only when larger than the symbol size. Significant differences between RB and RB+ treatments are shown as $P_{RB}$. For significant linear effects ($P_{lin}$) of peak wavelength among the RB+ treatments, a trendline together with the respective *P*-value is depicted. Only $P<0.1$ are shown, $P<0.05$ are depicted as bold.

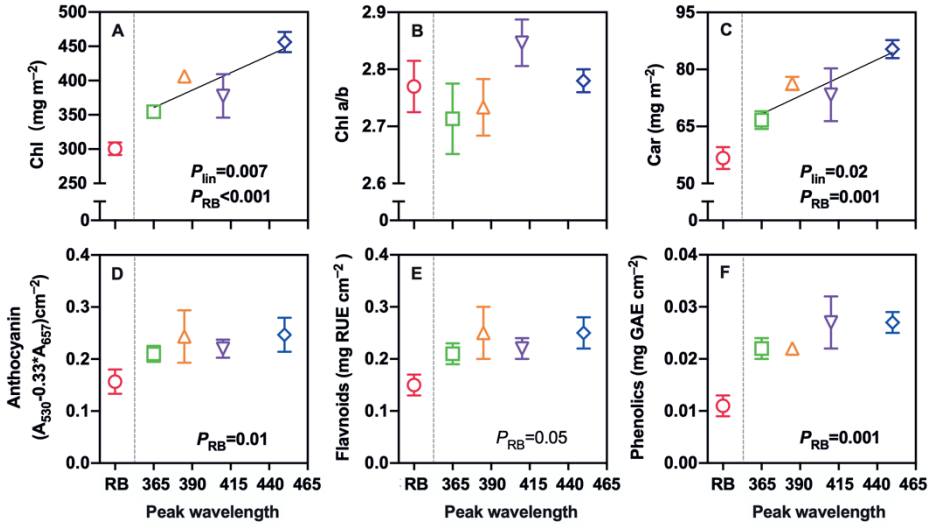


**Figure 3.** Pigmentation of tomato leaves acclimated to a mixture of red (R; 95 µmol $m^{-2}$ $s^{-1}$) and blue (B; 5 µmol $m^{-2}$ $s^{-1}$) light (RB), as well as additional spectra in the UV-A1 and blue region with an intensity of 50 µmol $m^{-2}$ $s^{-1}$ light intensity peaking at 365, 385, 410 and 450 nm (RB+). A: chlorophyll concentration, B: chlorophyll a/b ratio, C: carotenoid concentration, D: anthocyanin concentration, E: flavonoid concentration (rutin equivalent (RUE) used as the standard reference), F: phenolics concentration (gallic acid equivalent (GAE) used as the standard reference). Error bars show ± SEM (n = 3, where each replicate represents the mean of six replicate plants). SEM is visible only when larger than the symbol size. Significant differences between RB and RB+ treatments are shown as $P_{RB}$. For significant linear effects ($P_{lin}$) of peak wavelength among the RB+ treatments, a trendline together with the respective *P*-value is depicted. Only *P*<0.1 are shown, *P*<0.05 are depicted as bold.

## 3.2 Steady-state leaf photosynthesis traits

Judging from light and $CO_2$ response curves of photosynthetic gas exchange and chlorophyll fluorescence, photosynthetic capacity and $g_s$ were the lowest in RB-acclimated leaves, and progressively increased with peak wavelength in RB+ treated leaves (Figs. 4A-C; S2). This was confirmed by statistical analysis of parameters extracted from these curves: $A_{sat}$, $R_d$, $V_{cmax}$, $J$ and TPU were all strongly reduced ($P$<0.001 in all cases), resulting in maximum differences (between RB and RB+450) of ~40% for $A_{sat}$ and $J$ (Fig. 4D, H), and ~60% for $V_{cmax}$ (Fig. 4G). Somewhat surprisingly, however, the apparent maximum quantum yield (α) was significantly larger in RB than in RB+ treated leaves (Fig. 4E). Among the RB+ treated leaves, several traits related to photosynthetic capacity ($A_{sat}$ and $V_{cmax}$) showed significant linear increases with peak wavelength, while the linear correlation with $J$ was not significant (Fig. 4D, G, H).

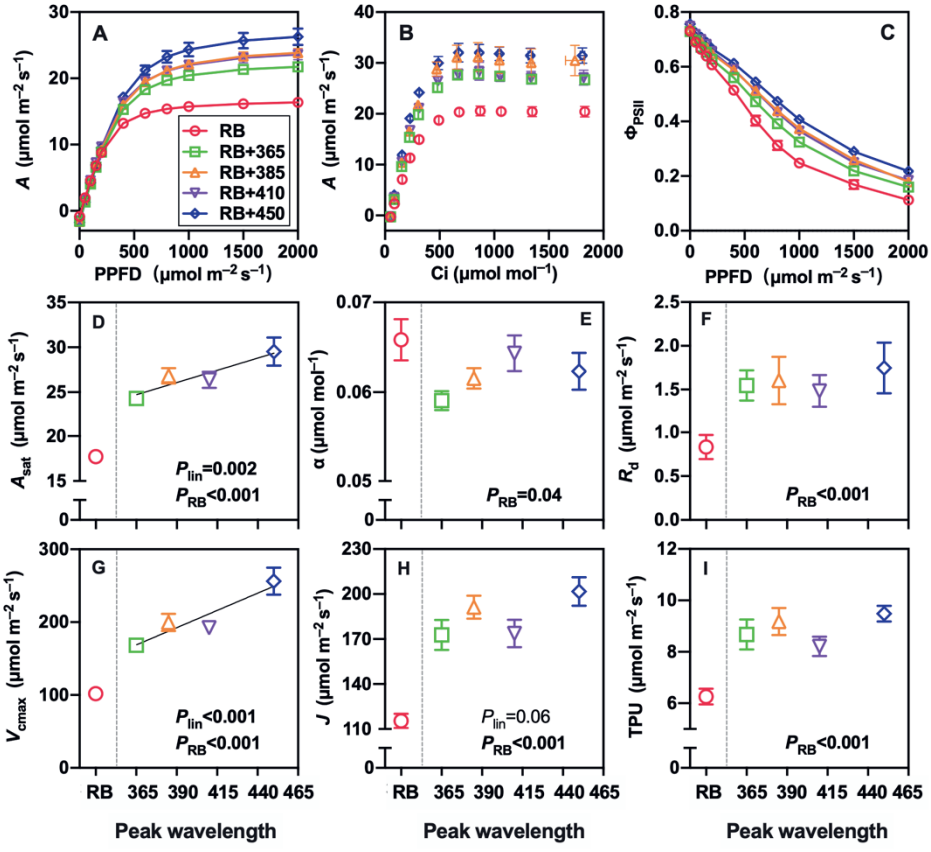


**Figure 4.** Steady-state responses of photosynthesis and chlorophyll fluorescence to light intensity and [$CO_2$] in leaves acclimated to a mixture of red (R; 95 µmol $m^{-2}$ $s^{-1}$) and blue (B; 5 µmol $m^{-2}$ $s^{-1}$) light (RB), as well as additional spectra in the UV-A1 and blue region with an intensity of 50 µmol $m^{-2}$ $s^{-1}$ peaking at 365, 385, 410 and 450 nm (RB+). During all measurements, a spectrum of 90% red and 10% blue light was used. A: light response curve of net photosynthesis rate ($A$), B: response curve of $A$ to leaf internal $CO_2$ partial pressure ($C_i$), C: light response curves of electron transport efficiency through photosystem II ($\Phi_{PSII}$), D: light-saturated $A$ ($A_{sat}$), E: maximum apparent quantum yield of $CO_2$ fixation ($\alpha$), F: mitochondrial respiration rate ($R_d$), G: maximum carboxylation rate ($V_{cmax}$), H: electron transport rate at 1500 µmol $m^{-2}$ $s^{-1}$ ($J$), I: maximum rate of triose phosphate use (TPU). Error bars show ± SEM (n = 5, five replicate plants were measured in two batches). SEM is visible only when larger than the symbol size. Significant differences between RB and RB+ treatments are shown as $P_{RB}$. For significant linear effects ($P_{lin}$) of peak wavelength among the RB+ treatments, a trendline together with the respective $P$-value is depicted. Only $P$<0.1 are shown, $P$<0.05 are depicted as bold.

## 3.3 Dynamic photosynthesis

Under high light intensity, $A$, $g_s$, and $\Phi_{PSII}$ all showed maximum values in RB+450 acclimated leaves, while minimum values were found under RB (Fig. 5A, B, D), similar to many steady-state photosynthesis traits (Fig. 4). The rate of photosynthetic induction was not affected by extra UV-A1 or blue light treatments, as indicated by an absence of significant effects on $IS_{60}$ and no significant treatment effects on times to reach 90% of full photosynthetic induction ($t_{90}$-$A$; Figs. 5J; S3). While a quadratic response in $t_{50}$-$A$ was observed (Fig. 5G), there was no significant linear relationship between $g_s$ before photosynthetic induction and $t_{90}$-$A$ (Fig. S4). The rate of stomatal opening ($\tau_i$) showed a quadratic response with peak wavelength (due to smaller values in the 410 nm treatment; Fig. 5H) while the rate of stomatal closure ($\tau_d$) showed a negative linear response with peak wavelength (Fig. 5I), suggesting that stomata in leaves acclimated to blue light closed faster than those acclimated to UV-A1 radiation.

Time courses of NPQ under dynamic light intensities were mostly unaffected by different light intensity treatments (RB vs. RB+), but showed some differences among the RB+ treatments (Fig. 5E): After the switch from low to high light intensity, RB+450 treated leaves induced NPQ much more rapidly than all other leaves (Fig. 5K), whereas rates of NPQ relaxation after the reverse switch were unaffected (Fig. 5L). During high light exposure, NPQ in RB+450 treated leaves quickly levelled off, whereas it kept rising in other treatments (Fig. 5E), resulting in a significant negative relationship between NPQ reached after 40 min. of high light exposure and peak wavelength ($P$=0.006), and significantly larger NPQ in RB compared to RB+ treated leaves ($P$=0.004; Fig. S5). After the switch to low light, $qE$ showed a significant ($P$=0.02) negative linear relationship with peak wavelength among the RB+ treatments (Fig. 5M), whereas $qZ$ and $qT$ as well as apparent $qI$ did not show significant linear reductions ($P$=0.05 in both cases) with peak wavelength (Fig. 5N, O).

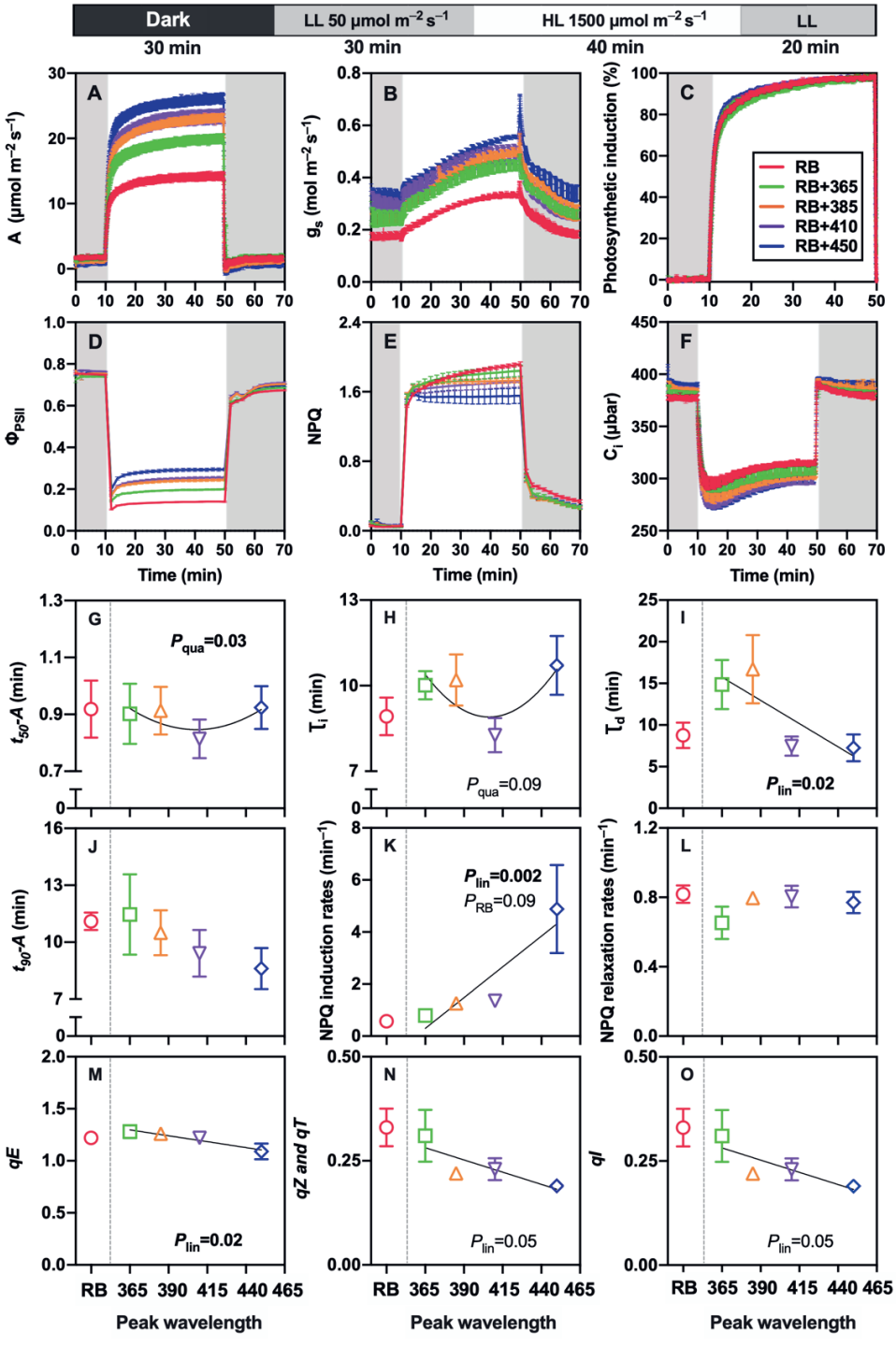
Dark
LL 50 µmol m⁻² s⁻¹
HL 1500 µmol m⁻² s⁻¹
LL
30 min
30 min
40 min
20 min
A
A (µmol m⁻² s⁻¹)
B
gs (mol m⁻² s⁻¹)
C
Photosynthetic induction (%)
RB
RB+365
RB+385
RB+410
RB+450
D
ΦPSII
E
NPQ
F
Ci (µbar)
Time (min)
G
Pqua=0.03
t50-A (min)
H
Ti (min)
Pqua=0.09
I
Td (min)
Plin=0.02
J
t90-A (min)
K
Plin=0.002
PRB=0.09
NPQ induction rates (min⁻¹)
L
NPQ relaxation rates (min⁻¹)
M
qE
Plin=0.02
N
qZ and qT
Plin=0.05
O
qI
Plin=0.05
RB 365 390 415 440 465
Peak wavelength

**Figure 5.** Dynamic photosynthesis, stomatal and photoprotection responses to step changes in light intensity in leaves acclimated to a mixture of red (R; 95 µmol $m^{-2}$ $s^{-1}$) and blue (B; 5 µmol $m^{-2}$ $s^{-1}$) light (RB), as well as additional spectra in the UV-A1 and blue region with an intensity of 50 µmol $m^{-2}$ $s^{-1}$ peaking at 365, 385, 410 and 450 nm (RB+). During all measurements, a spectrum of 90% red and 10% blue light was used. A: net photosynthesis rate (*A*), B: stomatal conductance ($g_s$), C: photosynthetic induction (%), D: photosystem II electron transport efficiency ($\Phi_{PSII}$), E: non-photochemical fluorescence quenching (NPQ), F: leaf internal $CO_2$ partial pressure ($C_i$), G and J: times to reach 50 and 90% of full photosynthetic induction ($t_{50}$-*A* and $t_{90}$-*A*), H and I: time constants of stomatal opening ($\tau_i$) and closure ($\tau_d$), K and L: rate constants of NPQ induction and relaxation; M-O: components of NPQ relaxation, *qE* (energy-dependent quenching), *qZ* (zeaxanthin-dependent quenching) and *qT* (state transition-dependent quenching), *qI* (photoinhibition). Initially dark-adapted leaves (black bar) for 30 min were adapted to 50 µmol $m^{-2}$ $s^{-1}$ for 30 min (grey bars), were then exposed to a sudden increase in light intensity to 1,500 µmol $m^{-2}$ $s^{-1}$ for 40 min (light bars), and were exposed to a sudden decrease in light intensity to 50 µmol $m^{-2}$ $s^{-1}$ (grey bars). Error bars show ± SEM (n = 5, five replicate plants were measured in two batches). SEM is visible only when larger than the symbol size. Significant differences between RB and RB+ treatments are shown as $P_{RB}$. For significant linear ($P_{lin}$) or quadratic ($P_{quad}$) effects of peak wavelength among the RB+ treatments, a trendline together with the respective *P*-value is depicted. Only $P<0.1$ are shown, $P<0.05$ are depicted as bold.

## 3.4 Responses to short-term high light and long-term fluctuating light exposure

Maximum quantum yield of photosystem II ($F_v/F_m$) was assessed before and after HL (1500 $m^{-2}$ $s^{-1}$) exposure for 30 min, as well as during a 5-day FL exposure (Figs. 6, 7F). Before exposure to HL, $F_v/F_m$ in leaves of most treatments was >0.8, except for RB+365, which had a value of only 0.76 (Fig. 6A). Additionally, RB+ treated leaves showed a strong positive linear relationship between peak wavelength and $F_v/F_m$ (Fig. 6A). After HL exposure, $F_v/F_m$ in leaves of all treatments was reduced, while the mentioned linear relationship among RB+ treated leaves was still apparent (Fig. 6A). Additionally, we observed that thetreatment effect on the extent of $F_v/F_m$ reduction under HL was not significant (Fig. 6B).

When plants were transferred to FL for five days, we noted an interaction between light spectrum treatments and the duration of FL exposure ($P<0.001$; Fig. 7F): notably, $F_v/F_m$ in leaves treated without UV-A1 was consistently above 0.8 during the 5-day FL exposure, while $F_v/F_m$ in RB+365 treated leaves started at 0.78 and gradually increased towards 0.81, which was a little higher than RB+385 (~0.8) at the 5-day FL exposure (Fig. 7F). Besides, RB treated leaves suffered a reduction in $F_v/F_m$ on days 3 and 5, and thus did not recover during FL exposure, while blue light treated leaves never showed a reduction during FL exposure (Fig. 7F).

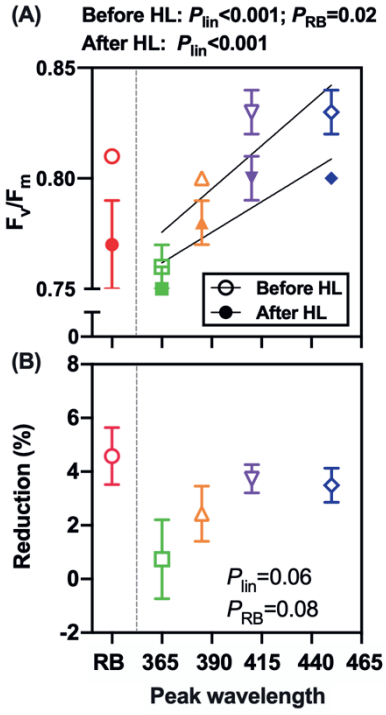


**Figure 6.** Maximum quantum yield of photosystem II ($F_v/F_m$) and its reduction after HL exposure for 30 min. A: $F_v/F_m$ before and after HL exposure; B: Percentage reduction in $F_v/F_m$ due to HL exposure. Plants were acclimated to a mixture of red (R; 95 µmol $m^{-2}$ $s^{-1}$) and blue (B; 5 µmol $m^{-2}$ $s^{-1}$) light (RB), as well as additional spectra in the UV-A1 and blue region with an intensity of 50 µmol $m^{-2}$ $s^{-1}$ peaking at 365, 385, 410 and 450 nm (RB+). After acclimation for 13 days, plants were exposed to a high light intensity (1500 µmol $m^{-2}$ $s^{-1}$) for 30 min. Error bars show ± SEM (n = 12, replicate plants were measured in two separate batches (six plants per batch). SEM is visible only when larger than the symbol size. Significant differences between RB and RB+ treatments are shown as $P_{RB}$. For significant linear effects ($P_{lin}$) of peak wavelength among the RB+ treatments, a trendline together with the respective *P*-value is depicted. Only *P*<0.1 are shown, *P*<0.05 are depicted as bold.

Leaf photosynthetic traits were also assessed during 5-day FL exposure, along with growth traits measured before and after FL exposure (Figs. 7; S5). Values of $A$, $g_s$ and $\Phi_{PSII}$ measured at high irradiance ($A_{1000}$, $g_{s1000}$, $\Phi_{PSII1000}$) in leaves acclimated to RB started out much lower than those of all other treatments, but increased steadily as exposure time to FL progressed (Figs. 7A, D; S5). In contrast, $A$ measured at 150 µmol $m^{-2}$ $s^{-1}$ showed no significant differences between treatments (Fig. 7B), while no interaction between light spectrum treatments and duration of FL exposure was observed on $\Phi_{PSII150}$ (Fig. 7E). $R_{dark}$ was initially significantly smaller in RB and RB+365 treated leaves, but similarly to $A_{1000}$ and $\Phi_{PSII1000}$, this difference

disappeared with duration of FL exposure (Fig. 7C). In addition, shoot dry weight, leaf area, and dry mass content increased, and SLA decreased, in all treatments during FL exposure (Fig. 7G, H, I, L). The increase in shoot dry weight was significantly smaller ($P$=0.01), and the increase in leaf area was not significant, in RB compared to RB+ treated leaves (Fig. 7G, H). Nevertheless, there was no significant treatment effect on the percentage change in shoot dry weight or leaf area (Fig. 7J, K).

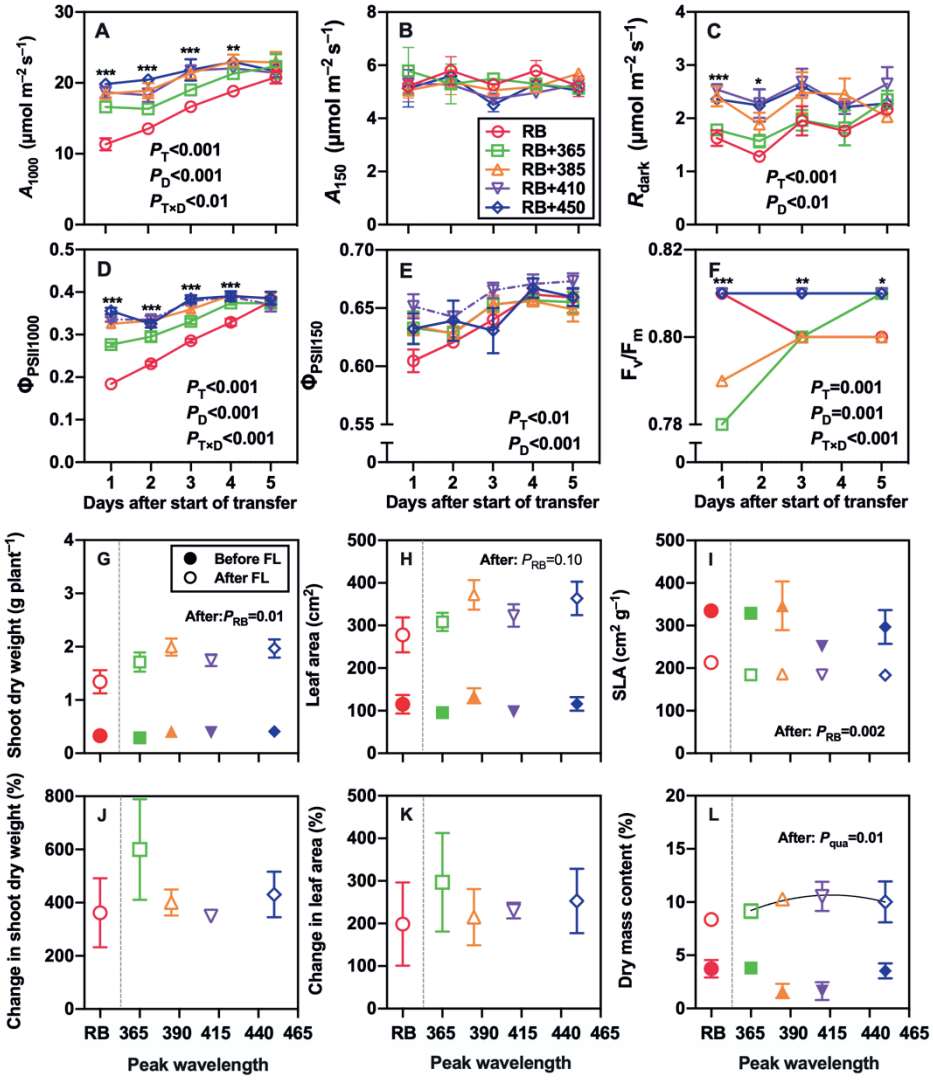


**Figure 7.** Leaf photosynthesis and growth traits of plants acclimated to various light spectra in response to FL exposure. Plants were initially acclimated to a mixture of red (R; 95 µmol $m^{-2}$ $s^{-1}$) and blue (B; 5 µmol $m^{-2}$ $s^{-1}$) light (RB), as well as additional spectra in the UV-A1 and blue region with an intensity of 50 µmol $m^{-2}$ $s^{-1}$ peaking at 365, 385, 410 and 450 nm (RB+), for 10 days. Thereafter, they were transferred to FL exposure for 5 days. For gas exchange measurements, a spectrum of 90% red and 10% blue light was used. A: net leaf photosynthesis rate at 1000 µmol $m^{-2}$ $s^{-1}$ ($A_{1000}$), B: net leaf photosynthesis rate at 150 µmol $m^{-2}$ $s^{-1}$ ($A_{150}$), C: dark respiration rate ($R_{dark}$), D: photosystem II electron transport efficiency at 1000 µmol $m^{-2}$ $s^{-1}$ ($\Phi_{PSII1000}$), E: $\Phi_{PSII}$ measured at 150 µmol $m^{-2}$ $s^{-1}$ ($\Phi_{PSII150}$), F: maximum quantum yield of photosystem II ($F_v/F_m$), G: shoot dry weight, H: leaf area, I: specific leaf area (SLA), J-K: increase of shoot dry weight and leaf area before and after FL exposure, respectively, L: dry mass content. Error bars show ± SEM (n = 6, six replicate plants measured in two batches, i.e. three plants per batch). Two-way ANOVA was performed for each parameter, and

the *P*-value of the main effect of treatment ($P_T$) and days after start of treatment ($P_D$), as well as the interaction effect of the two factors ($P_{T\times D}$), is shown. Asterisks indicate the significance among treatments on the given day after FL exposure (∗*P*<0.05, ∗∗*P*<0.01, ∗∗∗*P*<0.001). Significant differences between RB and RB+ treatments are shown as $P_{RB}$. For significant quadratic ($P_{quad}$) or linear effects ($P_{lin}$) of peak wavelength among the RB+ treatments, a trendline together with the respective *P*-value is depicted. Only *P*<0.1 are shown, *P*<0.05 are depicted as bold.

# 4. Discussion

UV-A radiation is a significant component of sunlight, but its effects on plant biology, including photosynthetic acclimation to UV-A, are poorly understood. We investigated how acclimation to UV-A1 (350-400 nm) radiation affects leaf photosynthetic traits (steady and dynamic) and photoprotective capacities as well as plant morphology and growth, compared to acclimation to blue light. We found that additional UV-A1 and blue light affected steady-state photosynthesis and photoprotective traits in a wavelength-dependent manner such that, generally, the effects of UV-A1 were weaker than those of blue light.

## 4.1 Shallow gradient response in leaf photosynthetic acclimation and plant morphology within the UV-A1 and blue light wavebands

We confirmed our first hypothesis, namely that radiation in the UV-A1 range is effective in triggering photosynthetic acclimation and changes in plant morphology, however to a lesser extent than blue light. Firstly, relative to the RB treatment (100 µmol $m^{-2}$ $s^{-1}$; 95% red and 5% blue), many traits of the RB+ treatments (RB plus 50 µmol $m^{-2}$ $s^{-1}$) were considerably increased (Figs. 2-5), signifying strong effects of the additional 50 µmol $m^{-2}$ $s^{-1}$ PFD in the 365-450 nm range. Secondly, among the RB+ treatments, we observed in many traits significant linear correlations with peak wavelength: these were found in shoot biomass and dry mass content, apparent leaf thickness (i.e., specific leaf area) and leaf light absorption, chlorophyll and carotenoid concentrations (though not other pigments), photosynthetic capacity and stomatal conductance ($g_s$), as well as NPQ and $F_v/F_m$ (Figs. 2-7). Also, a major component of NPQ, *qE*, showed significant a linear correlation with peak wavelength (Fig. 5M). From this comprehensive collection of traits at various integration levels emerges a general picture that suggests the following: generally, no qualitative difference seems to exist for plants between

UV-A1 and blue light – if it did, one would expect to see stark differences in phenotypes under one waveband compared to the other. Instead, plants respond in a continuous fashion to the peak wavelength that they are exposed to.

How can these linear responses in the 365-450 nm range be explained? Given that UV-A1 and blue light share the same photoreceptors, namely phototropins and cryptochromes (Rai et al., 2021), these are unlikely to account for the response gradients observed here. More likely, these responses are related to the molecular mechanisms of photosynthetic acclimation, which is strongly driven by retrograde signals that are predominantly produced in photosynthesizing chloroplasts, and sensed in the nucleus (Bräutigam et al., 2009; Dietz, 2015). Because of wavelength-selective screening of light in the epidermis by flavonoids and other phenylpropanoids ('sunscreen pigments'), the epidermal transmittance for UV radiation is very low: In a survey of 37 species, Barnes et al. (2016) observed that epidermal UV transmittance ranged from ~5-25%, which implies that most UV radiation does not reach the chloroplasts. Furthermore, in isolated chloroplasts, absorbance in the 350-450 nm range was linearly and negatively correlated with wavelength (Merzlyak et al., 2009), meaning that even without sunscreen pigments, chloroplasts absorb much more light at 450 nm than at 365 nm. Together, these results would imply that rates of photosynthetic electron transport in each photosynthesizing cell are reduced the lower the peak wavelength in the 365-450 nm range is, in turn leading to gradual suppression of retrograde signaling and thus photosynthetic acclimation. However, the molecular mechanisms underlying UV-A1 vs. blue light acclimation are relatively unknown, and future work with e.g. retrograde signaling mutants (e.g. Leister, 2012) may shed more light on this matter.

Despite the many differences in morphological and physiological traits between RB and RB+ treated plants, plant growth under the RB treatment was not different from those of the RB+ treatments (Fig. 2B, 7G). This lack of a difference is likely partially caused by the relatively short treatment duration (10-14 days), which may have masked any treatment effects on growth rate. Moreover, we recently showed that the addition of UV-A1 radiation (peaking at 365 nm) to low (150 $m^{-2}$ $s^{-1}$) or high (550 $m^{-2}$ $s^{-1}$) intensities of white light barely affected growth in a number of horticultural species (including tomato) and the model plant Arabidopsis thaliana

(Sun et al., 2023). These results suggest that even though it powers photosynthesis (Johnson & Day, 2002; Mantha et al., 2001; McCree, 1971; Sun et al., 2024), UV-A1 is also stressful for plants (Fig. 6A). The carbon gain due to addition of UV-A1 radiation may be outweighed by the stress that UV-A1 radiation imposes on plants in the form of photoinhibition (see below).

## 4.2 UV-A1 and blue light wavebands barely affect dynamic leaf photosynthetic traits

Acclimation to the various wavelengths clearly affected steady-state photosynthesis traits related to photosynthetic capacity (Fig. 4), but barely affected dynamic photosynthesis traits (Fig. 5). This general lack of treatment effects on the rate of photosynthetic induction (Fig. 5C, G, J; S3) confirms our second hypothesis, and aligns well with previous research, which showed very limited effects of acclimation to far-red and various red/blue ratios on photosynthetic induction (Ernstsen et al., 1999; Kang et al., 2021; Zhang et al., 2019). From a different point of view, this lack of treatment effects is nevertheless surprising, given that the treatments had relatively large effects on both steady-state (Fig. S2) and dynamic $g_s$ (Fig. 5B).

Photosynthetic induction proceeded relatively quickly in all treatments here (Fig. 5C), resulting in small average values for $t_{50\text{-}A}$ (~1 min) and $t_{90\text{-}A}$ (~10 min; Fig. 5G, J). These values are similar to those published by Kaiser et al. (2017b, 2020) and Zhang, Y. et al. (2022), who reported values of 1-1.5 min and 7.5-11 min for $t_{50\text{-}A}$ and $t_{90\text{-}A}$ of young, unstressed tomato leaves, but which are somewhat smaller compared to Zhang, N. et al. (2022, 2024) and Shao et al. (2024), who reported 2-3.5 min and 15-20 min for $t_{50\text{-}A}$ and $t_{90\text{-}A}$, respectively. These six studies and our current study used similar environmental conditions during dark/low light adaptation and measurements, so differences in these values are unlikely to be caused by experimental protocols. Also, a range of different tomato cultivars was used in these studies. While we cannot be sure what caused the differences in photosynthetic induction rates between these studies, two possible answers lie in genotypic effects and leaf age: among three tomato cultivars, Zhang, N. et al. (2022) observed ranges of 3-5 min for $t_{50\text{-}A}$ and 15-20 min for $t_{90\text{-}A}$ (such variation was even stronger for different cultivars of e.g. *Chrysanthemum*, showing ranges of 2-8 and 20-30 min for $t_{50\text{-}A}$ and $t_{90\text{-}A}$, respectively). As for leaf age, Zhang, Y. et al. (2022) observed progressive

increases from 1 to 2 min for $t_{50\text{-}A}$ and 10-25 min for $t_{90\text{-}A}$ as leaves aged.

## 4.3 UV-A1 radiation induces photoinhibition and enhances plant resilience to high light, but blue light is most effective in protecting plants from high and fluctuating light

Due to its short wavelength, we hypothesized that UV-A1 radiation would cause stronger photoinhibition than blue light (Takahashi et al., 2010), and may lead to stronger photoprotective capacity. The first part of this hypothesis could clearly be proven, based on initial $F_v/F_m$ data before exposure to high (Fig. 6A) as well as fluctuating light (Fig. 7F): in both cases, $F_v/F_m$ was linearly related to peak wavelength, with the lowest values observed under the RB+365 treatment. As for the second part of the hypothesis, we found that RB+365 treated leaves showed an interesting combination of high NPQ under high light (Fig. 5E), as well as high values for NPQ components (Fig. 5M-O), coupled with a small (although not significantly different from other treatments) reduction in $F_v/F_m$ during 30 min high light exposure (Fig. 6A) and a strong increase in $F_v/F_m$ when undergoing acclimation to fluctuating light (FL; Fig. 7F). RB+385 treated leaves showed similar tendencies, but less strongly (Figs. 5-7) compared with RB+365 treated leaves. Conversely, RB+450 treated leaves increased NPQ most quickly after a shift from low to high light intensity (Fig. 5K), and both RB+410 and RB+450 treated leaves had large values of $F_v/F_m$ before and after high light exposure (Fig. 6A), as well as during the entire time course of acclimation to FL (Fig. 7F). Thus, based on our data we cannot clearly conclude that acclimation to UV-A1 radiation resulted in a greater photoprotective capacity than acclimation to blue light, and we suggest that further studies on the topic are needed.

Plants grown under RB showed no significant difference in the reduction of $F_v/F_m$ when exposed to HL compared to RB+ treatments. One may speculate, however, that under longer exposure to HL, these differences between treatments would have been exacerbated. This speculation can be supported by the FL experiment, which showed a reduction of $F_v/F_m$ throughout the 5 day FL exposure in RB grown plants, whereas in all other treatments, $F_v/F_m$ was either constant (blue light acclimated plants) or increased (UV-A1 acclimated plants; Fig. 7F). Additionally, photosynthetic capacity ($A_{sat}$) was initially lowest in RB treated plants, and

almost double while linearly increasing during FL exposure (Fig. 7A), all the while 'losing out' on high rates of $CO_2$ assimilation during high light intensity events (Fig. 5A) imposed by the FL pattern (Fig. 1B). In fact, FL exposure was so stressful, and high light events (Fig. 7B) were so inefficiently used, that RB treated plants ended up having reduced shoot dry weight and leaf area, compared to RB+ treatments, despite the fact that before the start of FL exposure there had been no differences for these traits between treatments (Fig. 7G, H). It should be emphasized here that during FL exposure, all plants received the same light sum, so differences in growth rate are solely related to different initial acclimation states due to prior RB and RB+ treatments.

To what extent did the various RB+ treatments prepare plants for FL? Judging from data related to photosynthetic capacity and photoinhibition (Fig. 7A, D, F), both blue light treatments were clearly most effective in that role, confirming previous research (Kang et al., 2021). In contrast, UV-A1 and RB treated leaves lacked photosynthetic capacity initially, but managed to increase it during five days of FL exposure (Fig. 7A, D). The fact that $F_v/F_m$ in UV-A1 treated leaves was initially lowest but increased during FL exposure, whereas $F_v/F_m$ declined in RB treated leaves (Fig. 7F), suggests that the rate of photoinhibition was lower under FL exposure than in the UV-A1 treatment, but was higher than in the RB treatment. Additionally (or alternatively), this may suggest that UV-A1 treated leaves were able to acclimate their photoprotective capacity more quickly to FL than RB treated leaves were.

# 5. Conclusions

Unlike people, plants do not categorize light into different, distinct colors. This was nicely exemplified by many traits tested here responding in a continuous linear manner to light treatments within the 365-450 nm range, rather than exhibiting sharp differences between UV-A1 and blue light. Also, effects of the RB+385 and the RB+410 treatments were undistinguishable for most traits (Figs. 2-5, 7), despite the fact that 385 nm is in the UV-A1 range and 410 nm is part of blue light. This is a reminder that categories that are based on human vision (e.g. blue, green, yellow, red) can be distracting when studying plant-environment interactions. As understandable as such categories are as mental shortcuts, they

can be misleading. At the very least, scientists should provide information of the light spectrum used when reporting on the effects of any 'light color' on plant biology. Also, our results are a reminder that a 'full' array of peak wavelengths is very likely more informative than only using one peak wavelength per light color (see also Battle et al., 2020; Chen et al. 2024): for example, if in the current experiment, we had only used one blue (e.g. 450 nm) and one UV-A1 (e.g. 365 nm) light source, we would have likely drawn very different conclusions than we have using a gradient of four peak wavelengths.

# References


Acevedo-Siaca, L. G., Coe, R., Wang, Y., Kromdijk, J., Quick, W. P., & Long, S. P. (2020). Variation in photosynthetic induction between rice accessions and its potential for improving productivity. *New Phytologist*, *227*(4), 1097–1108. https://doi.org/10.1111/nph.16454

Baker, N. R. (2008). Chlorophyll fluorescence: A probe of photosynthesis in vivo. *Annual Review of Plant Biology*, *59*, 89–113. https://doi.org/10.1146/annurev.arplant.59.032607.092759

Barnes, P. W., Flint, S. D., Tobler, M. A., & Ryel, R. J. (2016). Diurnal adjustment in ultraviolet sunscreen protection is widespread among higher plants. *Oecologia*, *181*(1), 55–63. https://doi.org/10.1007/s00442-016-3558-9

Battle, M. W., Vegliani, F., & Jones, M. A. (2020). Shades of green: Untying the knots of green photoperception. *Journal of Experimental Botany*, *71*(19), 5764–5770. https://doi.org/10.1093/jxb/eraa312

Bräutigam, K., Dietzel, L., Kleine, T., Ströher, E., Wormuth, D., Dietz, K. J., Radke, D., Wirtz, M., Hell, R., Dörmann, P., Nunes-Nesi, A., Schauer, N., Fernie, A. R., Oliver, S. N., Geigenberger, P., Leister, D., & Pfannschmidt, T. (2009). Dynamic plastid redox signals integrate gene expression and metabolism to induce distinct metabolic states in photosynthetic acclimation in Arabidopsis. *Plant Cell*, *21*(9), 2715–2732. https://doi.org/10.1105/tpc.108.062018

Brelsford, C. C., Morales, L. O., Nezval, J., Kotilainen, T. K., Hartikainen, S. M., Aphalo, P. J., & Robson, T. M. (2019). Do UV-A radiation and blue light during growth prime leaves to cope with acute high light in photoreceptor mutants of Arabidopsis thaliana? *Physiologia Plantarum*, *165*(3), 537–554. https://doi.org/10.1111/ppl.12749

Busch, F. A., Ainsworth, E. A., Amtmann, A., Cavanagh, A. P., Driever, S. M., Ferguson, J. N., Kromdijk, J., Lawson, T., Leakey, A. D. B., Matthews, J. S. A., Meacham-Hensold, K., Vath, R. L., Vialet-Chabrand, S., Walker, B. J., & Papanatsiou, M. (2024). A guide to photosynthetic gas exchange measurements: Fundamental principles, best practice and potential pitfalls. *Plant Cell and Environment*, *December 2023*. https://doi.org/10.1111/pce.14815

Cannell, M. G. R., & Thornley, J. H. M. (1998). Temperature and $CO_2$ responses of leaf and canopy photosynthesis: a clarification using the non-rectangular hyperbola model of photosynthesis. *Annals of Botany*, *82*(6), 883–892. https://doi.org/10.1006/anbo.1998.0777

Chen, Y., Li, T., Yang, Q., Zhang, Y., Zou, J., Bian, Z., & Wen, X. (2019). UVA radiation is beneficial for yield and quality of indoor cultivated lettuce. *Frontiers in Plant Science*, *10*. https://doi.org/10.3389/fpls.2019.01563

Dietz, K. J. (2015). Efficient high light acclimation involves rapid processes at multiple mechanistic levels. *Journal of Experimental Botany*, *66*(9), 2401–2414. https://doi.org/10.1093/jxb/eru505

Durand, M., & Robson, T. M. (2023). Fields of a thousand shimmers: canopy architecture determines high-frequency light fluctuations. *New Phytologist*, *238*(5), 2000–2015. https://doi.org/10.1111/nph.18822

Ernstsen, J., Woodrow, I. E., & Mott, K. A. (1999). Effects of growth-light quantity, growth-light quality and $CO_2$ concentration on Rubisco deactivation during low PFD or darkness. *Photosynthesis Research*, *61*(1), 65–75. https://doi.org/10.1023/A:1006289901858

Fankhauser, C., & Chory, J. (1997). Light Control of Plant Development. *Annual Review of Cell and Developmental Biology, 13*(1)*,* 203–229. *https://doi.org/10.1146/annurev.cellbio.13.1.203*

Ferguson, J. N., Jithesh, T., Lawson, T., & Kromdijk, J. (2023). Excised leaves show limited and species-specific effects on photosynthetic parameters across crop functional types. *Journal of Experimental Botany*, *74*(21), 6662–6676. https://doi.org/10.1093/jxb/erad319

Franklin, K. A. (2008). Shade avoidance. *New Phytologist*, *179*(4), 930–944. https://doi.org/10.1111/j.1469-8137.2008.02507.x

Harley, P. C., Loreto, F., Marco, G. Di, & Sharkey, T. D. (1992). Theoretical considerations when estimating the mesophyll conductance to $CO_2$ flux by analysis of the response of photosynthesis to $CO_2$. *Plant Physiology*, *98*(4), 1429–1436. https://doi.org/10.1104/pp.98.4.1429

Hoffmann, A. M., Noga, G., & Hunsche, M. (2015). High blue light improves acclimation and photosynthetic recovery of pepper plants exposed to UV stress. *Environmental and Experimental Botany*, *109*, 254–263. https://doi.org/10.1016/j.envexpbot.2014.06.017

Hogewoning, S. W., Trouwborst, G., Maljaars, H., Poorter, H., van Ieperen, W., & Harbinson, J. (2010). Blue light dose-responses of leaf photosynthesis, morphology, and chemical composition of Cucumis sativus grown under different combinations of red and blue light. *Journal of Experimental Botany*, *61*(11), 3107–3117. https://doi.org/10.1093/jxb/erq132

Jiang, B., Zhong, Z., Gu, L., Zhang, X., Wei, J., Ye, C., Lin, G., Qu, G., Xiang, X., Wen, C., Gateas, M., Bailey-Serres, J., Wang, Q., He, C., Wang, X., & Lin, C. (2023). Light-induced LLPS of the CRY2/SPA1/FIO1 complex regulating mRNA methylation and chlorophyll homeostasis in Arabidopsis. *Nature Plants* , *9*(12), 2042–2058. https://doi.org/10.1038/s41477-023-01580-0

Johnson, G. A., & Day, T. A. (2002). Enhancement of photosynthesis in Sorghum bicolor by ultraviolet radiation. *Physiologia Plantarum*, *116*(4), 554–562. https://doi.org/10.1034/j.1399-3054.2002.1160415.x

Kaiser, E., Morales, A., Harbinson, J., Heuvelink, E., Prinzenberg, A. E., & Marcelis, L. F. (2016). Metabolic and diffusional limitations of photosynthesis in fluctuating irradiance in Arabidopsis thaliana. *Scientific Reports*, *6*(1). https://doi.org/10.1038/srep31252

Kaiser, E., Kromdijk, J., Harbinson, J., Heuvelink, E., & Marcelis, L. F. M. (2017a). Photosynthetic induction and its diffusional, carboxylation and electron transport processes as affected by $CO_2$ partial pressure, temperature, air humidity and blue irradiance. *Annals of Botany*, *119*(1), 191–205. https://doi.org/10.1093/aob/mcw226

Kaiser, E., Kusuma, P., Vialet-Chabrand, S., Folta, K. M., Liu, Y., Poorter, H., Woning, N., Shrestha, S., Ciarreta, A., VanBrenk, J., Karpe, M., Ji, Y., David, S., Zepeda, C., Zhu, X., Huntenburg, K., Verdonk, J. C., Woltering, E., Gauthier, P. P., … Marcelis, L. F. (2024). Vertical farming goes dynamic: optimizing resource use efficiency, product quality, and energy costs. *Frontiers in Plant Sciences*, *September*. https://doi.org/10.3389/fsci.2024.1411259

Kaiser, E., Morales, A., Harbinson, J., Heuvelink, E., & Marcelis, L. F. M. (2020). High Stomatal Conductance in the Tomato Flacca Mutant Allows for Faster Photosynthetic Induction. *Frontiers in Plant Science*, *11*(August), 1–12. https://doi.org/10.3389/fpls.2020.01317

Kaiser, E., Morales, A., Harbinson, J., Kromdijk, J., Heuvelink, E., & Marcelis, L. F. M. (2015). Dynamic photosynthesis in different environmental conditions. *Journal of Experimental Botany*. *66*(9), 2415–2426. https://doi.org/10.1093/jxb/eru406

Kaiser, E., Ouzounis, T., Giday, H., Schipper, R., Heuvelink, E., & Marcelis, L. F. M. (2019). Adding blue to red supplemental light increases biomass and yield of greenhouse-grown tomatoes, but only to an optimum. *Frontiers in Plant Science*, *9*(January), 1–11. https://doi.org/10.3389/fpls.2018.02002

Kaiser, E., Zhou, D., Heuvelink, E., Harbinson, J., Morales, A., & Marcelis, L. F. M. (2017b). Elevated $CO_2$ increases photosynthesis in fluctuating irradiance regardless of photosynthetic induction state. *Journal of Experimental Botany*, *68*(20), 5629–5640. https://doi.org/10.1093/jxb/erx357

Kang, C., Zhang, Y., Cheng, R., Kaiser, E., Yang, Q., & Li, T. (2021). Acclimating Cucumber Plants to Blue Supplemental Light Promotes Growth in Full Sunlight. *Frontiers in Plant Science*, *12*(November), 1–14. https://doi.org/10.3389/fpls.2021.782465

Kelly, N., & Runkle, E. S. (2023). End-of-production Ultraviolet A and blue Light similarly increase lettuce coloration and phytochemical concentrations. *HortScience*, *58*(5), 525–531. https://doi.org/10.21273/HORTSCI17108-23

Khanam, U. K. S., Oba, S., Yanase, E., & Murakami, Y. (2012). Phenolic acids, flavonoids and total antioxidant capacity of selected leafy vegetables. *Journal of Functional Foods*, *4*(4), 979–987. https://doi.org/10.1016/j.jff.2012.07.006

Leister, D. (2012). Retrograde signaling in plants: From simple to complex scenarios. *Frontiers in Plant Science*, *3*(JUN), 1–10. https://doi.org/10.3389/fpls.2012.00135

Liang, Y., Kang, C., Kaiser, E., Kuang, Y., Yang, Q., & Li, T. (2021). Red/blue light ratios induce morphology and physiology alterations differently in cucumber and tomato. *Scientia Horticulturae*, *281*(February), 109995. https://doi.org/10.1016/j.scienta.2021.109995

Lichtenthaler, H. K., & Buschmann, C. (2001). Chlorophylls and carotenoids: Measurement and characterization by UV-VIS spectroscopy. *Current Protocols in Food Analytical Chemistry*, *1*(1), F4.3.1-F4.3.8. https://doi.org/10.1002/0471142913.faf0403s01

Lin, C. (2000). Plant blue-light receptors. *Trends in Plant Science*, *5*(8), 337–342. https://doi.org/10.1016/S1360-1385(00)01687-3

Liu, C. C., Chi, C., Jin, L. J., Zhu, J., Yu, J. Q., & Zhou, Y. H. (2018). The bZip transcription factor HY5 mediates CRY1a-induced anthocyanin biosynthesis in tomato. *Plant Cell and Environment*, *41*(8), 1762–1775. https://doi.org/10.1111/pce.13171

Long, S. P., Taylor, S. H., Burgess, S. J., Carmo-Silva, E., Lawson, T., De Souza, A. P., Leonelli, L., & Wang, Y. (2022). Into the shadows and back into sunlight: Photosynthesis in fluctuating light. *Annual Review of Plant Biology*, *73*, 617–648. https://doi.org/10.1146/annurev-arplant-070221-024745

Mantha, S. V., Johnson, G. A., & Day, T. A. (2001). Evidence from action and fluorescence spectra that UV-induced biolet-blue-green fluorescence enhances leaf photosynthesis¶. *Photochemistry and Photobiology*, *73*(3), 249–256. https://doi.org/10.1562/0031-8655(2001)0730249efaafs2.0.co2

Matsuda, R., Ohashi-Kaneko, K., Fujiwara, K., Goto, E., & Kurata, K. (2004). Photosynthetic characteristics of rice leaves grown under red light with or without supplemental blue light. *Plant and Cell Physiology*, *45*(12), 1870–1874. https://doi.org/10.1093/pcp/pch203

McCree, K. J. (1971). The action spectrum, absorptance and quantum yield of photosynthesis in crop plants. *Agricultural Meteorology*. https://doi.org/10.1016/0002-1571(71)90022-7

Merzlyak, M. N., Chivkunova, O. B., Zhigalova, T. V., & Naqvi, K. R. (2009). Light absorption by isolated chloroplasts and leaves: effects of scattering and "packing". *Photosynthesis Research*, *102*(1), 31–41. https://doi.org/10.1007/s11120-009-9481-8

Miyata, K., Noguchi, K., & Terashima, I. (2012). Cost and benefit of the repair of photodamaged photosystem II in spinach leaves: Roles of acclimation to growth light. *Photosynthesis Research*, *113*(1–3), 165–180. https://doi.org/10.1007/s11120-012-9767-0

Morales, A., & Kaiser, E. (2020). Photosynthetic acclimation to fluctuating irradiance in plants. *Frontiers in Plant Science*, *11*(March), 1–12. https://doi.org/10.3389/fpls.2020.00268

Murchie, E. H., & Niyogi, K. K. (2011). Manipulation of photoprotection to improve plant photosynthesis. *Plant Physiology*, *155*(1), 86–92. https://doi.org/10.1104/pp.110.168831

Poorter, H., Niinemets, Ü., Ntagkas, N., Siebenkäs, A., Mäenpää, M., Matsubara, S., & Pons, T. L. (2019). A meta-analysis of plant responses to light intensity for 70 traits ranging from molecules to whole plant performance. *New Phytologist*, *223*(3), 1073–1105. https://doi.org/10.1111/nph.15754

Rai, N., Morales, L. O., & Aphalo, P. J. (2021). Perception of solar UV radiation by plants: photoreceptors and mechanisms. *Plant Physiology*, *186*(3), 1382–1396. https://doi.org/10.1093/PLPHYS/KIAB162

Rai, N., Neugart, S., Yan, Y., Wang, F., Siipola, S. M., Lindfors, A. V., Winkler, J. B., Albert, A., Brosché, M., Lehto, T., Morales, L. O., & Aphalo, P. J. (2019). How do cryptochromes and UVR8 interact in natural and simulated sunlight? *Journal of Experimental Botany*, *70*(18), 4975–4990. https://doi.org/10.1093/jxb/erz236

Sharkey, T. D. (2016). What gas exchange data can tell us about photosynthesis. *Plant Cell and Environment*, *39*(6),

1161–1163. https://doi.org/10.1111/pce.12641

Sun, X., Kaiser, E., Aphalo, P. J., Marcelis, L. F. M., & Li, T. (2023). Plant responses to UV-A1 radiation are genotype and background irradiance dependent. *Environmental and Experimental Botany*, *219*, 105621. https://doi.org/10.1016/j.envexpbot.2023.105621

Sun, X., Kaiser, E., Zhang, Y., Marcelis, L. F. M., & Li, T. (2024). Quantifying the Photosynthetic Quantum Yield of Ultraviolet-A1 Radiation. *Plant Cell and Environment*, 1–13. https://doi.org/10.1111/pce.15145

Takahashi, S., Milward, S. E., Yamori, W., Evans, J. R., Hillier, W., & Badger, M. R. (2010). The solar action spectrum of photosystem II damage. *Plant Physiology*, *153*(3), 988–993. https://doi.org/10.1104/pp.110.155747

Trouwborst, G., Hogewoning, S. W., van Kooten, O., Harbinson, J., & van Ieperen, W. (2016). Plasticity of photosynthesis after the 'red light syndrome' in cucumber. *Environmental and Experimental Botany*, *121*, 75–82. https://doi.org/10.1016/j.envexpbot.2015.05.002

Turnbull, T. L., Barlow, A. M., & Adams, M. A. (2013). Photosynthetic benefits of ultraviolet-A to Pimelea ligustrina, a woody shrub of sub-alpine Australia. *Oecologia*, *173*(2), 375–385. https://doi.org/10.1007/s00442-013-2640-9

van Delden, S. H., SharathKumar, M., Butturini, M., Graamans, L. J. A., Heuvelink, E., Kacira, M., Kaiser, E., Klamer, R. S., Klerkx, L., Kootstra, G., Loeber, A., Schouten, R. E., Stanghellini, C., van Ieperen, W., Verdonk, J. C., Vialet-Chabrand, S., Woltering, E. J., van de Zedde, R., Zhang, Y., & Marcelis, L. F. M. (2021). Current status and future challenges in implementing and upscaling vertical farming systems. *Nature Food*, *2*(12), 944–956. https://doi.org/10.1038/s43016-021-00402-w

Verdaguer, D., Jansen, M. A. K., Llorens, L., Morales, L. O., & Neugart, S. (2017). UV-A radiation effects on higher plants: Exploring the known unknown. *Plant Science*. *255*, 72–81. https://doi.org/10.1016/j.plantsci.2016.11.014

Vialet-Chabrand, S. R. M., Matthews, J. S. A., McAusland, L., Blatt, M. R., Griffiths, H., & Lawson, T. (2017). Temporal dynamics of stomatal behavior: Modeling and implications for photosynthesis and water use. *Plant Physiology*, *174*(2), 603–613. https://doi.org/10.1104/pp.17.00125

Walters, R. G. (2005). Towards an understanding of photosynthetic acclimation. *Journal of Experimental Botany*, *56*(411), 435–447.https://doi.org/10.1093/jxb/eri060

Wennicke, H., & Schmid, R. (1987). Control of the photosynthetic apparatus of Acetabularia mediterranea by blue Light . *Plant Physiology*, *84*(4), 1252–1256. https://doi.org/10.1104/pp.84.4.1252

Yang, L., Fanourakis, D., Tsaniklidis, G., Li, K., Yang, Q., & Li, T. (2021). Contrary to red, blue monochromatic light improves the bioactive compound content in broccoli sprouts. *Agronomy*, *11*(11). https://doi.org/10.3390/agronomy11112139

Yin, X., Struik, P. C., Romero, P., Harbinson, J., Evers, J. B., Van Der Putten, P. E. L., & Vos, J. (2009). Using combined measurements of gas exchange and chlorophyll fluorescence to estimate parameters of a biochemical C3 photosynthesis model: A critical appraisal and a new integrated approach applied to leaves in a wheat (Triticum aestivum) canopy. *Plant, Cell and Environment*, *32*(5), 448–464. https://doi.org/10.1111/j.1365-3040.2009.01934.x

Zhang, N., Berman, S. R., Joubert, D., Vialet-Chabrand, S., Marcelis, L. F. M., & Kaiser, E. (2022). Variation of photosynthetic iInduction in major horticultural crops is mostly driven by differences in stomatal traits. *Frontiers in Plant Science*, *13*(April), 1–19. https://doi.org/10.3389/fpls.2022.860229

Zhang, N., Berman, S. R., van den Berg, T., Chen, Y., Marcelis, L. F. M., & Kaiser, E. (2024). Biochemical versus stomatal acclimation of dynamic photosynthetic gas exchange to elevated $CO_2$ in three horticultural species with contrasting stomatal morphology. *Plant Cell and Environment*, *July*. https://doi.org/10.1111/pce.15043

Zhang, Y., Kaiser, E., Zhang, Y., Zou, J., Bian, Z., Yang, Q., & Li, T. (2020). UVA radiation promotes tomato growth through morphological adaptation leading to increased light interception. *Environmental and Experimental*

*Botany*. https://doi.org/10.1016/j.envexpbot.2020.104073

Zhang, Y., Sun, X., Aphalo, P. J., Zhang, Y., Cheng, R., & Li, T. (2023). Ultraviolet-A1 radiation induced a more favorable light-intercepting leaf-area display than blue light and promoted plant growth. *Plant Cell and Environment*, *46*(10), 1–16. https://doi.org/10.1111/pce.14727

Zhang, Y., Kaiser, E., Li, T., & Marcelis, L. F. M. (2022). NaCl affects photosynthetic and stomatal dynamics by osmotic effects and reduces photosynthetic capacity by ionic effects in tomato. *Journal of Experimental Botany*, *73*(11), 3637–3650. https://doi.org/10.1093/jxb/erac078

Zhang, Y., Kaiser, E., Zhang, Y., Yang, Q., & Li, T. (2019). Red/blue light ratio strongly affects steady-state photosynthesis, but hardly affects photosynthetic induction in tomato (Solanum lycopersicum). *Physiologia Plantarum*, *167*(2), 144–158. https://doi.org/10.1111/ppl.12876

Zipperlen, S. W., & Press, M. C. (1997). PhotosyntheticiInduction and stomatal oscillations in relation to the light environment of two dipterocarp rain forest Tree Species. *The Journal of Ecology*, *85*(4), 491. https://doi.org/10.2307/2960572

# Supplementary material

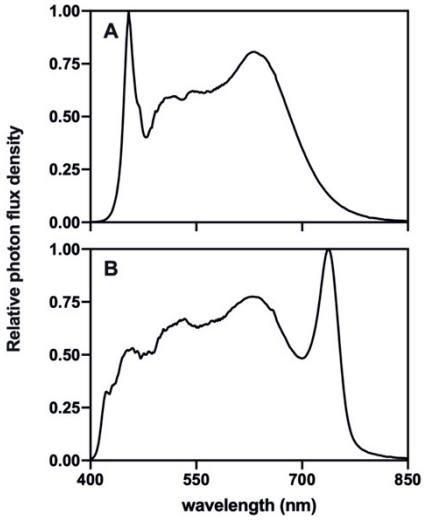


**Figure S1.** Spectral photon irradiance normalized to its maximum in each panel, in light treatments used for germination (A), high light and fluctuating light intensity exposure (B).

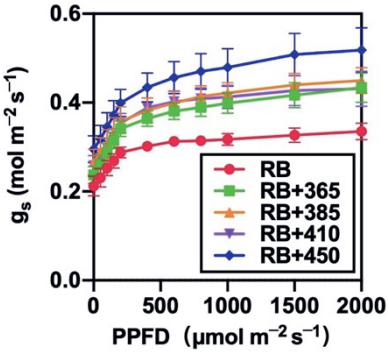


**Figure S2.** Steady-state responses of stomatal conductance (gs) to light intensity in leaves acclimated to different spectra in the UV-A1 and blue region. Error bars show ± SEM (n = 5, five biological replicates measured in two batches). SEM is visible only when larger than the symbol size. For experimental details, see Fig. 4.

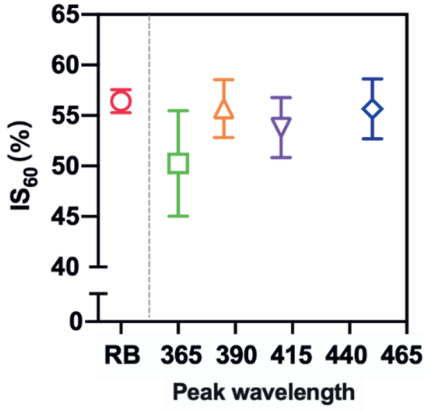


**Figure S3.** Photosynthetic induction state 60 s after light intensity increase ($IS_{60}$) in leaves acclimated to additional spectra in the UV-A1 and blue region. Error bars show ± SEM (n = 5, five biological replicates measured in two separate batches). For experimental details, see Fig. 5.

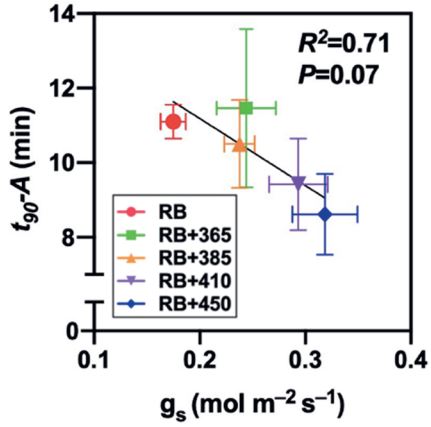


**Figure S4.** Relationship between initial, steady-state stomatal conductance ($g_s$) at low light intensity (50 µmol $m^{-2}$ $s^{-1}$) and the time to reach 90% of full photosynthetic induction ($t_{90\text{-}A}$). Error bars show ± SEM (n = 5, five biological replicates measured in two separate batches). The black line and numbers in the panels represent a linear regression based on the means. For experimental details, see Fig. 5.

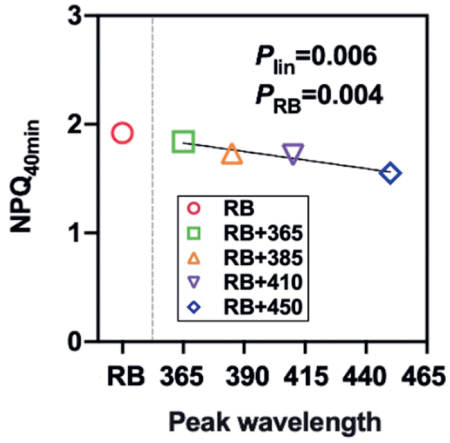


**Figure S5.** Non-photochemical fluorescence quenching (NPQ) reached after 40 minutes of high light exposure in leaves acclimated to different spectra in the UV-A1 and blue region ($NPQ_{40min}$), during photosynthetic induction. Error bars show ± SEM (n = 5, five biological replicates measured in two separate batches). Significant differences between RB and RB+ treatments are shown as $P_{RB}$. For significant linear effects ($P_{lin}$) of peak wavelength among the RB+ treatments, a trendline together with the respective *P*-value is depicted. For experimental details, see Fig. 5.



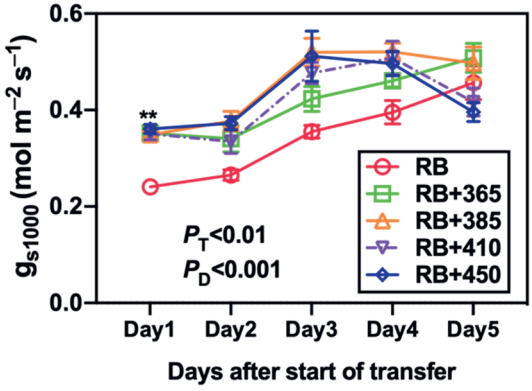


**Figure S6.** Stomatal conductance at 1000 µmol m$^{-2}$ s$^{-1}$ ($g_{s1000}$) in plants pretreated with light spectrum treatments during FL exposure. Error bars show ± SEM (n = 6, six biological replicates measured in two batches). Two-way ANOVA was performed, and the *P*-value of the main effect of treatment ($P_T$) and days after start of treatment ($P_D$), is shown. Asterisks indicate significance among treatments on the given day after fluctuating irradiance exposure (∗*P*<0.05, ∗∗*P*<0.01, ∗∗∗*P*<0.001). For experimental details, see Fig. 7.

**Table S1.** Detailed treatment information for each experiment.

| Experiment | Treatment duration | Type of measurement | No. of growth batches | No. of replicate plants per batch |
|---|---|---|---|---|
| Light spectrum treatments | 14 days | Plant growth | 3 | 6 |
| | | Pigmentation | 3 | 6 |
| | | Photoinhibition | 2 | 6 |
| | 10-13 days | Photosynthesis | 2 | 2 plants in batch 1<br>3 plants in batch 2 |
| High light exposure | 30 min | Photoinhibition | 2 | 6 |
| Fluctuating light exposure | 5 days | Plant growth | 2 | 3 |
| | 1-5 days | Photosynthesis | 2 | 3 |
| | 1, 3, 5 days | Photoinhibition | 2 | 3 |

**Table S2.** Growth traits of tomato plants acclimated to different spectra in UV-A1 and blue region. A mixture of red (R; 95 µmol $m^{-2}$ $s^{-1}$) and blue (B; 5 µmol $m^{-2}$ $s^{-1}$) light was provided as background, 50 µmol $m^{-2}$ $s^{-1}$ light intensity peaking at 365, 385, 410 and 450 nm was added, respectively. Dry mass partitioning to each organ was calculated by dividing dry weight of each organ to total shoot dry weight. Error bars show mean ± SEM (n = 3, each batch represents the mean from 6 individual plants). Significant differences between RB and RB+ treatments are shown as $P_{RB}$. Significant linear effects ($P_{lin}$) of peak wavelength among the RB+ treatments are also shown. Only $P$<0.1 are shown, $P$<0.05 are depicted as bold.

| Parameter | Treatment | | | | | $P_{lin}$ | $P_{RB}$ |
|---|---|---|---|---|---|---|---|
| | RB | RB365 | RB385 | RB410 | RB450 | | |
| **Leaf** | | | | | | | |
| Leaf number | 4.89±0.24 | 5.06±0.20 | 5.06±0.34 | 5.61±0.47 | 5.11±0.31 | | |
| Leaf fresh weight | 4.62±0.89 | 4.6±0.86 | 5.75±0.69 | 5.92±0.92 | 6.33±0.79 | | |
| Leaf dry weight | 0.51±0.06 | 0.51±0.08 | 0.65±0.05 | 0.69±0.07 | 0.78±0.07 | **0.02** | 0.07 |
| **Stem** | | | | | | | |
| Stem fresh weight | 2.52±0.22 | 2.01±0.26 | 2.26±0.07 | 2.36±0.12 | 2.36±0.15 | | |
| Stem dry weight | 0.12±0.01 | 0.10±0.01 | 0.12±0 | 0.13±0 | 0.15±0.01 | **0.001** | |
| **Petiole** | | | | | | | |
| Petiole fresh weight | 2.90±0.47 | 1.97±0.29 | 2.92±0.21 | 3.24±0.29 | 3.30±0.36 | **0.02** | |
| Petiole dry weight | 0.13±0.02 | 0.1±0.01 | 0.14±0.01 | 0.16±0.01 | 0.17±0.01 | **0.004** | |
| **Shoot** | | | | | | | |
| Shoot fresh weight | 10.22±1.39 | 8.76±1.25 | 11.18±0.73 | 11.80±1.03 | 12.29±0.97 | 0.05 | |
| Dry mass partitioning to leaf (%) | 67.20±0.61 | 72.1±0.58 | 71.2±0.73 | 70.20±1.65 | 71.10±0.93 | | **0.01** |
| Dry mass partitioning to stem (%) | 16.0±1.0 | 14.30±0.60 | 13.60±0.98 | 13.90±1.08 | 13.50±0.68 | | 0.052 |
| Dry mass partitioning to petiole (%) | 16.80±0.60 | 13.60±0.15 | 15.20±0.26 | 15.90±0.61 | 15.40±0.32 | **0.02** | **0.004** |

# CHAPTER 4

## Quantifying the photosynthetic quantum yield of ultraviolet-A1 radiation

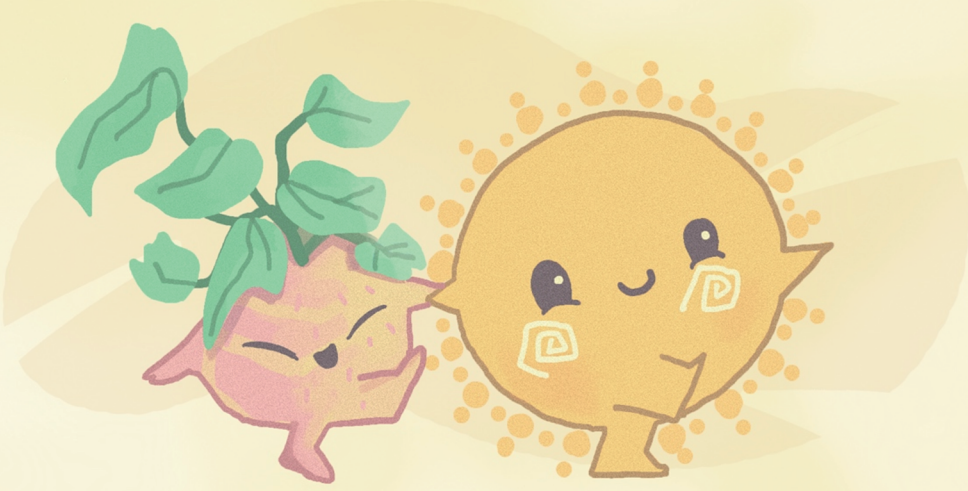

Xuguang Sun, Elias Kaiser, Yuqi Zhang, Leo F. M. Marcelis, Tao Li

*Published in Plant, Cell & Environment (2024)*
*https://doi.org/10.1111/pce.15145*

# Abstract

Although it powers photosynthesis, ultraviolet-A1 radiation (UV-A1) is usually not defined as photosynthetically active radiation (PAR). However, the quantum yield (QY) with which UV-A1 drives net photosynthesis rate (*A*) is unknown, as are the kinetics of *A* and chlorophyll fluorescence under constant UV-A1 exposure. We measured *A* in leaves of six genotypes at four spectra peaking at 365, 385, 410 and 450 nm, at intensities spanning 0-300 μmol $m^{-2}$ $s^{-1}$. All treatments powered near-linear increases in *A* in a wavelength- dependent manner. QY at 365 and 385 nm was linked to the apparent concentration of flavonoids, implicating the pigment in reductions of photosynthetic efficiency under UV-A1; in several genotypes, *A* under 365 and 385 nm was negative regardless of illumination intensity, suggesting very small contributions of UV-A1 radiation to $CO_2$ fixation. Exposure to treatment spectra for 30 min caused slow increases in non-photochemical quenching, transient reductions in *A* and dark-adapted maximum quantum yield of photosystem II, that depended on wavelength and intensity, but were generally stronger the lower the peak wavelength was. We conclude that UV-A1 generally powers *A*, but its definition as PAR requires additional evidence of its capacity to significantly increase whole-canopy carbon uptake in nature.

## Keywords:

UV-A1, photosynthesis, photoinhibition, photosynthetic quantum yield, chlorophyll fluorescence

# 1. Introduction

Ultraviolet-A radiation (UV-A, 315-400 nm) accounts for ~95% of all solar ultraviolet radiation (UV; 280-400 nm) on Earth, amounting to ~5-12% of photosynthetically active radiation (PAR; typically defined as 400-700 nm) (Kerr & Fioletov, 2008; Robson et al., 2019). Although the effects of UV-A on net photosynthesis rate ($A$; μmol $m^{-2}$ $s^{-1}$) have not been studied systematically, it has been shown that UV-A powers $A$ in both algae and higher plants (Halldal, 1964; Johnson & Day, 2002; Mantha et al., 2001; McCree, 1971; McCree & Keener, 1974; Turnbull et al., 2013). In the field, the UV-A present in solar radiation was suggested to increase $A$ by 12% (Turnbull et al., 2013). When measured in the laboratory at non-saturating light intensity, UV radiation produced through the use of cut-off filters below 311 nm enhanced $A$ by only 1%, while narrow-band UV radiation peaking at 340 nm enhanced $A$ by 8~10%, compared with $A$ under 400 nm (Johnson & Day, 2002; Mantha et al., 2001). In addition, McCree observed a relative photosynthetic quantum yield at 375 nm of <0.2, normalized to a maximum at 625 nm of 1.00 (McCree, 1971). However, the intensity of UV-A radiation was not quantified in any of these cases, making it impossible to calculate how efficiently UV-A radiation powers $A$ compared to blue (400-500 nm), green, red or far-red light. Nevertheless, several mechanisms through which UV-A may power $A$ have been proposed: i) Leaves illuminated by UV radiation can emit blue-green fluorescence, which upon re-absorption by chlorophylls and carotenoids can power $A$ (Johnson & Day, 2002; Mantha et al., 2001). Substances emitting blue-green fluorescence upon UV exposure are phenolic compounds, including flavonoids and hydroxycinnamic acids in the epidermis and mesophyll cells (Lang et al., 1991; Mazza et al., 2000). ii) Re-absorption of UV-induced blue-green fluorescence by chloroplasts in guard cells can promote stomatal opening and would thus potentially reduce diffusional limitations on $A$ (Johnson & Day, 2002).

Apart from powering photochemistry, per photon, UV-A can cause high rates of photodamage, due to its short wavelength (Jones & Kok, 1966). Especially when it exceeds the capacity for $CO_2$ fixation, excess radiation can cause the formation of reactive oxygen species (ROS), which tend to attack and damage the D1 protein in photosystem II (PSII), leading to photoinhibition (Li et al., 2009). The most deleterious effect of ROS is photobleaching of

photosynthetic pigments (Kulandaivelu & Noorudeen, 1983; Murchie & Niyogi, 2011). To minimize this damage, plants have developed several photoprotective mechanisms, such as leaf movement to reduce light absorption, accumulation of ROS scavenging compounds, and fast relaxation of dissipative energy processes, also known as non-photochemical quenching (NPQ; Malnoë, 2018; Ruban & Wilson, 2021; Wang et al., 2020). NPQ has multiple components, of which energy-dependent quenching (qE) is usually the major component (Müller et al., 2001). When strongly upregulated, NPQ can compete with photosynthetic electron transport and thereby reduce photosynthetic quantum yield (QY). However, to what extent UV-A radiation induces NPQ and whether this process is wavelength-dependent currently unknown.

It is often assumed that UV-A radiation functions similarly to blue light in mediating plant processes, as both wavebands share several photoreceptors (phototropins and cryptochromes; Lin, 2000), although in a recent study we found that leaf morphology and gene expression were differentially affected by UV-A and blue light (Zhang et al., 2023). Nevertheless, to what extent UV-A and blue light differ in powering *A* and photoinhibition is less well explored. Blue light may alter the impact of UV-A on *A*, as it may help to alleviate photoinhibition induced by UV-A (Hoffmann et al., 2015; Rai et al., 2019), and there may thus be interaction effects on photoinhibition between these two wavebands.

It has recently been suggested to divide UV-A into two regions based on the photoreceptors involved in their sensing: short-wavelength UV-A radiation (315–350 nm, UV-A2) requires UV Resistance Locus 8 (UVR8), whereas long-wavelength UV-A radiation sensing (350–400 nm, UV-A1) requires cryptochromes and phototropins (Rai et al., 2021). Effects of UV-A1 and UV-A2 on *A* remain largely unexplored, and it thus remains to be described how specific wavelengths in these waveband ranges affect QY. Recent advances in LED lighting technology have made it possible to utilize UV-A1 for plant biological research (Chen et al., 2019; Lee et al., 2019; Zhang et al., 2020, 2023). It is also unknown how strongly the effects of UV-A on *A* differ between genotypes. Further, leaf structural acclimation to various growth environments may change their ability to utilize UV-A (Aphalo & Sadras, 2021; Hakala-Yatkin et al., 2010), which may be ascribed to altered concentrations of UV-absorbing compounds in the epidermis (Bidel et al., 2007; Gotz et al., 2010). McCree & Keener (1974) showed that UV-A1 powered *A* in leaves with the epidermis removed. Epidermal tissues filter

out much of the incoming UV radiation, to prevent it from reaching the chloroplasts and thereby causing photodamage (Caldwell et al., 1983; Robberecht & Caldwell, 1978). Thus, higher concentrations of UV-absorbing compounds, such as flavonoids, result in lower UV transmittance of the epidermis (Barnes et al., 2000; Neugart et al., 2021). Nevertheless, it is unknown to what extent the presence of UV-absorbing compounds affects the relationship between UV-A and *A*, and how this relationship differs with that of blue light.

We aimed to quantify QY under various UV-A1 and blue light wavelengths across a range of horticultural crops (cucumber, tomato, and lettuce) and woody species (hydrangea and red dogwood). Further, we explored how *A*, photoinhibition and chlorophyll fluorescence respond to longer-term UV-A1 exposure in cucumber and lettuce, compared to responses under blue light. We hypothesized that QY decreases the shorter the peak wavelength of UV-A1 is, and that upon longer exposure of leaves to UV-A1 radiation, *A* declines, due to progressive build-up of photoinhibition and/or photoprotection. We found that UV-A1 powered photosynthesis in all genotypes tested, but the efficiency of this strongly depended on the concentration of UV-absorbing compounds.



# 2. Materials and methods

## 2.1 Plant material and growth conditions

Seeds of cucumber (*Cucumis sativus* cv. Xiamei No.2, China) and romaine lettuce (*Lactuca sativa* 'Tiberius', Rijk Zwaan, Netherlands) were sown in rockwool plugs (Grodan, Roermond, the Netherlands) and germinated in a growth room at a photosynthetic photon flux density (PPFD) of 100 µmol $m^{-2}$ $s^{-1}$ white light (WL; ZWS01D-LED120-180, PanAnGreenlight, Jinhua, China; for spectra see Fig. S1), a photoperiod of 16 h, day/night temperature of 23.0 ± 0.6 /22.6 ± 0.5 °C, relative humidity (RH) of 70 ± 5 %, and a $CO_2$ partial pressure that was close to ambient. Environmental factors were monitored by a climate sensor (TR-76Ui-S; T&D Co. Ltd., Nagano, Tokyo, Japan). Seedlings were transferred to rockwool cubes (7.5 cm × 7.5 cm × 5 cm; Grodan) upon unfolding of the 1st-2nd true leaf, and then were grown in the same growth room. Growth units with dimensions of 115 cm length × 70 cm width × 115 cm height

were set up. Opaque black-white plastic films were wrapped around each unit, which harbored one treatment, with the white side facing the plants, to avoid light contamination between units. Two ventilation fans (12 V, 0.90 A, 0.5 $m^3$ $min^{-1}$) were installed on both sides of each unit to ensure uniform air circulation. Plants were watered regularly by hand with a modified Hoagland nutrient solution (pH = 5.8, EC = 2.0 dS $m^{-1}$). Every other day, plants inside each treatment were rotated and relocated relative to each other, to avoid position effects on plant growth. Light intensity and spectrum were monitored using a spectroradiometer (Avaspec-2048CL, Avates, Apeldoorn, the Netherlands). The spectroradiometer was calibrated by using a standard light source (Avalight-DH-S-BAL, Avates, Apeldoorn, the Netherlands), which delivers a highly stable, continuous spectrum in the range of 215 to 2500 nm. Most measurements were conducted on plants that had been grown under WL of 100 µmol $m^{-2}$ $s^{-1}$. Additionally, some plants were grown under WL of high intensity (HL; 300 µmol $m^{-2}$ $s^{-1}$), and WL (100 µmol $m^{-2}$ $s^{-1}$) supplemented with UV-A (20 µmol $m^{-2}$ $s^{-1}$; WLUVA20; peak wavelength at 365 nm; ZWS01D-LED120-180, PanAnGreenlight, Jinhua, China; for spectra see Fig. S1). All other growth conditions were identical between growth experiments. When plants were ~4 weeks old (11–14 days after transplanting), the uppermost fully expanded leaf was used for measurements. Many rounds of plants were continuously grown under growth conditions, and plants were randomly chosen for measurements. Per treatment, five biological replicates were used (n = 5, one leaf per plant).

Additional measurements were conducted in April 2024 on four biological replicates each (n=4) of tomato (*Solanum lycopersicum* cv. Moneymaker), butterhead lettuce (*Lactuca sativa* 'Klee', Rijk Zwaan, Netherlands), hydrangea (*Hydrangea macrophylla* L.) and red dogwood (*Cornus alba* L.). Measurements were conducted 43 days after sowing in tomato, and the growth period in the glass greenhouse was from March to April of 2024, at average day/night temperatures of 24.9 / 18.8 °C, and RH of 53 / 71%. Measurements on lettuce 'Klee' were conducted 66 days after sowing, and the growth period in the Chinese solar greenhouse was from February to April of 2024, at average day/night temperatures of 27.3 / 12.3 °C and RH of 49 / 90%. Leaves of hydrangea and red dogwood that had been grown in the open field at the Chinese academy of agricultural sciences campus, Beijing, China, respectively, were collected for measurements.

## 2.2 Treatments

Four separate LED light sources (ZWS01D-LED120-180; PanAnGreenlight, Jinhua, China; for spectra see Fig. 1A) that had adjustable output and different peak wavelengths in the UV-A1 and blue light wavebands were applied for treatments. Lamp output peaked at 365 ± 13 (full width at half maximum), 385 ± 14, 410 ± 16 and 450 ± 20 nm, respectively; we refer to these treatment spectra by their peak wavelength in the remainder of this article. LED lamps were installed in a compartment (Fig. 1C, D) inside the growth room, with the same dimensions as the growth units, such that during measurements, environmental factors apart from light climate remained the same as during growth of chamber-grown plants. Plants were exposed to treatment spectra at a number of intensities and for different durations, depending on the type of measurement conducted (described below; Table 1).

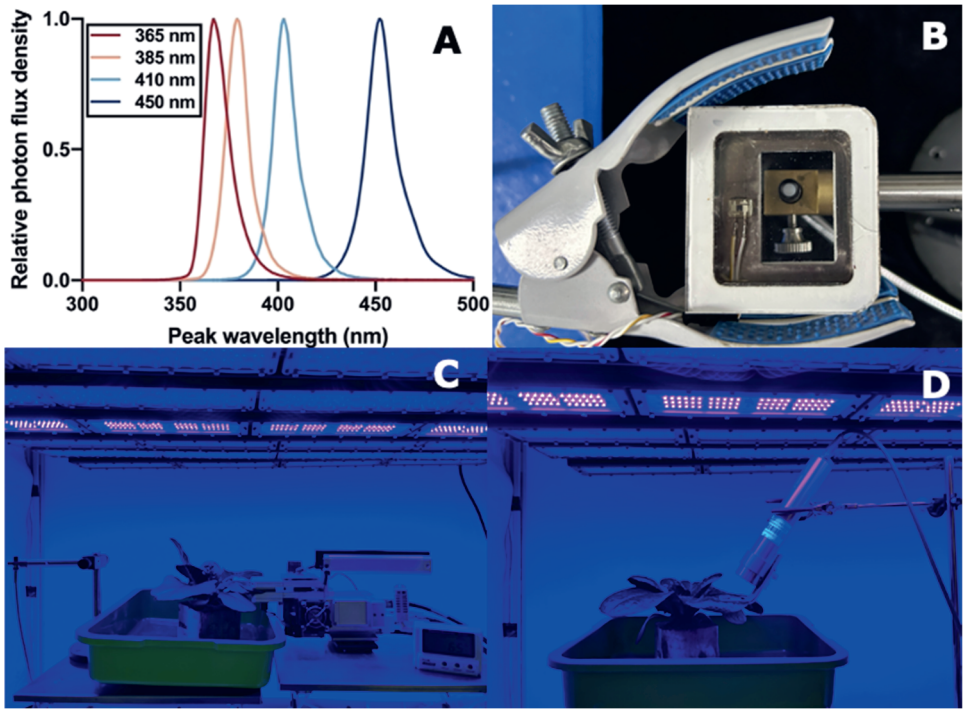


**Figure 1.** Set up of measurements of photosynthesis and chlorophyll fluorescence. (A) Spectra of the treatment lamps used in this study; (B) Leaf chamber with transparent quartz cover and instantaneous light intensity measured via the spectroradiometer (Avaspec-2048CL, Avates, Apeldoorn, the Netherlands); (C) Measurement of leaf gas exchange: LI-6400 portable gas exchange system (Li-Cor Biosciences, Lincoln, Nebraska, USA); (D) Set-up of monitoring PAM fluorometer (Heinz Walz GmbH, Effeltrich, Germany). *Note*: Pictures in C and D were photographed under the 410 nm treatment.

**Table 1.** Overview of growth environments, genotypes and measurements in the experimental setup.

| Growth environment | Genotype | Type of measurement | | | |
|---|---|---|---|---|---|
| | | light response curve | Time course of photosynthesis | Chlorophyll fluorescence | Flavonoid indices |
| Climate chamber | Cucumber | ✓ | ✓ | ✓ | |
| | Lettuce 'Tiberius' | ✓ | ✓ | ✓ | |
| Greenhouse | Lettuce 'Klee' | ✓ | | | ✓ |
| | Tomato | ✓ | | | ✓ |
| Field | Hydrangea | ✓ | | | ✓ |
| | Red dogwood | ✓ | | | ✓ |

## 2.3 Measurements

### *2.3.1 Photosynthetic gas exchange*

In chamber-grown plants, when plants were ~4 weeks old (11-14 days after transplanting), the uppermost fully expanded leaf was used for measurements. In greenhouse-grown plants, pots of lettuce 'Klee' and rockwool cubes of tomato were randomly brought to the laboratory just before measurements. In field-grown plants, 20 cm long shoots collected from hydrangea and red dogwood were cut under water in a plastic bag and transported to the laboratory, and were measured within 1 h. Only leaf material from well-watered plants was used, and all measurements were conducted on the uppermost, fully expanded and vertically orientated leaves. Photosynthetic gas exchange was measured using the LI-6400XT photosynthesis system (Li-Cor Biosciences, Lincoln, Nebraska, USA), which was placed inside the treatment setup (Fig. 1C). The transparent leaf cuvette was used, and its standard plastic cover was replaced by a 2 mm thick quartz plate, to allow for UV-A1 to reach the leaf surface. At 365 nm, the transmittance was 83%, while at the other three wavelengths, it was 91%; these differences in transmittance were accounted for when conducting photosynthetic gas exchange measurements. Light intensity and spectrum inside the cuvette were measured using a spectroradiometer (Avaspec-2048CL; Fig. 1B). During measurements, $CO_2$ partial pressure was 400 µbar (unless specified otherwise), leaf temperature was 25 °C, leaf-to-air vapor

pressure deficit was 0.7–1.0 kPa, the flow rate of air through the system was 200 μmol $s^{-1}$, and the duration of internal data averaging in the system was 4 s. To eliminate the effect of the time of day on *A*, the order of measurements was fully randomized between replicates and measurement protocols.

To assess QY of *A* under the treatment spectra, leaves were exposed to light intensities in the 0-300 μmol $m^{-2}$ $s^{-1}$ range, at 25-50 μmol $m^{-2}$ $s^{-1}$ increments. Upon reaching steady-state *A* (~3 min per step), gas exchange parameters were logged every 10 s for 1 min, and averages of these values were determined per replicate. QY was calculated as the slope ($R^2$: 0.80-0.99 in all cases) of the light response curve of *A* at low light intensities ranging from 50 to 200 μmol $m^{-2}$ $s^{-1}$, and was expressed in μmol $CO_2$ / μmol photons; intensities below 50 μmol $m^{-2}$ $s^{-1}$ were excluded to avoid the 'Kok effect', which strongly affects the slope of *A* vs. light intensity in the 0-30 μmol $m^{-2}$ $s^{-1}$ range (Evans, 1987; Tcherkez et al., 2017). The percentage difference between QY at 450 nm ($QY_{450}$) and QY at 365 nm ($QY_{365}$) was calculated as: $\Delta QY_{450\text{-}365} = ((QY_{450}\text{-}QY_{365})/QY_{450})*100$. Percentage differences between $QY_{450}$ and $QY_{385}$, $QY_{410}$ were done analogously.

To assess how *A* changes when exposed to a stable UV-A1 intensity in isolation or combination with background light in chamber-grown plants, leaves were inserted in the Li-6400 cuvette and either kept in the dark, or illuminated with white background light (100 μmol $m^{-2}$ $s^{-1}$), for ~5 min. Treatment LED lamps were then turned on in a step change (intensity: 100 or 300 μmol $m^{-2}$ $s^{-1}$), and gas exchange was logged every 10 s, for 30 min, after which treatment lights were again turned off. In some cases, leaves were then exposed to background light for another 10 min, to follow the recovery of *A* after treatment lights had turned off. [$CO_2$] in the cuvette was 400 or 1500 μbar, depending on experiment. Several traits were quantified from time courses of *A* under treatment light exposure: the largest value of *A* reached during treatment light exposure ($A_{high}$); final *A* after 30 min of treatment light exposure ($A_{final}$); difference between $A_{high}$ and $A_{final}$ (Reduction); time to reach $A_{high}$ during treatment light exposure (time); and average *A* during the 30 min treatment ($A_{avgL}$). To assess the recovery of *A* when the treatment lamps were off and leaves were illuminated with white light, the average value of *A* during the last 5 min of white light exposure was determined ($A_{avgE}$). For calculating $A_{high}$ and $A_{final}$, gas exchange parameters were logged every 10 s for 1 min, and averages of these values were determined per replicate.

### *2.3.2 Chlorophyll fluorescence*

To monitor chlorophyll fluorescence under 30 min exposure under treatment spectra in chamber-grown plants, the MONI-PAM multi-channel fluorometer (Heinz Walz GmbH, Effeltrich, Germany) was placed in the treatment setup. Selected leaflets were then placed in the leaf clip consisting of two aluminum frames (35×25 mm), which was mounted at a distance of 25 mm from the optical window, so that leaf area and longitudinal axis of the fluorometer formed an angle of 120 ° (Fig. 1D). Plants were first dark-adapted for ~30 min, and maximum chlorophyll *a* fluorescence ($F_m$) of leaves of dark-adapted plants was logged. Leaves were exposed to treatment light intensities of 300 µmol $m^{-2}$ $s^{-1}$, and data were logged every 2 min during the entire 30 min treatment duration. Measuring beam intensity was 1 µmol $m^{-2}$ $s^{-1}$, and maximum flash intensity was 4,000 µmol $m^{-2}$ $s^{-1}$. Fluorescence yield under actinic light ($F_s$) and maximal fluorescence yield of a light-adapted leaf ($F_m$') were logged repeatedly. Photosystem II operating efficiency ($\Phi_{PSII}$) was calculated as $\Phi_{PSII} = (F_m' - F_s)/F_m'$, non-photochemical quenching (NPQ) was calculated as $NPQ = F_m/F_m' - 1$, quantum yield of regulatory energy dissipation ($\Phi_{NPQ}$) was calculated as $\Phi_{NPQ} = F_s/F_m' - F_s/F_m$, and quantum yield of non-regulatory energy dissipation ($\Phi_{NO}$) was calculated as $\Phi_{NO} = F_s/F_m$ (Baker, 2008; Hendrickson et al., 2004).

To measure maximum quantum yield of PSII ($F_v/F_m$) of chamber-grown plants before and after 30 min of treatment light exposure, $F_m$ and minimum ($F_o$) chlorophyll *a* fluorescence of dark-adapted plants (≥20 min of dark adaptation) were measured, using a chlorophyll *a* fluorescence imager (IMAG-MAXI; Heinz Walz, Effeltrich, Germany). $F_v/F_m$ was calculated as $(F_m - F_o)/F_m$ (Baker, 2008). Plants were initially dark-adapted for 20 min, after which $F_v/F_m$ was determined. Plants were then exposed to the treatment spectra (300 µmol $m^{-2}$ $s^{-1}$) for 30 min, dark-adapted again for 20 min, and $F_v/F_m$ was measured again.

### *2.3.3 Pigment indices*

For chamber-grown plants, indices of chlorophyll and anthocyanin concentrations were determined non-destructively by a Dualex (Dualex Scientific+; Force-A, Orsay, France), after exposure to treatment spectra for 30 min. Measurements were taken on the uppermost fully

expanded leaf. Four technical replicates per leaf were taken randomly, and an average value was calculated per leaf. In the other genotypes, indices of chlorophyll, anthocyanin and flavonoid concentrations were determined non-destructively using a MPM100 device (Opti-sciences; 8 Winn Avenue, Hudson, USA). Two technical replicates per leaf were taken randomly, and an average value was calculated per leaf.

### 2.4 Statistics

One-way ANOVA was performed to test for significant effects of different treatment wavelengths. Data were first tested for normality (Shapiro–Wilk test) and homogeneity of variances (Fligner–Killeen test) at $p$=0.05. The least significant difference test was used to test for differences between any two treatments at the $p$=0.05 level. If the requirement for normal distribution was not fulfilled, Kruskal-Wallis one-way ANOVA was performed. Additionally, to estimate the linear relationship between treatment wavelength and the extent of photoinhibition, flavonoid index and ΔQY, simple linear regressions were performed, respectively. All analyses were performed using SPSS 24 (SPSS Inc., Chicago, IL). Data is presented as the mean ± standard deviation (SD) of five biological replicates per treatment in chamber-grown plants, four biological replicates per treatment in greenhouse- and field-grown plants.



## 3. Results

### 3.1 Photosynthetic quantum yield (QY) and pigment indices

Leaf exposure to light intensities in the 0-300 μmol $m^{-2}$ $s^{-1}$ range produced the characteristic light response curves of photosynthesis ($A$) expected within this light intensity range. All four treatment spectra powered increases in $A$ in a wavelength-dependent manner, and did so broadly similarly in both horticultural crops and woody species (Fig. 2). At every light intensity, $A$ tended to increase with wavelength in all species, especially in the 200-300 μmol $m^{-2}$ $s^{-1}$ range in cucumber and lettuce ‘Tiberius’ (Fig. 2B, C). However, in lettuce ‘Klee’, hydrangea and red dogwood, the increase in $A$ under 365 and 385 nm illumination was so shallow that $A$ remained negative or was very close to zero at all tested intensities (Fig. 2D, F, G). QY derived from light response curves increased with wavelength: at 365 nm, QY had the lowest value in

all species, which was 35%, 60%, and 55% lower compared with 450 nm in cucumber, lettuce 'Tiberius' and tomato, respectively (Fig. 2); it was ~80% lower compared with 450 nm in lettuce 'Klee', which had the highest flavonoid and anthocyanin concentrations, as well as in woody species (Figs. 2B-G; 3B, 3C). The differences between the three remaining treatment spectra in the 385-450 nm range were more subtle; for example, in cucumber, QY at 385 nm was only 5% lower than QY at 410 nm (Fig. 2B). Although QY in the UV-A1 range was lower than that in the blue light range across all species (Fig. 2), photosynthetic efficiency under UV-A1 exposure was always positive. Treatment light effects on *A* did not seem to be caused by differences in $g_s$, which did not vary much under the experimental conditions (Fig. S3).

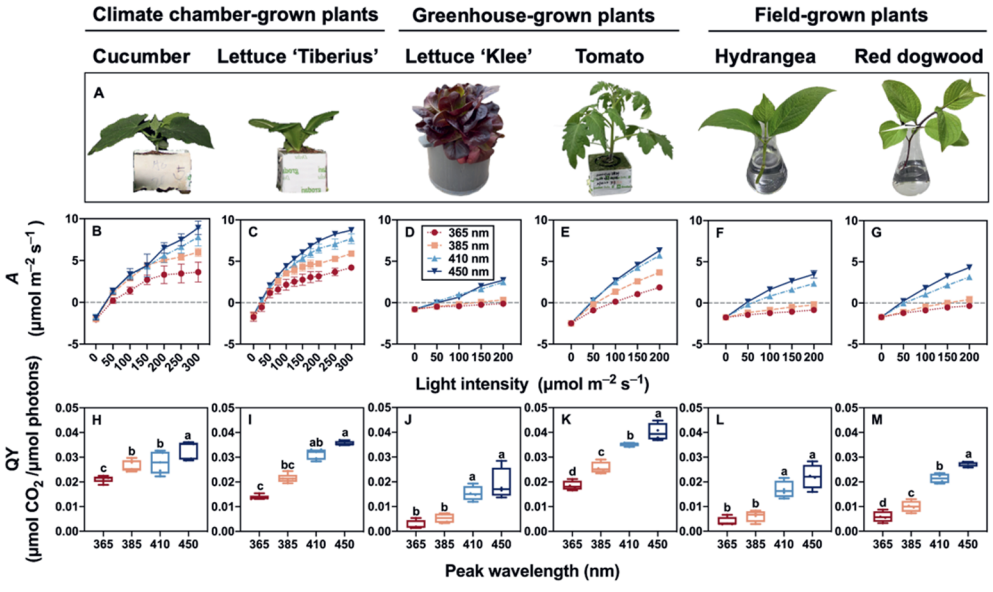


**Figure 2.** Light response of photosynthesis in leaves of six genotypes from three growing environments under UV-A1 and blue light. A: representative images of leaves used for measurements; B-G: light responses curves of net photosynthesis rate (*A*); H-M: photosynthetic quantum yield (QY). Mean values ± SD of five biological replicates for climate chamber-grown plants, four biological replicates for greenhouse- and field-grown plants; SD is visible only when larger than the symbol size. Boxplots (center line, median; box limits, upper and lower quartiles; whiskers, 1.5× interquartile range; points, outliers) represent all measurements from five biological replicates for climate chamber-grown plants, four biological replicates for greenhouse- and field-grown plants. Different letters show statistically significant differences among treatments ($p < 0.05$). QY was calculated as the slope ($R^2$: 0.80-0.99 in all cases) of the light response curve at low light intensities ranging from 50 to 200 µmol $m^{-2}$ $s^{-1}$ and expressed in µmol $CO_2$ / µmol photons.

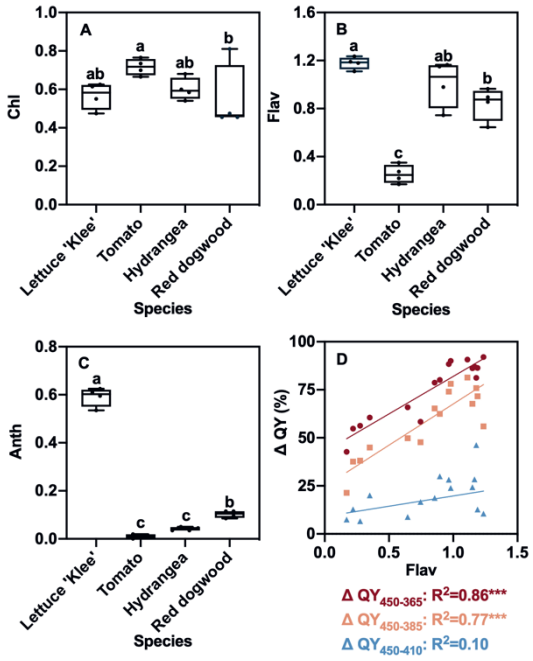


**Figure 3.** Pigment indices and their relationship with photosynthetic quantum yield across several species. A: chlorophyll concentration index; B: flavonoid concentration index; C: anthocyanin concentration index; D: linear regressions between the percentage difference of QY at 450 nm and at 365, 385 and 410 nm, respectively, and flavonoid concentration index, per replicate. Different letters show statistically significant differences among treatments ($p < 0.05$). Boxplots (center line, median; box limits, upper and lower quartiles; whiskers, 1.5× interquartile range; points, outliers) represent all measurements from four biological replicates. Numbers below the panel D represent Pearson coefficients as determined by simple linear regression, and asterisks indicate the significance of the linear relationship (***$p < 0.001$).

Further, growing cucumber leaves under a mixture of white light (100 µmol $m^{-2}$ $s^{-1}$) and UV-A1 radiation (20 µmol $m^{-2}$ $s^{-1}$) had no major effects on the response of *A* to different intensities of 365 nm treatment light, compared to leaves grown under only white light of 100 µmol $m^{-2}$ $s^{-1}$ (Fig. S3). Growth under a higher intensity of white light (300 µmol $m^{-2}$ $s^{-1}$), however, caused a clear increase of mitochondrial respiration, and reduced the slope of the light response curve of *A* measured under 365 nm, thus resulting in lower QY compared to leaves grown under 100 µmol $m^{-2}$ $s^{-1}$ white light (Fig. S3).

Measurements of pigmentation indices in greenhouse- and field-grown genotypes suggested minor differences in chlorophyll concentration (Fig. 3A), much smaller flavonoid concentrations in tomato than in the other three genotypes (Fig. 3B), and much larger anthocyanin concentrations in the purple-leaved lettuce 'Klee' than in the other three genotypes (Fig. 3C). To test for possible connections between pigmentation and QY under UV-A1 in these four genotypes, we calculated the percentage difference of QY at 365, 385 and 410 nm relative to QY at 450 nm ($\Delta QY_{450\text{-}365}$, $\Delta QY_{450\text{-}385}$, and $\Delta QY_{450\text{-}410}$, respectively), and correlated these to the pigmentation indices shown in Fig. 3A-C. This analysis showed very strong positive correlations ($p$<0.001; $R^2$ = 0.76-0.86) between flavonoid index and $\Delta QY_{450\text{-}365}$ as well as $\Delta QY_{450\text{-}385}$ (Fig. 3D), and a weaker positive correlation ($p$=0.03; $R^2$ = 0.30) between anthocyanin index and $\Delta QY_{450\text{-}365}$ (Fig. S4B); other tested correlations were not significant (Fig. S4). This analysis thus suggests that strong reductions in QY under UV-A1 (relative to QY under blue light) were linked to high flavonoid concentrations, and to a minor extent high anthocyanin concentrations.

## 3.2 Time courses of photosynthetic gas exchange and chlorophyll fluorescence

After a switch from darkness to 300 µmol $m^{-2}$ $s^{-1}$ treatment light, $A$ gradually increased within minutes under all treatment spectra (Fig. 4A, B). Under 450 nm, the highest value of $A$ during treatment light exposure ($A_{high}$) occurred within ~20 min and then stabilized (Figs. 4A, 4B; S6A, S6C, S6I, S6K). Under 365-410 nm, $A$ showed decreases after having reached an initial maximum within approx. 3-9 min of light exposure, and this decrease was larger and occurred sooner the lower the peak wavelength was (Figs. 4A, 4B; S6J, S6L). Final $A$ after 30 min of treatment light exposure ($A_{final}$) under 365 and 385 nm light was ~75% and ~65% lower than $A_{final}$ under 450 nm light, respectively, in both chamber-grown species (Figs. 4A, 4B; S6B, S6D). In addition, $A_{high}$, $A_{final}$ and average $A$ during the 30 min treatment ($A_{avgL}$) showed that $A$ under blue light spectra was significantly higher than UV-A1 (Fig. S6A-D, S6E, S6G).

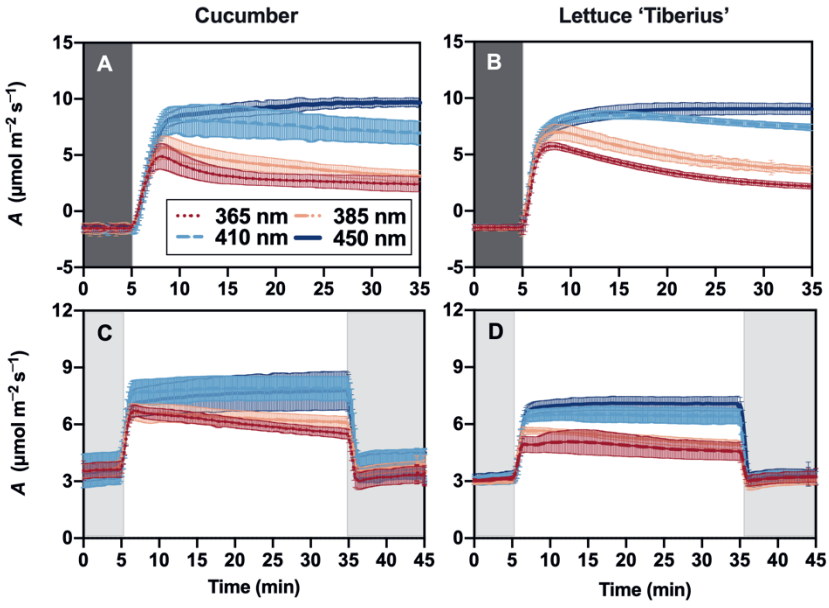


**Figure 4.** Time courses of photosynthetic gas exchange (*A*) in cucumber and lettuce 'Tiberius' leaves under UV-A1 and blue light (365-450 nm). A and B: Leaves that had initially been darkened for 5 min (dark grey bars) were exposed to 300 µmol $m^{-2}$ $s^{-1}$ of treatment light for 30 min. C and D: Leaves initially under 100 µmol $m^{-2}$ $s^{-1}$ of white light for 5 min (light grey bars) were exposed to an additional 100 µmol $m^{-2}$ $s^{-1}$ of treatment light for 30 min, then the treatment light was switched off and leaves were again exposed under 100 µmol $m^{-2}$ $s^{-1}$ of white light for 10 min (light grey bars). Mean values ± SD of five biological replicates (n = 5).

When 100 µmol $m^{-2}$ $s^{-1}$ treatment light was added to 100 µmol $m^{-2}$ $s^{-1}$ background white light in both chamber-grown species, *A* again increased and within a few minutes reached stable levels under both blue light spectra, whereas under both UV-A1 spectra it showed a continuous, near-linear decline that lasted the entire 30 min period (Fig. 4C, D). After treatment lights were switched off and *A* was logged under background white light (minutes 35-45 in Fig. 4C, D), *A* showed a decline and stabilized in all cases. Interestingly, the average value of *A* during the last 5 min of white light exposure ($A_{avgE}$) exhibited no significant effects among treatments in both chamber-grown species (Fig. S6F, H), suggesting that reductions of *A* under weak (100 µmol $m^{-2}$ $s^{-1}$) UV-A1 light exposure caused no carry-over effects for *A* under background light. Further, the decline in *A* under 30 min exposure to 365 nm light was likely not related to potential changes in $CO_2$ gas diffusion into the leaf (i.e., stomatal and mesophyll conductance), as a similarly strong reduction in *A* was observed in cucumber leaves at 1500 µbar [$CO_2$] (Fig. S7), compared to when measured at 400 µbar [$CO_2$] (Fig. 4A).

In darkened leaves that were suddenly exposed to 300 μmol $m^{-2}$ $s^{-1}$ treatment light, non-photochemical quenching (NPQ) initially increased quickly towards an initial peak value (3–4 min) in all cases, and then relaxed toward a lower value for another 3-4 min (Fig. 5A, B). Thereafter, in leaves exposed to 365 and 385 nm (and to a lesser extent in lettuce 'Tiberius' under 410 nm, Fig. 5B), NPQ gradually increased until the end of light exposure (Fig. 5A, B). Under 410 and 450 nm, NPQ tended to relax toward a lower, stable value after 30 min of light exposure. As a result, final NPQ after 30 min of treatment light exposure under 450 nm was 63% lower than that under 365 nm in cucumber, and 36% lower in lettuce 'Tiberius', respectively (Fig. 5A, B). The effect of treatment wavelengths in the UV-A1 range on the NPQ increase coincided with a modest reduction in maximum chlorophyll fluorescence ($F_m$), which showed an opposite trend to NPQ (Fig. S8). Photosystem II operating efficiency ($\Phi_{PSII}$) displayed an opposite trend to NPQ in both chamber-grown species (Fig. 5C, D), roughly mirroring the changes in *A* (Fig. 4A, B). Quantum yield of regulatory energy dissipation ($\Phi_{NPQ}$) displayed the same trend as NPQ (Fig. 5E, F). Non-regulatory energy dissipation ($\Phi_{NO}$) showed a short, transient increase and relaxation after which it remained flat, with relatively small differences between treatments (Fig. 5G, H).

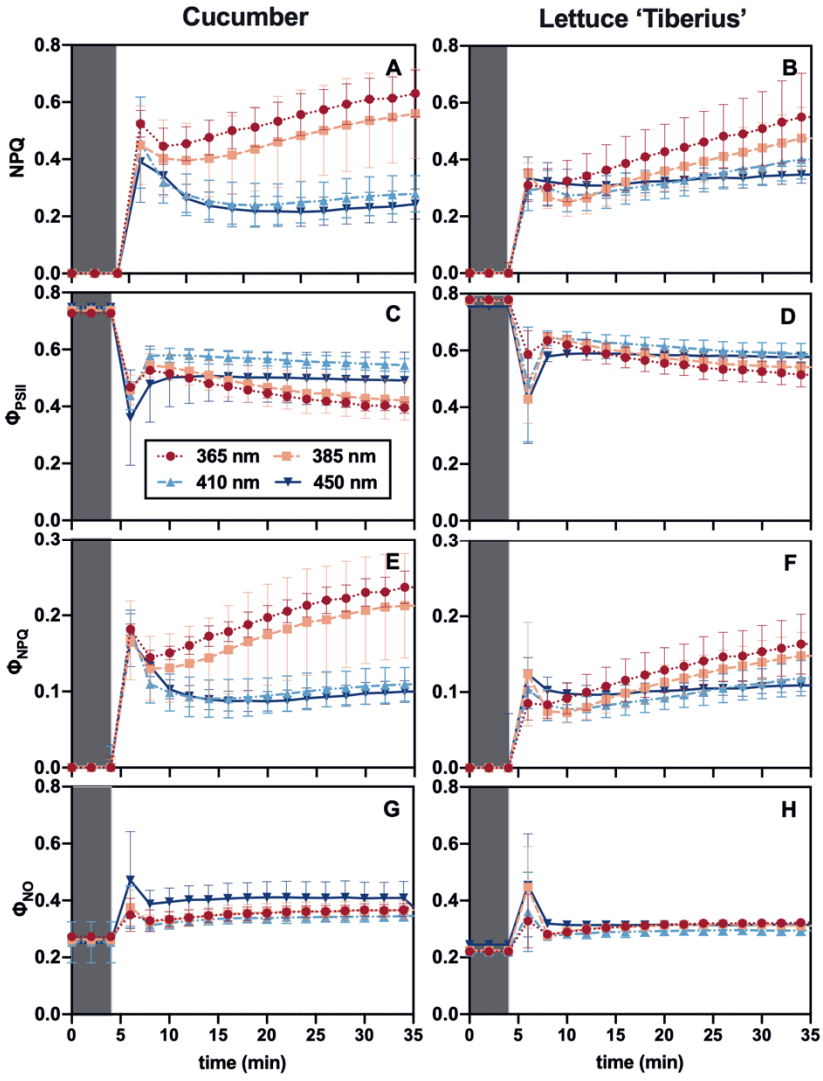


**Figure 5.** Time courses of chlorophyll fluorescence in cucumber and lettuce 'Tiberius' leaves under UV-A1 and blue light (365-450 nm). Initially darkened leaves for 30 min (dark grey bars) were exposed to 300 µmol $m^{-2}$ $s^{-1}$ of treatment light for 30 min, and data were logged every 2 min. A and B: non-photochemical fluorescence quenching (NPQ); C and D: photosystem II operating efficiency ($\Phi_{PSII}$); E and F: quantum yield of regulatory energy dissipation ($\Phi_{NPQ}$); G and H: quantum yield of non-regulatory energy dissipation ($\Phi_{NO}$). Mean values ± SD of five biological replicates (n = 5); SD is visible only when larger than the symbol size.

### 3.3 Photoinhibition and leaf pigmentation index before and after treatments

The maximum quantum yield of PSII ($F_v/F_m$) in cucumber and lettuce 'Tiberius' was measured before and after 30 min exposure to treatment lights (300 µmol $m^{-2}$ $s^{-1}$). Before exposure, $F_v/F_m$ in leaves of both chamber-grown species was > 0.8; after exposure, $F_v/F_m$ declined in all cases, but did so much more strongly under UV-A1 than under blue light (Fig. 6). Leaves showed the highest $F_v/F_m$ under 450 nm in both chamber-grown species (~0.79), and leaves under 365 nm showed the lowest $F_v/F_m$ of approx. ~0.55-0.7 (Fig. 6B), representing a 16% and 32% decrease in cucumber and lettuce 'Tiberius', respectively, compared to the initial value. Leaves exposed to 385 and 410 nm showed intermediate drops in $F_v/F_m$, resulting in near-linear declines in $F_v/F_m$ the shorter the wavelength was (Fig. 6B). Furthermore, lettuce 'Tiberius' was more sensitive to UV-A1 exposure compared with cucumber, as indicated by the steeper slope of the $F_v/F_m$ vs. wavelength relationship (Fig. 6B). Indices of chlorophyll and anthocyanin concentrations did not show treatment effects, although in cucumber leaves there was a tendency for the anthocyanin index to increase after exposure to lower wavelengths (Fig. S9).

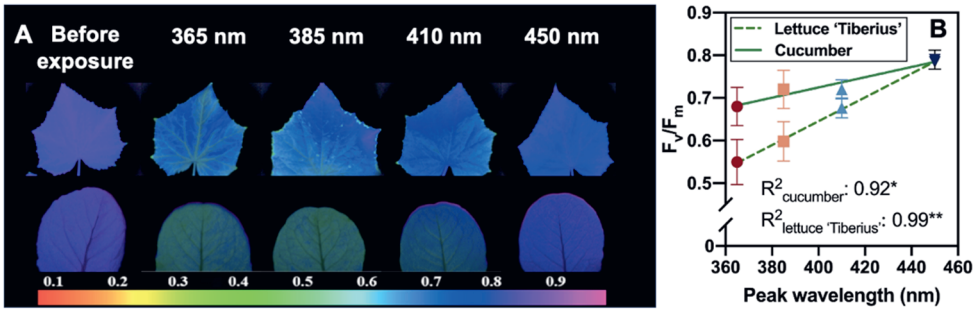


**Figure 6.** Photoinhibition in cucumber and lettuce 'Tiberius' leaves is affected by UV-A1 and blue light (365-450 nm). Leaves were exposed to one of four treatment spectra (365-450 nm) at a light intensity of 300 µmol $m^{-2}$ $s^{-1}$, for 30 min. Averaged maximum quantum efficiency of photosystem II photochemistry ($F_v/F_m$) before treatment spectra in cucumber and lettuce was 0.81 and 0.80, respectively. A: Representative false color images of $F_v/F_m$ distribution before and after light exposure. B: $F_v/F_m$ after exposure to different treatment lights. The green line in panel B represents the best-fit model, as determined by simple linear regression, and asterisks indicate the significance of the linear relationship (∗$p$<0.05, ∗∗$p$<0.01). Mean values ± SD of five biological replicates (n = 5); SD is visible only when larger than the symbol size.

# 4. Discussion

Previous studies have assessed the contribution of UV-A to net photosynthesis rate (*A*) (Johnson & Day, 2002; Mantha et al., 2001; McCree, 1971; Turnbull et al., 2013), but so far did not properly quantify these effects. To our knowledge, we have for the first time quantified *A* under several peak wavelengths in the UV-A1 range across several genotypes from three growing environments, and compared this to the response under blue light, using narrow-bandwidth UV-A1 and blue light LEDs at a range of light intensities. Also, we assessed how *A* and chlorophyll fluorescence change when leaves are exposed to UV-A1 for up to 30 min. Our results indicate that i) UV-A1 powers *A* with roughly half the photosynthetic quantum yield (QY) of blue light across horticultural crops grown in both climate chamber and greenhouses (except for lettuce 'Klee', which had purple leaves) and about one-third of blue light in woody species grown in the field; ii) the larger the flavonoid concentration, the stronger the reduction in QY is under UV-A1 light (relative to blue light); iii) after several minutes of exposure to UV-A1 radiation, *A* and $\Phi_{PSII}$ start to decline, whereas photoprotection (NPQ) rises, and iv) part of the decline in *A* under longer-term UV-A1 exposure is likely caused by photoinhibition, which is stronger the shorter the peak wavelength of the treatment light is.



## 4.1 The quantum yield of photosynthesis under UV-A1 declines with exposure time and increases with peak wavelength

Our results are in agreement with previous findings that QY is wavelength-dependent (Evans, 1987; McCree, 1971). The fact that the lowest QY was found at 365 nm may be attributed to a lack of absorption by photosynthetic and non-photosynthetic pigments, as well as a stronger excitation of photosystem II relative to photosystem I (Fig. 2H-M; Hogewoning et al., 2012). The maximum absorption of the photosynthetic pigments chlorophyll *a* and *b*, as well as of carotenoids, was found to be around 430-450 nm, but dropped below 425 nm; chlorophyll *b* and carotenoids have absorption tails reaching 365 nm (Chazaux et al., 2022; Lichtenthaler & Buschmann, 2001). On the other hand, flavonoids, major non-photosynthetic pigments, absorb in the range 330 to 360 nm (Edreva, 2005; Taniguchi et al., 2023). Hence, photosynthetic pigments harvest light most efficiently in the visible range, while flavonoids screen out UV

radiation, likely contributing to the strong increase in QY seen in the 365-450 nm range (Fig. 2H-M; Agati & Tattini, 2010; Simkin et al., 2022). Further, it was previously found that the average absorptance in leaves of 22 species was near-identical in the UV-A1 (0.92-0.94) and the blue light ranges (0.94-0.96; (McCree, 1971, 1972), suggesting that any differences in *A* between these two wavelength ranges were likely not caused by differences in absorptance.

We found that QY declines with exposure time to UV-A1 radiation (Fig. 4), and this reduction was likely not caused by changes in diffusional limitations to *A* (Fig. S7). There are several potential causes for this reduction, including NPQ, photoinhibition, the accumulation of UV-absorbing compounds and photobleaching (Barnes et al., 2016b; Murchie & Niyogi, 2011). The strong increases in NPQ observed under 300 µmol $m^{-2}$ $s^{-1}$ of 365 and 385 nm suggest the build-up of photoinhibition (qI) as well as zeaxanthin-dependent quenching (qZ; (Fig. 5A, B; Nilkens et al., 2010). The decrease in $\Phi_{PSII}$ under UV-A1 exposure that was similar to the reduction of *A* indicated that the rate of conversion of light energy into chemical energy decreased under UV-A1 (Figs. 4C, 4D; 5C, 5D). Besides, the excess energy dissipated through non-regulatory dissipation ($\Phi_{NO}$) was higher than that of regulatory dissipation ($\Phi_{NPQ}$), which indicated that the trend of *A* under both UV-A1 and blue light resulted primarily from the fraction of open reaction centers instead of changes in antenna size (Figs. 4; 5E-H; (Kramer et al., 2004). The notion that leaves became photoinhibited under 30 minutes of 300 µmol $m^{-2}$ $s^{-1}$ UV-A1 radiation is further supported by the strong reduction in $F_v/F_m$ (Fig. 6). However, after exposure to only 100 µmol $m^{-2}$ $s^{-1}$ treatment light for 30 min, *A* measured under low white light intensity was not significantly reduced in UV-A1 treated leaves (Figs. 4C, 4D; S6F, S6H), suggesting that 100 µmol $m^{-2}$ $s^{-1}$ UV-A1 light was too weak to cause strong photoinhibition. In addition, photobleaching can result in elevated NPQ and in reduced $F_v/F_m$ (Lingvay et al., 2020; Merzlyak et al., 1998); however, a lack of chlorophyll pigment degradation and only modest reductions in maximum chlorophyll fluorescence ($F_m$) during 30 min of UV-A1 exposure make it unlikely that photobleaching occurred (Figs. S8; S9C, D). Finally, although exposure to UV-A1 may induce an accumulation of UV-absorbing compounds within minutes to hours, changes in leaf UV sunscreen protection usually takes place over much longer time scales (several days; Barnes et al., 2016b), suggesting that the reduction in *A* within 30 min is unlikely to have been caused by changes in pigmentation.

Another potential reason for a reduction in *A* could be chloroplast avoidance movement, which reduces the amount of light absorbed by the leaf (Wada et al., 2003). However, the action spectrum of chloroplast movement has a maximum near 450 nm, with another minor peak around 370 nm (Blatt, 1983; Brugnoli & Björkman, 1992), therefore one would expect to see a reduction in *A* under 450 nm, which was clearly not observed (Fig. 4A, B). Therefore, we assume that chloroplast movement is an unlikely candidate to explain the observed reduction in *A* under UV-A1 light.

## 4.2 Concentrations of UV-absorbing compounds may determine photosynthetic efficiency in the UV-A1 range

Field- and greenhouse-grown plants are subject to growth in a much more complex and fluctuating environment compared to chamber-grown plants. Lettuce 'Klee' grown in the greenhouse and woody species grown in the field showed lower QY under both UV-A1 and blue light, which may suggest that growth environments affect photosynthetic efficiency (Fig. 2). However, tomato plants grown in the greenhouse had similar QY as chamber-grown cucumber and lettuce plants (Fig. 2), suggesting that both genotype and environment (as well as their interaction) likely determine QY. In addition, it is well known that UV-absorbing compounds filter out part of the UV radiation absorbed by the leaf (Barnes et al., 2016a). Strong correlations between apparent flavonoid concentrations and reductions in QY at 365 and 385 nm, relative to QY at 450 nm (Fig. 3D), as well as a weaker correlation between apparent anthocyanin concentrations and the reduction in QY at 365 nm (Fig. S4), are another indication that UV absorbing compounds can directly influence photosynthesis under UV-A1 illumination. Indeed, in lettuce 'Klee', hydrangea and red dogwood, all of which had large concentration indices for flavonoids (Fig. 3B), *A* under 365 and 385 nm illumination was below or around zero at all radiation intensities (Fig. 2D, F, G). We also found that QY in low-light grown plants (growth light intensity: 100 μmol $m^{-2}$ $s^{-1}$) was significantly higher than that of plants grown under a higher light intensity (growth light intensity: 300 μmol $m^{-2}$ $s^{-1}$; Fig. S4C). This suggests that plant leaves acclimated to different environments may possess different abilities to use UV-A1, and these may be caused by differences in UV-absorbing compound concentrations, the structure of the leaf epidermis, tissue thickness, waxes and trichomes (Gotz et al., 2010; Holmes & Keiller, 2002).

## 4.3 Should UV-A1 be defined as PAR?

Both UV-A and far-red radiation (700-800 nm) are excluded from the conventional PAR waveband (400–700 nm; McCree, 1971; Sheerin & Hiltbrunner, 2017). Far-red radiation applied alone is inefficient for driving *A*, but together with shorter-wavelength red light – such as in natural sunlight - it has been demonstrated to enhance *A* due to a more balanced excitation of the two photosystems (Emerson et al., 1957; Zhen et al., 2019; Zhen & Bugbee, 2020; Zhen & van Iersel, 2017). Based on this, a new definition of PAR, namely ePAR (400-750 nm), was recently proposed by Zhen et al. (2021).

Unlike far-red radiation, we found that UV-A1 powered *A* independently of PAR (Figs. 2; 4A, 4B) as well as in the presence of PAR (Fig. 4C, D). The finding that the solar fraction of UV radiation increased *A* by ~12% in the field (Turnbull et al., 2013) is an indication that the contribution of this part of the solar spectrum to plant productivity is substantial. Also, the UV-A1 portion of UV radiation can reach crops grown in greenhouses, but the extent of this depends on the covering materials (Serrano & Moreno, 2020; Timmermans et al., 2020). All of these results argue in favor of including UV-A1 in a re-definition of PAR (or ePAR). However, because in several genotypes UV-A1 only had minute effects on the increase of *A* (Fig. 2D, F, G), it can be argued that our data are not sufficiently compelling to redefine UV-A1 as PAR just yet.

## 4.4 Limitations and future research

Our current knowledge of UV-A and its effects on plants is still shrouded in mystery (Verdaguer et al., 2017). Most importantly, more mathematical modelling and experimental work is required at several spatial scales to quantify the relative contributions of UV-A and far-red light (Zhen et al., 2022) to whole-canopy carbon gain in the field and in controlled environment agriculture. It also remains to be shown to what extent UV-A1 powers photosynthesis in leaves of $C_4$ and CAM species, although for $C_4$ leaves some experimental evidence exists that it does (Barnes et al., 2016a; Johnson & Day, 2002). Also, it remains to be seen whether longer exposure to UV-A1 radiation would further reduce *A*, or whether instead the leaf is able to acclimate and therefore can recover *A* (Kang et al., 2021; Schumann et al., 2017). It was

previously shown that UV-absorbing compound concentrations were modulated within minutes to hours of UV-radiation exposure (Barnes et al., 2016a; 2016b), but it is unclear to what extent such changes affect QY under UV-A1. Additionally, it remains unknown whether UV-A exhibits a threshold effect that balances between positive effects by powering *A*, and negative effects by causing photoinhibition. The topics of photoprotection and photoinhibition under UV radiation exposure, as well as their interaction, deserve further exploration, including the role of NPQ induction and relaxation kinetics under dynamically changing sunlight (Murchie & Ruban, 2020).

# 5. Conclusions

Our study shows that UV-A1 radiation acts as an energy source for photosynthesis, both in the presence or absence of white background light, in several genotypes grown in various environments, but that it also acts as a stress that induces photoinhibition. Under longer exposure to UV-A1 radiation, photosynthesis showed declines, while regulated photoprotection (non-photochemical quenching) and photoinhibition increased. All of these effects were strongly wavelength-dependent. While photosynthetic quantum yield was clearly positive in all species tested, new research should aim to quantify the possible contribution of UV-A1 to whole-canopy carbon gain in the field.

# References


Agati, G., & Tattini, M. (2010). Multiple functional roles of flavonoids in photoprotection. *New Phytologist*, *186*(4), 786–793. https://doi.org/10.1111/j.1469-8137.2010.03269.x

Aphalo, P. J., & Sadras, V. O. (2021). Explaining pre-emptive acclimation by linking information to plant phenotype. *Journal of Experimental Botany*, *73*(15), 5213–5234. https://doi.org/10.1093/jxb/erab537

Baker, N. R. (2008). Chlorophyll fluorescence: A probe of photosynthesis in vivo. *Annual Review of Plant Biology*, *59*, 89–113. https://doi.org/10.1146/annurev.arplant.59.032607.092759

Barnes, P. W., Flint, S. D., Tobler, M. A., & Ryel, R. J. (2016a). Diurnal adjustment in ultraviolet sunscreen protection is widespread among higher plants. *Oecologia*, *181*(1), 55–63. https://doi.org/10.1007/s00442-016-3558-9

Barnes, P. W., Tobler, M. A., Keefover-Ring, K., Flint, S. D., Barkley, A. E., Ryel, R. J., & Lindroth, R. L. (2016b). Rapid modulation of ultraviolet shielding in plants is influenced by solar ultraviolet radiation and linked to alterations in flavonoids. *Plant Cell and Environment*, *39*(1), 222–230. https://doi.org/10.1111/pce.12609

Barnes, P. W., Searles, P. S., Ballaré, C. L., Ryel, R. J., & Caldwell, M. M. (2000). Non-invasive measurements of leaf epidermal transmittance of UV radiation using chlorophyll fluorescence: Field and laboratory studies. *Physiologia Plantarum*, *109*(3), 274–283. https://doi.org/10.1034/j.1399-3054.2000.100308.x

Bidel, L. P. R., Meyer, S., Goulas, Y., Cadot, Y., & Cerovic, Z. G. (2007). Responses of epidermal phenolic compounds to light acclimation: In vivo qualitative and quantitative assessment using chlorophyll fluorescence excitation spectra in leaves of three woody species. *Journal of Photochemistry and Photobiology B: Biology*, *88*(2–3), 163–179. https://doi.org/10.1016/j.jphotobiol.2007.06.002

Bilger, W., Rolland, M., & Nybakken, L. (2007). UV screening in higher plants induced by low temperature in the absence of UV-B radiation. *Photochemical & Photobiological Sciences*, *6*(2), 190–195. https://doi.org/10.1039/b609820g

Blatt, M. R. (1983). The action spectrum for chloroplast movements and evidence for blue-light-photoreceptor cycling in the alga Vaucheria. *Planta*, *159*(3), 267–276. https://doi.org/10.1007/BF00397535

Brugnoli, E., & Björkman, O. (1992). Chloroplast movements in leaves: Influence on chlorophyll fluorescence and measurements of light-induced absorbance changes related to ΔpH and zeaxanthin formation. *Photosynthesis Research*, *32*(1), 23–35. https://doi.org/10.1007/BF00028795

Caldwell, M. M., Robberecht, R., & Flint, S. D. (1983). Internal filters: Prospects for UV-acclimation in higher plants. *Physiologia Plantarum*, *58*(3), 445–450. https://doi.org/10.1111/j.1399-3054.1983.tb04206.x

Chazaux, M., Schiphorst, C., Lazzari, G., & Caffarri, S. (2022). Precise estimation of chlorophyll a, b and carotenoid content by deconvolution of the absorption spectrum and new simultaneous equations for Chl determination. *Plant Journal*, *109*(6), 1630–1648. https://doi.org/10.1111/tpj.15643

Chen, Y., Li, T., Yang, Q., Zhang, Y., Zou, J., Bian, Z., & Wen, X. (2019). UVA radiation is beneficial for yield and quality of indoor cultivated lettuce. *Frontiers in Plant Science*, *10*, 1563. https://doi.org/10.3389/fpls.2019.01563

Edreva, A. (2005). The importance of non-photosynthetic pigments and cinnamic acid derivatives in photoprotection. *Agriculture, Ecosystems and Environment*, *106*(2-3), 135–146. https://doi.org/10.1016/j.agee.2004.10.002

Emerson, R., Chalmers, R., & Cederstrand, C. (1957). Some factors influencing the long-wave limit of photosynthesis. *Proceedings of the National Academy of Sciences*, *43*(1), 133–143. https://doi.org/10.1073/pnas.43.1.133

Evans, J. (1987). The dependence of quantum yield on wavelength and growth irradiance. *Functional Plant Biology*, *14*(1), 69. https://doi.org/10.1071/pp9870069

Gotz, M., Albert, A., Stich, S., Heller, W., Scherb, H., Krins, A., Langebartels, C., Seidlitz, H. K., & Ernst, D. (2010). PAR modulation of the UV-dependent levels of flavonoid metabolites in Arabidopsis thaliana (L.) Heynh. leaf rosettes: cumulative effects after a whole vegetative growth period. *Protoplasma*, *243*(1–4), 95–103. https://doi.org/10.1007/s00709-009-0064-5

Hakala-Yatkin, M., Mntysaari, M., Mattila, H., & Tyystjärvi, E. (2010). Contributions of visible and ultraviolet parts of sunlight to photoinhibition. *Plant and Cell Physiology*, *51*(10), 1745–1753. https://doi.org/10.1093/pcp/pcq133

Halldal, P. (1964). Ultraviolet action spectra of photosynthesis and photosynthetic inhibition in a green and a red alga. *Physiologia Plantarum*. *17*(2), 414–421. https://doi.org/10.1111/j.1399-3054.1964.tb08174.x

Hendrickson, L., Furbank, R. T., & Chow, W. S. (2004). A simple alternative approach to assessing the fate of absorbed light energy using chlorophyll fluorescence. *Photosynthesis Research*, *82*(1), 73–81. https://doi.org/10.1023/B:PRES.0000040446.87305.f4

Hoffmann, A. M., Noga, G., & Hunsche, M. (2015). High blue light improves acclimation and photosynthetic recovery of pepper plants exposed to UV stress. *Environmental and Experimental Botany*, *109*, 254–263. https://doi.org/10.1016/j.envexpbot.2014.06.017

Hogewoning, S. W., Wientjes, E., Douwstra, P., Trouwborst, G., van Ieperen, W., Croce, R., & Harbinson, J. (2012). Photosynthetic quantum yield dynamics: From photosystems to leaves. *Plant Cell*, *24*(5), 1921–1935. https://doi.org/10.1105/tpc.112.097972

Holmes, M. G., & Keiller, D. R. (2002). Effects of pubescence and waxes on the reflectance of leaves in the ultraviolet and photosynthetic wavebands: A comparison of a range of species. *Plant, Cell and Environment*, *25*(1), 85–93. https://doi.org/10.1046/j.1365-3040.2002.00779.x

Jenkins, G. I. (2014). The UV-B photoreceptor UVR8: from structure to physiology. *Plant Cell*, *26*(1), 21–37. https://doi.org/10.1105/tpc.113.119446

Johnson, G. A., & Day, T. A. (2002). Enhancement of photosynthesis in Sorghum bicolor by ultraviolet radiation. *Physiologia Plantarum*, *116*(4), 554–562. https://doi.org/10.1034/j.1399-3054.2002.1160415.x

Jones, L. W., & Kok, B. (1966). Photoinhibition of chloroplast reactions. i. Kinetics and action spectra. *Plant Physiology*, *41*(6), 1037–1043. https://doi.org/10.1104/pp.41.6.1037

Kang, C., Zhang, Y., Cheng, R., Kaiser, E., Yang, Q., & Li, T. (2021). Acclimating cucumber plants to blue supplemental light promotes growth in full sunlight. *Frontiers in Plant Science*, *12*, 782465. https://doi.org/10.3389/fpls.2021.782465

Kerr, J. B., & Fioletov, V. E. (2008). Surface ultraviolet radiation. *Atmosphere - Ocean*, *46*(1), 159–184. https://doi.org/10.3137/ao.460108

Kramer, D. M., Johnson, G., Kiirats, O., & Edwards, G. E. (2004). New fluorescence parameters for the determination of QA redox state and excitation energy fluxes. *Photosynthesis research*, *79*, 209-218. https://doi.org/10.1023/B:PRES.0000015391.99477.0d

Kulandaivelu, G., & Noorudeen, A. M. (1983). Comparative study of the action of ultraviolet-C and ultraviolet- B radiation on photosynthetic electron transport. *Physiologia Plantarum*, *58*(3), 389–394. https://doi.org/10.1111/j.1399-3054.1983.tb04199.x

Lang, M., Stober, F., & Lichtenthaler, H. K. (1991). Fluorescence emission spectra of plant leaves and plant constituents. *Radiation and Environmental Biophysics*, *30*, 333–347.

Lee, J. H., Oh, M. M., & Son, K. H. (2019). Short-term ultraviolet (UV)-A light-emitting diode (LED) radiation improves biomass and bioactive compounds of Kale. *Frontiers in Plant Science*, *10*, 1042. https://doi.org/10.3389/fpls.2019.01042

Li, Z., Wakao, S., Fischer, B. B., & Niyogi, K. K. (2009). Sensing and responding to excess light. *Annual Review of Plant Biology*, *60*, 239–260. https://doi.org/10.1146/annurev.arplant.58.032806.103844

Lichtenthaler, H. K., & Buschmann, C. (2001). Chlorophylls and carotenoids: Measurement and characterization by

UV-VIS spectroscopy. *Current Protocols in Food Analytical Chemistry*, *1*(1), F4-3. https://doi.org/10.1002/0471142913.faf0403s01

Lin, C. (2000). Plant blue-light receptors. *Trends in Plant Science*, *5*(8), 337–342. https://doi.org/10.1016/S1360-1385(00)01687-3

Lingvay, M., Akhtar, P., Sebők-Nagy, K., Páli, T., & Lambrev, P. H. (2020). Photobleaching of chlorophyll in light-harvesting complex II increases in lipid environment. *Frontiers in Plant Science, 11*, 1–14. https://doi.org/10.3389/fpls.2020.00849

Malnoë, A. (2018). Photoinhibition or photoprotection of photosynthesis? Update on the (newly termed) sustained quenching component qH. *Environmental and Experimental Botany*, *154*, 123–133. https://doi.org/10.1016/j.envexpbot.2018.05.005

Mantha, S. V., Johnson, G. A., & Day, T. A. (2001). Evidence from action and fluorescence spectra that UV-induced violet-blue-green fluorescence enhances leaf photosynthesis¶. *Photochemistry and Photobiology*. https://doi.org/10.1562/0031-8655(2001)0730249efaafs2.0.co2

Mazza, C. A., Boccalandro, H. E., Giordano, C. V., Battista, D., Scopel, A. L., & Ballare, C. L. (2000). Functional significance and induction by solar radiation of ultraviolet-absorbing sunscreens in field-grown soybean crops. *Plant Physiology*, *122*(1), 117–125. https://doi.org/10.1104/pp.122.1.117

McCree, K. J. (1971). The action spectrum, absorptance and quantum yield of photosynthesis in crop plants. Agricultural Meteorology. https://doi.org/10.1016/0002-1571(71)90022-7

McCree, K. J. (1972). Test of current definitions of photosynthetically active radiation against leaf photosynthesis data. *Agricultural Meteorology*, *10*, 443–453. https://doi.org/10.1016/0002-1571(72)90045-3

McCree, K. J., & Keener, M. E. (1974). Effect of atmospheric turbidity on the photosynthetic rates of leaves. *Agricultural Meteorology*, *13*(3), 349–357. https://doi.org/10.1016/0002-1571(74)90075-2

Merzlyak, M. N., Gitelson, A. A., Pogosyan, S. I., Lekhimena, L., & Chivkunova, O. B. (1998). Light-induced pigment degradation in leaves and ripening fruits studied in situ with reflectance spectroscopy. *Physiologia Plantarum*, *104*(4), 661-667. https://doi.org/10.1034/j.1399-3054.1998.1040420.x

Müller, P., Li, X. P., & Niyogi, K. K. (2001). Non-photochemical quenching. A response to excess light energy. *Plant Physiology*, *125*(4), 1558–1566. https://doi.org/10.1104/pp.125.4.1558

Murchie, E. H., & Ruban, A. V. (2019). Dynamic non-photochemical quenching in plants: from molecular mechanism to productivity. *Plant Journal*, *101*(4), 885–896. https://doi.org/10.1111/tpj.14601

Murchie, E. H., & Niyogi, K. (2010). Manipulation of photoprotection to improve plant photosynthesis. *Plant Physiology*, *155*(1), 86–92. https://doi.org/10.1104/pp.110.168831

Neugart, S., Tobler, M. A., & Barnes, P. W. (2021). Rapid adjustment in epidermal UV sunscreen: Comparison of optical measurement techniques and response to changing solar UV radiation conditions. *Physiologia Plantarum*, *173*(3), 725–735. https://doi.org/10.1111/ppl.13517

Nilkens, M., Kress, E., Lambrev, P., Miloslavina, Y., Müller, M., Holzwarth, A. R., & Jahns, P. (2010). Identification of a slowly inducible zeaxanthin-dependent component of non-photochemical quenching of chlorophyll fluorescence generated under steady-state conditions in Arabidopsis. *Biochimica et Biophysica Acta - Bioenergetics*, *1797*(4), 466–475. https://doi.org/10.1016/j.bbabio.2010.01.001

Rai, N., Morales, L. O., & Aphalo, P. J. (2021). Perception of solar UV radiation by plants: photoreceptors and mechanisms. *Plant Physiology*, *186*(3), 1382–1396. https://doi.org/10.1093/PLPHYS/KIAB162

Rai, N., Neugart, S., Yan, Y., Wang, F., Siipola, S. M., Lindfors, A. V., Winkler, J. B., Albert, A., Brosché, M., Lehto, T., Morales, L. O., & Aphalo, P. J. (2019). How do cryptochromes and UVR8 interact in natural and simulated sunlight? *Journal of Experimental Botany*, *70*(18), 4975–4990. https://doi.org/10.1093/jxb/erz236

Robberecht, R., & Caldwell, M. M. (1978). Leaf epidermal transmittance of ultraviolet radiation and its implications for plant sensitivity to ulraviolet-radiation induced injury. *Oecologia*, *32*(3), 277–287. https://doi.org/10.1007/BF00345107

Robson, T. M., Aphalo, P. J., Banaś, A. K., Barnes, P. W., Brelsford, C. C., Jenkins, G. I., Kotilainen, T. K., Łabuz, J., Martínez-Abaigar, J., Morales, L. O., Neugart, S., Pieristè, M., Rai, N., Vandenbussche, F., & Jansen, M. A. K. (2019). A perspective on ecologically relevant plant-UV research and its practical application. *Photochemical and Photobiological Sciences*, *18*(5), 970–988. https://doi.org/10.1039/c8pp00526e

Ruban, A. V., & Wilson, S. (2021). The mechanism of non-photochemical quenching in plants: Localization and driving forces. *Plant and Cell Physiology*, *62*(7), 1063–1072. https://doi.org/10.1093/pcp/pcaa155

Schumann, T., Paul, S., Melzer, M., Dormann, P., & Jahns, P. (2017). Plant growth under natural light conditions provides highly flexible short-term acclimation properties toward high light stress. *Front Plant Sci*, *8*, 681. https://doi.org/10.3389/fpls.2017.00681

Serrano, M. A., & Moreno, J. C. (2020). Spectral transmission of solar radiation by plastic and glass materials. *Journal of Photochemistry and Photobiology B: Biology*, *208*, 111894. https://doi.org/10.1016/j.jphotobiol.2020.111894

Sheerin, D. J., & Hiltbrunner, A. (2017). Molecular mechanisms and ecological function of far-red light signalling. *Plant Cell and Environment*, *40*(11), 2509–2529. https://doi.org/10.1111/pce.12915

Simkin, A. J., Kapoor, L., Doss, C. G. P., Hofmann, T. A., Lawson, T., & Ramamoorthy, S. (2022). The role of photosynthesis related pigments in light harvesting, photoprotection and enhancement of photosynthetic yield in planta. *Photosynthesis Research*, *152*(1), 23–42. https://doi.org/10.1007/s11120-021-00892-6

Taniguchi, M., LaRocca, C. A., Bernat, J. D., & Lindsey, J. S. (2023). Digital database of absorption spectra of diverse flavonoids enables structural comparisons and quantitative evaluations. *Journal of Natural Products*, *86*(4), 1087–1119. https://doi.org/10.1021/acs.jnatprod.2c00720

Tcherkez, G., Gauthier, P., Buckley, T. N., Busch, F. A., Barbour, M. M., Bruhn, D., Heskel, M. A., Gong, X. Y., Crous, K., Griffin, K. L., Way, D. A., Turnbull, M. H., Adams, M. A., Atkin, O. K., Bender, M., Farquhar, G. D., & Cornic, G. (2017). Tracking the origins of the Kok effect, 70 years after its discovery. *New Phytologist*, *214*(2), 506–510. https://doi.org/10.1111/nph.14527

Timmermans, G. H., Hemming, S., Baeza, E., van Thoor, E. A. J., Schenning, A. P., & Debije, M. G. (2020). Advanced optical materials for sunlight control in greenhouses. *Advanced Optical Materials*, *8*(18). https://doi.org/10.1002/adom.202000738

Turnbull, T. L., Barlow, A. M., & Adams, M. A. (2013). Photosynthetic benefits of ultraviolet-A to Pimelea ligustrina, a woody shrub of sub-alpine Australia. *Oecologia*, *173*(2), 375–385. https://doi.org/10.1007/s00442-013-2640-9

Verdaguer, D., Jansen, M. A. K., Llorens, L., Morales, L. O., & Neugart, S. (2017). UV-A radiation effects on higher plants: Exploring the known unknown. *Plant Science*, *255*, 72–81. https://doi.org/10.1016/j.plantsci.2016.11.014

Wada, M., Kagawa, T., & Sato, Y. (2003). Chloroplast movement. *Annual Review of Plant Biology*, *54* (1), 455–468. https://doi.org/10.1146/annurev.arplant.54.031902.135023

Wang, Y., Burgess, S. J., de Becker, E. M., & Long, S. P. (2020). Photosynthesis in the fleeting shadows: an overlooked opportunity for increasing crop productivity? *Plant Journal*, *101*(4), 874–884. https://doi.org/10.1111/tpj.14663

Zhang, Y., Kaiser, E., Zhang, Y., Zou, J., Bian, Z., Yang, Q., & Li, T. (2020). UVA radiation promotes tomato growth through morphological adaptation leading to increased light interception. *Environmental and Experimental Botany*, *176*, 104073. https://doi.org/10.1016/j.envexpbot.2020.104073

Zhang, Y., Sun, X., Aphalo, P. J., Zhang, Y., Cheng, R., & Li, T. (2023). Ultraviolet-A1 radiation induced a more favorable light-intercepting leaf-area display than blue light and promoted plant growth. *Plant Cell and Environment*, *46*(10), 1–16. https://doi.org/10.1111/pce.14727

Zhen, S., & Bugbee, B. (2020). Far-red photons have equivalent efficiency to traditional photosynthetic photons: Implications for redefining photosynthetically active radiation. *Plant Cell and Environment*, *43*(5), 1259–

1272. https://doi.org/10.1111/pce.13730

Zhen, S., Haidekker, M., & van Iersel, M. W. (2019). Far-red light enhances photochemical efficiency in a wavelength-dependent manner. *Physiologia Plantarum*, *167*(1), 21–33. https://doi.org/10.1111/ppl.12834

Zhen, S., van Iersel, M., & Bugbee, B. (2021). Why far-red photons should be included in the definition of photosynthetic photons and the measurement of horticultural fixture efficacy. *Frontiers in Plant Science*, *12*, 1158. https://doi.org/10.3389/fpls.2021.693445

Zhen, S., & van Iersel, M. W. (2017). Far-red light is needed for efficient photochemistry and photosynthesis. *Journal of Plant Physiology*, *209*, 115–122. https://doi.org/10.1016/j.jplph.2016.12.004

Zhen, S., van Iersel, M. W., & Bugbee, B. (2022). Photosynthesis in sun and shade: the surprising importance of far-red photons. *New Phytologist*, *236*(2), 538–546. https://doi.org/10.1111/nph.18375

# Supplementary material

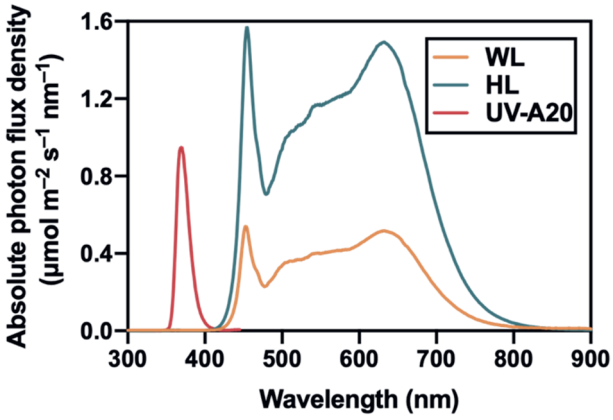


**Figure S1.** Spectral photon irradiance for growth light treatments. Plants were grown under white light of low intensity (WL; 100 µmol $m^{-2}$ $s^{-1}$), high intensity (HL; 300 µmol $m^{-2}$ $s^{-1}$), and white light (100 µmol $m^{-2}$ $s^{-1}$) supplemented with UV-A1 (20 µmol $m^{-2}$ $s^{-1}$; WLUVA20).

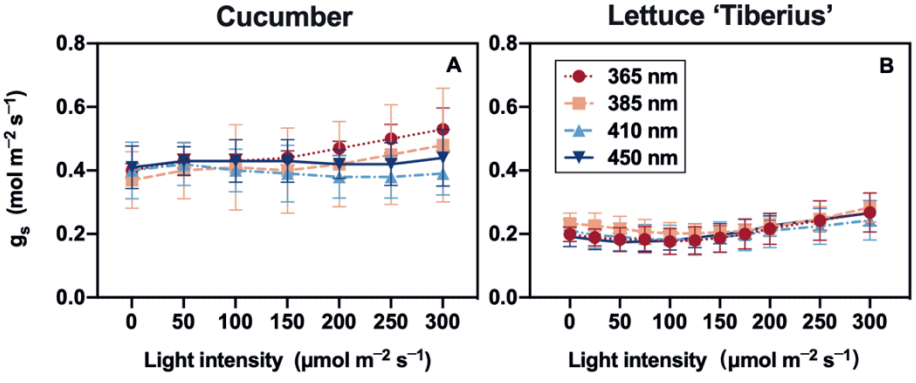


**Figure S2.** Stomatal conductance ($g_s$) in cucumber and lettuce 'Tiberius' leaves during the measurement of photosynthesis light response curves (Fig. 2A, B) under four spectra (365-450 nm). Mean values ± SD of five biological replicates (n = 5); SD is visible only when larger than the symbol size.

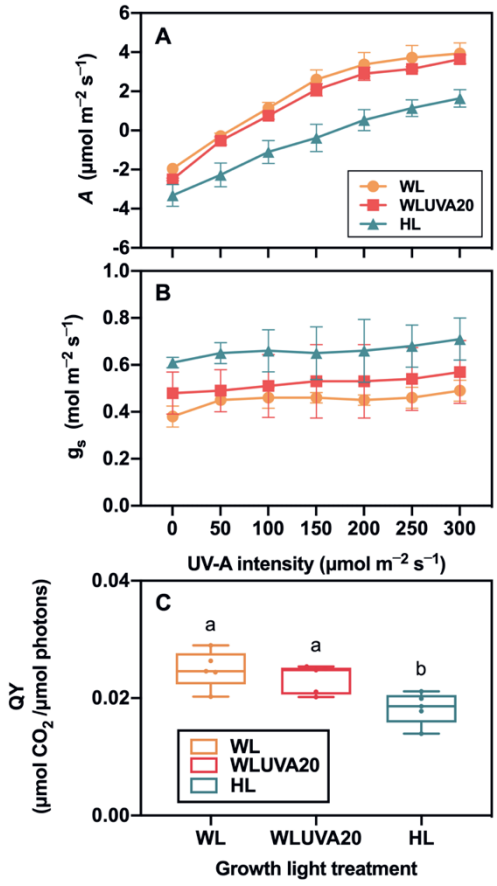


**Figure S3.** Partial light response curves of photosynthesis in cucumber leaves under 365 nm, when plants were grown under either white light (WL; 100 µmol $m^{-2}$ $s^{-1}$), white light supplemented with UV-A1 light intensity of 20 µmol $m^{-2}$ $s^{-1}$ (WLUVA20), or high light (HL; 300 µmol $m^{-2}$ $s^{-1}$), respectively. A: net photosynthesis rate (*A*); B: stomatal conductance ($g_s$). C: photosynthetic quantum yield (QY). Mean values ± SD of five biological replicates (n = 5); SD is visible only when larger than the symbol size. QY was calculated as the slope ($R^2$: 0.87-0.99 in all cases) of the light curve at low light intensities ranging from 50 to 200 µmol $m^{-2}$ $s^{-1}$ and expressed in µmol $CO_2$ /µmol photons. Boxplots (center line, median; box limits, upper and lower quartiles; whiskers, 1.5× interquartile range; points, outliers) represent all measurements from five biological replicates. Different letters show statistically significant differences among treatments ($p < 0.05$).

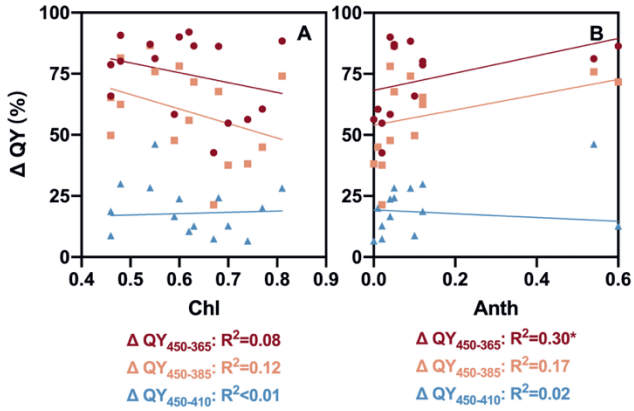


**Figure S4.** Pigment indices and their relationship with reductions in photosynthetic quantum yield across several species. A and B: linear regressions between the percentage difference of QY at 450 nm and at 365, 385 and 410 nm, respectively, and chlorophyll concentration index measured in the same leaf, per replicate, as well as anthocyanin concentration index. Numbers below the panel represent Pearson coefficients as determined by simple linear regression, and asterisks indicate the significance of the linear relationship (*$p < 0.05$).

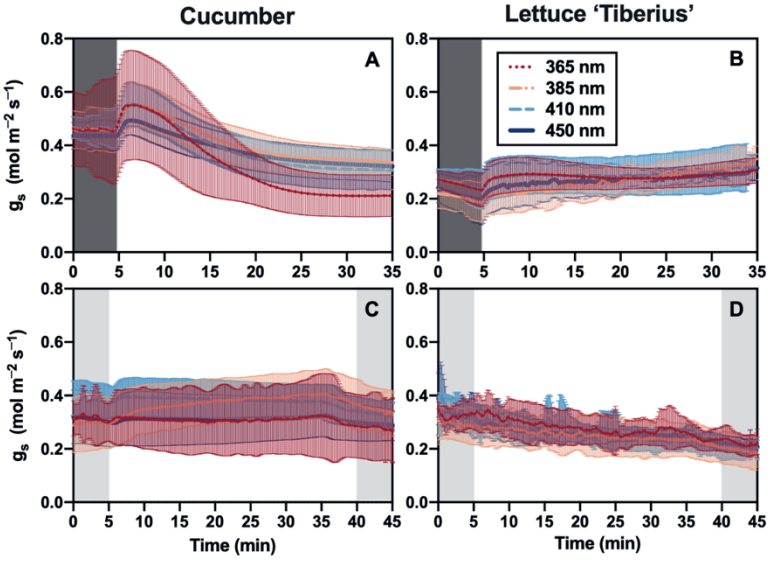


**Figure S5.** Time courses of stomatal conductance ($g_s$) in cucumber and lettuce 'Tiberius' leaves under four spectra (365-450 nm). A and B: Initially darkened leaves (dark grey bars) were exposed to 300 µmol $m^{-2}$ $s^{-1}$ of treatment light for 30 min. C and D: Leaves initially exposed to 100 µmol $m^{-2}$ $s^{-1}$ of white light (light grey bars) were exposed to an additional 100 µmol $m^{-2}$ $s^{-1}$ of treatment light for 30 min, after which the treatment light was switched off and leaves were again exposed under 100 µmol $m^{-2}$ $s^{-1}$ of white light for 10 min (light grey bars). Mean values ± SD of five biological replicates (n = 5).

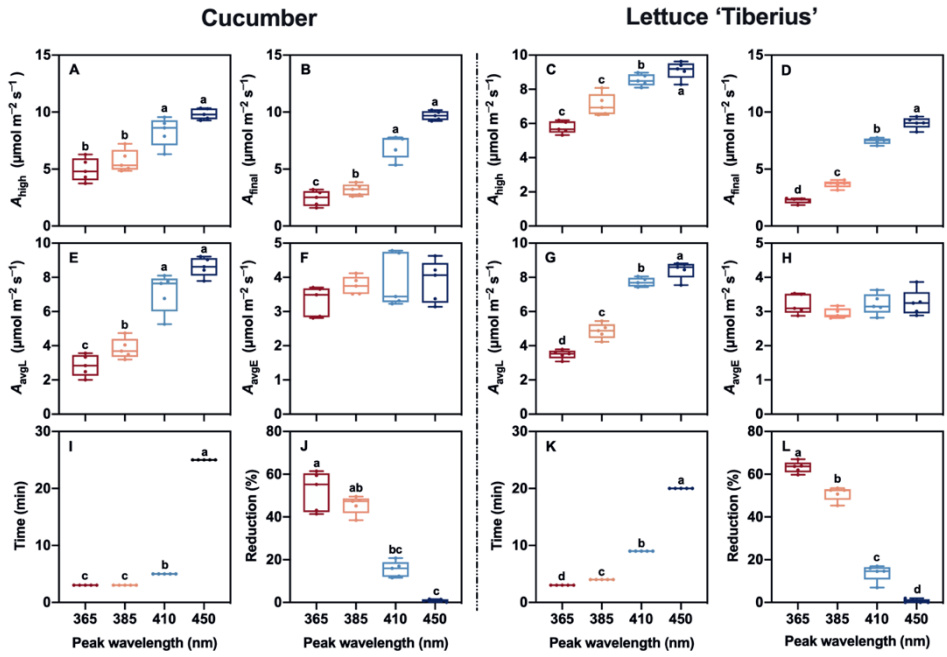


**Figure S6.** Traits of time courses of photosynthetic gas exchange (*A*) in cucumber and lettuce 'Tiberius' leaves under the four treatment spectra (365-450 nm), which are derived from Fig. 4. Traits derived from Fig. 4A, B including: $A_{high}$ (A, C), the highest *A* reached during treatment light exposure; $A_{final}$ (B, D), final *A* after 30 min of treatment light exposure; $A_{avgL}$ (E, G), average *A* across time courses during the 30 min of treatment light exposure; Time (I, K), time when $A_{high}$ was reached; Reduction (J, L), difference between $A_{high}$ and $A_{final}$. Traits derived from Fig. 4C, D refer to $A_{avgE}$ (F, H), which is average *A* over time courses from 40 to 45 min. Boxplots (center line, median; box limits, upper and lower quartiles; whiskers, 1.5× interquartile range; points, outliers) represent all measurements from five biological replicates. Different lowercase letters indicate statistically significant differences among treatments ($p < 0.05$).

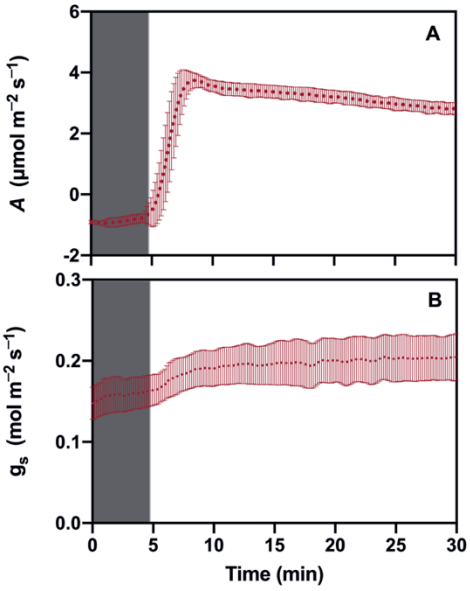


**Figure S7.** Time courses of photosynthetic gas exchange (*A*) and stomatal conductance ($g_s$) in cucumber leaves under UV-A1 radiation (wavelength at 365 nm), at 1500 µbar [$CO_2$]. Initially darkened leaves (dark grey bars) were exposed to 100 µmol $m^{-2}$ $s^{-1}$ of treatment light for 25 min. Mean values ± SD of five biological replicates (n = 5). SD is visible only when larger than the symbol size.



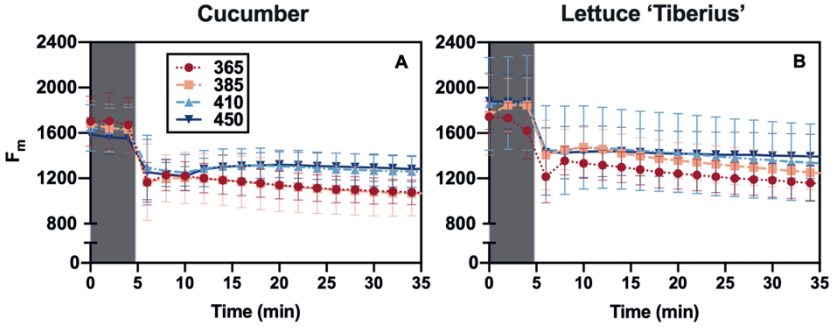


**Figure S8.** Time courses of maximum chlorophyll fluorescence (defined as $F_m$ in darkness, $F_m$' in light) in cucumber and lettuce 'Tiberius' leaves under UV-A1 and blue light (365-450 nm). Initially darkened leaves for 30 min (dark grey bars) were exposed to 300 µmol $m^{-2}$ $s^{-1}$ of treatment light for 30 min, and data were logged every 2 min. Mean values ± SD of five biological replicates (n = 5); SD is visible only when larger than the symbol size.

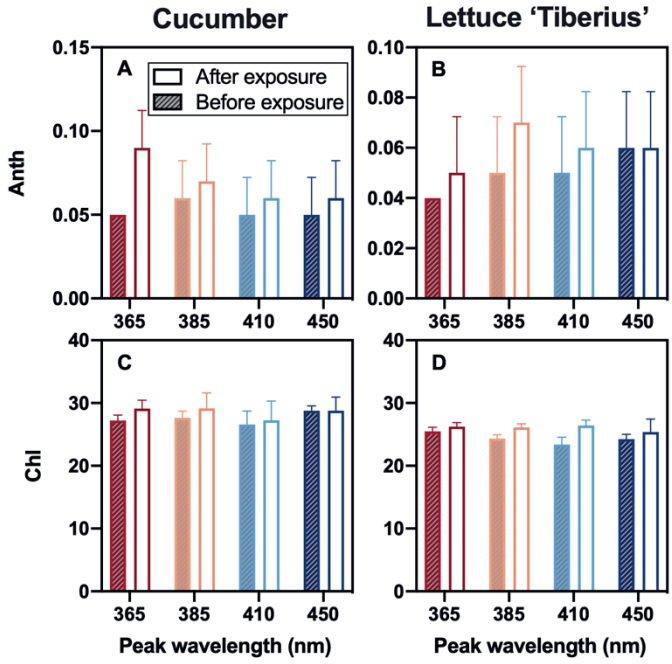


**Figure S9.** Leaf pigment concentrations in cucumber and lettuce 'Tiberius' leaves before and after exposure to one of four treatment light spectra (365-450 nm). A and B: Anthocyanin index; C and D: Chlorophyll index. Mean values ± SD of five biological replicates (n = 5). SD is visible only when larger than the symbol size.

# CHAPTER 5

## Tracking the leaf photosynthetic acclimation to the stress of UV-A1 exposure

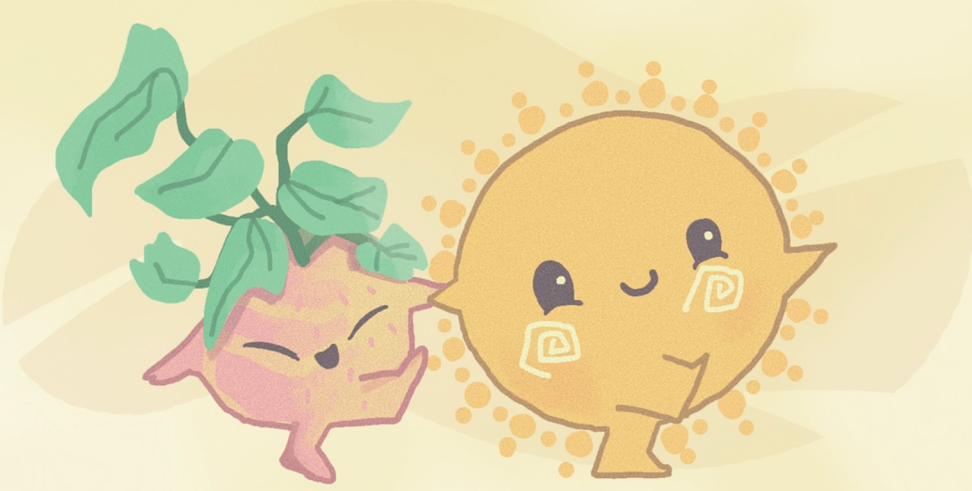

Xuguang Sun, Elias Kaiser, Leo F. M. Marcelis, Tao Li

(*to be submitted*)

# Abstract

Plants have plasticity that enables them to acclimate to stress. Previous research in **Chapter 2** demonstrated that short-term exposure to UV-A1 (350-400 nm; U) induced photoinhibition, thereby partially suppressing net photosynthesis rate (*A*). However, it is unknown whether photoinhibition caused by U suppresses *A* continuously, and how this compares to exposure to red (R) or blue (B) light. Lettuce seedlings were exposed to different light spectra in a series of three independent experiments: Exp.1) monochromatic R, B and U (peaking at 655, 456, 365 nm, respectively) at 200 µmol $m^{-2}$ $s^{-1}$ for 24 h; Exp.2) 200 µmol $m^{-2}$ $s^{-1}$ R, as well as R combined with either 200 µmol $m^{-2}$ $s^{-1}$ B or U for 24 h, resulting in R, RB and RU; and Exp. 3) R, RB and RU at each 400 µmol $m^{-2}$ $s^{-1}$ and a duration of 72 h. Results showed that exposure to U caused a rapid reduction in *A* and related traits in all experiments. Exposure to 400 µmol $m^{-2}$ $s^{-1}$ (Exp.3) was stressful for all plants, as indicated by lower maximum quantum yield of photosystem II ($F_v/F_m$), especially under RU, which is 24% and 28% lower than R and RB at 6 h, respectively; they acclimated by increasing photosynthetic capacity and eventually matched the *A* measured under R. We conclude that longer-term UV-A1 exposure is a severe stress, and leaves are able to acclimate by adjusting photosynthetic apparatus.

## Keywords:

UV-A1, photosynthesis, photosynthetic capacity, stress, pigmentation

# 1. Introduction

Exposure to light, such as monochromatic light or sudden transitions from low to high light intensity, can create moderate stress conditions for plants, as indicated by unbalanced activation of photoreceptors or excess light that cannot be fully utilized by photosynthesis (Izzo et al., 2020). High light intensities increase the chance of photoinhibition, i.e. the destruction of the D1 protein in the PSII reaction center by reactive oxygen species (ROS) happens at a faster rate than its repair (Takahashi & Badger, 2011), thereby reducing the efficiency of photosynthetic electron transport. Studying how leaves respond and acclimate to these stresses can help reveal acclimatory mechanisms, and may aid in optimizing supplemental lighting in vertical farming and greenhouses, reducing photooxidative damage, and enhancing photosynthetic efficiency, thus boosting crop growth and yield while minimizing stress-induced damage (van Delden et al., 2021). UV-A radiation (315-400 nm) is an important component of solar radiation, and affects plants both in the forms of energy and information (Verdaguer et al., 2017). As energy source, UV-A has been shown to power photosynthesis (*A*) in various species (Johnson & Day, 2002; McCree & Keener, 1974; Turnbull et al., 2013), but due to its comparably high energy content per photon can also cause high rates of photodamage (Takahashi et al., 2010). As a signal, UV-A may be divided into UV-A1 (350-400 nm) and UV-A2 (315-350 nm; Rai et al., 2021) according to the photoreceptor action spectrum: UV-A1 shares cryptochromes and phototropins with blue light, whereas UV-A2 shares photoreceptors with UVR8 (Christie, 2007; Rai et al., 2021). To date, few studies have focused on the extent to which UV-A radiation causes stress and how plants deal with it.



Longer-term UV-A1 exposure may impact *A* in multiple ways (Verdaguer et al., 2017): i) the quantum yield of UV-A1 is lower than that of visible light (McCree, 1971); ii) UV-A1 modulates stomatal aperture (Alexander et al., 2024; Ng, 2019), affecting the rate of $CO_2$ diffusion into the leaf and consequently photosynthetic efficiency; iii) UV-A1 may trigger chloroplast movement, similarly to blue light (Blatt, 1983), which would modulate leaf light absorptance; iv) UV-A1 impaired the repair of D1 and D2 proteins (Christopher & Mullet, 1994), affecting the function of the photosystem II reaction center. v) UV-A1 may inhibit the activity of Calvin cycle enzymes and through this effect reduce $CO_2$ fixation (Kataria et al.,

2014); and vi) leaves developed under UV-A1 functioned similarly as those developed under blue light in terms of their photosynthetic machinery (Zhang et al., 2020).

UV-A1 possesses a higher energy per photon than visible light, but powers photosynthesis to a lesser extent. It is therefore likely that plants engage high rates of photoprotection, e.g. in the form of non-photochemical chlorophyll fluorescence quenching (NPQ) to protect themselves from photoinhibition (Ruban, 2016). This may also mean that leaves acclimating to UV-A1 radiation build up strong photoprotective capacity, the extent of which may depend on the balance between photodamage and associated repair mechanisms (Takahashi & Badger, 2011). Maximum quantum yield of PSII ($F_v/F_m$) and PSII operating efficiency ($\Phi_{PSII}$) are considered to be reliable indicators of photoinhibition and photosynthetic performance, respectively (Murchie & Lawson, 2013). Additionally, mitochondrial respiration may increase to help synthesize antioxidants, maintain cellular energy supply and redox balance to reduce the generation of ROS (O'Leary et al., 2019). Besides, UV often causes an accumulation of UV-absorbing compounds in the epidermis, which protect leaves from UV-induced damage by reducing the amount of UV reaching the chloroplasts (Barnes et al., 2016; Caldwell et al., 1983). Acclimation to UV-A1 may occur within days, causing plants to be less susceptible to photoinhibition (Walters, 2005).

We previously showed that UV-A1 powered *A* and induced photoinhibition in a wavelength-dependent manner, both in the presence and absence of white background light (**Chapter 4**). Additionally, during 30 min of UV-A1 exposure, we observed a continuous decline in *A* that seemed to be driven by photoinhibition (**Chapter 4**). Based on this, we wondered whether leaves would be able to acclimate to longer-term UV-A1 exposure, and if so what the roles of photosynthetic capacity, mitochondrial respiration and photoprotection would be, as these processes work synergistically to maintain the metabolic balance and cope with environmental stress. In a series of experiments, we exposed plants to continuous light treatments of up to 72 h. We used lettuce (*Lactuca sativa*), as this was reported to be continuous light injury resistant (Velez-Ramirez et al., 2011). We hypothesized that UV-A1 can power photosynthesis under both short- and long-term radiation exposure, but that the extent of *A* would be dynamically modulated by photoinhibition, accumulation of UV-absorbing compounds and NPQ. Compared with blue light, we hypothesized that leaves would be more stressed under longer-term UV-A1 radiation, but would nevertheless be able to utilize high light.

# 2. Materials and methods

## 2.1 Plant material and growth conditions

Seeds of butterhead lettuce (*Lactuca sativa* cv. Klee, Rijk Zwaan, the Netherlands) were sown in rockwool plugs (Grodan, Roermond, the Netherlands) with one seed per plug, and germinated in a growth room at a photosynthetic photon flux density (PPFD) of 150 µmol $m^{-2}$ $s^{-1}$ white light (WL; ZWS01D-LED120-180, PanAnGreenlight, Jinhua, China; for spectra see Fig. S1) and a photoperiod of 16 h (06:00-22:00), a day/night temperature of 23.0 ± 0.6 /22.6 ± 0.5 °C, relative humidity of 70 ± 5 %, and a $CO_2$ partial pressure that was close to ambient. Environmental factors were monitored by a climate sensor (TR-76Ui-S; T&D Co. Ltd., Nagano, Tokyo, Japan). Seedlings were transferred to rockwool cubes (7.5 × 7.5 × 5 cm; Grodan) upon unfolding of the second leaf, and were placed in the same growth room at a PPFD of 200 µmol $m^{-2}$ $s^{-1}$ WL (ZWS01D-LED120-180, PanAnGreenlight, Jinhua, China; for spectra see Fig. S2). Opaque black-white plastic films were wrapped around each unit, which harbored one treatment, with the white side facing the plants, to avoid light contamination between units. Two ventilation fans (12 V, 0.90 A, 0.5 $m^3$ $min^{-1}$) were installed per unit to ensure uniform air circulation. A cooling system, including central air conditioning and ventilation, was used to provide uniform air quality in the growth chamber. Plants were regularly watered by hand with a modified Hoagland nutrient solution (pH = 5.8, EC = 1.6 dS $m^{-1}$). Every other day, plants inside each treatment were rotated and relocated relative to each other, to avoid position effects on plant growth. Light intensity was measured regularly using a spectroradiometer (Avaspec-2048CL, Avantes, Apeldoorn, the Netherlands). The spectroradiometer was calibrated by using a standard light source (Avalight-DH-S-BAL, Avates, Apeldoorn, the Netherlands), which delivers a highly stable, continuous spectrum in the range of 215 to 2500 nm. Every few days, new seeds were sown under these conditions, so that new starting material for the treatments (see below) was continuously available.

## 2.2 Treatments

When they were ~4 weeks old (12–14 days after transplanting), plants were transferred to light

treatments at 08:00 AM (2 h after start of photoperiod). Light treatments were provided by red (655 nm, termed 'R' hereafter), UV-A (365 nm, 'U') and blue (450 nm, 'B'; ZWS01D-LED120-180, PanAnGreenlight, Jinhua, China, 180W per lamp; Fig. S2A) LED lamps, and these were used either monochromatically, or B and U were each added to R (Table 1). LED lamps were installed in a cubicle with dimensions of 115 cm length × 70 cm width × 115 cm height inside the growth chamber, such that during treatments, environmental factors apart from light climate remained the same as during growth.

Three experiments were conducted in series (Table 1): Exp. 1) 24 h exposure to monochromatic U, B and R, each at an intensity of 200 µmol $m^{-2}$ $s^{-1}$; Exp. 2) 24 h exposure to either R (at 200 µmol $m^{-2}$ $s^{-1}$), or addition of U plus B, and U plus R (RU and RB, respectively), each at a combined intensity of 400 µmol $m^{-2}$ $s^{-1}$; Exp. 3) 72 h exposure to either R, RB or RU, each at an intensity of 400 µmol $m^{-2}$ $s^{-1}$. During each experiment, treatments were applied consecutively and in random order, since only one cubicle was available for treatment application.

**Table 1.** Overview of light treatments in the three experiments.

| Exp. no. | Color | Light intensity (µmol $m^{-2}$ $s^{-1}$) | Duration (h) | No. of replicate plants | Type of operational measurement | | | | |
|---|---|---|---|---|---|---|---|---|---|
| | | | | | *A* | *A* (LL) | *A* (HL) | CF | Leaf light abs. pigmentation plant growth |
| 1 | R | 200 | 24h | 5 | ✓ | ✓ | | | |
| | U | 200 | | 5 | | | | | |
| | B | 200 | | 5 | | | | | |
| 2 | R | 200 | 24h | 5 | ✓ | ✓ | | | |
| | RU | 200 + 200 | | 5 | | | | | |
| | RB | 200 + 200 | | 5 | | | | | |
| 3 | R | 400 | 72h | 10 | ✓ | ✓ | ✓ | ✓ | ✓ |
| | RU | 200 + 200 | | 10 | | | | | |
| | RB | 200 + 200 | | 10 | | | | | |

**Note:** R, red light peaking at 656 nm; B, blue light peaking at 450 nm; U, long-wavelength UV-A radiation peaking at 365 nm; PFD, photon flux density; *A*, operational photosynthesis under the treatment spectra; *A* (LL) and *A* (HL), photosynthesis under a standard red/blue spectrum at 100 and 1500 umol $m^{-2}$ $s^{-1}$, respectively; CF, chlorophyll fluorescence; Leaf light abs., leaf light absorptance in the 400-700 nm range. For CF measurements, only six replicate plants in one batch were used.

## 2.3 Measurements

### *2.3.1 Gas exchange and chlorophyll fluorescence*

When plants were ~4 weeks old (12–14 days after transplanting), the youngest fully expanded leaf -was used for measurements. All photosynthesis measurements were conducted at the following time points after treatment had started: 0 (5 min after start of treatment in Exp. 1 and 2), 1, 3, 6, 12, 24 (Exp. 1 and 2), 36, 48, 60 and 72 h (Exp. 3). The same plant was used for different time points. In Exp.1 and 2, measurements were conducted on five replicates plants, while in Exp. 3, measurements were conducted on ten replicates plants. Operational chlorophyll fluorescence measurements were only conducted during Exp. 3, on six replicates plants.

***Operational photosynthesis and stomatal conductance***

To assess operational gas exchange, *A* and $g_s$ were repeatedly measured under the different treatment spectra using the LI-6400XT photosynthesis system (Li-Cor Biosciences, Lincoln, Nebraska, USA), with the cuvette placed inside the treatment setup. The standard plastic film of the transparent cuvette was replaced by a 2 mm thick quartz plate, to allow for UV-A to reach the leaf surface. Light intensity and spectrum inside the cuvette were measured using a spectroradiometer (Fig. S1B). During measurements, $CO_2$ partial pressure was 400 µbar, leaf temperature was 25 °C, leaf-to-air vapor pressure deficit was 0.7–1.0 kPa and the flow rate of air through the system was 200 µmol $s^{-1}$. Upon reaching steady-state *A* (~3 mins at each sampling time), gas exchange was logged every 10 s for 1 min, and averages of these values were determined.

To monitor operational chlorophyll fluorescence, the MONI-PAM multi-channel fluorometer (Heinz Walz GmbH, Effeltrich, Germany) was placed in the treatment setup. Plants were dark-adapted in the same room for ~30 min. Selected leaflets were then placed in the leaf clip consisting of two aluminum frames (35×25 mm), and the leaf clip was mounted at a distance of 25 mm from the optical window, so that leaf clip area and the longitudinal axis of the MONI-head formed an angle of 120 °. Leaves were exposed to light intensities of 400 µmol $m^{-2}$ $s^{-1}$, and data were logged every 30 min during the experiment. Measuring beam intensity was 1 µmol $m^{-2}$ $s^{-1}$, and maximum flash intensity was 4,000 µmol $m^{-2}$ $s^{-1}$. Fluorescence yield under actinic light ($F_s$) and maximal fluorescence yield of a light-adapted leaf ($F_m$') were logged

repeatedly. Photosystem II operating efficiency ($\Phi_{PSII}$) was calculated as $\Phi_{PSII} = (F_m' - F_s)/F_m'$, NPQ was calculated as $NPQ = F_m/F_m' - 1$, the quantum yield of regulatory energy dissipation ($\Phi_{NPQ}$) was calculated as $\Phi_{NPQ} = F_s/F_m' - F_s/F_m$ , and the quantum yield of non-regulatory energy dissipation ($\Phi_{NO}$) was calculated as $\Phi_{NO} = F_s / F_m$ (Baker, 2008; Hendrickson et al., 2004).

To measure maximum quantum yield of photosystem II ($F_v/F_m$), $F_m$ and minimum ($F_o$) chlorophyll *a* fluorescence of dark-adapted plants (⩾20 min of dark adaptation) were measured, using a chlorophyll *a* fluorescence imager (IMAG-MAXI; Heinz Walz, Effeltrich, Germany). $F_v/F_m$ was then calculated as $(F_m - F_o)/ F_m$ (Baker, 2008).

***Respiration rate, photosynthetic quantum yield and photosynthetic capacity***

After measuring *A* and $g_s$ under the treatment spectrum, the same leaf was enclosed in the leaf chamber fluorometer of the Li-6800 (Li-Cor Part No.6800–01A, enclosed leaf area: 2 $cm^2$) to determine net photosynthesis rate at 100 µmol $m^{-2}$ $s^{-1}$ ($A_{100}$), apparent rate of respiration in darkness ($R_{dark}$), and maximum photosynthesis rate under light- and $CO_2$ saturation ($A_{max}$) during the treatment (Busch et al., 2024), under a standard light source. At each time point, leaves were exposed to 1500, 100 and 0 µmol $m^{-2}$ $s^{-1}$ PPFD in the fluorometer, respectively, $CO_2$ partial pressure was 1500 µbar under 1500 $m^{-2}$ $s^{-1}$ PPFD, and 400 µbar under 100 and 0 µmol $m^{-2}$ $s^{-1}$ PPFD, leaf temperature was ~25 °C, leaf vapor pressure deficit was 0.7–1.0 kPa, and air flow rate through the system was 200 µmol $s^{-1}$. Irradiance was provided by a mixture of red (90%) and blue (10%) LEDs in the fluorometer; peak intensities of red and blue LEDs were at wavelengths of 635 and 465 nm, respectively. After steady-state *A* was reached at each light intensity (~2 min, except for the highest light intensity, where this took 5-10 min), photosynthetic gas exchange was logged every 10 s for 1 min, and averaged values were later used. Additionally, chlorophyll fluorescence was measured at 1500 and 100 µmol $m^{-2}$ $s^{-1}$ PPFD, using a rectangular saturating flash of 16000 µmol $m^{-2}$ $s^{-1}$ intensity that was applied for 500 ms, and a data acquisition rate of 100 Hz. The maximum efficiency of $CO_2$ uptake ($\Phi CO_2$) was calculated as: $\Phi CO_2 = (A - R_{dark})/(PPFD * \text{leaf light absorptance})$.

***2.3.2 Plant growth***

Destructive measurements were carried out after 0, 24, 48 and 72 h during Exp. 3. Fresh and dry weights of leaves were determined. Plant organs were dried for 48 h at 80 °C in a ventilated oven (DHG-9070A, Shanghai Jinghong, Shanghai, China). Leaves that were longer than 2 cm

from the base to the tip were counted. Leaf area was measured using a leaf area meter (LI-3100C, Li-Cor Biosciences). Specific leaf area (SLA; $cm^2\ g^{-1}$) was calculated by dividing leaf area by leaf dry weight. Dry mass content was calculated as the ratio of shoot dry to fresh weight. Measurements were conducted on three plants per sampling time point and batch, in two separate batches in total.

### *2.3.3 Leaf light absorptance*

Light reflectance (Rf) and transmittance (Tr) of the adaxial side of the leaf were measured with a spectrometer (Ocean optics USB2000+, Dunedin, USA), in combination with two integrating spheres (FOIS-1, ISP-REF, Ocean Optics). Leaf light absorptance (Abs), ranging from 400 to 700 nm, was calculated as Abs=1−(Rf+Tr). Additionally, leaf light absorptance was measured every 5 minutes within the first ~30 min of treatment, to observe possible effects of chloroplast movement on leaf optical properties.

### *2.3.4 Leaf biochemical components*

On four time points (0, 24, 48 and 72 h), biochemical measurements were conducted on two plants per batch (plants were chosen randomly per time point), and this was repeated in six separate batches of plants. Leaf samples were pooled per pair of plants and frozen in liquid nitrogen, which means six replicates plants were used.

#### *Chlorophyll concentration*

Fresh leaf tissue (0.1 g) was ground in liquid nitrogen, using a high-throughput tissue grinder (SCIENTZ-48, Xinzhi, Ningbo, China), and then incubated in 10 mL 95% ethanol in the dark at 4 °C, for 24 h. After centrifugation for 5 min at 4 °C, the absorbance of the extract was measured at 470, 649, 664 and 750 nm, using a spectrophotometer (UV-1800, Shimadzu, Japan). The concentrations of chlorophyll *a*, chlorophyll *b*, their sum and ratio, as well as total carotenoid contents, were calculated using the equations derived by Lichtenthaler and Buschmann (2001).

#### *Anthocyanin*

Fresh leaf tissue (0.1 g) was ground as described above, incubated with 600 µL extraction buffer (99% methanol and 1% HCl), and vortexed. Extracts were placed in an ultrasonic bath for 10

minutes and then incubated overnight and in the dark, at 4 °C. After extraction, 400 µL of water and 400 µL of chloroform were added. Absorbance (Abs) of extracts was measured at 530 and 657 nm, using a microplate reader (Infinite 200 PRO, TECAN, Switzerland), and anthocyanin content was calculated after Liu et al. (2018).

***UV-absorbing compounds***

Fresh samples (0.1 g) were ground as described above, and incubated with 5 mL of acidified methanol solution (70% methanol, 29% $H_2O$ and 1% HCl) at -20°C, for 48 h. Absorbance of extracts was measured at 330 nm, using a microplate reader (Infinite 200 PRO), and the concentration of UV-absorbing compounds was determined following Barnes et al. (2016).

***Phenolic and flavonoid contents***

Fresh samples (0.1 g) were extracted with 1 mL of 80% aqueous methanol in an ultrasonic bath (10 min), and were then centrifuged (15,000× g for 10 min). Total phenolic and flavonoid concentrations were determined using the Folin Ciocalteu and the aluminum chloride colorimetric assays (Khanam et al., 2012), respectively. The absorbances at 750 and 510 nm were determined, respectively, using a microplate reader (Infinite 200 PRO). For total phenolics and flavonoid content, gallic acid and rutin were used as the standard reference, respectively. Both gallic acid equivalent (GAE) and rutin equivalent (RUE) were determined as mg per g fresh mass following Yang et al. (2021).

***Indices of pigment concentrations***

Indices of chlorophyll and anthocyanin concentrations were regularly determined non-destructively by a Dualex (Dualex Scientific+; Force-A, Orsay, France). Measurements were taken on the youngest mature leaves. Three technical replicates per leaf were chosen randomly, and an average value was calculated per leaf.

## 2.4 Experimental design and statistics

Three experiments each with three light treatments were conducted consecutively (Table 1), and treatments were also applied consecutively. Exp. 1 and 2 were conducted once, Exp. 3 was conducted twice. During Exp. 1 and 2, 5 replicate plants were measured; during Exp. 3, 10

replicate plants were measured, except for measurements of chlorophyll fluorescence in which case 6 replicate plants were measured. Statistical analyses were performed in R (version 4.1.3., R Core Development Team, 2022). The Q-Q plot was used to test the distribution of data graphically, and the *bartlett.test* was used to test the homogeneity of variance of residuals at $P$=0.05. When data did not fulfil the assumptions for an ANOVA, they were log-transformed and the tests on residuals were repeated. If the log-transformed data failed to satisfy the assumptions for an ANOVA, the *kruskal-wallis.test* was used on original non-transformed data. Linear mixed effects models were fitted using the *lme* function in the *nlme* package, considering independent plant as a random effect when the same plant were used for different time points. The effects of the factors were analyzed, i.e. the effect of light spectrum treatment, the sampling time of treatment, and their interaction.

# 3. Results

## 3.1 Photosynthesis under continuous exposure to monochromatic U, B and R light

When lettuce leaves were exposed to monochromatic UV-A1 radiation (U), operational net photosynthesis rate ($A_{op}$) was initially ca. 60-70% lower than that under red (R) or blue (B) light (Fig. 1A). Within the first hour of U exposure, there was an additional sharp decline, and $A_{op}$ did not recover in the remainder of the 24 h treatment (Fig. 1A). While $A_{op}$ in R and B showed slight decreases (10-20%), the reduction under U was notably larger (~70%, Fig. 1A), compared to $A_{op}$ after 5 min of treatment. The operational stomatal conductance ($g_{sop}$) of U and R treated leaves showed strong initial reductions in the first hours, and these were accompanied with reductions in leaf internal $CO_2$ partial pressure ($C_{iop}$) in R but not U treated leaves (Fig. 1C, D). In contrast, $g_{sop}$ remained stable in B treated leaves, causing $C_{iop}$ to be stable as well (Fig. 1C, D).

When measured under a standard spectrum at low light intensity, photosynthesis ($A_{100}$) in U-treated leaves initially showed strong reductions with a later recovery, whereas $A_{100}$ in R and B treated leaves was relatively stable (Fig. 1E). At the same time, apparent respiration rate in darkness ($R_{dark}$) was much lower in U-treated leaves than in R or B treated leaves (Fig. 1B), so

the reduction in $A_{op}$ and $A_{100}$ under U cannot be explained by increased respiration rate. Electron transport efficiency through photosystem II ($\Phi_{PSII\_100}$) roughly followed the same trend as $A_{100}$, although between 12 and 24 h, $\Phi_{PSII\_100}$ in U-treated leaves stayed relatively low, whereas $A_{100}$ recovered (Fig. 1A, F).

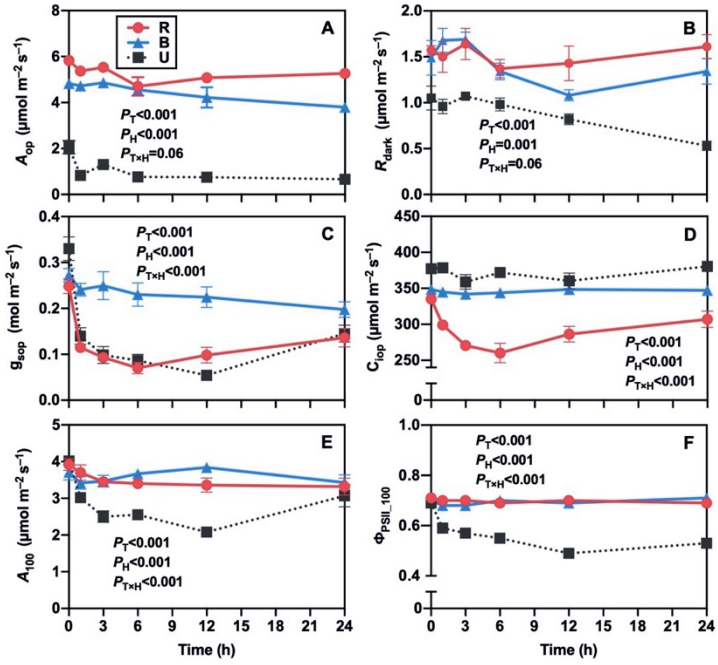


**Figure 1.** Effects of 24 h exposure to monochromatic UV-A (U), blue (B) and red light (R) on leaf photosynthetic gas exchange and chlorophyll fluorescence in lettuce. A) Operational net photosynthesis rate (*A*) under the treatment spectra ($A_{op}$), B) apparent respiration rate in darkness ($R_{dark}$), C) operational stomatal conductance ($g_{sop}$), D) operational leaf internal $CO_2$ partial pressure ($C_{iop}$), E) *A* under a standard red/blue spectrum at 100 umol m$^{-2}$ s$^{-1}$ ($A_{100}$), F) electron transport efficiency through photosystem II, under identical conditions as $A_{100}$ ($\Phi_{PSII\_100}$). UV-A radiation (U), blue (B) and red light (R) were used as treatment spectra at 200 µmol m$^{-2}$ s$^{-1}$. Mean values ± SEM of five replicates plants (n = 5). Numbers show *P*-values for the main effects of light spectrum treatment ($P_T$) and sampling time of treatment ($P_H$), and their interaction ($P_{T\times H}$). *(Experiment 1)*

## 3.2 Effect of adding U or B to R light for 24 hours on photosynthesis

To compare the effects of U and B within a broader light spectrum, these were each added to R light (at total intensities of 400 µmol m$^{-2}$ s$^{-1}$), and compared to the effects of monochromatic R light (200 µmol m$^{-2}$ s$^{-1}$). $A_{op}$ under RU and RB was initially higher than $A_{op}$ under R (Fig.

2A), owing to the twice as high light intensity in RU and RB compared to R. However, just as under monochromatic U exposure (Fig. 1A), exposure to RU caused a rapid decline in $A_{op}$ within the first hour of treatment, causing $A_{op}$ to have roughly the same or lower rates than $A_{op}$ under R (Fig. 2A). Under RB, $A_{op}$ also declined, but it did so less strongly than under RU (Fig. 2A). Similarly to U and R (Fig. 1C), $g_{sop}$ under RU and R showed strong initial reductions that later recovered to some extent, whereas $g_{sop}$ under RB was more variable (Fig. 2C). Because of the strong reductions in $A_{op}$, $C_{iop}$ in RU treated leaves was relatively stable, whereas in R treated leaves the reductions in $g_{sop}$ (at relatively stable $A_{op}$) caused a drop and later partial recovery in $C_{iop}$ (Fig. 2A, C, D). $A_{100}$ and $\Phi_{PSII\_100}$ showed strong reductions under RU and lesser reductions under RB, while under R these traits stayed very stable (Fig. 2E, F). $R_{dark}$ tended to be smaller in RU and RB leaves compared to R, but varied over time in all three treatments (Fig. 2B).

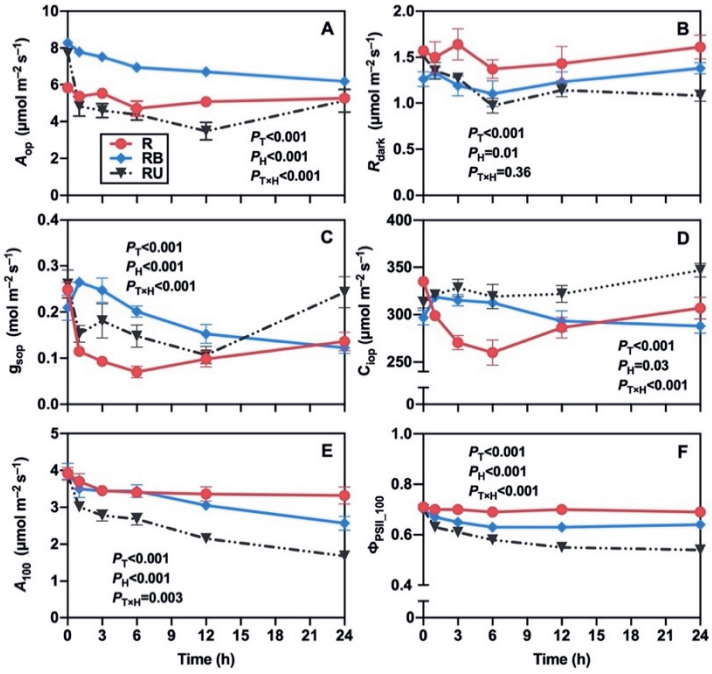


**Figure 2.** Effects of 24 h exposure to monochromatic R or dichromatic RB or RU light spectrum treatments on leaf photosynthesis in lettuce. A) Operational net photosynthesis rate ($A$) under the treatment spectra ($A_{op}$), B) apparent respiration rate in darkness ($R_{dark}$), C) operational stomatal conductance ($g_{sop}$), D) operational leaf internal $CO_2$ partial pressure ($C_{iop}$), E) $A$ under a standard red/blue spectrum at 100 umol m$^{-2}$ s$^{-1}$ ($A_{100}$), F) electron transport efficiency through photosystem II, under identical conditions as $A_{100}$ ($\Phi_{PSII\_100}$). Red light (R; 200 µmol m$^{-2}$ s$^{-1}$) was used as background spectrum, and treatment light (200 µmol m$^{-2}$ s$^{-1}$) of either of two peak wavelengths was added: 365 (RU)

and 450 (RB) nm. Mean values ± SEM of five replicates plants (n = 5). Numbers show *P*-values for the main effects of light spectrum treatment ($P_T$) and sampling time of treatment ($P_H$), and the interaction between them ($P_{T\times H}$). *(Experiment 2)*

## 3.3 Effect of partially substituting R by U or B light for 72 hours on photosynthesis, photoprotection and photoinhibition

Following the time courses of photosynthesis observed within 24 h of exposure to U, B, R, RB and RU, we asked whether $A_{op}$ under U would be able to recover fully at a longer treatment duration, and what role photoinhibition, photoprotection and changes in photosynthetic capacity may play in this recovery. To answer these questions, we exposed plants for 72 h to continuous light (400 μmol $m^{-2}$ $s^{-1}$) of either R, RB or RU, and conducted a large number of measurements.

In RU leaves, $A_{op}$ showed an initial drop similar to those seen before (Figs. 1A, 2A), but throughout the entire 72 h exposure, it recovered almost entirely (Fig. 3A). RB treated leaves, on the other hand, showed a continuous decline in $A_{op}$ by ~50% after 72 h, whereas $A_{op}$ in R treated leaves showed a lesser reduction on days 2 and 3 of the treatment (Fig. 3A). $g_{sop}$ showed strong initial increases in RB treated leaves, but this declined within 24 h, and then showed slow, continuous reductions similar to those seen in R treated leaves (Fig. 3B). In contrast, $g_{sop}$ in RU treated leaves showed a strong initial reduction and then was relatively constant (Fig. 3B). $C_{iop}$ was mostly stable in RU and RB treated leaves, while it was reduced in R treated leaves (Fig. 3C). No major treatment effects were observed on $R_{dark}$ (which stayed relatively constant; Fig. 3I) within 72 h. Leaf light absorptance showed increases over time in all treatments (Fig. 3J). While, during 30 min of treatment exposure, RB treated leaves showed a continuous reduction in leaf light absorptance, whereas R and RU treated leaves did not (Fig. S3).

Traits measured under a standard spectrum and at a low light intensity (100 $m^{-2}$ $s^{-1}$), namely $A_{100}$, $\Phi_{PSII\_100}$ and $\Phi_{CO2\_100}$ (Fig. 3D-F), showed similar patterns as $A_{op}$ (Fig. 3A): in all three traits, a rapid reduction with a later recovery was visible in RU treated leaves, whereas $A_{100}$ and $\Phi_{CO2\_100}$ showed near-linear reductions over time in RB and R treated leaves. $\Phi_{PSII\_100}$, on the

other hand, was remarkably stable in RB and R treated leaves (Fig. 3E). There were no large differences in $R_{dark}$ between treatments (Fig. 3I). When measured under saturating irradiance and [$CO_2$], $A_{max}$ in RU treated leaves showed an initial reduction, but thereafter increased constantly, so that after 72h it was ~20% higher than at the start of the treatment (Fig. 3G). In the RB and R treatments, on the other hand, $A_{max}$ showed reductions that resulted in ~20-50% reductions, respectively; the treatment effect on $A_{max}$ was not reflected in $\Phi_{PSII\_max}$, which showed small increases in RU and RB treated leaves, but was almost stable in R treated leaves (Fig. 3H).

In RU treated leaves, dark-adapted $F_v/F_m$ showed massive reductions directly after the start of treatment, resulting in a minimum after 6h of treatment that was ~30% lower than the initial value (~0.81; Fig. 3K). Thereafter, however, $F_v/F_m$ in RU treated leaves increased steadily, recovering to a final value of 0.73 (Fig. 3K). In RB treated leaves, there was only a slight reduction in $F_v/F_m$, whereas in R treated leaves a relatively strong reduction was observed within the first 24h that did not fully recover until the end of the experiment (Fig. 3K). Operational NPQ measured under the treatment lights showed continuous and strong increases in RB and R treated leaves, but was very low and declined further in RU treated leaves (Fig. 3L). The three competing energy partitioning pathways - $\Phi_{NPQ}$, $\Phi_{PSII}$ and $\Phi_{NO}$ - fluctuated over time in RU treated leaves but otherwise showed no significant trends (Fig. 3M-O). In RB treated leaves, on the other hand, $\Phi_{NPQ}$ and $\Phi_{PSII}$ both increased over time, resulting in declining $\Phi_{NO}$; in R treated leaves $\Phi_{NPQ}$ increased while $\Phi_{PSII}$ was relatively stable, and $\Phi_{NO}$ declined as a result of the increase in $\Phi_{NPQ}$ (Fig. 3M-O).

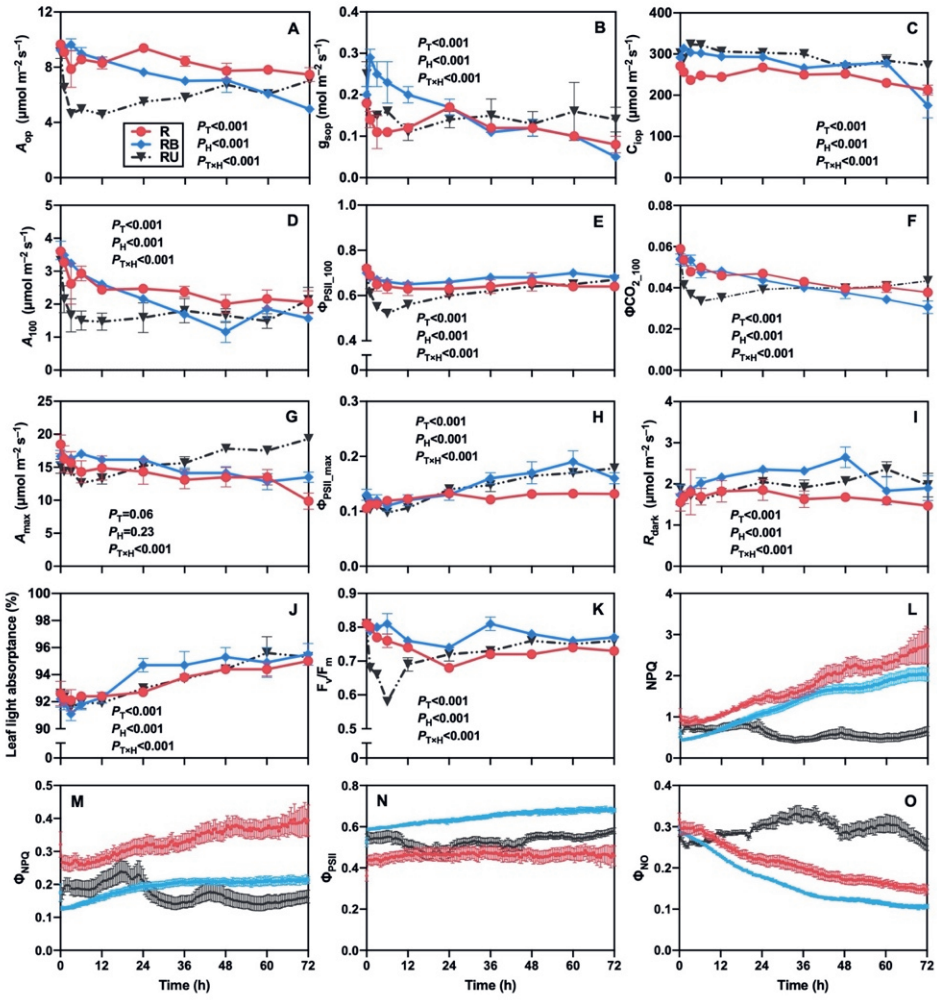


**Figure 3.** Effects of 72 h exposure to monochromatic R or dichromatic RB or RU light spectrum on leaf photosynthesis, photoprotection and photoinhibition in lettuce. A) Operational net photosynthesis rate (*A*) under the treatment spectra ($A_{op}$), B) operational stomatal conductance ($g_{sop}$), C) operational leaf internal $CO_2$ partial pressure ($C_{iop}$), D) *A* under a standard red/blue spectrum at 100 umol $m^{-2}$ $s^{-1}$ ($A_{100}$), E) electron transport efficiency through photosystem II (PSII), under identical conditions as $A_{100}$ ($\Phi_{PSII\_100}$), F) maximum efficiency of $CO_2$ uptake, under identical conditions as $A_{100}$ ($\Phi CO_{2\_100}$), G) *A* under a standard red/blue spectrum at 1500 umol $m^{-2}$ $s^{-1}$ ($A_{max}$), H) electron transport efficiency through photosystem II (PSII), under identical conditions as $A_{max}$ ($\Phi_{PSII\_max}$), I) apparent respiration rate in darkness ($R_{dark}$), J) leaf light absorptance in the 400-700 nm range, K) maximum quantum yield of photosystem II ($F_v/F_m$), L) non-photochemical fluorescence quenching (NPQ), M) quantum yield of regulatory energy dissipation ($\Phi_{NPQ}$), N) photosystem II electron transport efficiency ($\Phi_{PSII}$), O) quantum yield of non-regulatory energy dissipation ($\Phi_{NO}$). To obtain chlorophyll fluorescence parameters shown in L-O, initially darkened leaves were exposed to 400 µmol $m^{-2}$ $s^{-1}$ light intensity for 72h, and data were logged every 30 min; mean values ± SEM of six replicates plants (n = 6). For other photosynthetic parameters, mean values ± SEM of ten replicates plants (n = 10) are shown. Red light (200 µmol $m^{-2}$

$s^{-1}$) was used as background spectrum, and treatment light (200 µmol $m^{-2}$ $s^{-1}$) of either of three peak wavelengths was added: 365 (RU), 450 (RB) and 656 (R) nm. Numbers show *P*-values for the main effects of light spectrum treatment ($P_T$) and sampling time of treatment ($P_H$), and the interaction between them ($P_{T\times H}$). *(Experiment 3)*

## 3.4 Plant growth and pigmentation under 72 h treatment

All treatments caused a purplish coloration, and especially RB treated plants appeared more compact and dark purple after 72 h (Fig. 4A). The RU treatment resulted in slightly reduced shoot fresh and dry weights compared to the other two treatments, along with a tendency for reduced leaf area (Fig. 4C, D, F). Leaf number and SLA tended to be larger under RU, and SLA as well as dry mass content showed the fastest treatment responses in RB treated leaves, but none of these traits showed significant differences after 72 h of treatment (Fig. 4B, E, G). Treatment with RU caused stronger increases in chlorophyll concentrations than either RB or R (Fig. 5A), whereas the concentrations of anthocyanins, UV-absorbing compounds, phenolics and flavonoids were strongly increased in RB treated leaves compared to other treatments, which increased under all treatments but did not strongly differ from one another in R and RU treated leaves (Fig. 5C-F). Carotenoid concentrations also increased in all treatments, but showed no major treatment effects (Fig. 5B).

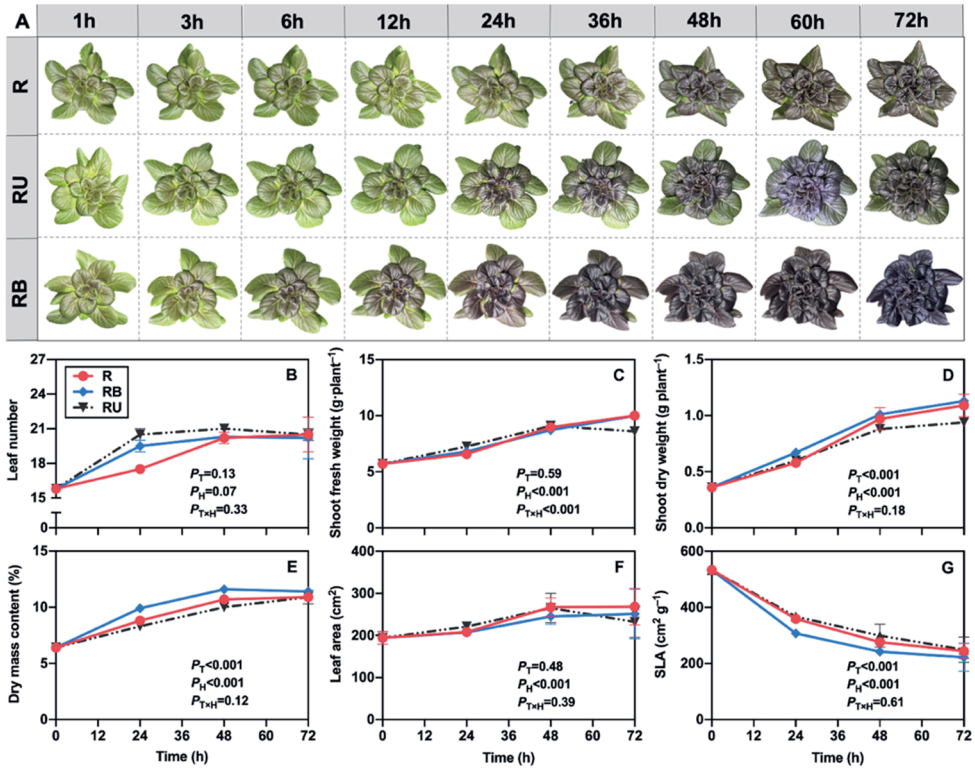


**Figure 4.** Effects of 72 h exposure to monochromatic R or dichromatic RB or RU on plant appearance and growth in lettuce. A: Appearance of representative plants that were repeatedly photographed, B: leaf number, C: shoot fresh weight, D: shoot dry weight, E: dry mass content, F: leaf area, G: specific leaf area (SLA). Mean values ± SEM of six replicates plants (n = 6). Red light (200 µmol $m^{-2}$ $s^{-1}$) was used as background spectrum, and treatment light (200 µmol $m^{-2}$ $s^{-1}$) of either of three peak wavelengths was added: 365 (RU), 450 (RB) and 656 (R) nm. Numbers show *P*-values for the main effects of light spectrum treatment ($P_T$) and sampling time of treatment ($P_H$), and their interaction ($P_{T\times H}$). *(Experiment 3)*

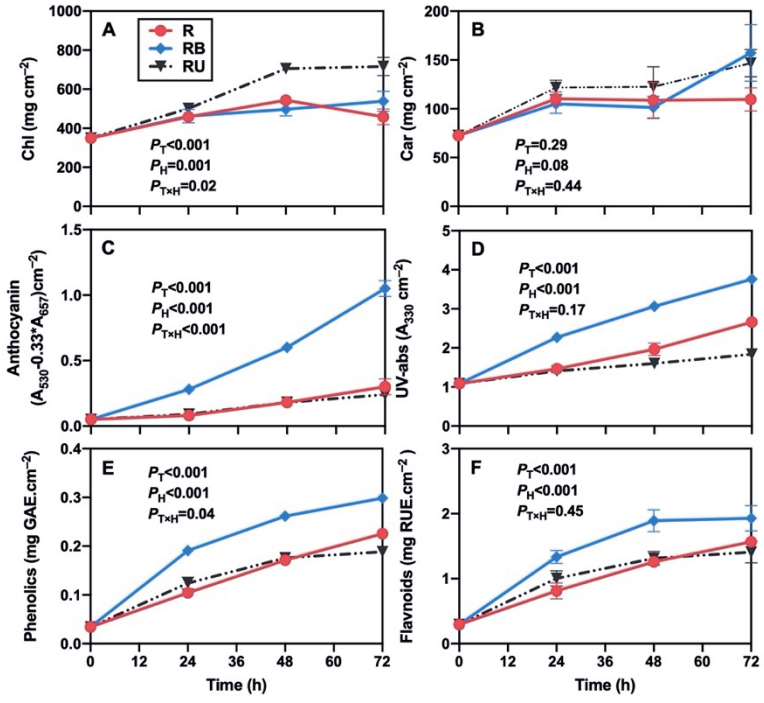


**Figure 5.** Effects of 72 h exposure to monochromatic R or dichromatic RB or RU spectrum treatment on leaf biochemical compounds in lettuce. A: chlorophyll concentration, B: carotenoids, C: anthocyanin, D: UV-absorbing compounds, E: phenolics (gallic acid equivalent (GAE) used as the standard reference), F: flavonoids (rutin equivalent (RUE) used as the standard reference). Red light (200 µmol $m^{-2}$ $s^{-1}$) was used as background light, to which treatment light (200 µmol $m^{-2}$ $s^{-1}$) of either of three peak wavelengths was added: 365 (RU), 450 (RB) and 656 (R) nm. Mean values ± SEM of 12 replicates plants (n = 12). Numbers show *P*-values for the main effects of light spectrum treatment ($P_T$) and sampling time of treatment ($P_H$), and their interaction ($P_{T\times H}$). *(Experiment 3)*



# 4. Discussion

As a significant component of sunlight, UV-A radiation may contribute to plant growth, but also may be a significant stressor that plants need to protect themselves from; both of these facets of UV-A radiation are currently understudied. We investigated several time series of *A* in lettuce under continuous exposure to a number of light treatments, including monochromatic and dichromatic R and UV-A1. Overall, we found that while exposure to 200 µmol $m^{-2}$ $s^{-1}$ of UV-A1 radiation combined with 200 µmol $m^{-2}$ $s^{-1}$ red light caused significant stress, leaves were able to acclimate to this stress within three days.

## 4.1 Transferring plants from growth light to continuous treatment light could induce stress, with UV-A being the most stressful light quality

In several treatments (Exp. 2 and 3) we used 400 μmol $m^{-2}$ $s^{-1}$ as treatment light intensity, which was twice the growth light intensity of 200 μmol $m^{-2}$ $s^{-1}$ (Table 1) and while plants were raised at a photoperiod of 16h, during treatment period the plants were continuously exposed to light. This was a deliberate choice to introduce a stress whose effects we could then study over time (Figs. 2-5). It turned out that exposure to UV-A1 was the most stressful, especially at the first three hours, as indicated by lowest $A_{op}$ and $F_v/F_m$ (Figs. 1-3). Under either monochromatic or hybrid light treatments, the intensity of UV-A1 was kept at 200 μmol $m^{-2}$ $s^{-1}$, which is an intensity that can be almost reached in nature under very high light intensities (Turnbull et al., 2013), so using this intensity in an experiment like ours is high, but not unrealistically so.

When plants grown under low background light intensity were transferred to continuous high light exposure, pigment concentrations increased under in all treatments (Fig. 5). Hence, leaf light absorptance increased over time in all treatments (Fig. 3J), enhancing the ability of all plants to capture light. Nevertheless, these plants may have been unable to fully utilize all the absorbed energy: plants grown under RB and R dissipated the excess energy as heat via thermal dissipation (Fig. 3L), while RU induced non-regulatory dissipation of energy (Fig. 3O), a process that does not benefit the plant in terms of photoprotection and that indicates stress (Samson et al., 2019). Furthermore, chloroplast movement can induce changes in leaf light absorptance (Davis et al., 2011): We observed that leaf light absorptance was affected by light spectrum treatments (Fig. S3): blue light seemed to trigger leaf light absorptance changes, while in R or RU treated leaves it did not, which also confirms prior research that chloroplast movement is wavelength-dependent (Blatt, 1983).

A sharp decline in $A_{op}$ under sole U (100 μmol $m^{-2}$ $s^{-1}$) was observed in Exp. 1 (Fig. 1A), again suggesting that UV-A1 exposure was stressful for the lettuce leaves. It was unknown whether $A$ would drop even further or show recovery at a longer exposure time; to investigate this, we decided to treat plants to even longer exposure times of continuous light. Continuous light promoted the accumulation of pigments under all treatments in a wavelength dependent manner (Fig. 5). Blue light applied just prior to harvest could be utilized to trigger the synthesis of novel

colors and flavors that are liked by consumers (Ilić & Fallik, 2017; Min et al., 2021). To sum up, treatment light intensity being higher than growth light together with continuous light lead to a reduction in $A_{op}$ in all cases, and RU-treated plants showed both strong photoinhibition and acclimation capabilities (discussed below), compared to the other treatments (Fig. 3).

## 4.2 Leaves under UV-A1 are initially strongly stressed, but manage to acclimate within 72 h

Plants interact with the environment in an intricate manner (Aphalo & Sadras, 2022; Janda et al., 2020). The rapid suppression of $A_{op}$ under UV-A1 was caused by several processes: first of all, it is known that UV-A1 powers photosynthesis with a relatively low quantum yield (**Chapter 4**; McCree, 1971). Additionally, leaves were clearly photoinhibited (low $F_v/F_m$; Fig. 3K), and initially showed low photosynthesis rates even when measured under a standard spectrum ($A_{100}$; Figs. 1E, 2E, 3D); this, together with broadly unaffected $R_{dark}$ (Figs. 1B, 2B, 3I) resulted in strong initial reductions in $\Phi_{CO2}$ (Fig. 3F). Hence, it is likely that photoinhibition initially reduced photosynthetic efficiency in UV-A1 treated leaves through a strong reduction of active PSII reaction centres (Takahashi & Badger, 2011). This is also shown by impaired photosynthetic electron transport around PSII resulting in lower $\Phi_{PSII}$ (Fig. 1F, 2F, 3E; (Vass et al., 2002), thereby preventing the light from being fully utilized by plants. Interestingly, under 72h RU exposure, $A_{op}$ under RU increased to such an extent that it was not different from $A_{op}$ under R (Fig. 3A), suggesting that plants under RU managed to successfully acclimate to UV-A1 exposure within 72 h.

Surprisingly, this acclimation under RU was not accomplished through increases in NPQ or UV-absorbing compounds, but by increases in photosynthetic capacity (Figs. 3G, L, M; 5C-F), which goes against our hypothesis. Plants can achieve photoprotection through various mechanisms (i.e., ROS scavenging, screening of radiation by UV-absorbing compounds in the epidermis, NPQ, leaf and chloroplast movement) (Takahashi & Badger, 2011). The increase of NPQ under R and RB at 72 h co-occurred with a reduction in $A_{op}$ (Fig. 3A, L). NPQ of RU was slightly higher than that of RB during first 12 h exposure, indicating that NPQ alleviated photoinhibition to a certain extent (Fig. 3 A, K, M). Besides, accumulation of carotenoids may further absorb UV-A1 radiation to prevent it from arriving at the chloroplast

(Fig. 5B) (Edreva, 2005). The concentrations of UV-absorbing compounds did not strongly increase under UV-A1 exposure similar as blue light (Fig. 5C-D), which was also against our hypothesis. This lack of change in UV absorbing compounds under UV-A1 exposure may be regulated by UVR8, instead of UV-A photoreceptors (Jenkins, 2014). However, this explanation is incomplete, as exposure to blue light did cause an accumulation of these compounds, which supports prior findings that blue light promotes flavonoid accumulation by inducing gene expression in the phenylpropanoid pathway (Palma et al., 2021, 2022). Another possible reason is that UV radiation regulates specific phenolic compounds rather than total flavonoid concentration (Kotilainen et al., 2008). It is also possible that UV-A1 is less effective than blue light at the transcriptional level (Zhang et al., 2023). In addition, under continuous light exposure (Table 1), the duration of UV-A1 exposure also affects both flavonoid synthesis and accumulation (Kotilainen et al., 2010; Palma et al., 2021). Besides, plants continuously exposed to light in the current study exhibited varying intensities of purple, which likely resulted from different concentrations of UV-screening pigments (Figs. 4A, 5D-F). This confirms that the accumulation of UV-absorbing compounds under UV-A1 exposure is heavily regulated by light spectrum (Palma et al., 2021; Qian et al., 2019). In addition, future research should also determine how quickly photoprotection and photoinhibition can recover from UV-A1 exposure.

The increase in $A_{max}$ under RU may suggest that HL can enhance the activity of Rubisco involved in the Calvin cycle (Fig. 3G) (Ernstsen et al., 1999; Kataria et al., 2014), further accelerating the rate of $CO_2$ fixation under HL. Further, contrary to our expectations, $R_{dark}$ was not increased under UV-A1 exposure, it even decreased under sole UV-A1 radiation (Fig. 1B, 2B, 3I), thus failing to provide a surplus of ATP to reduce the risk of photo-oxidative damage (Millar et al., 2011). Thus, low $A_{op}$ under RU likely explains reduced plant growth, compared to other treatments, as neither $R_{dark}$ nor projected leaf area were reduced under RU (Figs. 3A, I; 4). Plants inevitably encounter UV radiation in nature (Verdaguer et al., 2017), and early acclimation to UV-A1 treatments such as in our experiments may prime seedlings to possess high resistance to photo-oxidative damage.

### 4.3 Stomatal conductance ($g_s$) differentiates between UV-A1 and blue light

Distinct mechanisms are involved in stomatal opening regulated by different wavelengths (Kuiper, 1964), but it is unclear how the stomatal response to UV-A1 fits into the known responses, such as the blue light and the red light response. On the one hand, UV-A1 is adjacent to and similar to blue light in some respect, as both are sensed by phototropins which regulate $g_s$ (Christie, 2007); on the other hand, photons in the UV-A1 range possessing high energy may activate protection mechanisms and thereby indirectly affect $g_s$ (Alexander et al., 2024). The contrasting trend of $g_{sop}$ between B and RB was ascribed to both light intensity and light quality (Figs. 1C, 2C), which reflected the prominent role of B inducing stomata opening in the presence of strong R as background light (Baroli et al., 2008). However, red light had no such effects on RU treatment (Fig. 2C), indicating that UV-A1 regulation of stomatal opening is an independent mechanism different from both red and blue light. Further, $g_{sop}$ decreased under both R and RU, but $C_{iop}$ showed opposite trends in two treatments (Fig. 2C, D), potentially ruling out effects of UV-A1-driven mesophyll photosynthesis (Matthews et al., 2020). We note that there is currently a knowledge gap in the role of UV-A1 on stomata, but studies using photoreceptor mutants together with narrowband UV-A lamps will likely illuminate this.

## 5. Conclusions

This study highlights the stress responses and acclimation mechanisms of lettuce plants exposed to different combinations of UV-A1 radiation, red and blue light. Continuous exposure to 400 μmol $m^{-2}$ $s^{-1}$ light for up to 72 h was generally stressful for plants grown under 200 μmol $m^{-2}$ $s^{-1}$, with UV-A1 being the most stressful, a situation that plants responded to by acclimating their photosynthetic apparatus and especially their photosynthetic capacity.

Chapter 5

# References


Alexander, A., Jansen, M. A. K., Grace, J., & Urban, O. (2024). Unravelling the neglected role of ultraviolet radiation on stomata: A meta-analysis with implications for modelling ecosystem–climate interactions. *Plant Cell and Environment*, *November 2023*, 1–13. https://doi.org/10.1111/pce.14841

Aphalo, P. J., & Sadras, V. O. (2022). Explaining pre-emptive acclimation by linking information to plant phenotype. *Journal of Experimental Botany*, *73*(15), 5213–5234. https://doi.org/10.1093/jxb/erab537

Baker, N. R. (2008). Chlorophyll fluorescence: A probe of photosynthesis in vivo. *Annual Review of Plant Biology*, *59*, 89–113. https://doi.org/10.1146/annurev.arplant.59.032607.092759

Barnes, P. W., Tobler, M. A., Keefover-Ring, K., Flint, S. D., Barkley, A. E., Ryel, R. J., & Lindroth, R. L. (2016). Rapid modulation of ultraviolet shielding in plants is influenced by solar ultraviolet radiation and linked to alterations in flavonoids. *Plant Cell and Environment*, *39*(1), 222–230. https://doi.org/10.1111/pce.12609

Baroli, I., Price, G. D., Badger, M. R., & Von Caemmerer, S. (2008). The contribution of photosynthesis to the red light response of stomatal conductance. *Plant Physiology*, *146*(2), 737–747. https://doi.org/10.1104/pp.107.110924

Blatt, M. R. (1983). The action spectrum for chloroplast movements and evidence for blue-light-photoreceptor cycling in the alga Vaucheria. *Planta*, *159*(3), 267–276. https://doi.org/10.1007/BF00397535

Busch, F. A., Ainsworth, E. A., Amtmann, A., Cavanagh, A. P., Driever, S. M., Ferguson, J. N., Kromdijk, J., Lawson, T., Leakey, A. D. B., Matthews, J. S. A., Meacham-Hensold, K., Vath, R. L., Vialet-Chabrand, S., Walker, B. J., & Papanatsiou, M. (2024). A guide to photosynthetic gas exchange measurements: Fundamental principles, best practice and potential pitfalls. *Plant Cell and Environment*, *December 2023*. https://doi.org/10.1111/pce.14815

Caldwell, M. M., Robberecht, R., & Flint, S. D. (1983). Internal filters: Prospects for UV-acclimation in higher plants. *Physiologia Plantarum*, *58*(3), 445–450. https://doi.org/10.1111/j.1399-3054.1983.tb04206.x

Christie, J. M. (2007). Phototropin blue-light receptors. *Annu Rev Plant Biol*, *58*, 21–45. https://doi.org/10.1146/annurev.arplant.58.032806.103951

Christopher, D. A., & Mullet, J. E. (1994). Separate photosensory pathways co-regulate blue light/ultraviolet-A-activated psbD-psbC transcription and light-induced D2 and CP43 degradation in barley (*Hordeum vulgare*) chloroplasts. *Plant Physiology*, *104*(4), 1119–1129. https://doi.org/10.1104/pp.104.4.1119

Davis, P. A., Caylor, S., Whippo, C. W., & Hangarter, R. P. (2011). Changes in leaf optical properties associated with light-dependent chloroplast movements. *Plant, Cell and Environment*. https://doi.org/10.1111/j.1365-3040.2011.02402.x

Edreva, A. (2005). The importance of non-photosynthetic pigments and cinnamic acid derivatives in photoprotection. *Agriculture, Ecosystems and Environment*, *106*(2-3 SPEC. ISS.), 135–146. https://doi.org/10.1016/j.agee.2004.10.002

Ernstsen, J., Woodrow, I. E., & Mott, K. A. (1999). Effects of growth-light quantity, growth-light quality and $CO_2$ concentration on Rubisco deactivation during low PFD or darkness. *Photosynthesis Research*, *61*(1), 65–75. https://doi.org/10.1023/A:1006289901858

Hendrickson, L., Furbank, R. T., & Chow, W. S. (2004). A simple alternative approach to assessing the fate of absorbed light energy using chlorophyll fluorescence. *Photosynthesis Research*, *82*(1), 73–81. https://doi.org/10.1023/B:PRES.0000040446.87305.f4

Ilić, Z. S., & Fallik, E. (2017). Light quality manipulation improves vegetable quality at harvest and postharvest: A review. *Environmental and Experimental Botany*, *139*(July), 79–90. https://doi.org/10.1016/j.envexpbot.2017.04.006

Izzo, L. G., Hay Mele, B., Vitale, L., Vitale, E., & Arena, C. (2020). The role of monochromatic red and blue light in tomato early photomorphogenesis and photosynthetic traits. *Environmental and Experimental Botany*, *179*(May), 104195. https://doi.org/10.1016/j.envexpbot.2020.104195

Janda, T., Hideg, É., & Vanková, R. (2020). Editorial: The role of light in abiotic stress acclimation. *Frontiers in Plant Science*, *11*. https://doi.org/10.3389/fpls.2020.00184

Johnson, G. A., & Day, T. A. (2002). Enhancement of photosynthesis in *Sorghum bicolor* by ultraviolet radiation. *Physiologia Plantarum*, *116*(4), 554–562. https://doi.org/10.1034/j.1399-3054.2002.1160415.x

Kataria, S., Jajoo, A., & Guruprasad, K. N. (2014). Impact of increasing Ultraviolet-B (UV-B) radiation on photosynthetic processes. *Journal of Photochemistry and Photobiology B: Biology*, *137*, 55–66. https://doi.org/10.1016/j.jphotobiol.2014.02.004

Khanam, U. K. S., Oba, S., Yanase, E., & Murakami, Y. (2012). Phenolic acids, flavonoids and total antioxidant capacity of selected leafy vegetables. *Journal of Functional Foods*, *4*(4), 979–987. https://doi.org/10.1016/j.jff.2012.07.006

Kotilainen, T., Tegelberg, R., Julkunen-Tiitto, R., Lindfors, A., & Aphalo, P. J. (2008). Metabolite specific effects of solar UV-A and UV-B on alder and birch leaf phenolics. *Global Change Biology*, *14*(6), 1294–1304. https://doi.org/10.1111/j.1365-2486.2008.01569.x

Kotilainen, T., Tegelberg, R., Julkunen-Tiitto, R., Lindfors, A., O'Hara, R. B., & Aphalo, P. J. (2010). Seasonal fluctuations in leaf phenolic composition under UV manipulations reflect contrasting strategies of alder and birch trees. *Physiologia Plantarum*, *140*(3), 297–309. https://doi.org/10.1111/j.1399-3054.2010.01398.x

Kuiper, P. J. C. (1964). Dependence upon wavelength of stomatal movement in epidermal tissue of senecio odoris . *Plant Physiology*, *39*(6), 952–955. https://doi.org/10.1104/pp.39.6.952

Lichtenthaler, H. K., & Buschmann, C. (2001). Chlorophylls and Carotenoids: measurement and characterization by UV-VIS spectroscopy. *Current Protocols in Food Analytical Chemistry*, *1*(1), F4.3.1-F4.3.8. https://doi.org/10.1002/0471142913.faf0403s01

Liu, C. C., Chi, C., Jin, L. J., Zhu, J., Yu, J. Q., & Zhou, Y. H. (2018). The bZip transcription factor HY5 mediates CRY1a-induced anthocyanin biosynthesis in tomato. *Plant Cell and Environment*, *41*(8), 1762–1775. https://doi.org/10.1111/pce.13171

Ribarova, F., Atanassova, M., Marinova, D., Ribarova, F., & Atanassova, M. (2005). Total phenolics and flavonoids in Bulgarian fruits and vegetables. *JU Chem. Metal*, *40*(3), 255-60.

Matthews, J. S. A., Vialet-Chabrand, S., & Lawson, T. (2020). Role of blue and red light in stomatal dynamic behaviour. *Journal of Experimental Botany*, *71*(7), 2253–2269. https://doi.org/10.1093/jxb/erz563

McCree, K. J. (1971). The action spectrum, absorptance and quantum yield of photosynthesis in crop plants. *Agricultural Meteorology*. https://doi.org/10.1016/0002-1571(71)90022-7

McCree, K. J., & Keener, M. E. (1974). Effect of atmospheric turbidity on the photosynthetic rates of leaves. *Agricultural Meteorology*, *13*(3), 349–357. https://doi.org/10.1016/0002-1571(74)90075-2

Millar, A. H., Whelan, J., Soole, K. L., & Day, D. A. (2011). Organization and regulation of mitochondrial respiration in plants. *Annual Review of Plant Biology*, *62*, 79–104. https://doi.org/10.1146/annurev-arplant-042110-103857

Min, Q., Marcelis, L. F. M., Nicole, C. C. S., & Woltering, E. J. (2021). High light intensity applied shortly before harvest improves lettuce nutritional quality and extends the shelf life. *Frontiers in Plant Science*, *12*(January). https://doi.org/10.3389/fpls.2021.615355

Murchie, E. H., & Lawson, T. (2013). Chlorophyll fluorescence analysis: A guide to good practice and understanding some new applications. *Journal of Experimental Botany*, *64*(13), 3983–3998. https://doi.org/10.1093/jxb/ert208

Ng, C. K. Y. (2019). Plant cell biology: UVA on guard. *Current Biology*, *29*(15), R740–R742. https://doi.org/10.1016/j.cub.2019.06.036

O'Leary, B. M., Asao, S., Millar, A. H., & Atkin, O. K. (2019). Core principles which explain variation in respiration across biological scales. *New Phytologist*, *222*(2), 670–686. https://doi.org/10.1111/nph.15576

Palma, C. F. F., Castro-Alves, V., Morales, L. O., Rosenqvist, E., Ottosen, C. O., Hyötyläinen, T., & Strid, Å. (2022). Metabolic changes in cucumber leaves are enhanced by blue light but differentially affected by UV interactions with light signalling pathways in the visible spectrum. *Plant Science*, *321*, 111326. https://doi.org/10.1016/j.plantsci.2022.111326

Palma, C. F. F., Castro-Alves, V., Rosenqvist, E., Ottosen, C. O., Strid, Å., & Morales, L. O. (2021). Effects of UV radiation on transcript and metabolite accumulation are dependent on monochromatic light background in cucumber. *Physiologia Plantarum*, *173*(3), 750–761. https://doi.org/10.1111/ppl.13551

Qian, M., Kalbina, I., Rosenqvist, E., Jansen, M. A. K., Teng, Y., & Strid, Å. (2019). UV regulates the expression of phenylpropanoid biosynthesis genes in cucumber (Cucumis sativus L.) in an organ and spectrum dependent manner. *Photochemical and Photobiological Sciences*, *18*(2), 424–433. https://doi.org/10.1039/C8PP00480C

Rai, N., Morales, L. O., & Aphalo, P. J. (2021). Perception of solar UV radiation by plants: photoreceptors and mechanisms. *Plant Physiology*, *186*(3), 1382–1396. https://doi.org/10.1093/PLPHYS/KIAB162

Ruban, A. V. (2016). Nonphotochemical chlorophyll fluorescence quenching: Mechanism and effectiveness in protecting plants from photodamage. *Plant Physiology*, *170*(4), 1903–1916. https://doi.org/10.1104/pp.15.01935

Samson, G., Bonin, L., & Maire, V. (2019). Dynamics of regulated YNPQ and non-regulated YNO energy dissipation in sunflower leaves exposed to sinusoidal lights. *Photosynthesis Research*, *141*(3), 315–330. https://doi.org/10.1007/s11120-019-00633-w

Takahashi, S, & Badger, M. R. (2011). Photoprotection in plants: a new light on photosystem II damage. *Trends Plant Sci*, *16*(1), 53–60. https://doi.org/10.1016/j.tplants.2010.10.001

Takahashi, Shunichi, & Badger, M. R. (2011). Photoprotection in plants: A new light on photosystem II damage. *Trends in Plant Science*, *16*(1), 53–60. https://doi.org/10.1016/j.tplants.2010.10.001

Takahashi, Shunichi, Milward, S. E., Yamori, W., Evans, J. R., Hillier, W., & Badger, M. R. (2010). The solar action spectrum of photosystem II damage. *Plant Physiology*, *153*(3), 988–993. https://doi.org/10.1104/pp.110.155747

Turnbull, T. L., Barlow, A. M., & Adams, M. A. (2013). Photosynthetic benefits of ultraviolet-A to *Pimelea ligustrina*, a woody shrub of sub-alpine Australia. *Oecologia*. https://doi.org/10.1007/s00442-013-2640-9

van Delden, S. H., SharathKumar, M., Butturini, M., Graamans, L. J. A., Heuvelink, E., Kacira, M., Kaiser, E., Klamer, R. S., Klerkx, L., Kootstra, G., Loeber, A., Schouten, R. E., Stanghellini, C., van Ieperen, W., Verdonk, J. C., Vialet-Chabrand, S., Woltering, E. J., van de Zedde, R., Zhang, Y., & Marcelis, L. F. M. (2021). Current status and future challenges in implementing and upscaling vertical farming systems. *Nature Food*, *2*(12), 944–956. https://doi.org/10.1038/s43016-021-00402-w

Vass, I., Turcsányi, E., Touloupakis, E., Ghanotakis, D., & Petrouleas, V. (2002). The mechanism of UV-A radiation-induced inhibition of photosystem II electron transport studied by EPR and chlorophyll fluorescence. *Biochemistry*, *41*(32), 10200–10208. https://doi.org/10.1021/bi020272+

Velez-Ramirez, A. I., Van Ieperen, W., Vreugdenhil, D., & Millenaar, F. F. (2011). Plants under continuous light. *Trends in Plant Science*, *16*(6), 310–318. https://doi.org/10.1016/j.tplants.2011.02.003

Verdaguer, D., Jansen, M. A. K., Llorens, L., Morales, L. O., & Neugart, S. (2017). UV-A radiation effects on higher plants: Exploring the known unknown. *Plant Science*. https://doi.org/10.1016/j.plantsci.2016.11.014

Walters, R. G. (2005). Towards an understanding of photosynthetic acclimation. *Journal of Experimental Botany*. https://doi.org/10.1093/jxb/eri060

Yang, L., Fanourakis, D., Tsaniklidis, G., Li, K., Yang, Q., & Li, T. (2021). Contrary to red, blue monochromatic light improves the bioactive compound content in broccoli sprouts. *Agronomy*, *11*(11).

https://doi.org/10.3390/agronomy11112139

Zhang, Y., Kaiser, E., Zhang, Y., Zou, J., Bian, Z., Yang, Q., & Li, T. (2020). UVA radiation promotes tomato growth through morphological adaptation leading to increased light interception. *Environmental and Experimental Botany*. https://doi.org/10.1016/j.envexpbot.2020.104073

Zhang, Y., Sun, X., Aphalo, P. J., Zhang, Y., Cheng, R., & Li, T. (2023). Ultraviolet-A1 radiation induced a more favorable light-intercepting leaf-area display than blue light and promoted plant growth. *Plant Cell and Environment*, *46*(10), 1–16. https://doi.org/10.1111/pce.14727

Zhen, S., Kusuma, P., & Bugbee, B. (2024). Photons at the ultraviolet-visible interface: Effects on leaf expansion and photoinhibition. *Scientia Horticulturae*, *326*(August 2023), 112785. https://doi.org/10.1016/j.scienta.2023.112785

# Supplementary material

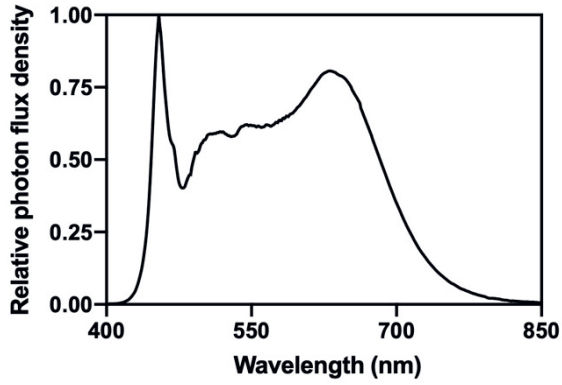


**Figure S1.** Spectral photon irradiance of germination and growth light (normalized to maximum).

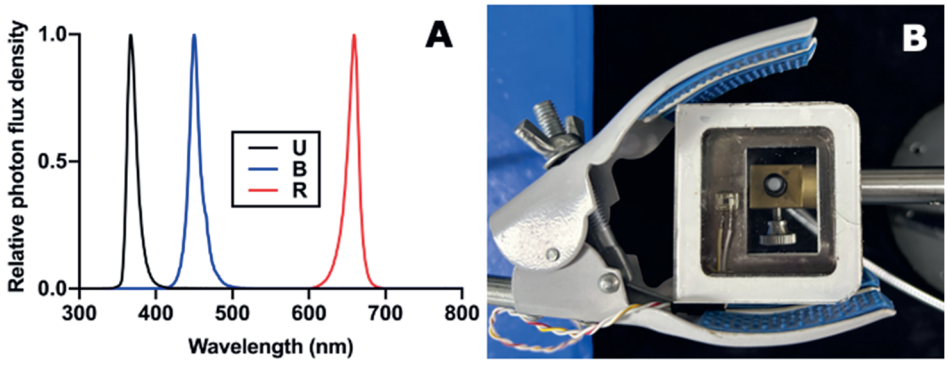


**Figure S2.** Set up of measurements of operational photosynthesis and chlorophyll fluorescence. (A) Spectra of the treatment lamps used in this study; (B) Leaf chamber with transparent quartz cover and setup to measure light intensity using the spectroradiometer (Avaspec-2048CL, Avates, Apeldoorn, the Netherlands).

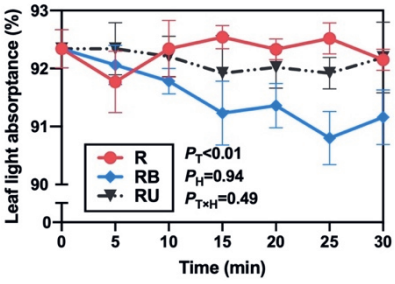


**Figure S3.** Time courses of chloroplast movement (leaf light absorptance within 30 min) under different treatment spectra. Red light (200 µmol $m^{-2} s^{-1}$) as the background light for treatment spectra, to which treatment light (200 µmol $m^{-2} s^{-1}$) of either of three peak wavelengths was added: 365 (RU), 450 (RB) and 656 (R) nm. Mean values ± SEM of 5 replicates plants (n = 5). Numbers show *P*-values for the main effects of light spectrum treatment ($P_T$) and sampling time of treatment ($P_H$), and their interaction ($P_{T\times H}$). *(Experiment 3)*

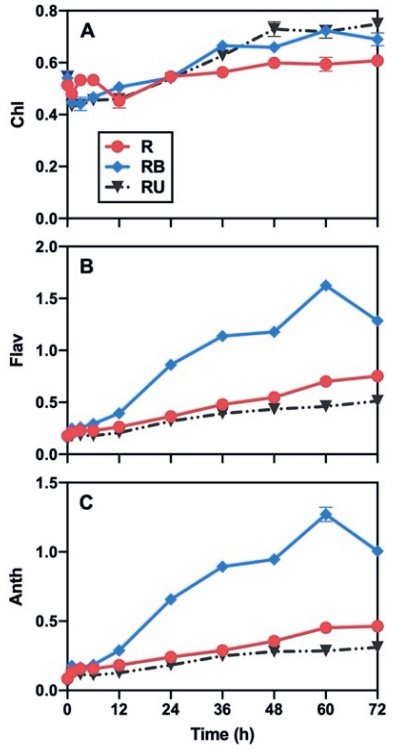


**Figure S4.** Indices of pigment concentrations under different treatment spectra in experiment 3. A: Chlorophyll index; B: Flavonoids index; C: Anthocyanin index. Red light (200 µmol $m^{-2} s^{-1}$) was used as background light, to which treatment light (200 µmol $m^{-2} s^{-1}$) of either of three peak wavelengths was added: 365 (RU), 450 (RB) and 656 (R) nm. Mean values ± SEM of 10 replicates plants (n = 10). *(Experiment 3)*

Chapter 5

# CHAPTER 6

## General discussion

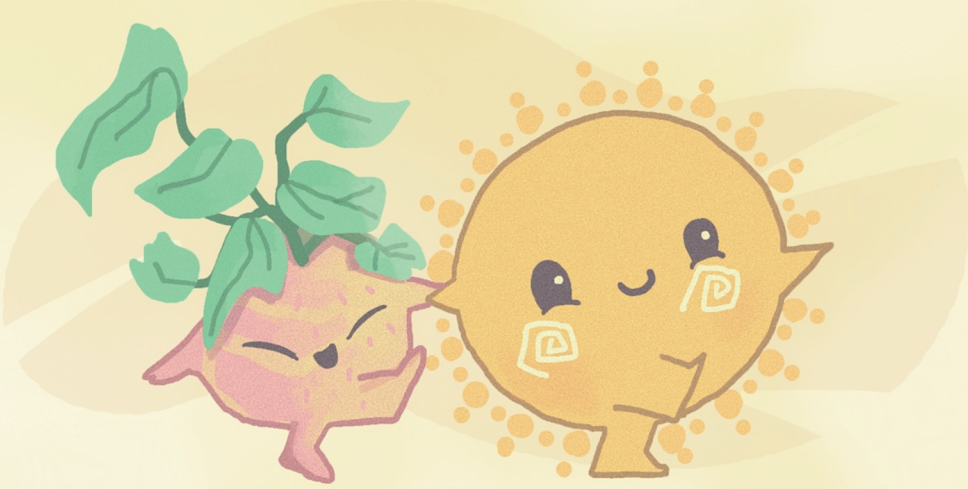

Xuguang Sun

Currently, there are only a few reviews on the effects of UV-A (315-400 nm) on plant growth and physiology (Neugart & Schreiner, 2018; Rai et al., 2021; Verdaguer et al., 2017), and these reviews indicate that the knowledge of UV-A photobiology is limited. This is partially because previous insights into UV-A effects on plants were obtained from measurements conducted in the field. In this thesis, I studied UV-A1 wavelength, UV-A1 dose and species in a well-controlled environment, and the main findings are that UV-A1 radiation triggers wavelength-dependent photosynthetic performance and photoprotective acclimation as well as photoinhibition, with the net result that plant growth was barely affected by UV-A exposure **(Chapters 2-5)**. This thesis filled some knowledge gaps around the effects of UV-A1 on plants, by using novel LEDs. In this general discussion, I will discuss how UV-A1 affects plant growth, leaf photosynthesis and photosynthetic acclimation in a broader perspective and then compare it to the effects of blue light, summarize UV applications in protected agriculture, and present perspectives for future research on this topic.

# Integrated effects of UV-A1 on plant physiology

In this section, I explore the intricate balance between photosynthesis, photosynthetic acclimation and plant growth, offering insights into why plant growth was barely affected by UV-A1 exposure despite the enhancement of photosynthetic capacity. When UV-A1 acts as a stimulus of photosynthetic performance, the rate of photosynthesis and photosynthetic capacity due to light acclimation are enhanced by UV-A1 (**Chapters 3-5**), though this does not seem to directly contribute to plant growth. Similarly, when UV-A1 serves as a stressor with high energy per photon leading to photoinhibition (Takahashi et al., 2010), this inhibitory effect does not seem to generally reduce plant growth **(Chapters 2-3)**. My results generally suggest that plants achieve a balance to maintain growth under UV-A1 exposure through a series of regulatory mechanisms.

The inspiration for this thesis was provided by earlier studies, which showed that UV-A1 promoted whole-plant light interception by inducing photomorphogenesis with a larger leaf area and steeper leaf angle (Zhang et al., 2023), leading to higher dry mass accumulation

compared to the treatment without UV-A1 supplemented (Chen et al., 2019). Surprisingly, in this thesis, we found that neither the addition of different intensities (0-100 μmol $m^{-2}$ $s^{-1}$) of 365 nm radiation nor different wavelengths (365 and 385 nm) in the UV-A1 range of the same intensity (50 μmol $m^{-2}$ $s^{-1}$) had significant effects on plant growth, compared with treatments without UV-A1 supplementation **(Chapters 2-3)**. Although UV-A1 could stimulate photosynthesis by inducing light-intercepting leaf-area display formation and increasing efficiency of energy conversion with photosynthetic pigments accumulation **(**Zhang et al., 2023; **Chapters 4-5)**, this benefit comes at a cost that UV-A1 induces photoinhibition and triggers photoprotective mechanisms such as non-photochemical quenching (NPQ). Besides, the photosynthetic quantum efficiency of UV-A was generally low **(Chapter 4),** and the presence of UV- absorbing compounds in the leaf epidermis further reduced this. It could be hypothesized that with a reduced UV-A1 radiation reaching the photosynthetic pigments, plants may require a lower photoprotective capacity, allowing them to allocate more resources towards growth rather than defense.

In conclusion, my results suggest that UV-A1 radiation has a dual role in plants: it enhances photosynthetic performance to some extent, but simultaneously induces stress responses. Plants seem to be generally able to maintain a balance between these effects, thereby sustaining normal growth. The effects of UV-A1 on plant growth, photosynthesis, and photosynthetic acclimation will be further discussed below, and results will be compared with those of other studies.

## Plant growth under UV-A1 exposure

In this thesis, both intensities and wavelengths of UV-A1 had no notable impacts on plant growth. However, when considering the available data, there is still no consensus on the effects of UV-A on plant growth. To be more specific, He et al. (2021) found that additional UV-A applied alone at an intensity of 10 μmol $m^{-2}$ $s^{-1}$ had no effects on the biomass of lettuce 'Yanzhi' and 'Red butter' grown under 300 μmol $m^{-2}$ $s^{-1}$ white background light. While, Kang et al. (2018) showed that additional broad-spectrum UV-A fluorescent lamps supplemented with a mixture of blue and red lamps at a background light intensity of 220

μmol $m^{-2}$ $s^{-1}$ increased the dry weight and leaf area of tomato 'Beijing cherry'. Unfortunately, the authors mentioned above did not provide information on the specific UV-A spectrum used. However, Chen et al. (2019) showed that an additional 20 μmol $m^{-2}$ $s^{-1}$ of UV-A1 at 365 nm promoted the growth of lettuce 'Klee', which is at odds with my experimental results exhibited the same UV-A1 intensity had minor effects on plant growth of the same genotype (**Chapter 2**). When comparing the experimental setups between **Chapter 2** and Chen et al. (2019), a core difference was the spectrum of the background light. In **Chapter 2**, I used white light as background, which contains a large fraction of green and blue light (35% and 22% of total photosynthetically active radiation (PAR), respectively), while in the study of Chen et al. (2019) the percentage of green and blue light was about 8% and 15% of the total PAR. The light spectrum regulates plant growth through different photoreceptors. Photoreceptors of UV-A1 (phototropins and cryptochromes) are also triggered by blue light, while green light can be absorbed by cryptochromes (Battle et al., 2020; Christie, 2007). Perhaps the presence of blue light that triggers cryptochromes caused UV-A1 not to have strong additional effects on the cryptochromes, or the presence of green light may have reversed UV-A1- effects by interrupting signaling by cryptochrome (Zhang & Folta, 2012). More evidence on the role of background light spectrum in UV-A1-mediated plant growth is needed to explain the conflicting results mentioned above. Light spectra should be considered when designing UV-A plant photobiology studies, as well as light intensity and photoperiod. Other environmental factors, such as temperature, humidity, and nutrients may also interact with UV-A1 and hence affect plant performance (Poorter et al., 2012). Adding UV-A1 to red light was effective in alleviating the downward curling of leaves (Zhang et al., 2020, 2023), and this phenomenon was only found under monochromatic red light; use of monochromatic red is an extreme condition and is not comparable to growth conditions in these chapters (**Chapters 2-3**). All of these studies exemplify that researchers need to clearly specify and carefully interpret the effects of experimental conditions.

## Balance between photochemistry, photoprotection and photoinhibition

UV-A can have both beneficial and detrimental effects on photosynthesis (Verdaguer et al., 2017). Although McCree (1971) suggested the range of PAR to be 400 to 700 nm,

photosynthesis is also powered by UV-A1, though to a lesser extent than blue light (**Chapter 4**). At the same time, a UV-A1 photon has a higher energy content than a blue photon, thereby driving photoinhibition to a larger extent. When plants cannot fully absorb UV-A1 radiation, various photosynthetic processes could be affected. For example, UV-A1 impaired photosynthetic electron transport around photosystem II (PSII; Hirosawa & Miyachi, 1983), thereby preventing the light from being fully utilized by plants. Besides, UV-A was found to damage a number of protein complexes in PSII isolated from spinach, with the water-oxidizing complex of PSII to be the most sensitive (Vass et al., 2002). However, when entire leaves instead of isolated PSII are exposed to light, UV-absorbing compounds in the epidermis function as a barrier, protecting the chloroplasts from UV-induced damage (Caldwell et al., 1983). Prior to this thesis, no studies have reported on the relationship between the concentration of UV-absorbing compounds and photosynthesis; my data suggest that a higher concentration of UV-absorbing compounds in the leaf leads to lower photosynthetic efficiency under UV-A1 (**Chapter 3**). More research is needed to explore how UV-absorbing compounds affect photosynthesis mechanistically.

Plants exposed to UV-A may develop a variety of photoprotective mechanisms to prevent light energy from inducing damage, with photobleaching and cell death as extreme examples (Murchie & Niyogi, 2011). NPQ is an important protective mechanism (Ruban & Wilson, 2021) and in my thesis showed distinct responses to short-term (several minutes), mid-term (three days of continuous exposure) and long-term (two weeks) UV-A1 exposure. NPQ-dependent photoprotection is activated more rapidly by UV-A1 than by blue light under short-term exposure (**Chapter 4**; Tokutsu et al., 2021). In contrast, mid-term acclimation to UV-A1 did not seem to be accomplished through increased NPQ (**Chapter 5**). However, long-term UV-A1 treated leaves showed an interesting combination of high NPQ under high light (**Chapter 3**). Based on these results, I cannot clearly conclude how UV-A1 regulates NPQ, and suggest that further studies on this topic are needed.

The thylakoid PSII auxiliary protein photosystem II protein 33 (PSB33) was found to have an important role in sustaining a functional PSII pool by regulating the *de novo* synthesis of PSII under UV-A radiation (Nilsson et al., 2020). Furthermore, since PSII absorbs more

strongly in the UV-A region compared to PSI, the relative excitation pressure between the photosystems is unbalanced, which may additionally lead to photoinhibition (Bellaflore et al., 2005). Apart from the protective role of UV-absorbing compounds in the epidermis, leaf hairs and waxes play a significant role in reflecting ultraviolet radiation (Caldwell et al., 1983; Holmes & Keiller, 2002). Besides, chloroplast avoidance movement may serve as an alternative protection to reduce the amount of light absorbed by chloroplasts (Wada et al., 2003). Chloroplast avoidance movement was also previously shown to be active under UV-A1 radiation (370 nm; (Blatt, 1983; **Chapter 5**). At the plant level, plant growth did not benefit from UV-A1 exposure and in some cases was even slightly reduced depending on genotype and UV-A1 intensity used **(Chapters 2-3).** This may in part be because the energy required for repairing UV-A1 induced photodamage could otherwise be used for growth (Miyata et al., 2012).

Manipulating photoprotective pathways is a strategy to improve both stress tolerance and photosynthetic efficiency in crops (Murchie & Niyogi, 2011). UV-A1 radiation at 50 µmol $m^{-2}$ $s^{-1}$ intensity indeed triggered the build-up of photoprotective capacity in tomato, and this might be ascribed to the high energy per photon (peak wavelength: 365 nm; (**Chapter 3**). However, plants acclimated under blue light at the same intensity as UV-A1 also exhibited strong photoprotective capacity, and did not experience photoinhibition (**Chapter 3**), which suggests UV-A1 induces photoprotective capacity at the cost of photoinhibition. Although continuous exposure for three days with UV-A1 intensity of 200 $m^{-2}$ $s^{-1}$ caused photoinhibition in lettuce 'Klee', photosynthetic capacity under high light was improved by UV-A1 and photoinhibition induced by UV-A1 gradually recovered over time (**Chapter 5**). Importantly, high yield potential and high stress tolerance are incompatible (Murchie et al., 2009), hence a compromise is required between these two aspects, and more research is needed to explore this trade-off for maintaining high yields under UV-A1 exposure without compromising stress tolerance.

## The role of UV-absorbing compounds in UV research

In higher plants, flavonoids and other phenylpropanoid derivatives accumulate in large quantities in the vacuoles of epidermal cells, and efficiently absorb the UV portion of sunlight,

thereby protecting the plant from UV damage (Mazza et al., 2000). The role of UV-absorbing compounds is often addressed in relation to acclimation, horticultural applications, and ecology (Barnes et al., 2000; Cockell & Knowland, 1999). The conventional method for measuring these compounds is measuring the UV absorbance of crude methanolic extracts, including that of enriched flavonoids and phenolics (Barnes et al., 2013, 2016; Beggs & Wellmann, 1985; Julkunen-Tiitto et al., 2014). Besides, total phenolics and total flavonoids are also extracted with methanol for subsequent content analysis (Khanam et al., 2012). Additionally, the concentration of UV-absorbing compounds in the leaf typically mirrors changes in epidermal UV transmittance (Neugart et al., 2021). Therefore, measuring the UV transmittance by use of instruments such as the Dualex (Dualex Scientific+; Force-A, Orsay, France) or UVA-PAM (UVA-PAM fluorometer; Gademann Messgeräte, Würzburg, Germany) (Barnes et al., 2013, 2015, 2016; Markstädter et al., 2001; Neugart et al., 2021) can serve as a proxy of the concentration of UV-absorbing compounds. Both methods are efficient and widely applied in horticultural and ecological research (Caldwell et al., 1983; Mazza et al., 2000; Pfündel et al., 2007), providing important data on plant responses and adaptive mechanisms to UV radiation.

Although some studies argue against the measurement of total phenolics and flavonoids, as UV-A modulates the concentrations of individual phenolic compounds rather than total phenolics and flavonoids pools (Kotilainen et al., 2008; Verdaguer et al., 2017), other studies still reported that UV-A can induce the bulk accumulation of these compounds (Chen et al., 2019; Kelly & Runkle, 2023; J. H. Lee et al., 2019; M. J. Lee et al., 2013, 2014). In this thesis, I used all the methods mentioned above to investigate the concentrations of UV-absorbing compounds in the leaf, as well as the concentrations of total flavonoids and phenolics (**Chapters 2-5**). I found that the concentrations of UV-absorbing compounds were not strongly affected by different wavelengths and intensities of UV-A1 in several genotypes (**Chapters 2-4**). This finding aligns with previous research: UV-A barely affected extracts of UV-absorbing compounds in leaves of cucumber, lettuce, *Betula pendula* and six woody species in the Mediterranean (Bernal et al., 2013; Krizek et al., 1997, 1998; Morales et al., 2010). However, this apparent lack of a UV-A effect on UV-absorbing compounds may in part be caused by the crude extraction method, which covered the entire UV spectrum., making it difficult to accurately measure the effect of UV-A1 on the specfic UV-absorbing compounds (Julkunen-

Tiitto et al.; 2014; Kotilainen et al., 2008; Verdaguer et al., 2017). Further, when UV-A1 was added to white background light, the concentration of UV-absorbing compounds and anthocyanins decreased significantly in arabidopsis, but not in tomato, lettuce and cucumber (**Chapter 2**), demonstrating that this effect is species specific (Kotilainen et al., 2010; Verdaguer et al., 2017). Also, a reduction of phenolic contents was observed in cucumber leaves grown under UV radiation (including both UV-A and UV-B) combined with white light (Palma et al., 2022), suggesting that the effect of UV-A depends on the experimental set-up (i.e. background light intensity, light quality and photoperiod) (**Chapters 2, 3 and 5**; Kotilainen et al., 2010; Palma et al., 2022; Qian et al., 2019). Differing experimental set-ups and species make inter-study comparisons challenging. Some studies showed that UV regulates transcript and metabolite accumulation in cucumber leaves in a spectrum-dependent manner (Palma et al., 2021, 2022); however, those experiments utilized broad-spectrum UV radiation, which complicates the comparison between the results presented in this thesis and those by Palma et al. (2021, 2022).

There are numerous studies on UV regulation of phenolic metabolism (reviewed in Neugart & Schreiner, 2018; Verdaguer et al., 2017), but many of those employ broad-spectrum UV treatments including UV-B, UV-A2, UV-A1, and plant responses to UV-B and UV-A2 are regulated by UVR8 (Rai et al., 2019). With advanced LED technology featuring specific, narrower wavebands, it will be very interesting to study changes in leaf phenolics under UV-A1 and UV-A2, respectively.

## UV-A1 and blue light: exploring their similarities and differences

Although UV-A1 and blue light share the same flavoprotein photoreceptors (Christie et al., 2015), it is not well described how plant responses to UV-A1 radiation are different from those to blue light. The similarities between UV-A1 and blue light in terms of effects on phototropism, chloroplast movement, and circadian rhythm are based on the hypothesis that they trigger the same photoreceptors (Lin, 2000), rather than on individual studies specifically reporting how UV-A regulates these aspects. For other processes of plant biology

regulated by blue light, such as morphogenesis, growth, and photosynthesis, I will combine the results found in this thesis with other studies to comprehensively discuss the differences and similarities between UV-A1 and blue light (Table 1).

Both UV-A1 and blue light can adjust leaf morphology, effectively alleviating the "red light syndrome" and maintaining normal photosynthetic performance (Inoue et al., 2008; Zhang et al., 2020, 2023). Additionally, UV-A1 is weaker than blue light in triggering the expression of genes related to auxin transport (Zhang et al., 2023), which may imply that the role of UV-A1 function differently as blue light in mediating plant processes. Blue light can induce characteristics of sun-type plants (Kang et al., 2021), with plant growth responding to blue light in a dose-dependent and species-specific manner (Hogewoning et al., 2010; Liang et al., 2021). In this thesis, a wide range of UV-A1 intensities had almost no effects on plant growth among horticultural species (**Chapters 2-3**). Further, both leaf photosynthesis and photosynthetic acclimation in the UV-A1 and blue light range followed a continuous shallow gradient when wavelength of the light increased (**Chapters 3-4**): a longer wavelength enhanced photosynthetic performance, while a shorter wavelength caused photoinhibition (Takahashi & Badger, 2011). I also found that the photoinhibition caused by UV-A1 was reversible, and that plants were able to fully acclimate to UV-A1 (**Chapters 2, 3, 5**). For stomata, UV-A1 and blue light may exhibit opposite regulatory patterns: short-term blue light exposure promotes stomatal opening (Christie et al., 2015), while short-term (3-6 h) UV-A1 exposure inhibits stomatal opening, but this effect decreases over time (Ng, 2019). These results align with my data, which showed that stomatal closure under long-term UV-A1 exposure was not observed, but neither was strong stomatal opening (**Chapter 3**). Besides, both blue light and UV-A1 can promote flowering in long-day plants (**Chapter 2;** Guo et al., 1998), but whether UV-A1 induces floral initiation through the cryptochrome 2 pathway or as part of a stress response requires further research (Xu et al., 2014).

Table 1. Similarity and difference between UV-A1 and blue light effects on plant processes.

| process | Similarity | Difference | | Reference |
|---|---|---|---|---|
| | | UV-A1 | blue light | |
| **Waveband** | share phototropins/ cryptochromes | 350-400 nm | 400-500 nm | [1], [2] |
| **Plant morphology** | promote leaf expansion | only under monochromatic red light | optimal leaf positioning /flattening | [3], [4] |
| **Plant growth** | maintain plant growth | mild effects | dose-response; species-specific; 'sun-type' plants | (**Ch. 2-3**); [5]–[8] |
| **Photosynthesis** | wavelength-dependent | quantum yield in the blue light range is higher than in the UVA range | | (**Ch. 4**); [9] |
| **Photoinhibition** | induced by excess light | photons with high energy | extreme high light intensity | (**Ch. 2-5**); [10] |
| **Photoprotection** | resistance to high light | at the cost of photoinhibition | higher photosynthetic capacity | (**Ch. 3, 5**) |
| **Stomata** | unclear | inhibition under short-term exposure | stomatal opening promotion | [11], [12] |
| **Chloroplast movement** | phototropins involved | unclear | low- and high-light-dependent | [13], [14] |
| **Flowering** | floral initiation regulated by cryptochromes | flowering promotion through cryptochromes or stress | long-day plants promotion; short-day plants inhibition | (**Ch.2**); [15], [16] |
| **Transcriptome** | the transcription level | UV-A1 triggers weaker and later transcriptome-wide responses | | [4] |
| **UV-absorbing compounds** | of flavonoid pathway | blue light strongly promotes accumulation | | (**Ch.5**); [17] |

# Perspectives for UV applications in horticulture

Although UV radiation is outside the range of conventional PAR, it is biologically effective. With advancements in LEDs, the potential of UV light in horticultural application is growing, paving the way for innovative plant production practices.

## UV could be used in pre- and post-harvest applications

UV radiation can be applied during the plants cultivation used in pharmaceutical, cosmetic, and nutraceutical industries for increasing the production of health-promoting compounds (Jacobo-Velázquez et al., 2022). UV-A, having the longest wavelengths and being least harmful to humans among the different types of UV radiation, was sometimes used in pre-harvest studies to improve plant production and coloration (Chen et al., 2019; Kelly & Runkle, 2023; Lee et al., 2019). Also, using UV-B and UV-C in pre-harvest treatments had significant effects, with specific doses varying depending on the purpose of the experiment and the genotypes: UV-B leads to increased phenolic and flavonoid concentrations in vegetables and fruits (Mosadegh et al., 2018; Neugart & Schreiner, 2018; Ordidge et al., 2010), including active substances in medicinal plants (Takshak & Agrawal, 2019). UV-C at 1.0 kJ $m^{-2}$ applied one hour per week (~7 weeks in total) was found to increase total fruit number and fruit weight in tomato, and induced flowering in ornamental plants (Darras et al., 2012, 2020). In addition, UV-C was found to improve plant growth under salt stress conditions (Ouhibi et al., 2014), and both UV-B and UV-C increased disease resistance (Meyer et al., 2021; Urban et al., 2018).

UV generally has a capacity to extend shelf-life and increase antioxidant activity (Chen et al., 2021; Sonntag et al., 2023; Stevens et al., 2004). In addition, UV-B and UV-C can slow down product quality depletion, delay ripening time and improve fruits firmness (Liu et al., 2011; Park & Kim, 2015; Stevens et al., 2004). UV-A was found to be effective in preventing fruit degradation after harvesting (Lante et al., 2016). It can be concluded that UV radiation is a useful tool in several post-harvest applications.

In this thesis, UV-A1 application did not remarkably stimulate the concentration of total phenolics and flavonoids as well as plant growth (**Chapters 2-5**). The results of this thesis suggest that UV-A1 implementation in improving nutraceuticals and yield is not a good choice, especially compared to blue light. In my research, plants were grown under highly controlled conditions, with stable and relatively low light intensity, compared to full sunlight. Plants were grown with visible light only, or with UV-A1 plus visible light, which may result in the accumulation of less UV absorbing compounds compared to open field grown plants. This is because the synthesis of flavonoids, which are major UV absorbing compounds, is regulated by a UV-B photoreceptor, UVR8 (Jenkins, 2014). However, I also found that blue light strongly promoted the accumulation of UV-absorbing compounds (**Chapter 5**). Moreover, there was a positive correlation between UV-A intensity and flavonoid concentration in *Betula pendula* leaves, while the opposite trend was observed in *Brassica napus* leaves (Morales et al., 2010; Wilson et al., 2001), suggesting species-specific responses between UV-A dosage and flavonoid accumulation. UV-A was found to be strongly involved in the transcription of genes in the flavonoid pathway (Fuglevand et al., 1996; Guo & Wang, 2010), such as phenylalanine ammonia lyase and chalcone synthase, suggesting that UV-A affects the concentration of UV-absorbing compounds. Compared to UV-A1 radiation, high light intensity (550 μmol $m^{-2}$ $s^{-1}$) and continuous light exposure (72 h) can also promote the accumulation of UV-absorbing compounds **(Chapters 2, 5)**. For further research on this topic, I recommend to investigate the signaling pathways by using photoreceptor mutants, as well as the effects of antagonistic or synergistic interactions with other environmental factors.

## Precautions for using UV-LEDs

When applying different wavelengths and doses of UV radiation at various stages of plant development, the requirements for dose and wavelength may differ (Neugart & Schreiner, 2018; Paradiso & Proietti, 2022). Thus, it is crucial to understand the specific UV requirements of plants or harvested organs. Moreover, researchers should not blindly trust the output parameters advertised by lighting manufacturers (Rai et al., 2021). Instead, it is necessary to use a calibrated spectrometer to accurately measure and identify the radiation

spectrum (Albert & Mcleod, 2012): all UV wavelengths can be harmful to humans (Gallagher & Lee, 2006), so precautions must be taken when using UV LED lighting.

## UV-A radiation: from LEDs to sunlight

LED technology provides researchers with the opportunity to study photobiology in well-controlled environments. However, studies with narrow-band LEDs may misestimate the role of sunlight on plant processes. Given the presence of UV-A in nature (up to 250 μmol $m^{-2}$ $s^{-1}$; Fig. 1C), it is quite obvious that plants can and do fully acclimate to this intensity, at both the leaf and the plant level **(Chapters 2-5)**.

The percentage of UV-A1 relative to PAR in sunlight is around 6%, and the maximum PAR intensity on a clear summer day was measured to be around 2000 μmol $m^{-2}$ $s^{-1}$ in Beijing (Fig. 1). The average quantum yield in the UV-A1 range among six genotypes was found to be ~0.013 μmol $CO_2$/ μmol photons **(Chapter 4)**, which would mean that the maximum photosynthesis rate due to UV-A1 is ~1. 6 μmol $m^{-2}$ $s^{-1}$ during the middle of the day. In addition, solar UV radiation depends on seasonal variations (Fig. 1). The solar altitude angle, daylight length and ozone layer all affect the intensity of UV radiation, as they affect visible light.

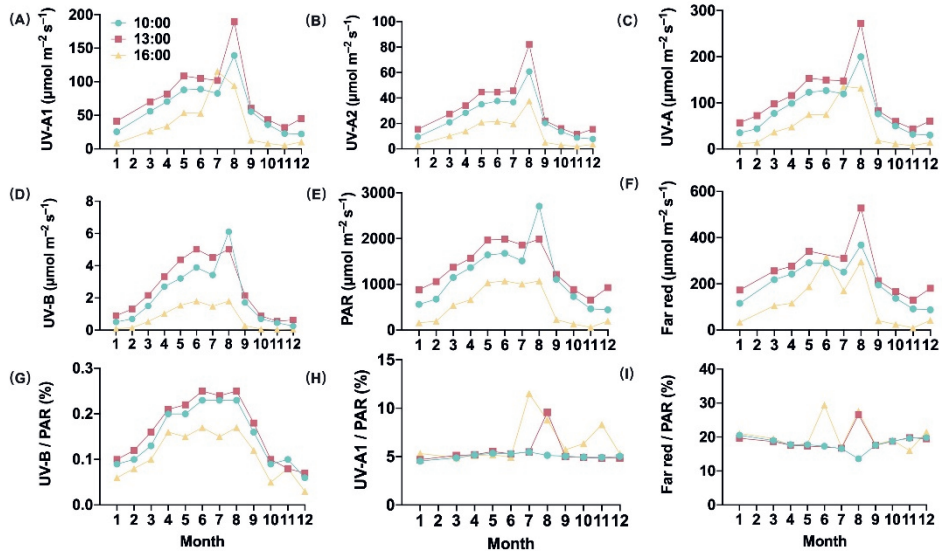


**Figure 1.** Annual solar irradiance of UV-A (315-400 nm), UV-B (280-315 nm) and far red (700-750 nm) radiation, and the changes in their ratios to PAR, at three moments of the day. Light intensity and spectrum were monitored using a spectroradiometer (Avaspec-2048CL, Avates, Apeldoorn, the Netherlands). Measurements were conducted on sunny days only, around the 23$^{rd}$ of each month in 2021, in the middle of Beijing, China. Care was taken that the spectroradiometer was not shaded during measurements.

# Future perspectives

This thesis is comprised of four research chapters as well as one general introduction and discussion. The intention of the thesis was to shed new light on plant responses to UV-A1 radiation. The data presented in this thesis may be used as a reference by growers and lamp manufacturers. Although notable advancements have been made in understanding the effects of UV-A1 radiation on plant growth, photosynthesis, photoprotection and leaf light acclimation, there still remain substantial knowledge gaps, as pointed out below:

1) The role of UV-A1 in photosynthesis remains an intriguing research area. Although not quantified in this thesis, UV-A may enhance photosynthesis in $C_4$ leaves (*Sorghum bicolor*; (Johnson & Day, 2002), and future studies should further determine how efficiently UV-A1 can drive photosynthesis in $C_4$ and in CAM

species. Controlled environment and novel UV-A1 LEDs could provide insights into the direct and indirect effects of UV-A1 on photosynthetic processes. Additionally, exploring the contribution of UV-A1 on whole-canopy photosynthesis is crucial, as this will provide a better estimate of photosynthetic quantum yield under full sunlight and may re-invigorate the discussion on a redefinition of PAR (Zhen and Bugbee, 2021). This could involve field studies using advanced UV sensors or remote sensing technologies and modeling approaches to understand how UV-A1 affects canopy structure, light distribution, and overall plant productivity.

2) Due to its high price and low energy efficiency, there are no reports of the effects of UV-A2 on plant growth, photosynthesis and photosynthetic acclimation, while those of UV-B have been explored comparably often. However, UV-A2, as a waveband between UV-B and UV-A1, may cause less photodamage than UV-B, but can nevertheless trigger UVR8 (Rai et al., 2020), potentially causing the synthesis of secondary metabolites and other health related compounds. Thus, UV-A2 could be used in pre- or post-harvest applications to improve the color, flavor and nutritional value of plants.

# References


Albert, A., & Mcleod, A. R. (2012). Beyond the Visible : A handbook of best practice in plant UV photobiology. In *Beyond the Visible : A handbook of best practice in plant UV photobiology* (Issue January). https://doi.org/10.31885/9789521083631

Battle, M. W., Vegliani, F., & Jones, M. A. (2020). Shades of green: Untying the knots of green photoperception. *Journal of Experimental Botany*, *71*(19), 5764–5770. https://doi.org/10.1093/jxb/eraa312

Barnes, P W, Tobler, M. A., Keefover-Ring, K., Flint, S. D., Barkley, A. E., Ryel, R. J., & Lindroth, R. L. (2016). Rapid modulation of ultraviolet shielding in plants is influenced by solar ultraviolet radiation and linked to alterations in flavonoids. *Plant Cell Environ*, *39*(1), 222–230. https://doi.org/10.1111/pce.12609

Barnes, P. W., Flint, S. D., Ryel, R. J., Tobler, M. A., Barkley, A. E., & Wargent, J. J. (2015). Rediscovering leaf optical properties: New insights into plant acclimation to solar UV radiation. *Plant Physiology and Biochemistry*, *93*, 94–100. https://doi.org/10.1016/j.plaphy.2014.11.015

Barnes, P. W., Kersting, A. R., Flint, S. D., Beyschlag, W., & Ryel, R. J. (2013). Adjustments in epidermal UV-transmittance of leaves in sun-shade transitions. *Physiologia Plantarum*, *149*(2), 200–213. https://doi.org/10.1111/ppl.12025

Barnes, P. W., Searles, P. S., Ballaré, C. L., Ryel, R. J., & Caldwell, M. M. (2000). Non-invasive measurements of leaf epidermal transmittance of UV radiation using chlorophyll fluorescence: Field and laboratory studies. *Physiologia Plantarum*, *109*(3), 274–283. https://doi.org/10.1034/j.1399-3054.2000.100308.x

Beggs, C. J., & Wellmann, E. (1985). Analysis of light-controlled anthocyanin formation in coleoptiles of Zea mays L.: The role of UV-B, blue, red and far-red light. *Photochemistry and Photobiology*, *41*(4), 481–486. https://doi.org/10.1111/j.1751-1097.1985.tb03515.x

Bellaflore, S., Barneche, F., Peltler, G., & Rochalx, J. D. (2005). State transitions and light adaptation require chloroplast thylakoid protein kinase STN7. *Nature*, *433*(7028), 892–895. https://doi.org/10.1038/nature03286

Bernal, M., Llorens, L., Badosa, J., & Verdaguer, D. (2013). Interactive effects of UV radiation and water availability onseedlings of six woody Mediterranean species. *Physiologia Plantarum*, *147*(2), 234–247. https://doi.org/10.1111/j.1399-3054.2012.01660.x

Blatt, M. R. (1983). The action spectrum for chloroplast movements and evidence for blue-light-photoreceptor cycling in the alga Vaucheria. *Planta*, *159*(3), 267–276. https://doi.org/10.1007/BF00397535

Caldwell, M. M., Robberecht, R., & Flint, S. D. (1983). Internal filters: Prospects for UV-acclimation in higher plants. *Physiologia Plantarum*, *58*(3), 445–450. https://doi.org/10.1111/j.1399-3054.1983.tb04206.x

Chen, Y., Fanourakis, D., Tsaniklidis, G., Aliniaeifard, S., Yang, Q., & Li, T. (2021). Low UVA intensity during cultivation improves the lettuce shelf-life, an effect that is not sustained at higher intensity. *Postharvest Biology and Technology*, *172*(September 2020), 111376. https://doi.org/10.1016/j.postharvbio.2020.111376

Chen, Y., Li, T., Yang, Q., Zhang, Y., Zou, J., Bian, Z., & Wen, X. (2019). UVA radiation is beneficial for yield and quality of indoor cultivated lettuce. *Frontiers in Plant Science*, *10*. https://doi.org/10.3389/fpls.2019.01563

Christie, J. M., (2007). Phototropin blue-light receptors. *Annu Rev Plant Biol*, *58*, 21–45. https://doi.org/10.1146/annurev.arplant.58.032806.103951

Christie, J. M., Blackwood, L., Petersen, J., & Sullivan, S. (2015). Plant flavoprotein photoreceptors. *Plant Cell Physiol*, *56*(3), 401–413. https://doi.org/10.1093/pcp/pcu196

Cockell, C. S., & Knowland, J. (1999). Ultraviolet radiation screening compounds. *Biological Reviews*, *74*(3), 311–345. https://doi.org/10.1111/j.1469-185X.1999.tb00189.x

Darras, A. I., Demopoulos, V., Bali, I., & Tiniakou, C. (2012). Photomorphogenic reactions in geranium (Pelargonium x hortotum) plants stimulated by brief exposures of ultraviolet-C irradiation. *Plant Growth Regulation*, *68*(3), 343–350. https://doi.org/10.1007/s10725-012-9722-2

Darras, A. I., Tsikaloudakis, G., Lycoskoufis, I., Dimitriadis, C., & Karamousantas, D. (2020). Low doses of UV-C irradiation affects growth, fruit yield and photosynthetic activity of tomato plants. *Scientia Horticulturae*, *267*, 109357. https://doi.org/10.1016/j.scienta.2020.109357

Fuglevand, G., Jackson, J. A., & Jenkins, G. I. (1996). UV-B, UV-A, and blue Light signal transduction pathways interact synergistically to regulate chalcone synthase gene expression in Arabidopsis. The Plant Cell, 8(12), 2347. https://doi.org/10.2307/3870473

Gallagher, R. P., & Lee, T. K. (2006). Adverse effects of ultraviolet radiation: A brief review. *Progress in Biophysics and Molecular Biology*, *92*(1), 119–131. https://doi.org/10.1016/j.pbiomolbio.2006.02.011

Guo, H., Yang, H., Mockler, T. C., & Lin, C. (1998). Regulation of flowering time by Arabidopsis photoreceptors. *Science*, *279*(5355), 1360–1363. https://doi.org/10.1126/science.279.5355.1360

Guo, J., & Wang, M. H. (2010). Ultraviolet A-specific induction of anthocyanin biosynthesis and PAL expression in tomato (*Solanum lycopersicum* L.). *Plant Growth Regulation*, *62*(1), 1–8. https://doi.org/10.1007/s10725-010-9472-y

He, R., Zhang, Y., Song, S., Su, W., Hao, Y., & Liu, H. (2021). UV-A and FR irradiation improves growth and nutritional properties of lettuce grown in an artificial light plant factory. *Food Chemistry*, *345*, 128727. https://doi.org/10.1016/j.foodchem.2020.128727

Hirosawa, T., & Miyachi, S. (1983). Inactivation of Hill reaction by long-wavelength ultraviolet radiation (UV-A) and its photoreactivation by visible light in the cyanobacterium, Anacystis nidulans. *Archives of Microbiology*, *135*(2), 98–102. https://doi.org/10.1007/BF00408016

Hogewoning, S. W., Trouwborst, G., Maljaars, H., Poorter, H., van Ieperen, W., & Harbinson, J. (2010). Blue light dose-responses of leaf photosynthesis, morphology, and chemical composition of Cucumis sativus grown under different combinations of red and blue light. *Journal of Experimental Botany*, *61*(11), 3107–3117. https://doi.org/10.1093/jxb/erq132

Holmes, M. G., & Keiller, D. R. (2002). Effects of pubescence and waxes on the reflectance of leaves in the ultraviolet and photosynthetic wavebands: A comparison of a range of species. *Plant, Cell and Environment*, *25*(1), 85–93. https://doi.org/10.1046/j.1365-3040.2002.00779.x

Inoue, S. I., Kinoshita, T., Takemiya, A., Doi, M., & Shimazaki, K. I. (2008). Leaf positioning of Arabidopsis in response to blue light. *Molecular Plant*, *1*(1), 15–26. https://doi.org/10.1093/mp/ssm001

Jacobo-Velázquez, D. A., Moreira-Rodríguez, M., & Benavides, J. (2022). UVA and UVB radiation as innovative tools to biofortify horticultural crops with nutraceuticals. *Horticulturae*, *8*(5), 1–12. https://doi.org/10.3390/horticulturae8050387

Jenkins, G. I. (2014). The UV-B photoreceptor UVR8: from structure to physiology. *Plant Cell*, *26*(1), 21–37. https://doi.org/10.1105/tpc.113.119446

Johnson, G. A., & Day, T. A. (2002). Enhancement of photosynthesis in Sorghum bicolor by ultraviolet radiation. *Physiologia Plantarum*. https://doi.org/10.1034/j.1399-3054.2002.1160415.x

Julkunen-Tiitto, R., Nenadis, N., Neugart, S., Robson, M., Agati, G., Vepsäläinen, J., Zipoli, G., Nybakken, L., Winkler, B., & Jansen, M. a. K. (2014). Assessing the response of plant flavonoids to UV radiation: an overview of appropriate techniques. *Phytochemistry Reviews*, *14*(2), 273–297. https://doi.org/10.1007/s11101-014-9362-4

Kang, C., Zhang, Y., Cheng, R., Kaiser, E., Yang, Q., & Li, T. (2021). Acclimating cucumber plants to blue supplemental light promotes growth in full sunlight. *Frontiers in Plant Science*, *12*, 1–14. https://doi.org/10.3389/fpls.2021.782465

Kang, S., Zhang, Y., Zhang, Y., Zou, J., Yang, Q., & Li, T. (2018). Ultraviolet-a radiation stimulates growth of indoor cultivated tomato (*Solanum lycopersicum*) seedlings. *HortScience*. https://doi.org/10.21273/HORTSCI13347-18

Kelly, N., & Runkle, E. S. (2023). End-of-production ultraviolet A and blue light similarly increase lettuce coloration and phytochemical concentrations. *HortScience*, *58*(5), 525–531. https://doi.org/10.21273/HORTSCI17108-23

Khanam, U. K. S., Oba, S., Yanase, E., & Murakami, Y. (2012). Phenolic acids, flavonoids and total antioxidant capacity of selected leafy vegetables. *Journal of Functional Foods*, *4*(4), 979–987. https://doi.org/10.1016/j.jff.2012.07.006

Kotilainen, T., Tegelberg, R., Julkunen-Tiitto, R., Lindfors, A., & Aphalo, P. J. (2008). Metabolite specific effects of solar UV-A and UV-B on alder and birch leaf phenolics. *Global Change Biology*, *14*(6), 1294–1304. https://doi.org/10.1111/j.1365-2486.2008.01569.x

Kotilainen, T., Tegelberg, R., Julkunen-Tiitto, R., Lindfors, A., O'Hara, R. B., & Aphalo, P. J. (2010). Seasonal fluctuations in leaf phenolic composition under UV manipulations reflect contrasting strategies of alder and birch trees. *Physiologia Plantarum*, *140*(3), 297–309. https://doi.org/10.1111/j.1399-3054.2010.01398.x

Krizek, D. T., Britz, S. J., & Mirecki, R. M. (1998). Inhibitory effects of ambient levels of solar UV-A and UV-B radiation on growth of cv. New Red Fire lettuce. *Physiologia Plantarum*, *103*(1), 1–7. https://doi.org/10.1034/j.1399-3054.1998.1030101.x

Krizek, D. T., Mirecki, R. M., & Britz, S. J. (1997). Inhibitory effects of ambient levels of solar UV-A and UV-B radiation on growth of cucumber. *Physiologia Plantarum*, *100*(4), 886–893. https://doi.org/10.1034/j.1399-3054.1997.1000414.x

Lante, A., Tinello, F., & Nicoletto, M. (2016). UV-A light treatment for controlling enzymatic browning of fresh-cut fruits. *Innovative Food Science and Emerging Technologies*, *34*, 141–147. https://doi.org/10.1016/j.ifset.2015.12.029

Lee, J. H., Oh, M. M., & Son, K. H. (2019). Short-term ultraviolet (UV)-A light-emitting diode (LED) radiation improves biomass and bioactive compounds of kale. *Frontiers in Plant Science*. https://doi.org/10.3389/fpls.2019.01042

Lee, M. J., Son, J. E., & Oh, M.-M. (2014). Growth and phenolic content of sowthistle grown in a closed-type plant production system with a UV-A or UV-B lamp. *Horticulture, Environment, and Biotechnology*, *54*(6), 492–500. https://doi.org/10.1007/s13580-013-0097-8

Lee, M. J., Son, J. E., & Oh, M. M. (2013). Growth and phenolic content of sowthistle grown in a closed-type plant production system with a UV-A or UV-B lamp. *Horticulture Environment and Biotechnology*, *54*(6), 492–500. https://doi.org/10.1007/s13580-013-0097-8

Liang, Y., Kang, C., Kaiser, E., Kuang, Y., Yang, Q., & Li, T. (2021). Red/blue light ratios induce morphology and physiology alterations differently in cucumber and tomato. *Scientia Horticulturae*, *281*, 109995. https://doi.org/10.1016/j.scienta.2021.109995

Lin, C. (2000). Plant blue-light receptors. *Trends in Plant Science*, *5*(8), 337–342. https://doi.org/10.1016/s1360-1385(00)01687-3

Liu, C., Han, X., Cai, L., Lu, X., Ying, T., & Jiang, Z. (2011). Postharvest UV-B irradiation maintains sensory qualities and enhances antioxidant capacity in tomato fruit during storage. *Postharvest Biology and Technology*, *59*(3), 232–237. https://doi.org/10.1016/j.postharvbio.2010.09.003

Markstädter, C., Queck, I., Baumeister, J., Riederer, M., Schreiber, U., & Bilger, W. (2001). Epidermal transmittance of leaves of Vicia faba for UV radiation as determined by two different methods. *Photosynthesis Research*, *67*(1–2), 17–25. https://doi.org/10.1023/A:1010676111026

Mazza, C. A., Boccalandro, H. E., Giordano, C. V., Battista, D., Soppel, A. L., & Ballare, C. L. (2000). Erratum: Functional significance and induction by solar radiation of ultraviolet-absorbing sunscreens in field-grown

soybean crops. *Plant Physiology*, *122*(4), 1461. https://doi.org/10.1104/pp.122.4.1461

McCree, K. J. (1971). The action spectrum, absorptance and quantum yield of photosynthesis in crop plants. *Agricultural Meteorology*. https://doi.org/10.1016/0002-1571(71)90022-7

Meyer, P., Van de Poel, B., & De Coninck, B. (2021). UV-B light and its application potential to reduce disease and pest incidence in crops. *Horticulture Research*, *8*(1). https://doi.org/10.1038/s41438-021-00629-5

Miyata, K., Noguchi, K., & Terashima, I. (2012). Cost and benefit of the repair of photodamaged photosystem II in spinach leaves: Roles of acclimation to growth light. *Photosynthesis Research*, *113*(1–3), 165–180. https://doi.org/10.1007/s11120-012-9767-0

Morales, L. O., Tegelberg, R., Brosche, M., Keinanen, M., Lindfors, A., & Aphalo, P. J. (2010). Effects of solar UV-A and UV-B radiation on gene expression and phenolic accumulation in *Betula pendula* leaves. *Tree Physiol*, *30*(7), 923–934. https://doi.org/10.1093/treephys/tpq051

Mosadegh, H., Trivellini, A., Ferrante, A., Lucchesini, M., Vernieri, P., & Mensuali, A. (2018). Applications of UV-B lighting to enhance phenolic accumulation of sweet basil. *Scientia Horticulturae*, *229*, 107–116. https://doi.org/10.1016/j.scienta.2017.10.043

Murchie, E. H., Pinto, M., & Horton, P. (2009). Agriculture and the new challenges for photosynthesis research. *New Phytologist*, *181*(3), 532–552. https://doi.org/10.1111/j.1469-8137.2008.02705.x

Murchie, Erik H., & Niyogi, K. K. (2011). Manipulation of photoprotection to improve plant photosynthesis. *Plant Physiology*, *155*(1), 86–92. https://doi.org/10.1104/pp.110.168831

Neugart, S., & Schreiner, M. (2018). UVB and UVA as eustressors in horticultural and agricultural crops. *Scientia Horticulturae*. *234*, 370–381. https://doi.org/10.1016/j.scienta.2018.02.021

Neugart, S., Tobler, M. A., & Barnes, P. W. (2021). Rapid adjustment in epidermal UV sunscreen: Comparison of optical measurement techniques and response to changing solar UV radiation conditions. *Physiologia Plantarum*, *173*(3), 725–735. https://doi.org/10.1111/ppl.13517

Ng, C. K. Y. (2019). Plant Cell Biology: UVA on guard. *Current Biology*, *29*(15), R740–R742. https://doi.org/10.1016/j.cub.2019.06.036

Nilsson, A. K., Pěnčík, A., Johansson, O. N., Bånkestad, D., Fristedt, R., Suorsa, M., Trotta, A., Novák, O., Mamedov, F., Aro, E. M., & Burmeister, B. L. (2020). PSB33 protein sustains photosystem II in plant chloroplasts under UV-A light. *Journal of Experimental Botany*, *71*(22), 7210–7223. https://doi.org/10.1093/jxb/eraa427

Ordidge, M., García-Macías, P., Battey, N. H., Gordon, M. H., Hadley, P., John, P., Lovegrove, J. A., Vysini, E., & Wagstaffe, A. (2010). Phenolic contents of lettuce, strawberry, raspberry, and blueberry crops cultivated under plastic films varying in ultraviolet transparency. *Food Chemistry*, *119*(3), 1224–1227. https://doi.org/10.1016/j.foodchem.2009.08.039

Ouhibi, C., Attia, H., Rebah, F., Msilini, N., Chebbi, M., Aarrouf, J., Urban, L., & Lachaal, M. (2014). Salt stress mitigation by seed priming with UV-C in lettuce plants: Growth, antioxidant activity and phenolic compounds. *Plant Physiology and Biochemistry*, *83*, 126–133. https://doi.org/10.1016/j.plaphy.2014.07.019

Palma, C. F. F., Castro-Alves, V., Morales, L. O., Rosenqvist, E., Ottosen, C. O., Hyötyläinen, T., & Strid, Å. (2022). Metabolic changes in cucumber leaves are enhanced by blue light but differentially affected by UV interactions with light signalling pathways in the visible spectrum. *Plant Science*, *321*(February). https://doi.org/10.1016/j.plantsci.2022.111326

Palma, C. F. F., Castro-Alves, V., Rosenqvist, E., Ottosen, C. O., Strid, Å., & Morales, L. O. (2021). Effects of UV radiation on transcript and metabolite accumulation are dependent on monochromatic light background in cucumber. *Physiologia Plantarum*, *173*(3), 750–761. https://doi.org/10.1111/ppl.13551

Paradiso, R., & Proietti, S. (2022). Light-Quality Manipulation to Control Plant Growth and Photomorphogenesis in Greenhouse Horticulture: The State of the Art and the Opportunities of Modern LED Systems. *Journal of Plant Growth Regulation*, *41*(2), 742–780. https://doi.org/10.1007/s00344-021-10337-y

Park, M. H., & Kim, J. G. (2015). Low-dose UV-C irradiation reduces the microbial population and preserves antioxidant levels in peeled garlic (*Allium sativum* L.) during storage. *Postharvest Biology and Technology*, *100*, 109–112. https://doi.org/10.1016/j.postharvbio.2014.09.013

Pfündel, E. E., Ben Ghozlen, N., Meyer, S., & Cerovic, Z. G. (2007). Investigating UV screening in leaves by two different types of portable UV fluorimeters reveals in vivo screening by anthocyanins and carotenoids. *Photosynthesis Research*, *9*3(1–3), 205–221. https://doi.org/10.1007/s11120-007-9135-7

Poorter, H., Fiorani, F., Stitt, M., Schurr, U., Finck, A., Gibon, Y., Usadel, B., Munns, R., Atkin, O. K., Tardieu, F., & Pons, T. L. (2012). The art of growing plants for experimental purposes: A practical guide for the plant biologist. *Functional Plant Biology*, *39*(11), 821–838. https://doi.org/10.1071/FP12028

Rai, N., Morales, L. O., & Aphalo, P. J. (2021). Perception of solar UV radiation by plants: photoreceptors and mechanisms. *Plant Physiology*, *186*(3), 1382–1396. https://doi.org/10.1093/PLPHYS/KIAB162

Rai, N., Neugart, S., Yan, Y., Wang, F., Siipola, S. M., Lindfors, A. V., Winkler, J. B., Albert, A., Brosché, M., Lehto, T., Morales, L. O., & Aphalo, P. J. (2019). How do cryptochromes and UVR8 interact in natural and simulated sunlight? *Journal of Experimental Botany*, *70*(18), 4975–4990. https://doi.org/10.1093/jxb/erz236

Rai, N., O'Hara, A., Farkas, D., Safronov, O., Ratanasopa, K., Wang, F., Lindfors, A. V., Jenkins, G. I., Lehto, T., Salojärvi, J., Brosché, M., Strid, Å., Aphalo, P. J., & Morales, L. O. (2020). The photoreceptor UVR8 mediates the perception of both UV-B and UV-A wavelengths up to 350 nm of sunlight with responsivity moderated by cryptochromes. *Plant Cell and Environment*. https://doi.org/10.1111/pce.13752

Ruban, A. V., & Wilson, S. (2021). The mechanism of non-photochemical quenching in plants: Localization and driving forces. *Plant and Cell Physiology*, *62*(7), 1063–1072. https://doi.org/10.1093/pcp/pcaa155

Sonntag, F., Liu, H., & Neugart, S. (2023). Nutritional and Physiological Effects of Postharvest UV Radiation on Vegetables: A Review. *Journal of Agricultural and Food Chemistry*, *71*(26), 9951–9972. https://doi.org/10.1021/acs.jafc.3c00481

Stevens, C., Liu, J., Khan, V. A., Lu, J. Y., Kabwe, M. K., Wilson, C. L., Igwegbe, E. C. K., Chalutz, E., & Droby, S. (2004). The effects of low-dose ultraviolet light-C treatment on polygalacturonase activity, delay ripening and Rhizopus soft rot development of tomatoes. *Crop Protection*, *23*(6), 551–554. https://doi.org/10.1016/j.cropro.2003.10.007

Takahashi, S, & Badger, M. R. (2011). Photoprotection in plants: a new light on photosystem II damage. *Trends Plant Sci*, *16*(1), 53–60. https://doi.org/10.1016/j.tplants.2010.10.001

Takahashi, Shunichi, Milward, S. E., Yamori, W., Evans, J. R., Hillier, W., & Badger, M. R. (2010). The solar action spectrum of photosystem II damage. *Plant Physiology*, *153*(3), 988–993. https://doi.org/10.1104/pp.110.155747

Takshak, S., & Agrawal, S. B. (2019). Defense potential of secondary metabolites in medicinal plants under UV-B stress. *Journal of Photochemistry and Photobiology B: Biology*, *193*(February), 51–88. https://doi.org/10.1016/j.jphotobiol.2019.02.002

Tokutsu, R., Fujimura-Kamada, K., Yamasaki, T., Okajima, K., & Minagawa, J. (2021). UV-A/B radiation rapidly activates photoprotective mechanisms in Chlamydomonas reinhardtii. *Plant Physiology*, *185*(4), 1894–1902. https://doi.org/10.1093/plphys/kiab004

Urban, L., Chabane Sari, D., Orsal, B., Lopes, M., Miranda, R., & Aarrouf, J. (2018). UV-C light and pulsed light as alternatives to chemical and biological elicitors for stimulating plant natural defenses against fungal diseases. *Scientia Horticulturae*, *235*, 452–459. https://doi.org/10.1016/j.scienta.2018.02.057

Vass, I., Turcsányi, E., Touloupakis, E., Ghanotakis, D., & Petrouleas, V. (2002). The mechanism of UV-A Radiation-Induced inhibition of photosystem II electron transport studied by EPR and chlorophyll fluorescence. *Biochemistry*, *41*(32), 10200–10208. https://doi.org/10.1021/bi020272

Verdaguer, D., Jansen, M. A. K., Llorens, L., Morales, L. O., & Neugart, S. (2017). UV-A radiation effects on higher plants: Exploring the known unknown. *Plant Science*. *255*, 72–81.https://doi.org/10.1016/j.plantsci.2016.11.014

Wada, M., Kagawa, T., & Sato, Y. (2003). Chloroplast Movement. *Annual Review of Plant Biology*, *54*, 455–468. https://doi.org/10.1146/annurev.arplant.54.031902.135023

Wilson, K. E., Thompson, J. E., Huner, N. P. A., & Greenberg, B. M. (2001). Effects of Ultraviolet-A exposure on Ultraviolet-B–induced accumulation of specific flavonoids in *Brassica napus*¶. *Photochemistry and Photobiology*, *73*(6), 678. https://doi.org/10.1562/0031-8655(2001)073<0678:eouaeo>2.0.co;2

Xu, M. Y., Zhang, L., Li, W. W., Hu, X. L., Wang, M. B., Fan, Y. L., Zhang, C. Y., & Wang, L. (2014). Stress-induced early flowering is mediated by miR169 in Arabidopsis thaliana. *Journal of Experimental Botany*, *65*(1), 89–101. https://doi.org/10.1093/jxb/ert353

Zhang, T., & Folta, K. M. (2012). Green light signaling and adaptive response. *Plant Signaling and Behavior*, *7*(1). https://doi.org/10.4161/psb.7.1.18635

Zhang, Y., Kaiser, E., Zhang, Y., Zou, J., Bian, Z., Yang, Q., & Li, T. (2020). UVA radiation promotes tomato growth through morphological adaptation leading to increased light interception. *Environmental and Experimental Botany*. *176*, 104073. https://doi.org/10.1016/j.envexpbot.2020.104073

Zhang, Y., Sun, X., Aphalo, P. J., Zhang, Y., Cheng, R., & Li, T. (2023). Ultraviolet-A1 radiation induced a more favorable light-intercepting leaf-area display than blue light and promoted plant growth. *Plant Cell and Environment*, *46*(10), 1–16. https://doi.org/10.1111/pce.14727

## References in Table 1


[1] Christie, J. M., Blackwood, L., Petersen, J., & Sullivan, S. (2014). Plant flavoprotein photoreceptors. *Plant and Cell Physiology*, *56*(3), 401–413. https://doi.org/10.1093/pcp/pcu196

[2] Rai, N., Morales, L. O., & Aphalo, P. J. (2021). Perception of solar UV radiation by plants: photoreceptors and mechanisms. *Plant Physiology*, *186*(3), 1382–1396. https://doi.org/10.1093/plphys/kiab162

[3] Inoue, S., Kinoshita, T., Takemiya, A., Doi, M., & Shimazaki, K. (2008). Leaf positioning of arabidopsis in response to blue light. *Molecular Plant*, *1*(1), 15–26. https://doi.org/10.1093/mp/ssm001

[4] Zhang, Y., Sun, X., Aphalo, P. J., Zhang, Y., Cheng, R., & Li, T. (2023). Ultraviolet-A1 radiation induced a more favorable light-intercepting leaf-area display than blue light and promoted plant growth. *Plant Cell & Environment*, *47*(1), 197–212. https://doi.org/10.1111/pce.14727

[5] Sun, X., Kaiser, E., Aphalo, P. J., Marcelis, L. F., & Li, T. (2024). Plant responses to UV-A1 radiation are genotype and background irradiance dependent. *Environmental and Experimental Botany*, *219*, 105621. https://doi.org/10.1016/j.envexpbot.2023.105621

[6] Hogewoning, S. W., Trouwborst, G., Maljaars, H., Poorter, H., Van Ieperen, W., & Harbinson, J. (2010). Blue light dose-responses of leaf photosynthesis, morphology, and chemical composition of Cucumis sativus grown under different combinations of red and blue light. *Journal of Experimental Botany*, *61*(11), 3107–3117. https://doi.org/10.1093/jxb/erq132

[7] Liang, Y., Kang, C., Kaiser, E., Kuang, Y., Yang, Q., & Li, T. (2021). Red/blue light ratios induce morphology and physiology alterations differently in cucumber and tomato. *Scientia Horticulturae*, *281*, 109995. https://doi.org/10.1016/j.scienta.2021.109995

[8] Kang, C., Zhang, Y., Cheng, R., Kaiser, E., Yang, Q., & Li, T. (2021). Acclimating cucumber plants to blue supplemental light promotes growth in full sunlight. *Frontiers in Plant Science*, *12*. https://doi.org/10.3389/fpls.2021.782465

[9] McCree, K. (1972). Test of current definitions of photosynthetically active radiation against leaf photosynthesis data. *Agricultural Meteorology*, *10*, 443–453. https://doi.org/10.1016/0002-1571(72)90045-3

[10] Takahashi, S., Milward, S. E., Yamori, W., Evans, J. R., Hillier, W., & Badger, M. R. (2010). The solar action spectrum of photosystem II damage. *Plant Physiology*, *153*(3), 988–993. https://doi.org/10.1104/pp.110.155747

[11] Inoue, S., & Kinoshita, T. (2017). Blue light regulation of stomatal opening and the plasma membrane H+-ATPASE. *Plant Physiology*, *174*(2), 531–538. https://doi.org/10.1104/pp.17.00166

[12] Isner, J., Olteanu, V., Hetherington, A. J., Coupel-Ledru, A., Sun, P., Pridgeon, A. J., Jones, G. S., Oates, M., Williams, T. A., Maathuis, F. J., Kift, R., Webb, A. R., Gough, J., Franklin, K. A., & Hetherington, A. M. (2019). Short- and Long-Term effects of UVA on arabidopsis are mediated by a novel CGMP phosphodiesterase. *Current Biology*, *29*(15), 2580-2585.e4. https://doi.org/10.1016/j.cub.2019.06.071

[13] Blatt, M. R. (1983). The action spectrum for chloroplast movements and evidence for blue-light-photoreceptor cycling in the alga Vaucheria. *Planta*, *159*(3), 267–276. https://doi.org/10.1007/bf00397535

[14] Königer, M., & Bollinger, N. (2012). Chloroplast movement behavior varies widely among species and does not correlate with high light stress tolerance. *Planta*, *236*(2), 411–426. https://doi.org/10.1007/s00425-012-1619-9

[15] Lin, C. (2000). Plant blue-light receptors. *Trends in Plant Science*, *5*(8), 337–342. https://doi.org/10.1016/s1360-1385(00)01687-3

[16] Xu, M. Y., Zhang, L., Li, W. W., Hu, X. L., Wang, M., Fan, Y. L., Zhang, C. Y., & Wang, L. (2013). Stress-induced early flowering is mediated by miR169 in Arabidopsis thaliana. *Journal of Experimental Botany*, *65*(1), 89–101. https://doi.org/10.1093/jxb/ert353

[17] Fuglevand, G., Jackson, J. A., & Jenkins, G. I. (1996). UV-B, UV-A, and blue light signal transduction pathways interact synergistically to regulate chalcone synthase gene expression in arabidopsis. *The Plant Cell*, *8*(12), 2347. https://doi.org/10.2307/3870473

Chapter 6

# Summary

Ultraviolet radiation (UV; 100–400 nm) is an important spectrum of solar radiation, with UV-A (315-400 nm) accounting for approximately 95% of all UV arriving at the Earth's surface. There is a large body of literature on plant responses to UV-B (280–315 nm), while knowledge on UV-A is limited. Existing studies point to a large variability of the effects of UV-A on plants, which may in part be caused by uncontrolled experimental conditions, various spectra and doses used, and genotype effects.

**Chapter 1** firstly introduced the composition of UV radiation and the photoreceptors sensing it. It further pointed out existing knowledge gaps and the limitations of current UV-A plant photobiology research, and then described the ambiguity of plant responses to UV-A radiation from three broad processes (i.e. plant growth, leaf photosynthesis and photosynthetic acclimation). Lastly, the structure of this thesis was introduced and research contents of each chapter were outlined.

**Chapter 2** explored how a range of UV-A1 (350- 400nm) intensities (0-100 μmol $m^{-2}$ $s^{-1}$) affect plant growth across four plant species, and how their responses to UV-A1 depend on low- (150 μmol $m^{-2}$ $s^{-1}$) and high- (550 μmol $m^{-2}$ $s^{-1}$) white background light intensity. Plant growth was barely affected under UV-A1, with some variations depending on genotype and background irradiance.

**Chapter 3** investigated how acclimation to several wavelengths in the UV-A1 (peaking at 365 and 385 nm) and blue light (peaking at 410 and 450 nm) range affects leaf photosynthetic and photoprotective performance in tomato. Both UV-A1 and blue light triggered leaf photosynthetic and photoprotective acclimation, thereby allowing plants to perform well under high and fluctuating irradiance. The extent of acclimation became stronger the longer the peak wavelength was. This study exemplified that plant growth and photosynthetic traits in response to light treatments within the 365-450 nm range follow a shallow-continuous pattern instead of showing strong differences between UV-A1 and blue light.

**Chapter 4** quantified the photosynthetic quantum yield of UV-A1 in horticultural crops (cucumber, tomato and lettuce) and woody species (hydrangea and red dogwood). UV-A1

powered photosynthesis and caused photoinhibition in a wavelength-dependent manner. Despite a positive quantum yield in all cases, plants grown in natural sunlight tended to show negative net photosynthesis rates under UV-A1 regardless of illumination intensity. This study found that the concentration of UV-absorbing compounds in the leaf was negatively correlated with photosynthetic efficiency under UV-A1. Furthermore, a slow increase in non-photochemical quenching (NPQ) and transient reduction in photosynthesis were observed under 30 min UV-A1 exposure. It was concluded that UV-A1 can power photosynthesis, but this was not sufficiently compelling to define UV-A1 as photosynthetically active radiation.

**Chapter 5** continued from the finding in chapter 4 that a continuous decline in photosynthesis was observed during 30 min of UV-A1 exposure. This observation triggered the question whether leaves could acclimate to continuous UV-A1 exposure of up to three days, and if so how plant processes work synergistically to cope with stress. It was demonstrated that lettuce successfully acclimated to exposure under different combinations of light quality (red light combined with either UV-A1 or blue light) and intensity (200 or 400 μmol $m^{-2}$ $s^{-1}$), with UV-A1 being the most stressful case. Our data suggest this acclimation was achieved by an increase in plants' photosynthetic rather than their photoprotective capacity.

**Chapter 6** summarized the findings of the thesis, and extended the interpretation and discussion of these findings. The insights gained throughout this thesis are related to existing literature to give a comprehensive overview of the state of knowledge about how UV-A1 affects plant growth, leaf photosynthesis and photosynthetic acclimation, in comparison with blue light. Moreover, the role of UV-A1 radiation in nature and its estimated contribution to leaf photosynthesis are evaluated. Finally, views on the application of UV radiation in protected agriculture and perspectives for future research were provided.

# Acknowledgements

The journey of pursuing a PhD is far from a solitary endeavor; it is enriched by the support, guidance, and companionship of many along the way. Thank you all for being part of this journey.

First and foremost, I would like to thank my supervisors Leo Marcelis, Elias Kaiser and Tao Li. I thank you all for your invaluable guidance, patience, and continuous support throughout the course of my PhD journey. Your expertise and insightful feedback have been instrumental in shaping this work. Thank you for allowing me to step on your shoulders, allowing me to view the world with an innovative and critical perspective. Leo, your passion for science inspires me. Your comments always predict the reviewers' questions in advance, making our paper better. Important decisions are always made under your guidance. In the final stage of my PhD, you always gave me timely feedback, helped me submit the thesis on time. Your dedication to both academic excellence and the personal development of students sets a remarkable example, one that I aspire to follow in my own career. Elias, you are my light on the road of scientific research, with detailed instructions for each step. I really admired your fast and high-quality feedback; you always have amazing ideas, you are an idol in the academia. Also, big thanks for helping me with language. Thank you for everything! Tao, the topic of diffuse light allowed us to know each other, thank you for providing such an opportunity for me to join this project. During the epidemic, you helped me set up the experiment, and this has been the foundation for all other experiments during my thesis. Thank you for your strict requirements and high aesthetic standards for the figures and layouts, so that we have a beautiful thesis book.

A very special thank you goes to Pedro Aphalo, my advisor during my PhD journey and my co-author in chapter 2. I greatly admire your knowledge and insights in UV, as well as your guidance on scientific writing. The initial cooperation not only guided my first research paper, but also had a profound impact on my entire thesis. Thank you Ep, for being a solid support

in statistics. Whenever I turned to you for help, the problem always got solved. Thank you Hendrik and Liana, for the stimulating talks after my work discussion. Your unique insights in your field have been a source of inspiration and support, greatly enriching my experience.

As a sandwich PhD, I did most of the research work in CAAS, China. I thank all the colleagues and students from the research group in CAAS for making my time as a PhD student a happy and fruitful experience. 感谢杨其长、程瑞锋、刘文科、张义、李琨、仝宇欣、方慧、伍纲、王君、张玉琪和黄思捷等老师在试验和生活上的关心和帮助。感谢查凌雁、张雅婷、邹洁、邵冰洁、杨利、文渊、张涵等小伙伴，在这段旅程中给予的支持和陪伴, 也让我的旅程更加充实和快乐。感谢国际教育处张明军老师对我的支持与帮助。Yuqi, thank you for always answering my questions and generously sharing your knowledge. You show both the gentleness and strength of the women, and your encouragement has supported me in both my studies and personal life. Yating, I have always enjoyed our discussions about UV-A, and the exchange of ideas has often sparked new insights. Congratulations on becoming a mother! I would not have had the opportunity to pursue a PhD without the wisdom and support of those who paved the way for me during my BSc and MSc studies. 感谢中国农业大学宋卫堂老师, 南京农业大学郭世荣、孙锦、束胜等老师, 给予的指导和支持。

My time in Wageningen was absolutely great. I thank all the people in the Horticulture and Product Physiology chair group - it was a pleasure getting to know all of you. I would like to thank my paranymphs, Ying and Jiayu, thank you for the time and effort you have invested in helping me navigate this important milestone. Ying, thank you for your contribution to my future publication, based on what is now Chapter 5. You not only helped with transcriptome data analysis, but also taught me how to interpret the data. Our collaboration has brought us closer, and I truly appreciate your generosity in sharing your knowledge and your encouragement and suggestions for the development of my career. Yongran, you are like an older brother to me in Wageningen. Thank you for your warm-hearted welcome. Bingjie, thank you for your company. The time we spent eating, drinking coffee, and gossiping together was always pleasant. Wannida, Sijia, and Balta, thank you for sharing valuable

information about submitting the thesis and preparing for the defense. It was reassuring and fun to fight this battle alongside you all. Max, thank you for your company and introducing me to Thai culture. Here I would like to take this opportunity to sincerely thank to Cab (Zhibo), Diego, Elahe, Elena, Ingeborg, Kartika, Katharina (Huntenburg), Kim (Wenqing), Kexin, Linfang, Maria, Martina, Nilson, Miaomiao, Peige, Samikshya, Shen, Silvère, Silvia, Wenqin, Willy, Xiaohan, Xin, Xixi, Yifei, Yunke, Yunong. Thank you, Katharina (Hanika), Kim (Vanderwolk), Linda, Pauline, Stefan (Vorage), Suzan and Tijmen. I would like to thank Claudius from the PE&RC graduate school for his support during the whole PhD program. My thanks go out as well to the many friends and colleagues who have helped me along the way, regardless of whether they are mentioned here.

Most importantly, I would like to thank my family for their unconditional love and encouragement. I love all of you so much! To my parents (爸爸、妈妈), your unwavering belief in me has been my greatest source of strength. No words in the world can fully express the love you have given me. To my sister, you have made my growth journey less lonely. To Jiandong, my boyfriend and my soulmate, thank you for always being there for me. I am looking forward to sharing every sweet moment of life with you. I also want to thank your family for their warm hospitality and delicious food. To my lovely nephew (圣智), your arrival has brought joy to our family, and I wish you a bright future!

I would like to thank myself. I thank myself for my resilience in the face of pressure and my determination to never give up when things got tough, which have brought me to where I am today and give me confidence for the future.

Finally, I express my sincere thanks to all the support and help from you, dear reader! I wish you all the best and full of happiness.

Xuguang Sun
Beijing, China
September 2024

# About the author

Xuguang Sun was born in June 1994 in Chifeng, China. In 2012, she started her BSc study majoring in protected horticulture at Nanjing Agricultural University and graduated with honors in 2016. She then continued in the same major at China Agricultural University for MSc degree and graduated with honors in June 2019. In December 2019, she started pursuing her PhD (sandwich PhD program), which was a collaboration between the Horticulture and Product Physiology group at Wageningen University and the Institute of Environment and Sustainable Development in Agriculture, Chinese Academy of Agricultural Sciences. The research was focused on the effects of UV-A radiation on plant growth, leaf photosynthesis and photosynthetic acclimation; she was supervised by Prof. Dr Leo F.M. Marcelis, Dr Elias Kaiser and Prof. Dr Tao Li. She is currently seeking a position in academia and looking forward to new chapters on plant research.

Contact: sunxuguang06@gmail.com

# List of Publications

**Sun, X.**, Kaiser, E., Marcelis, L. F. M., & Li, T. (2024). Leaf photosynthetic and photoprotective acclimation in the ultraviolet-A1 and blue light regions follow a continuous, shallow gradient. ***Plant Cell and Environment*** https://doi.org/10.1111/pce.15256

**Sun, X.**, Kaiser, E., Zhang, Y., Marcelis, L. F. M., & Li, T. (2024). Quantifying the photosynthetic quantum yield of ultraviolet-A1 radiation. ***Plant Cell and Environment*** https://doi.org/10.1111/pce.15145

**Sun, X.**, Kaiser, E., Aphalo, P. J., Marcelis, L. F. M., & Li, T. (2023). Plant responses to UV-A1 radiation are genotype and background irradiance dependent. ***Environmental and Experimental Botany*** https://doi.org/10.1016/j.envexpbot.2023.105621

Zhang, Yating, **Sun, X.**, Aphalo, P. J., Zhang, Y., Cheng, R., & Li, T. (2023). Ultraviolet-A1 radiation induced a more favorable light-intercepting leaf-area display than blue light and promoted plant growth. ***Plant Cell and Environment*** https://doi.org/10.1111/pce.14727

## PE&RC Training and Education Statement

With the training and education activities listed below the PhD candidate has complied with the requirements set by the Graduate School for Production Ecology and Resource Conservation (PE&RC) which comprises of a minimum total of 30 ECTS (= 20 weeks of activities)

**Review/project proposal (6 ECTS)**

- Exploring UVA radiation effects on plant growth, photosynthesis and leaf light acclimation

**Post-graduate courses (7.7 ECTS)**

- Plant Development and Molecular Biology, Peking University (2019)
- What a Plant Knows, Peking University (2019)
- Progress in Agricultural Science and Technology, CAAS (2020)
- Progress in Agricultural Bio-environment Engineering, CAAS (2020)
- Comprehensive Subject Evaluation, CAAS (2020)
- Basic statistics, PE&RC (2020)

**Deficiency, refresh, brush-up courses (18 ECTS)**

- Greenhouse Technology, FTE (2020)
- Advanced Methods for Plant-Climate Research in Controlled Environments, HPP (2020)
- Plant Plasticity and Adaptation, PPH (2020)

**Laboratory training and working visits (1.5 ECTS)**

- Laboratory training on photosynthesis, Institute of Botany, the Chinese Academy of Sciences (2019)
- Laboratory training on photosynthesis and modelling, Institute of Plant Physiology and Ecology, the Chinese Academy of Sciences (2021)
- Working visit on protected horticulture, College of Water Resources and Civil Engineering, China Agriculture University (2023)

**Competence, skills and career-oriented activities (4.8 ECTS)**

- Efficient and Effective Academic Development, WGS & CAAS (2019)

- Academic Writing & Presenting in English, WGS & CAAS (2019)
- Searching and Organizing Literature for PhD candidates, CAAS (2020)
- Career Orientation, CAAS (2020)
- Stress Management for WUR PhDs, PE&RC (2024)
- Writing Propositions for your PhD, WGS (2024)

**Scientific Integrity/Ethics in science activities (1.3 ECTS)**

- Research Integrity and Academic Norms, CAAS (2020)
- Ethics in Plant and Environmental Sciences, WGS (2024)

**PE&RC Annual meetings, seminars and PE&RC weekend/retreat (1.2 ECTS)**

- PE&RC Last Year Retreat (2024)
- Annual Meeting Experimental Plant Sciences (2024)

**National scientific meetings, local seminars, and discussion groups (12.6 ECTS)**

- Agricultural environmental sciences seminar, Institute of Environment and Sustainable Development in Agriculture, CAAS, Beijing, China (2019-2023)
- FLOP Photosynthesis, PE&RC (2020-2024)
- 3rd Network Meeting of the UV4 Plants Association and Training school, online meeting and training (2020)
- The 8th International horticulture research conference, Nanjing, China & Zoom (2021)
- International workshop on plant environment interactions, Beijing, China & online meeting (2024)

**International symposia, workshops and conferences (3.2 ECTS)**

- The 9th Japan-China-Korea Joint Symposium on Greenhouse Horticulture and Plant Factory, Online meeting (2021)
- Photosynthesis Physiology and Ecology Symposium, Shanghai, China (2021)

The research described in this thesis was financially supported by the Chinese Academy of Agricultural Sciences.

Financial support from Wageningen University for printing this thesis is gratefully acknowledged.

Cover design by Yilin Zou and Xuguang Sun

Printed by: ProefschriftMaken